


# MINE GROUNDING SYSTEMS

## Evaluation of In-Mine Grounding System and Codification of Ground Bed Construction and Measurement Techniques.

Prepared for
United States Department of the Interior
Bureau of Mines

by
College of Engineering
West Virginia University
Morgantown, West Virginia 26506




West Virginia University

Final Report for June 24, 1974 to June 30, 1979
on
Grant No. GO144138.

June 30, 1979

USBM Grant No. G0144138

# MINE GROUNDING SYSTEMS: EVALUATION OF IN-MINE GROUNDING SYSTEM AND CODIFICATION OF GROUND BED CONSTRUCTION AND MEASUREMENT TECHNIQUES

Dr. Wils L. Cooley
Dr. Robert L. McConnell

Department of Electrical Engineering
West Virginia University
Morgantown, WV 26505

June 1979

Prepared for the
U.S. Department of the Interior
Bureau of Mines
Washington, D.C. 20240

| 1. Report No. | 2. | 3. Recipient's Accession No. |
|---|---|---|
| | | |

| 4. Title and Subtitle | 5. Report Date |
|---|---|
| Mine Grounding Systems: Evaluation of In-Mine Grounding System and Codification of Ground Bed Construction and Measurement Techniques. | 30 June 1979 |
| | 6. |

| 7. Author(s) | 8. Performing Organization Report No. |
|---|---|
| Wils L. Cooley<br>Robert L. McConnell | |

| 9. Performing Organization Name and Address | 10. Project/Task/Work Unit No. |
|---|---|
| Engineering Experiment Station<br>West Virginia University<br>Morgantown, WV 26506 | 11. Contract or Grant No.<br>G0144138 |

| 12. Sponsoring Organization Name and Address | 13. Type of Report |
|---|---|
| Office of the Assistant Director - Mining<br>Bureau of Mines<br>Department of the Interior<br>Washington, D.C. 20241 | Final Report for 24 June 1974 to 30 June 1979. |
| | 14. |

15. Supplementary Notes

16. Abstract

Two major grounding topics are covered: mine ground systems and ground-check monitors. Performance characteristics of ground-check monitors for high-voltage surface mine distribution cables and low-voltage underground mine trailing cables are evaluated. Over 20 commercially available monitors are studied to determine their utility. Several monitoring concepts are incorporated into an unusual monitor design, the prototype of which is described in detail. A comparative study of the effectiveness of several alternate methods of grounding surface mine equipment supports the system currently proposed by MSHA. An instrument design to measure earth voltage gradients is described, as well as an instrument design for measuring the effectiveness of dc haulage current return systems. An extreme analysis is made of techniques for measuring earth resistivity and resistance of safety ground beds. Electrolytic corrosion studies of earth electrodes are reported extensively also.

| 17. Originator's Key Words | 18. Availability Statement |
|---|---|
| Safety ground bed, surface mine grounding, ground-check monitors, earth resistance, electrode corrosion, stray current, rail bonds. | |

| 19. U. S. Security Classif. of the Report | 20. U. S. Security Classif. of This Page | 21. No. of Pages | 22. Price |
|---|---|---|---|
| | | | |

## FOREWORD

This report was prepared by West Virginia University, Engineering Experiment Station, Morgantown, West Virginia under USBM Grant No. G0144138. The grant was initiated under the Coal Mine Health and Safety Research Program. It was administered under the technical direction of the Pittsburgh Mining and Safety Research Center with Mr. Roger L. King acting as Technical Project Officer. Mr. A. G. Young was the contract administrator for the Bureau of Mines.

This report is a summary of the work recently completed on this grant during the period 24 June 1974 to 30 June 1979. This report was submitted by the authors on 30 June 1979.

TABLE OF CONTENTS

Table of Contents - Continued

Table of Contents - Continued

Table of Contents - Continued

# EXECUTIVE SUMMARY

The technical tasks executed under research grant G0144138 were completed with mostly positive results. The tasks which involved laboratory investigation and theoretical study were completed as anticipated, while those involving instrument design and field measurement did not fully meet objectives. The design of instrumentation which can operate properly in the mine environment was definitely more difficult than anticipated.

Chapter 1 covers high-voltage ground wire monitor testing. A program was set up to evaluate the relative performance of various commercially available high-voltage ground wire monitors for surface coal mine applications under simulated conditions in the laboratory. Extensive work was carried out early in the grant period to estimate the frequency and severity of lightning transients. Based on this analysis, some guidelines were formed for monitor design. An evaluation program was set up based on accumulated knowledge of field conditions. Ten commercially available ground wire monitors were evaluated, four of which were dc, five were audio, and one was ac. Of all the monitors tested, the primary weakness was found to be in their high-voltage transient performance.

Chapter 2 deals with low-voltage ground-check monitors. Twelve commerical monitors were evaluated during the grant period, several of them more than once. In addition, suggestions were made to several of the developers of ways to improve the utility of their designs. In order to demonstrate several unusual monitoring concepts, two special monitors were designed under the grant. The first was a "modular monitor" which incorporated various monitoring modules that could be interconnected in several ways to match the monitor characteristics to existing mine conditions. It was tested underground and sent to MSHA for approval. The second monitor design was a "multipath monitor", which was meant to fulfill a monitoring need on a multiply interconnected grounding network, such as a haulage belt system. These are difficult to monitor because the motor frames are interconnected by both the safety ground wires and the belt frame work, and also because several separate motors may be controlled on the same power circuit. A monitor capable of checking grounds to five separate motors was built for delivery to USBM.

Chapter 3 details work on mine equipment shock hazard. One aspect of this work was a study of the effectiveness of grounding practice in surface coal mines. Systems were studied and analyses were made of the theoretical effectiveness of several proposed methods of grounding surface equipment. It was concluded that a separate safety-grounded system currently proposed by MSHA is probably the safest practical method. Another aspect of the work was the design and construction of a potential gradient plotter. This instrument was designed to make a rapid recording of surface voltage gradients in the earth near ground beds or grounded equipment, thereby providing valuable data on possible shock hazards. A prototype device was built and used several times. Experience to date indicates that it requires some refinement before it will be generally useful, but it did function as anticipated. A description of the device and the results of testing are presented.

Chapter 4 covers studies on ground beds. Methods of measuring the effective resistivity of non-homogeneous soils are investigated, and some totally new methods of measuring earth resistivity are suggested. Several methods of measuring ground-bed resistance were investigated also. Based on analysis and extensive modeling of non-homogeneous earth, it was determined that presently accepted techniques are often in error, and improved methods of resistance determination are presented. A protracted effort was aimed at improved methods of ground bed design, the results of which have become USBM IC 8767 and a Technology Transfer workshop. Corrosion of ground beds by stray dc current flow was evaluated by estimating the magnitude of dc flow in the ground bed, and then testing the corrosion rate of various electrode materials. Ten different electrodes were tested for susceptability to corrosion. The results indicate that popular electrode materials are highly susceptable to corrosion, especially by a critical narrowing of the electrode near the soil surface. Finally, the preliminary design of an instrument to measure the resistance of a connected ground bed is presented.

Chapter 5 deals with sources of stray and induced current in mine ground systems. Leakage of dc from track haulage systems is analyzed, and the results compared to field data. Other sources of ground current are discussed. An extensive theoretical study and computer simulation on the effects of rail bonds on dc leakage current shows that a bad bond is difficult to isolate. A design is presented for a mobile instrument to detect bad bonds. The chapter ends with a summary of induced ac current.

Many of the chapters refer extensively to previous annual reports and reports of other grants. Some of the pertinent information from these reports has been reproduced, but no attempt was made to include all of the work done on mine grounding in this final report.

# CHAPTER 1

# HIGH-VOLTAGE GROUND WIRE MONITOR TESTING

## 1.1 INTRODUCTION

The purpose of the testing program was to evaluate the relative performance of various commercially available high-voltage ground wire monitors for surface coal mine applications under simulated conditions in the laboratory.

The research work in the area of high-voltage monitors was started in 1976 when efforts were made to investigate the topography of power distribution systems for surface coal mines and estimate the severity of high-voltage transients caused by lightning, since it was thought to be a major contributor to monitor failure. This work has been described in earlier reports (56,58). Efforts have also been made to analyze the various other problems faced by monitors in surface applications. Based on this analysis, some guidelines were formed under which the testing program was carried out.

The report summarizes the problems faced by high-voltage monitors, other than the lightning problem which has already been described. Based on this, some design requirements for monitors are suggested. Finally, results from the laboratory evaluation of the commercially available monitors are presented.

## 1.2 PROBLEMS FACED BY HIGH-VOLTAGE MONITORS

The typical problems faced by monitors for surface applications are enumerated below. Some of them are the same as might exist in an underground system; others are characteristic of surface systems only.

### 1.2.1 Induced 60 Hz Voltages and Currents

Due to the unsymmetrical construction of SHD-GC cable, 60 Hz voltages will be induced in the ground and pilot wires, even though balanced currents may be flowing in the phase conductors. This voltage will be impressed directly across the terminals of the monitor. Due to extremely long feeder cables involved, this voltage could be substantial. A rough calculation shows in induced voltage on the order of approximately 66 mV/1000 m (20 mV/1000 ft) per ampere of current in the phase wires. This will amount to about 20 V for a 1500 m (5000 ft) cable and 200 A of current. However, at starting of motors this voltage can rise to approximately 100 V for a few seconds.

Also, if the machine has a low earth contact resistance (such as a dragline), the voltage induced in the neutral can circulate high currents in the ground wire. The path of current flow is shown in figure 1.1. This current can also give rise to monitoring problems.

### 1.2.2 Low-Resistance Parallel Paths

Most of the surface mining equipment has an extremely good connection to

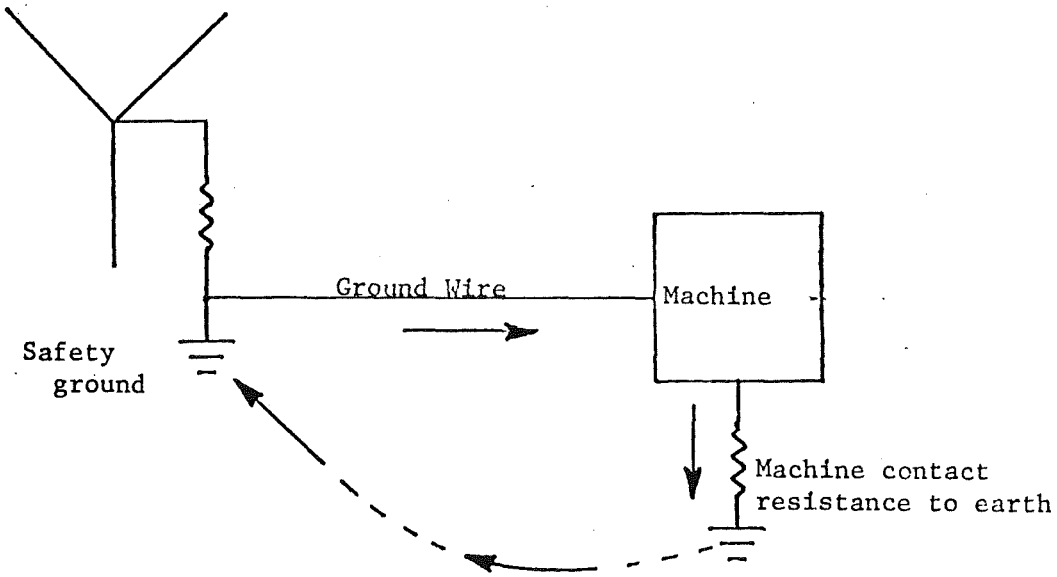


FIGURE 1.1. - Circuit to illustrate the path of ac stray currents flowing in the ground wire.

the ground due to the large metal surface in contact with earth. These additional ground paths (parallel paths) may have a resistance as low as the safety ground system itself. Even though these parallel paths do ground the equipment, they may only be temporary and therefore less desirable. Most of the monitors do not have the capability of distinguishing between a parallel path and the safety ground. They may therefore fail to trip when a parallel path is present even though the ground wire breaks.

### 1.2.3 Pilot-to-Ground Short Circuits

As a power cable deteriorates from use, it is possible that the pilot wire could become shorted to the ground wires somewhere within a cable. This pilot-to-ground short completes a monitoring loop that would ordinarily be completed only at the machine frame. This problem can be avoided by mounting components on the machine (resistors, filters, etc.) to distinguish between a legitimate monitoring loop and a shorted one.

### 1.2.4 Extreme Operating Temperatures

Normally, the monitor units are mounted in metal enclosures and left out in the open. Thus on a hot day the temperature inside the enclosure could be quite high. Temperatures as high as 70°C (158°F) are conceivable. Similarly, on a cold day the temperature could go well below freezing. Thus the monitors have to be built for operation within wide temperature limits. One may have difficulty in attaining these limits if solid-state components are used.

### 1.2.5 Phase-to-Pilot Faults

Due to the cable insulation degradation with the passage of time, there is a remote possibility that any of the phase conductors could short to the pilot wire. This type of fault can cause monitoring problems in high-voltage circuits. The effect will be illustrated with the help of the circuit in figure 1.2. Such a circuit results when a phase-to-pilot fault occurs. The supply voltage in the circuit is assumed to be 4160 V (line-to-line). $R_N$ is the neutral resistor and sized at 96Ω to limit the fault current to 25 A. $R_{MC}$ is the resistor mounted at the machine end to detect pilot-to-ground faults (typically sized at 4Ω). Thus, during the fault the voltage appearing across pilot-to-ground at the monitor terminals will be approximately 25 x 4 = 100 V which can cause monitoring problems.

### 1.2.6 Lightning Transients

The problem of high-voltage transients due to lightning has been discussed in detail in previous reports (56,58). Various pathways were analyzed through which high-voltage transients could be transferred to the monitor terminals. For the basis of this analysis, it was assumed that 1000 V appearing between the ground wire terminals and the frame of the monitor could cause monitor failure. The final results of this analysis are summarized in Table 1.1, which gives the frequency of occurrence of monitor failure per year due to each pathway. When all pathways are taken into account (assuming 8km, or 5 miles of pole line) the final result is summed up to be 1.97 or once every six months.

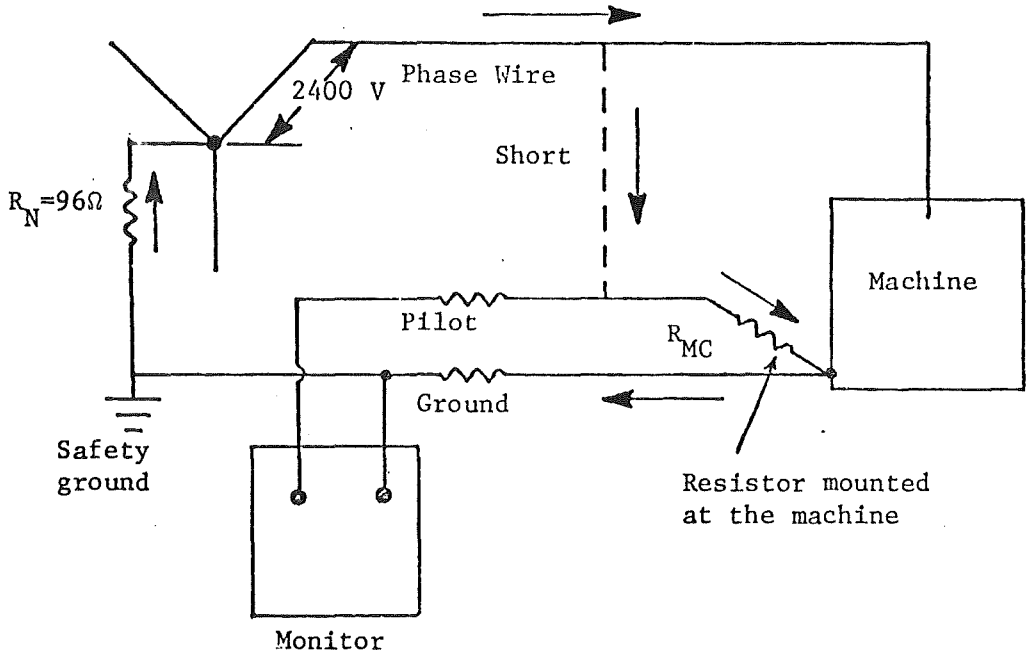


FIGURE 1.2. - Circuit to illustrate a phase-to-pilot short circuit. Arrows indicate the current flow.

TABLE 1.1-The frequency of occurrence of monitor damage due to various pathways

| Pathway | Frequency of Occurrence, per year |
|---|---|
| a. Incoming Static Wire | 0.017 |
| b. Incoming Phase Conductor | 0.212/1000 m (0.341/mile) |
| c. Dragline | 0.09892 |
| d. In-Line Breaker and Portable Substation | 0.053 |
| e. Primary Substation | 0.00565 |
| f. Earth Near Equipment | 0.00178 |
| g. Earth Near Cable | 0.001577 |

The results in Table 1.1 show that the incoming phase wire has the highest probability followed by the path through the static wire and dragline. Pathways d, e, f and g are of less significance. Protection efforts can be focused mainly on pathways a, b, c,and d.

## 1.3 MONITOR DESIGN REQUIREMENTS AND CONSIDERATIONS

Based on the analysis already presented, the following design requirements are suggested for high-voltage ground wire monitors.

### 1.3.1 Immunity to 60 Hz Voltages and Currents

The monitors should be immune to 60 Hz induced currents (up to 5 A) flowing in the ground wire. Also, 60 Hz voltages (up to 100 V) appearing between pilot and ground terminals should have no undesirable effect on the performance.

### 1.3.2 Ability to Monitor Long Lengths of Cable

As already seen, most of the cable lengths encountered in surface monitors are hundreds of meters (a few thousand feet). For these lengths and for monitors working in the audio frequency range the cable has to be treated as a distributed rather than a lumped element. This can give rise to grave monitoring problems. Preliminary studies done by WVU show that these transmission line effects are pronounced for cable lengths in excess of 1500 m (5000 ft) and monitoring frequencies of over 5 kHz. Dc monitors face no such problem.

### 1.3.3 Immunity to Parallel Paths

Most of the surface mining equipment frames are in good earth contact and can present low resistances which are sometimes hard for monitors to detect. However, it is a desirable feature for the monitors to have the ability to detect ground wire failure in spite of parallel paths.

### 1.3.4 Pilot-to-Ground Short Circuits

The monitor should have the ability to detect a pilot-to-ground short circuit. Usually, this can be accomplished by mounting a resistor or a filter at a machine between the pilot and the ground wire.

### 1.3.5 Large Temperature Variations

Due to the nature of their application the monitors should be able to operate efficiently under large temperature variations. The suggested values are -25°C to 70°C (-15°F to 160°F).

### 1.3.6 Immunity to High-Voltage Transients

As shown already, large voltage transients can be produced at the monitor terminals due to lightning strokes. However, at present no data is available on the peak value of these transients. As such, all the elements within the monitor connected directly to the input terminals (for example, supply transformers, rectifiers, relays, etc.) should have adequate BIL (Basic Impulse Level). High power surge protection should also be provided across the input supply terminals as well as across the ground terminal and case of the monitor.

### 1.3.7 Flags to Indicate Nature of Tripping

There can be several abnormal conditions within the system for which the monitor can trip. It is highly desirable that the monitor be capable of identifying the nature of fault, for example, ground wire open or pilot-to-ground short, etc. It would be of an added advantage if a rough indication of the location of the fault is also given.

### 1.3.8 Supply Voltage Variations

The monitor should operate satisfactorily if the supply voltage varies by -30% to +10% of its nominal value.

## 1.4 DESCRIPTION OF TESTS CARRIED OUT

The monitor test box which was fabricated for the testing of low-voltage monitors was used without any major modifications (figure 1.3). The following tests were carried out:

1. Sensitivity to changes in the resistance of ground and pilot wires.
2. Pilot-to-ground short circuits.
3. Stray ac and dc currents in the ground wire.
4. Parallel paths.
5. Environmental tests.
6. Supply voltage variations.
7. Tripping times under open ground and loss of power conditions.
8. High-voltage transient testing.

Test #5 could be carried out on only 3 monitors since the environmental chamber had to be returned to the USBM for their use. Test #8 needs some description which is given below.

### 1.4.1 High-Voltage Transient Testing

As previously indicated, high voltage transients due to lightning strokes are a major cause of many monitor failures. In the previous studies

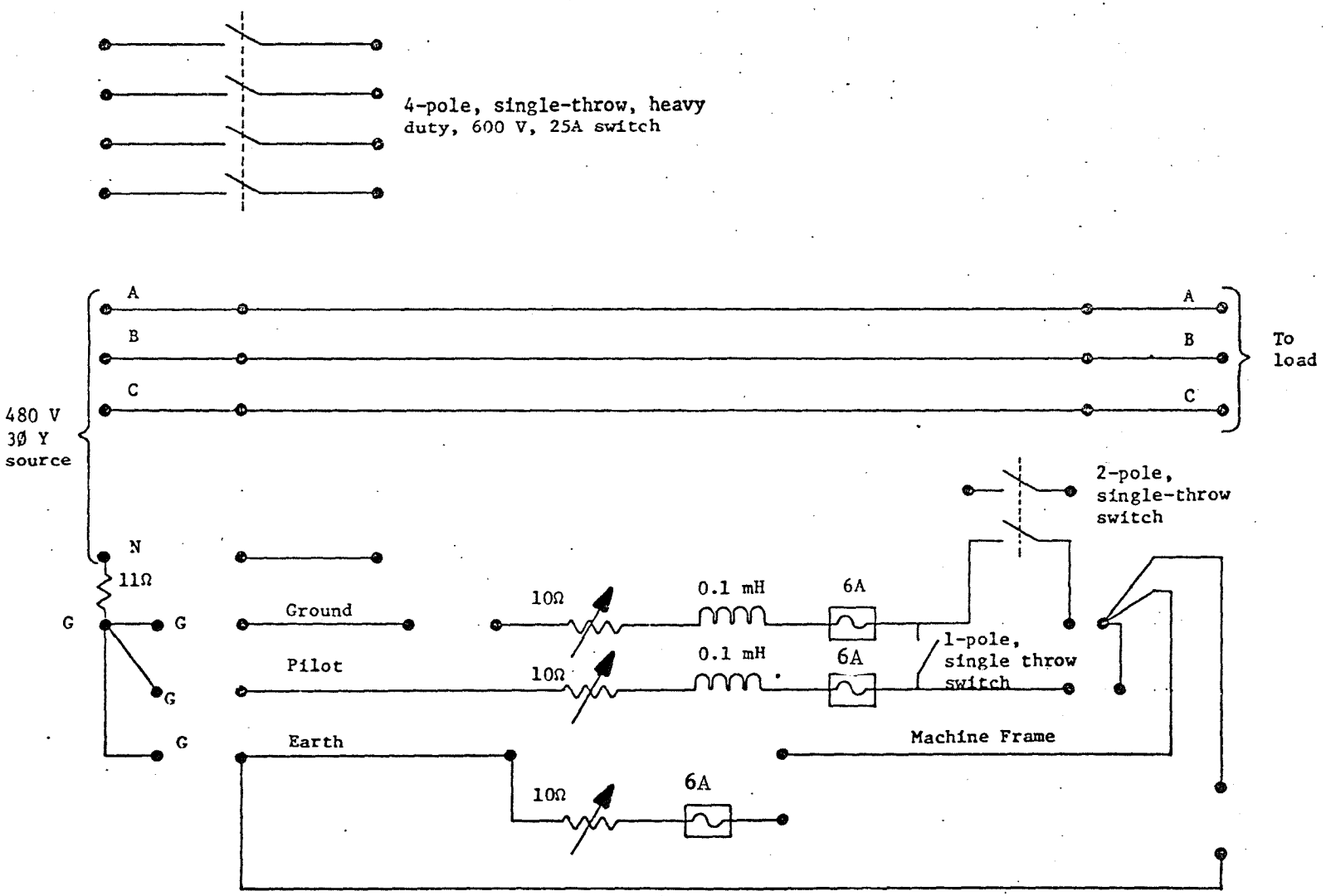


FIGURE 1.3. - Test panel for ground wire monitor.

## 1.5 LIST OF MONITORS TESTED

The available monitors on which testing was carried out are*:

1. Atkinson Armature Works Company Type AAW7700 Omser.
2. Central Electric Company Type RJL-300.
3. General Electric Company Type MEO-DP-3AM.
4. FEMCO Ground Sentinal II.
5. AMF Potter-Brumfield.
6. Line Power Mfg. P/N 170061.
7. Line Power Mfg. P/N 170013.
8. Consolidation Coal Company.
9. American Mine Research Type GM-200.
10. Ensign Electric Type 2401-865.

## 1.6 RESULTS FROM LABORATORY TESTS

The above-mentioned monitors were tested in the laboratory to evaluate their performance under simulated abnormal system conditions. However, since the tests were conducted strictly in a laboratory type environment, the actual performance in the field might differ somewhat. For the test routine it was assumed that all the monitors (except when clearly specified by the manufacturer, as in the case of the AMF monitor) were capable of monitoring multiple sections of cable in series, each section being approximately 300 m (1000 ft) in length. Also, none of the monitors tested was capable of monitoring through a junction box where a bigger cable teed-off into two smaller cables, unless the monitor was mounted in the junction box. For the tests carried out, all the monitors (except AMF) were set for a ground wire resistance of 0.5Ω and a pilot wire resistance of 4.0Ω which corresponds to about 1800 m (6000 ft) of 4/0 cable.

### 1.6.1 Atkinson Monitor

The connection diagram for the monitor is given in figure 1.5. Basically it is a dc monitor which uses a bridge circuit with a voltage comparator to measure resistance. A second comparator is used to detect a "too low" resistance representing a pilot-to-ground fault. In other words, the two comparators form a window detector. The monitor is equipped with pilot lights to indicate whether the tripping was due to pilot-to-ground resistance being too low or too high. It also uses a 4Ω resistor connected between pilot and the ground on the machine frame to detect pilot-to-ground short circuits. The open circuit pilot-to-ground voltage is 12 V.

The monitor was very sensitive to changes in the impedance of the ground and pilot wires and tripped for all abnormal conditions. It also tripped for pilot-to-ground shorts. Stray ac currents in the ground wire (up to 2.5 A) and induced voltages in the pilot-to-ground circuit (around 20 V) seemingly had no ill effect on the performance. However, the monitor tripped for stray dc currents in excess of 0.3 A. The monitor operated satisfactorily when the

*Reference to specific brands, equipment, or trade names in this report is made to facilitate understanding and does not imply endorsement by the Bureau of Mines.

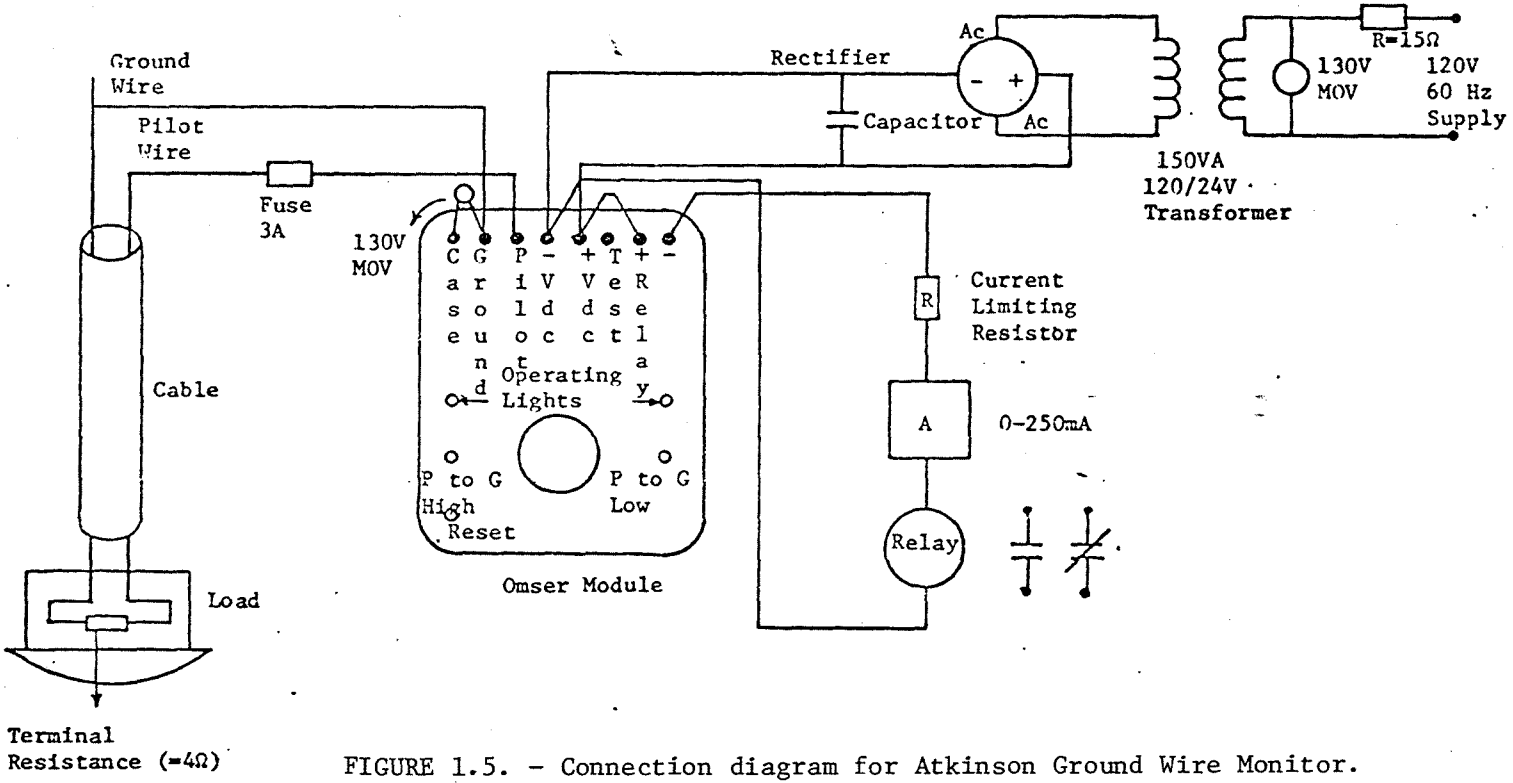


FIGURE 1.5. - Connection diagram for Atkinson Ground Wire Monitor.

supply voltage was increased by 10%. However, ppor performance was obtained when the voltage was decreased by more than 12% of the nominal value.

The monitor worked well when subjected to a temperature of 65° in an environmental chamber. However, when left at 80°C for some time, the main power supply failed.

The monitor does not have the ability to trip if the ground wire is opened in the presence of a low-resistance parallel path.

The output relay is normally energized and took approximately 165 ms to trip after the ground wire was opened. It took 2.4 seconds to trip after the power supply to the monitor was lost.

The monitor is protected against transients by two GE 130 V MOV's; one is connected across the supply transformer terminals and the second one is connected across the ground terminal and case of the monitor. The MOV across the supply terminals broke down at a peak transient voltage of approximately 2900 V (40 μs pulse width). Similiarly the one connected across the ground and case broke down at 1400 V. When the pulse width was increased to 1 ms the MOV across the supply terminals broke down at 1870 V while the one connected across the ground and case broke down at 1370 V. The supply terminals to case successfully withstood 3000 V in both the cases.

While the overall performance of the unit was satisfactory, it seems that the transient performance of the unit needs to be improved by using better surge arrestors.

### 1.6.2 Central Electric Company Monitor

The connection diagram is given in figure 1.6. In this monitoring technique a dc current (≙ 0.9 A) is circulated in the pilot-to-ground circuit. A small dc voltage (≃ 2 mV) which is developed across a ground-wire shunt is fed to a meter relay. The meter relay senses any decrease in the pick-up voltage and trips in case the voltage is less than the set-point. This will happen for any substantial increase in resistance of the pilot-ground circuit. There is a small circuit breaker in series with the pilot wire. This breaker is equipped with a thermal trip which is set for a time delay of approximately 10-15 seconds for a current of 2 A. In case there is a pilot-to-ground short-circuit the current will increase, thereby tripping the circuit-breaker and opening the pilot-ground circuit. This in turn will operate the monitor. The monitor also uses a 25Ω adjustable resistor connected between the pilot and ground at the machine frame. The dc voltage in the monitoring loop is around 24 V.

The monitor satisfactorily tripped for changes in the ground and pilot wire resistances under normal circumstances. However, if the monitor was originally set when a low parallel path was present and subsequently the parallel path was removed, the monitor failed to trip even when the ground wire resistance was increased to 10Ω. Stray ac flowing in the ground wire (up to 5 A) did not have any effect on the performance. However, the monitor

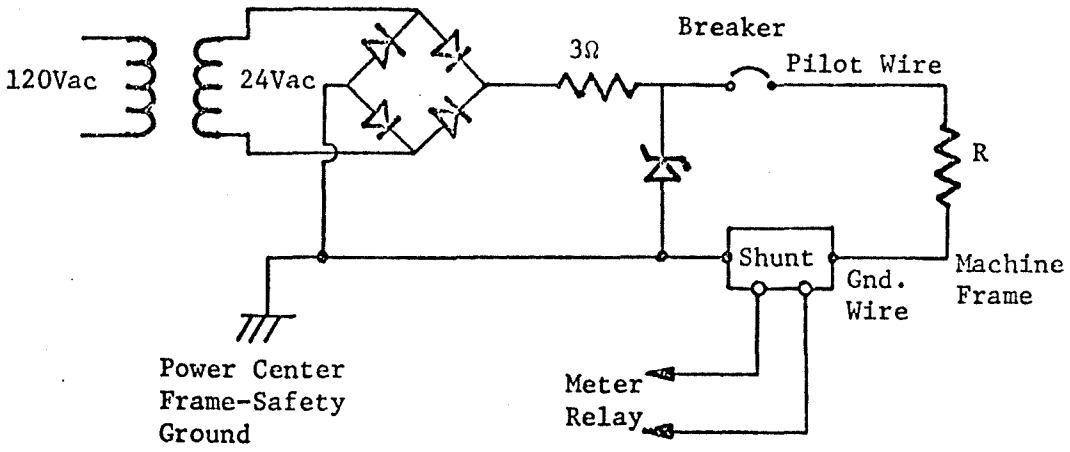


FIGURE 1.6.- Basic circuit diagram CEMSCO Monitor.

tripped in case the stray dc on the ground wire was more than 0.45 A. It did trip on a pilot-to-ground short circuit with a time delay of approximately 15 seconds. The unit performed well when the supply voltage was increased by 10% above the nominal. However, it seems to be sensitive to voltage dips in excess of 10% and showed very uncertain performance. According to the manufacturer this is because the recommended application for an individual length of cable is only 305 m (1000 ft) but not more than 914 m (3000 ft). However, this was not brought out in the instruction booklet supplied to WVU. The monitor is built quite ruggedly and showed no undesirable effects even when operated at 80°C for a few hours.

One of the major problems with the monitor could be the trip relay configurations. The trip relay must be energized to trip, therefore, the circuit is not fail-safe. It seems that a re-organization of this part could easily make the circuit fail-safe, assuming of course, that the meter relay itself is a fail-safe device.

The trip relay took an average of 465 ms to trip when the ground wire was opened.

A surge arrestor is provided across the supply transformer terminals. It broke down for a transient voltage in excess of 2000 V for a pulse width of 40 μs. The insulation between the supply terminals and the case broke down at 2400 V. The ground and the pilot wire terminals successfully withstood a 3000 V transient with respect to the case. However, the terminals going to the meter relay broke down at 2000 V with respect to the case. According to the manufacturer an isolation kit is provided with the monitor so that the frame of the monitor can be isolated from the frame of the substation, thus eliminating the problem of transient breakdown between the frame and terminals of the monitor. However, this isolation kit was not provided to WVU and hence its effectiveness could not be determined.

When the pulse width was increased to 1 ms, almost identical results as above were obtained. Thus there seems to be a need to improve the transient performance of the unit.

### 1.6.3 General Electric Monitor

The GE monitor is basically a dc series loop type monitor using a meter relay for sensing current. The monitoring current is approximately 2.5 A. The basic circuit is given in figure 1.7. The potentiometer (P) is used to adjust the current in the loop. The monitor also uses a 3Ω external resistor connected between ground and the pilot at the machine end. The output is protected by a thyrite and a capacitor connected across pilot-to-ground.

The monitor was set for approximately 1800 m (6000 ft) of 4/0 cable. This is equivalent to about 0.5Ω ground wire resistance and 4.0Ω of pilot wire resistance. The current sensitivity was set at ±0.5 A as suggested by the manufacturer to avoid nuisance tripping. During testing it was found that the correct adjustment of the potentiometer (P) was very important for sensitive monitor performance. In fact, for a high value of resistance (around 7Ω) the monitor failed to trip for a pilot-to-ground short circuit.

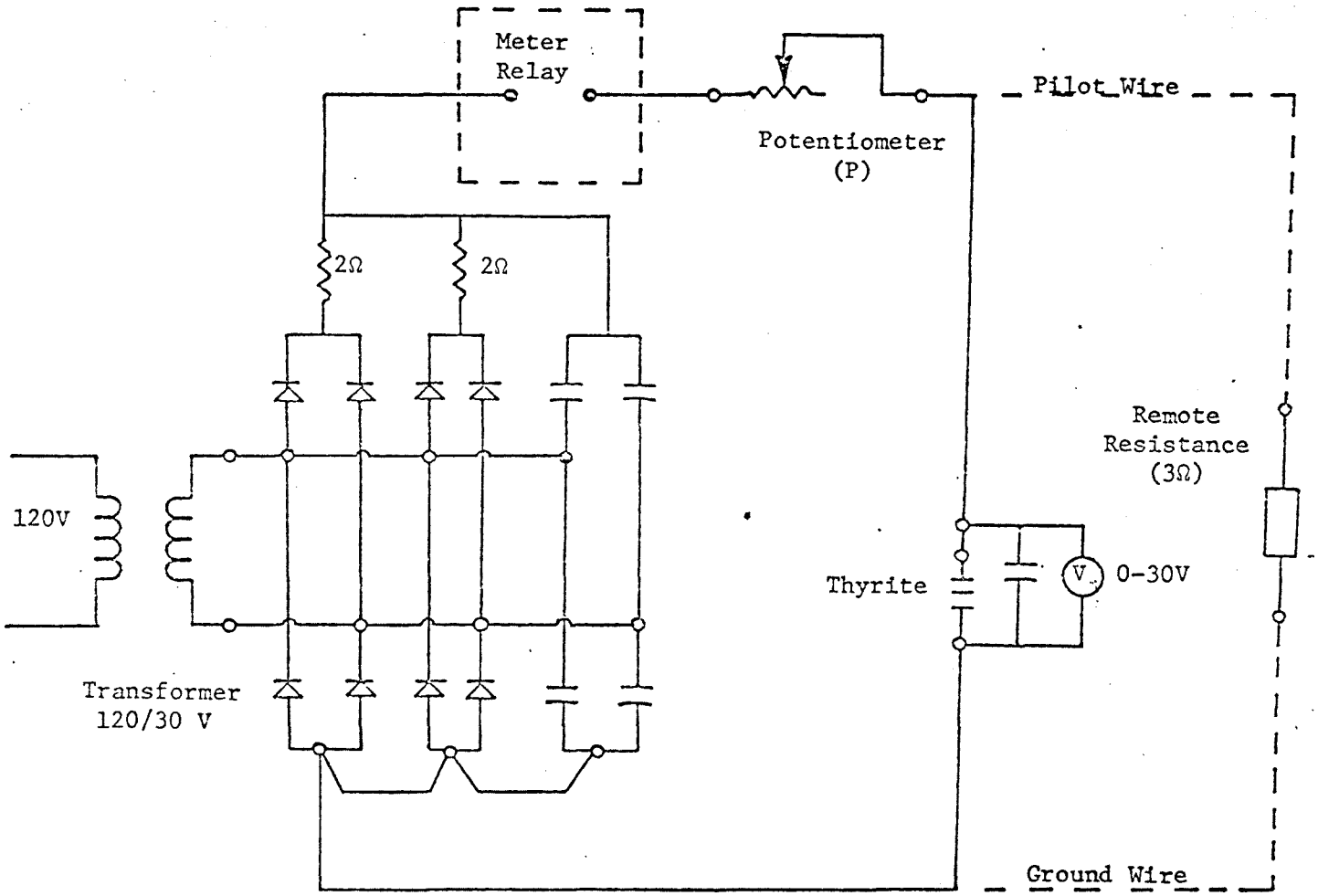


FIGURE 1.7. - Basic connection diagram of the GE Monitor.

For this test sequence the potentiometer was adjusted around 2Ω, which gave better sensitivity.

The monitor was also quite sensitive to changes in the ground and pilot wire resistances and tripped under a pilot-to-ground short circuit. Stray ac currents flowing in the ground wire (up to 2.5 A) did not have any ill effect on the performance. The monitor does not have the ability to detect parallel paths. It also seems quite sensitive to dips in the supply voltage. The monitor did not perform satisfactorily for dips in excess of 10%. The monitor was left in an environmental chamber at 65°C and showed no undesirable effects. However, when the temperature was increased to 80°C the reset knob of the monitor failed to function.

The input transformer terminals broke down for a transient voltage of 1900 V and 40 μs duration. The ground wire terminal to frame broke down at 2875 V. The supply terminals and the pilot wire terminal successfully withstood transients up to 3000 V with respect to the frame. Similar performance was obtained when the pulse width was increased to 1 ms.

### 1.6.4 AMF Potter-Brumfield Monitor

The connection diagram for the monitor is given in figure 1.8. The monitor has ratio and phase detectors which constantly measure the magnitude and phase of the impedance seen by the monitor. The monitor has a complex logic built into it by which it can differentiate between different kinds of faults as well as give a fair idea on the approximate location of the fault. The circuit also seems to have some redundancy built into it. The blocking impedance $Z_B$ is made up of the same size wire as the ground wire and prevents the signal from going through the machine frame into the ground.

According to the manufacturer each monitor is capable of monitoring only one section of a feeder cable. The printed circuit cards containing the monitoring circuitry are fabricated for different cable lengths (to be specified by the user) and hence need no adjustment in the field. This has its advantages and disadvantages. Since the monitor requires minimum adjustment in the field, it is likely to be free from installation errors due to unskilled personnel not familiar with monitor operation. However, a feeder cable feeding portable equipment is made up of many sections. Hence just to monitor one complete length of the cable one would require many monitors. Also, one has to be very careful to use the exact length of cable specified for the monitor. If the length of cable used is more than specified the monitor will become more sensitive and liable to cause nuisance tripping. On the other hand, if smaller length is used, the monitor may not trip for the set change in ground wire resistance. The tolerance of the monitor to these variations of cable length would of course depend on cable size used and other manufacturing tolerances.

The blocking impedance mounted at the machine is used to prevent parallel paths. However, this impedance itself is not monitored. If a break or a loose connection should occur within this impedance, one may lose the ground at the machine, but the monitor will still show a safe condition. However, the probability of such an occurrence is remote. In a revised design the

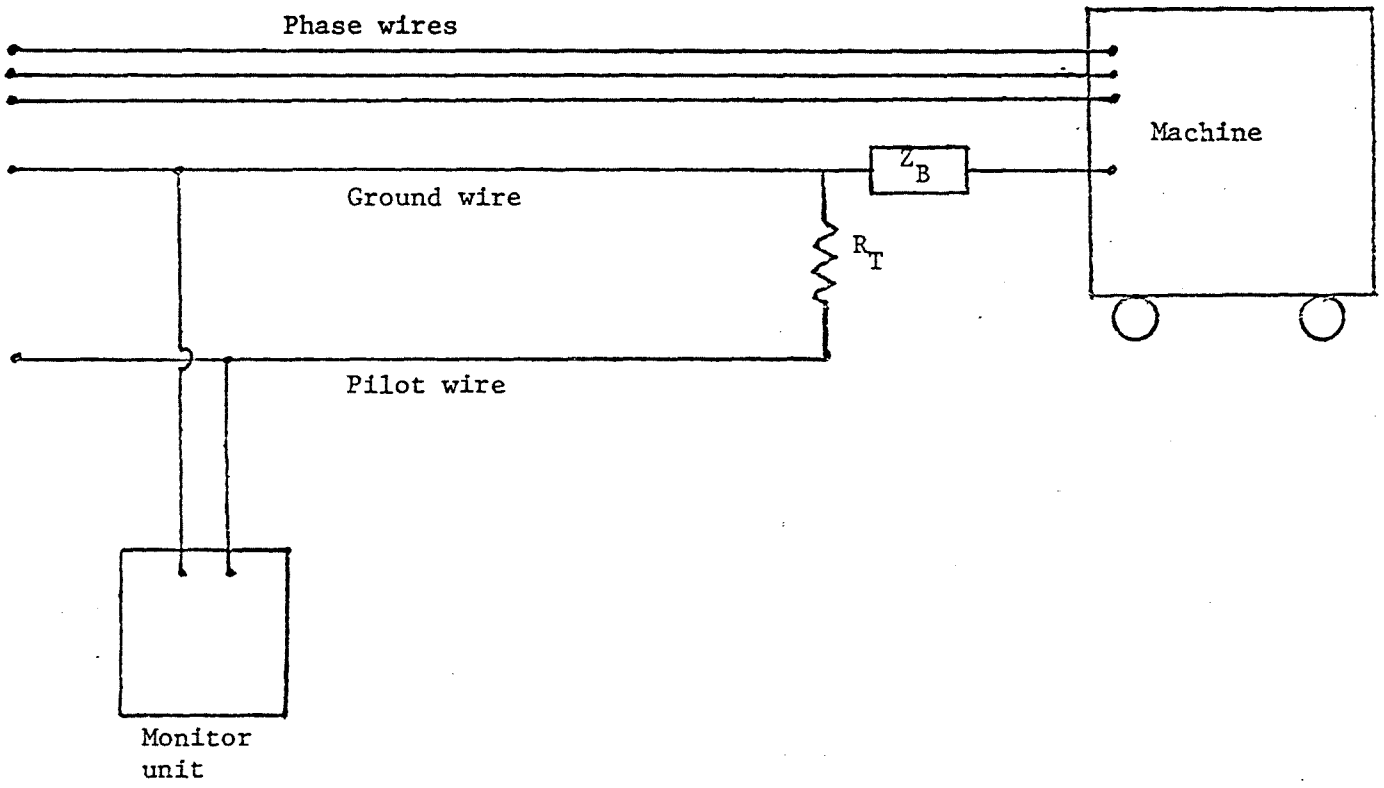


FIGURE 1.8. - Connection diagram for the AMF monitor.

blocking impedance is connected in series with the ground wire before the connection to the monitor. The only advantage gained by this modification is that the impedance can be mounted alongside the monitor where it can often be inspected.

The monitor showed excellent performance in detecting resistance changes in the pilot and the ground wires. It also tripped satisfactorily on a pilot-to-ground short circuit. Stray ac and dc on the ground wire (up to 2.5 A) seemingly did not have any effect in the performance characteristics. The monitor seemed to be immune to supply voltage variations. Satisfactory performance was obtained for the supply voltage variations of -40% to +15% of the nominal.

The monitor is equipped with flags to indicate the type of fault; that is a ground-wire break, pilot-to-ground short circuit, etc. According to the manufacturer, a combination of these flags would indicate whether the fault occurred in the cable close to the monitor unit or near the end of the cable. However, this facility did not function properly, and has been eliminated in a modified version of the monitor.

The monitor tripped on small increases in the line inductance. There is a possibility of a change in the cable inductance due to spooling or unspooling. However, since no experimental data is available in this respect, no conclusions can be derived.

All the above tests were carried out on an older version. The transient tests enumerated below were carried out on a modified version sent by the manufacturer.

When a transient voltage of 2000 V (40 μs width) was impressed across the supply terminals, a breakdown occurred. Similiarly the insulation between the supply terminals and the frame broke down at 2700 V. Breakdown also occurred when the pilot wire and ground wire terminals were subjected to a transient voltage of 2300 V with respect to the frame of the monitor. Similar performance was obtained when the pulse width was increased to 1 ms. Thus, the transient performance of the unit needs to be improved.

### 1.6.5 American Mine Research Monitor

This is a continuity-type rather than an impedance-type monitor. It is designed to trip when there is a break in the ground wire or when the impedance in the pilot-to-ground loop exceeds 75 ohms.

The connection diagram is shown in figure 1.9. The transmitter is directly coupled to the monitoring loop and injects a signal of approximately 4150 Hz into it. The return signal is picked up by a current transformer on the ground wire and is passed on to a receiver. If the signal strength falls below a threshold level (due to an increase in the impedance) the receiver sends a trip signal to the tripping relay.

The transmitter is connected to the loop through a coupling filter. The filter is made up in two parts; one consists of a series capacitor and an

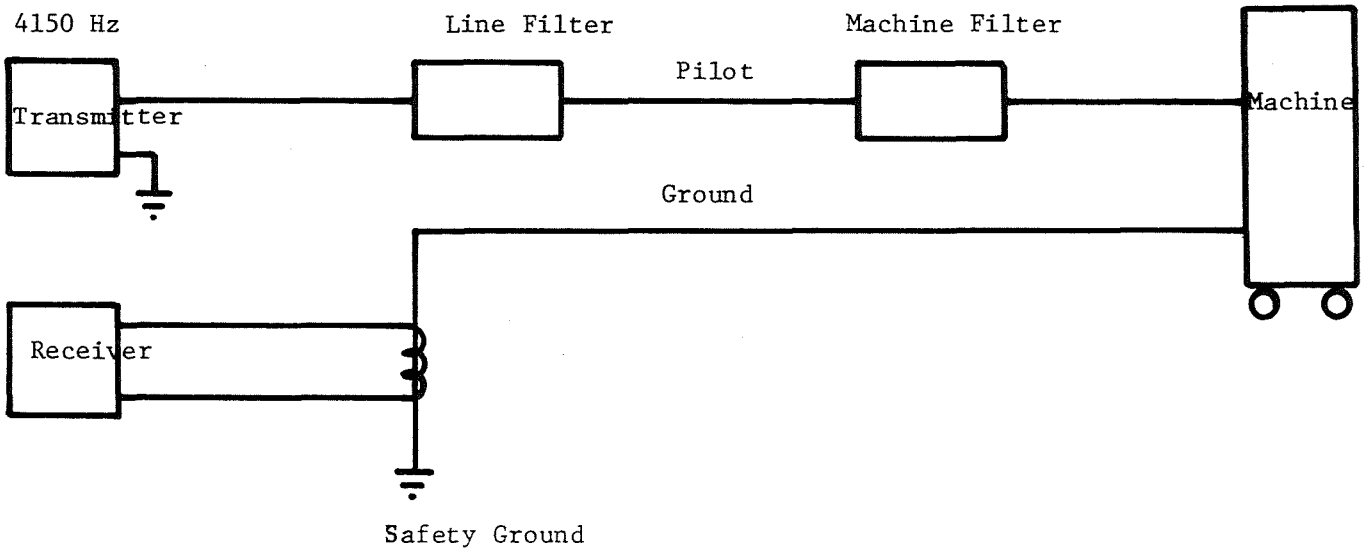


FIGURE 1.9. - Connection diagram for the American Mine Research Monitor.

inductor connected in series with the pilot wire at the monitoring end, and the other consists of a single inductor at the machine end. When used in series, these two form a tuned band-pass filter at about 4150 Hz. In case a pilot-to-ground short circuit occurs anywhere in the cable before the filter at the machine, the filter is detuned. This reduces signal current flow which is detected by the receiver.

The voltage in the monitoring loop was about 14.2 V. The monitor satisfactorily detected a break in the ground wire as well as a pilot-to-ground short circuit. Stray ac and dc currents up to 5 A had no effect on the performance. The monitor has the ability to operate in presence of low-resistance parallel paths because the signal is picked off a CT in the ground wire. However, very low-resistance parallel paths could cause nuisance tripping because the return signal would be shunted through this path rather than through the groundwire.

Supply voltage variations from -40% to +10% of the nominal had no undue effect on the performance.

The monitor trip relay took approximately 420 ms to operate after the ground wire was opened. It took an average of 295 ms to operate when the power supply for the monitor was cut off.

The power supply terminals have a surge suppressor connected across them to clamp the voltage down to a safe value in case of a high-voltage transient. The supply terminals successfully withstood a 1000 V transient (40 μs pulse width), but the surge suppressor broke down when the voltage was increased to approximately 1920 V. The supply terminals to the frame of the monitor safely withstood surges up to 3000 V. The transmitter ground terminal to frame successfully withstood 2000 V transients, but when a transient voltage of 2700 V was applied internal flash-over occurred. Similarly the transmitter in-out terminal broke down at approximately 3000 V. Fairly similar performance was obtained for a pulse width of 1 ms.

Overall, the monitor performed quite satisfactorily except that the transient performance needs to be improved using high-power surge suppressors.

### 1.6.6 Line Power Monitor P/N 170061

The connection diagram for this monitor is shown in figure 1.10. It is essentially a dc monitor using a Westinghouse type SC current relay for sensing the pilot-to-ground loop current as well as performing the function of tripping. The relay is normally energized and trips if the current through the relay falls below the set point. The normal operating current is approximately 1.5 A and the open circuit voltage in the monitoring loop is approximately 34 V. The monitor also uses a 6Ω resistor connected between the pilot and the ground at the machine.

The trip setting for the relay can be set by adjusting a screw at the base of the relay which must be set in the field depending upon the cable impedance to be monitored. In case the current in the monitoring loop increases due to a pilot-to-ground short circuit, the thyristor (marked SCR in figure 1.10) fires, thereby short circuiting the current relay.

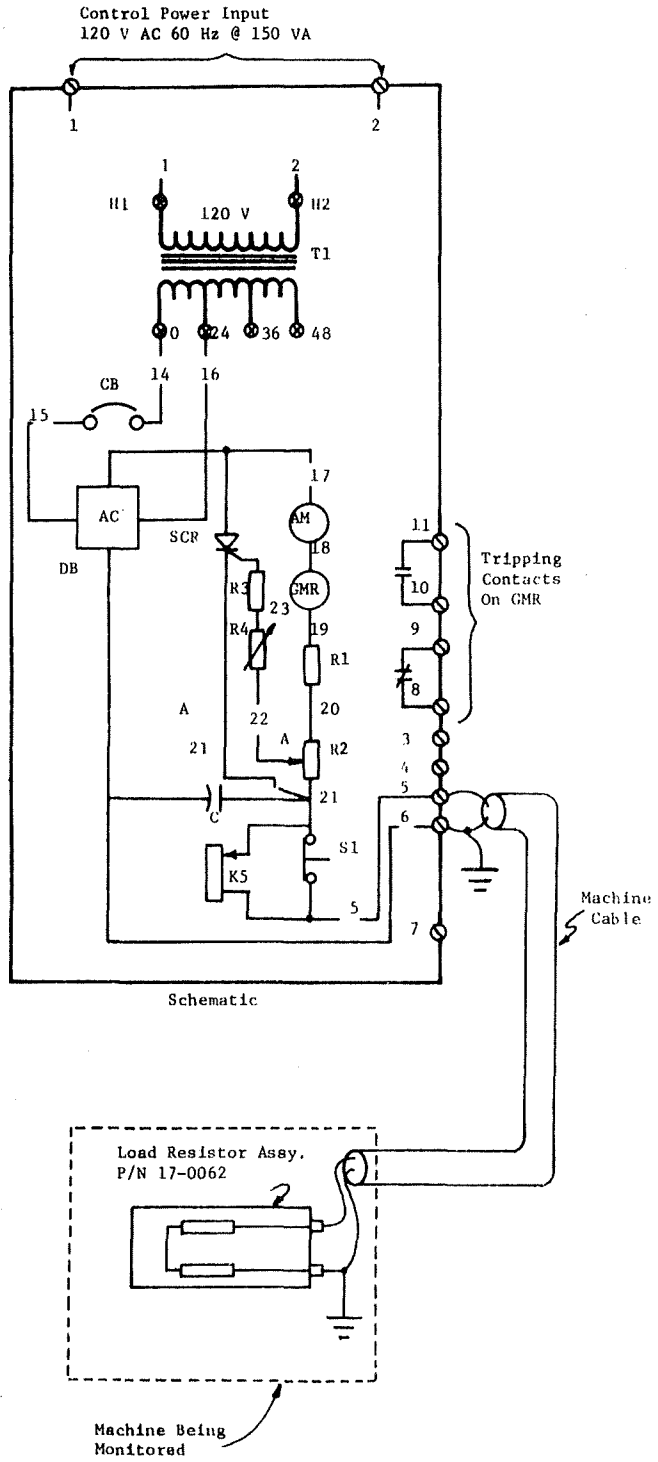


| Sym | Description |
|---|---|
| T1 | Transformer |
| R1 | Resistor 20 Ohm, 100 W |
| R2 | Resistor 2 Ohm, 100 W, Ad |
| R3 | Resistor 220 Ohm, 1 W |
| R4 | Potentiometer 1000 OHM, |
| R5 | Resistor 75 Ohm, 25 W, A |
| TB | Terminal Block |
| C | Capacitor |
| AM | Ammeter |
| DB | Rectifier Bridge |
| SCR | SCR |
| GMR | Relay Type SC |
| S1 | Push Button |
| S1 | Contact Block |
| CB | Circuit Breaker |

FIGURE 1.10. - Schematic diagram for Line Power Monitor P/N 17-0061.

The current through the relay decreases and thus trips it. The voltage at which the SCR fires can be set by varying resistors $R_4$ and $R_2$.

The monitor was very sensitive to increases in the ground and pilot wire resistance and tripped for any abnormal change (greater than 4 ohms). The monitor was also extremely sensitive to decreases in pilot wire resistance and tripped when the pilot wire resistance was decreased by 0.5Ω. Stray ac in the ground wire had no effect on the performance. However, the monitor was quite sensitive to dc strays and tripped when the stray current level exceeded 0.9 A. The monitor was also very sensitive to increases in the supply voltage; it tripped when the supply voltage was increased by just a few volts. It also tripped when the supply voltage was decreased below 102 V. The monitor does not have the ability to operate if the ground wire is opened in the presence of a low-resistance parallel path.

The current relay has a very fast operating time and took only 22 ms to operate after the ground wire was opened. It took approximately the same time after the power supply to the monitor was interrupted.

The main drawback of this monitor lies in the design of the operating relay. During normal operation the relay is energized and there is a flag to indicate this state. However, when the relay trips, the flag remains in this state and the operator has no visual indication of the tripping of the monitor. The only way one can find out is by looking at the position of the contacts through the window, which is not an easy task.

High-voltage transient testing could not be performed between the supply voltage terminals because the pulse waveform was quite distorted, presumably due to transformer inductance. The supply terminals-to-case successfully withstood surges up to 3000 V (40 μs width). The pilot-to-case withstood 2000 V but broke down at 2300 V. Similarly the ground-to-case withstood 2000 V but broke down at 2200 V. When the pulse width was increased to 1 ms the breakdown levels for the pilot and the ground terminals were reduced to 2000 V and 1950 V, respectively. The rest of the results remained unchanged.

### 1.6.7 Line Power Monitor P/N 170013

The connection diagram for this monitor is shown in figure 1.11. It is an ac impedance-type monitor. It also uses an Westinghouse SC current relay as a sensing and tripping element. The normal operating current is approximately 3.5 A and the voltage in the monitoring loop is 24 V.

Series capacitors prevent any stray dc from entering the monitoring loop. The toggle switch, S, reverses the phase of the current flowing in the loop and is used if trouble is experienced with stray ac currents. However, this does not seem to be a very effective solution. The pilot and the ground wire are solidly connected at the machine. Hence, the monitor is not capable of detecting pilot-to-ground short circuits. Also the monitor is not capable of operating if the ground wire is opened in the presence of a low-resistance parallel path.

The monitor was quite sensitive to increases in resistance in the pilot-to-ground loop and tripped for any resistance change greater than 4 ohms.

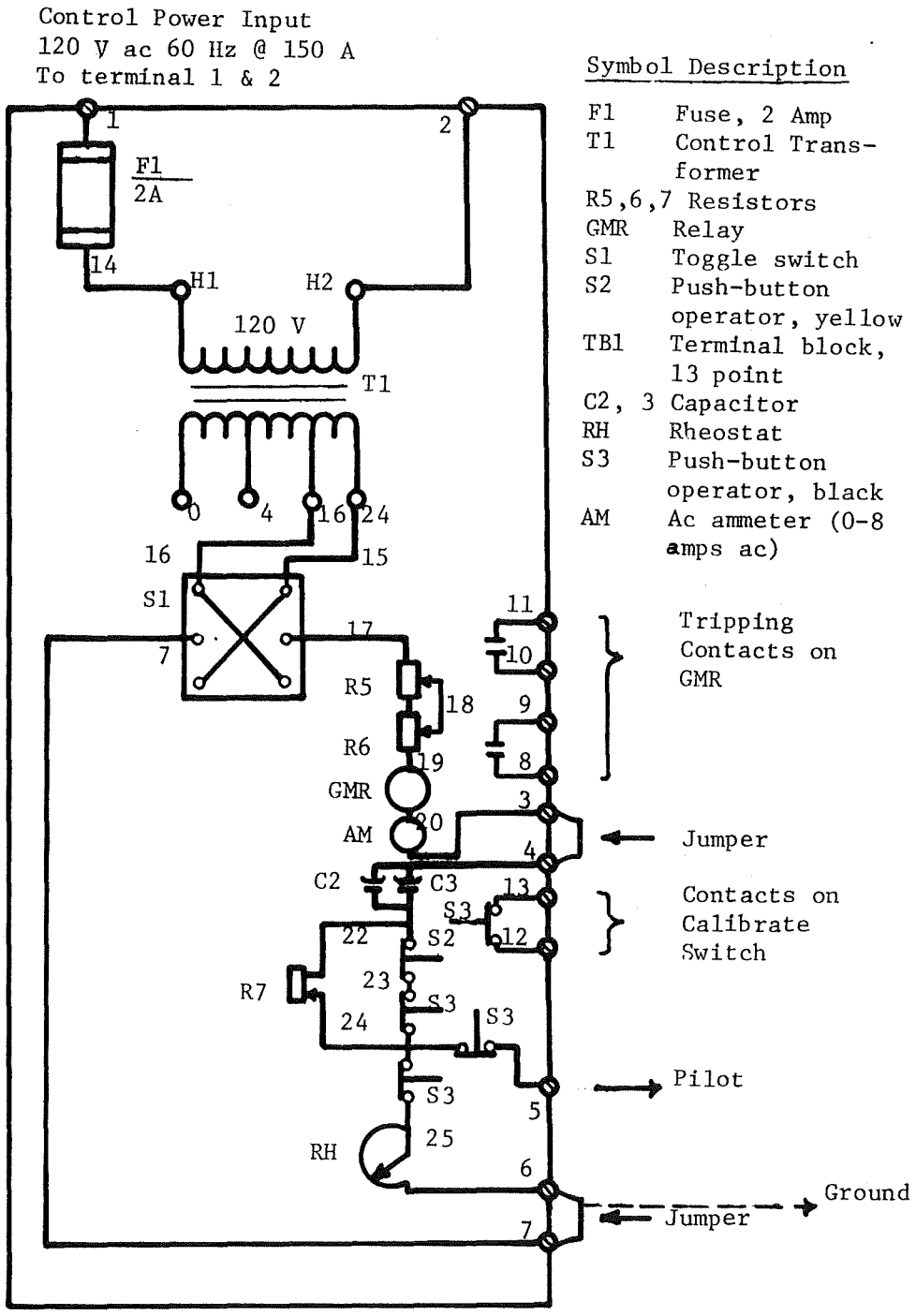


FIGURE 1.11. - Connection diagram for line power P/N 170013 Monitor.

Stray dc had no effect on the performance. Stray ac currents in the ground wire in excess of 6 A did trip the monitor. However, this could be a misleading figure because the trip level would be dependent on the phase relationship between the monitoring current and the stray current. An increase in the supply voltage by 10% had no undesirable effect, but when the voltage was decreased by more than 27% of the nominal value, it tripped.

The monitor took approximately 20 ms to trip after the ground wire was opened. It also took the same time to operate when the power supply to the monitor was cut off.

The supply terminals safely withstood surges up to 3000 V (40 μs width). Also the supply terminals-to-case, and ground terminal-to-case withstood surges up to 3000 V successfully. The same performance was obtained when the pulse width was increased to 1 ms. The supply terminals could not be tested because the pulse was completely deformed.

Thus the transient performance of this unit is satisfactory compared to the other monitors tested. The biggest disadvantage with this monitor (as with the dc model) is the current relay.

### 1.6.8 Consolidation Coal Company Monitor

This device is a homemade unit designed to operate at 1000 Hz. The connection diagram is shown in figure 1.12. The monitor has two subassemblies. One is a 1000 Hz, 2 A power supply. The other consists of the meter relay, auto-transformer, blocking capacitor, surge suppressors, etc. Only this portion of the monitor was supplied to WVU. The 1000 Hz power supply was obtained through a signal generator and a power amplifier.

The normal suggested operating current is 1 A. It was found that to detect a 4 ohm increase in the impedance of the circuit, the meter relay had to be adjusted to a sensitivity of ±0.25 A. Stray ac and dc currents up to 5 A had no undue effect on the performance. The monitor does not have the ability to detect a pilot-to-ground short circuit. This could be easily achieved by connecting a resistor between the pilot and ground at the machine end. The monitor also does not have the ability to operate if the ground wire is opened in the presence of a low-resistance parallel path.

However, the heart of the monitor is the 1000 Hz power supply. Since this was not provided to WVU, the test results are incomplete.

### 1.6.9 Ensign Electric Monitor

This device is an audio frequency monitor and can be used both in continuity-type and impedance-type applications.

To be used as a continuity-type monitor, it is connected as shown in figure 1.13. A transmitter couples a 2650 Hz signal to the monitoring loop through a current transformer. The signal returns through the resonant filter and is coupled to the receiver through a current transformer. Hence the monitor is completely isolated from the ground and the pilot wire terminals.

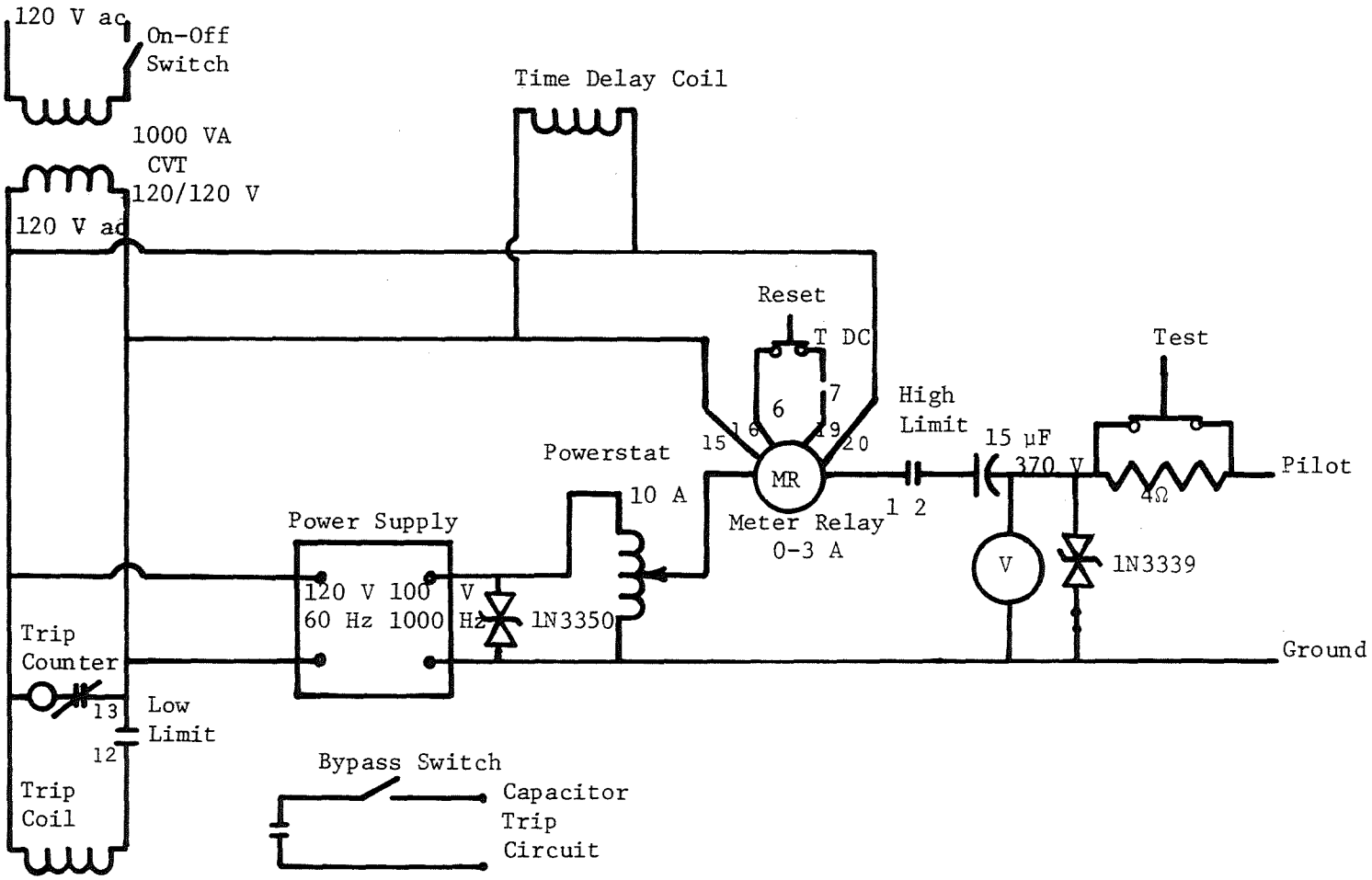


FIGURE 1.12. - Connection diagram for the CONSOL Monitor.

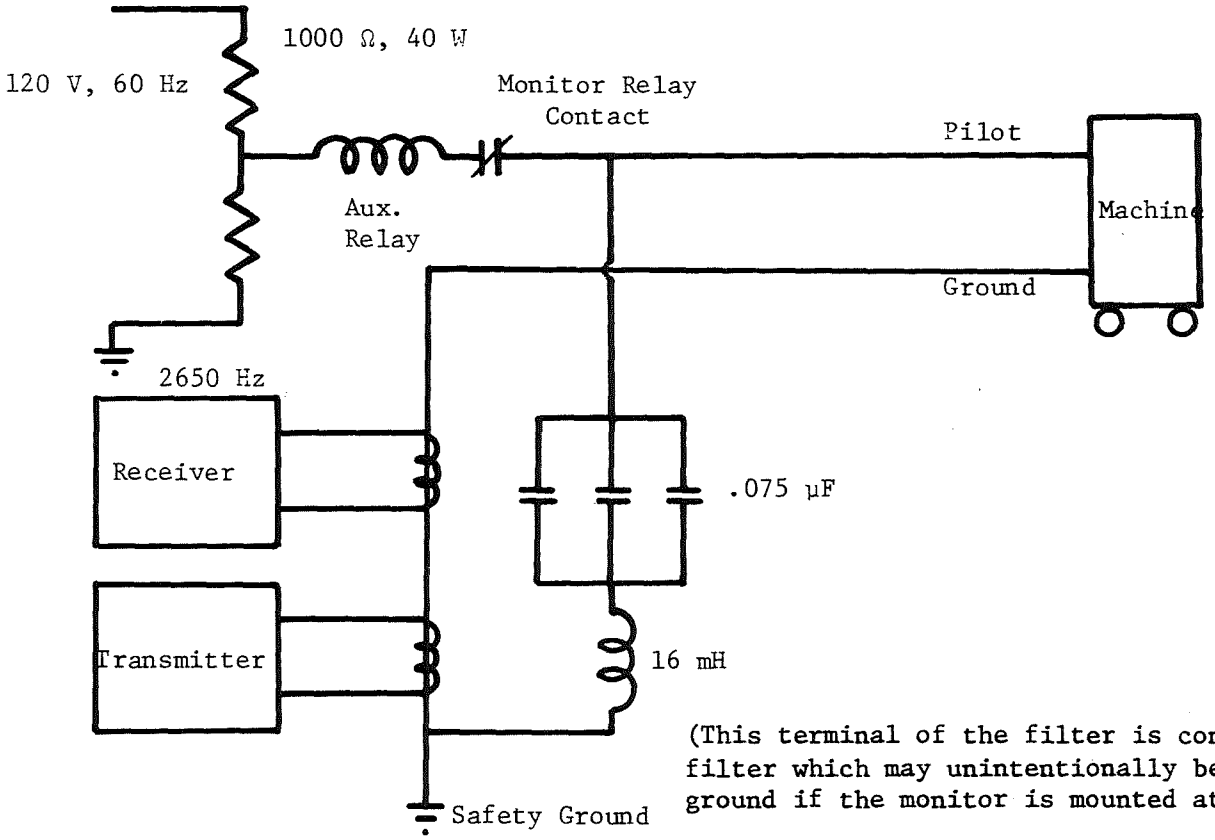


FIGURE 1.13. - Ensign Monitor used as a continuity monitor.

The transmitter is tuned to trip the monitor relay if the pilot-to-ground resistance exceeds 75 ohms. The auxiliary relay is connected to detect an open circuit in the pilot wire. Normally the monitor relay contact is closed and the auxiliary relay is energized through a voltage divider circuit. When the pilot wire is open the auxiliary relay loses the voltage, thus initiates tripping of the circuit breaker.

The voltage divider consists of two 1000 Ω, 40 W resistors and is connected so that the voltage on the pilot wire does not exceed 60 volts. However, should one of the resistors fail open, the pilot wire could be elevated to the full 120 volts which can be a dangerous situation.

As can be seen in figure 1.13 one of the terminals of the filter is connected to the safety ground. This terminal is also connected solidly to the case of the filter which in turn is mounted on the frame of the substation. Normally a surface substation frame is connected to the station ground, which according to CFR77.801-2 must be isolated from the safety ground by at least 7.6 m (25 ft). Hence, once the monitor is mounted on the substation, the two grounds are connected together.

When used as a continuity monitor, it does drop out for a resistance in excess of 75 ohms as claimed by the manufacturer. Stray dc and ac currents up to 5 A have no undue effect on the performance of the monitor. In this configuration, the monitor does not have the ability to detect a pilot-to-ground short circuit nor can it operate if the ground wire is opened in the presence of a low-resistance parallel path.

The monitor took approximately 240 ms to operate after the ground wire was opened. It also took an average of 116 ms to operate after the power supply to the monitor was cut off.

Large power supply variations had little effect on the performance of the monitor. It worked satisfactorily when the supply voltage was varied by -50% to +10% of the nominal value.

When used for impedance-type applications, the monitor is connected as shown in figure 1.14. The pilot and ground wire are short-circuited at the monitoring end, thus forming a loop. However, at machine starting large voltages can be induced between the pilot and ground (≃ 100 V). This large voltage can cause tremendous circulating currents since the current is only limited by the total impedance of the pilot and ground wires, which is quite small. This is bound to cause monitoring problems. The current can be limited by putting a series resistor at the monitoring end. However, in this case the monitor will have to be adjusted to drop out at a higher value of impedance.

In this configuration, the monitor is quite sensitive to a change in impedance in the monitoring loop and tripped when the impedance in the ground wire was increased beyond 4 ohms. It was immune to ac and dc stray currents to 10 A. It also performed satisfactorily when the supply voltage was varied by -50% to +10% of the nominal. The monitor took an average of 223 ms to trip after the ground wire was opened. It took approximately 110 ms to trip after the power supply to the monitor was cut off.

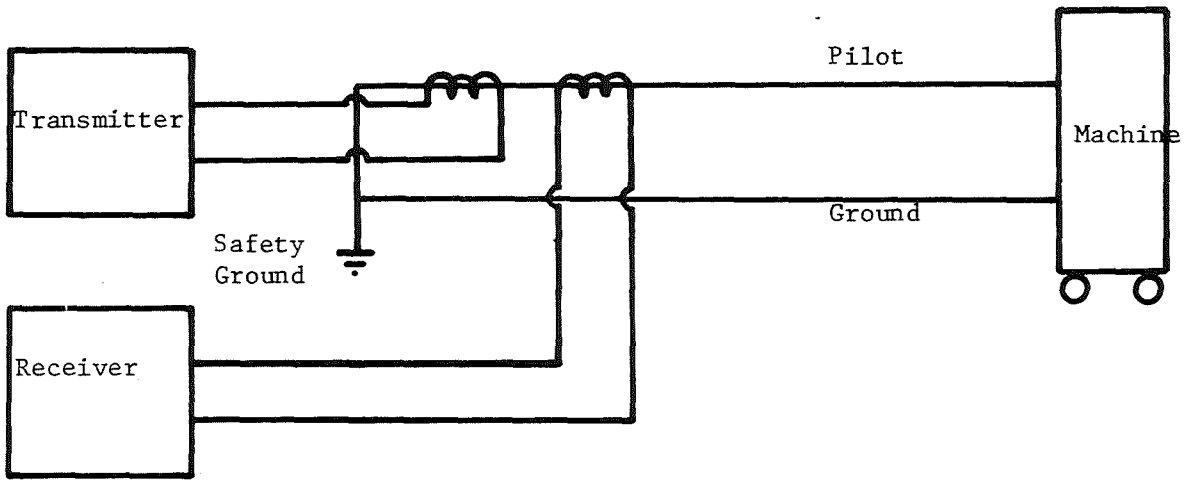


FIGURE 1.14. - Ensign Monitor used as an impedance monitor.

The monitor in this case also does not have the ability to detect a pilot-to-ground short circuit. It also fails to operate in case the ground wire is broken in the presence of a low-resistance parallel path. This problem could be solved to some extent if the transmitter signal were coupled to the ground wire instead of the pilot. The received CT would still be on the pilot wire.

Since the ground and pilot wires are not coupled to the terminals of the monitor, it provides excellent immunity against high-voltage transients appearing on the pilot and the ground wire. The only path through which the transients could be coupled to the monitor is through the supply voltage terminals. These terminals are protected by a surge suppressor but the protection was not found to be totally adequate. It did withstand a transient of 1000 V (40 μs pulse width) but broke down when the voltage was increased to 1920 V. It broke down at approximately the same voltage when the pulse width was increased to 1 ms.

The filter, when tested separately, showed resonance at approximately 2550 Hz. At this stage the current through the filter was approximately 21 mA, while the voltage drop was 0.2 V. This corresponded to an impedance of approximately 10 Ω. It was also found that the current was rich in harmonics, probably due to saturation in the inductor. The filter design could perhaps be improved by using larger value capacitors and a smaller inductor.

### 1.6.10 FEMCO Ground Sentinel II Monitor

The connection diagram for the FEMCO monitor is shown in figure 1.15. The monitoring signal is approximately 4 kHz and the circuit has to be tuned in the field depending on the length of the cable being monitored. Also the sensitivity of the monitor to detect resistance changes has to be adjusted in the field. Hence it is imperative that the installation of the monitor in the field be carried out by persons who are quite familiar with the monitor operation.

The monitor showed satisfactory performance in detecting changes in the resistance of pilot and ground wires and pilot-to-ground short circuits. It showed immunity to stray ac and dc (around 2.5 A) and the tripping point did not change considerably. Variations in the supply voltage seemingly had no effect in the performance characteristics. Excellent performance was obtained when the supply voltage was varied from -40% to +15% of the nominal value.

The arc trap in series with ground wire serves the purpose of eliminating parallel paths. However, the arc trap by itself is not monitored and if any break in connection occurs, the monitor fails to indicate an unsafe condition.

There are two LED's to indicate monitor tripping. One of them goes off when the abnormal condition which caused the monitor to trip is removed. The other stays on till the monitor is reset. However, there is no indication as to the mode of monitor trip, that is whether the tripping was caused by an open ground or pilot-to-ground short, etc.

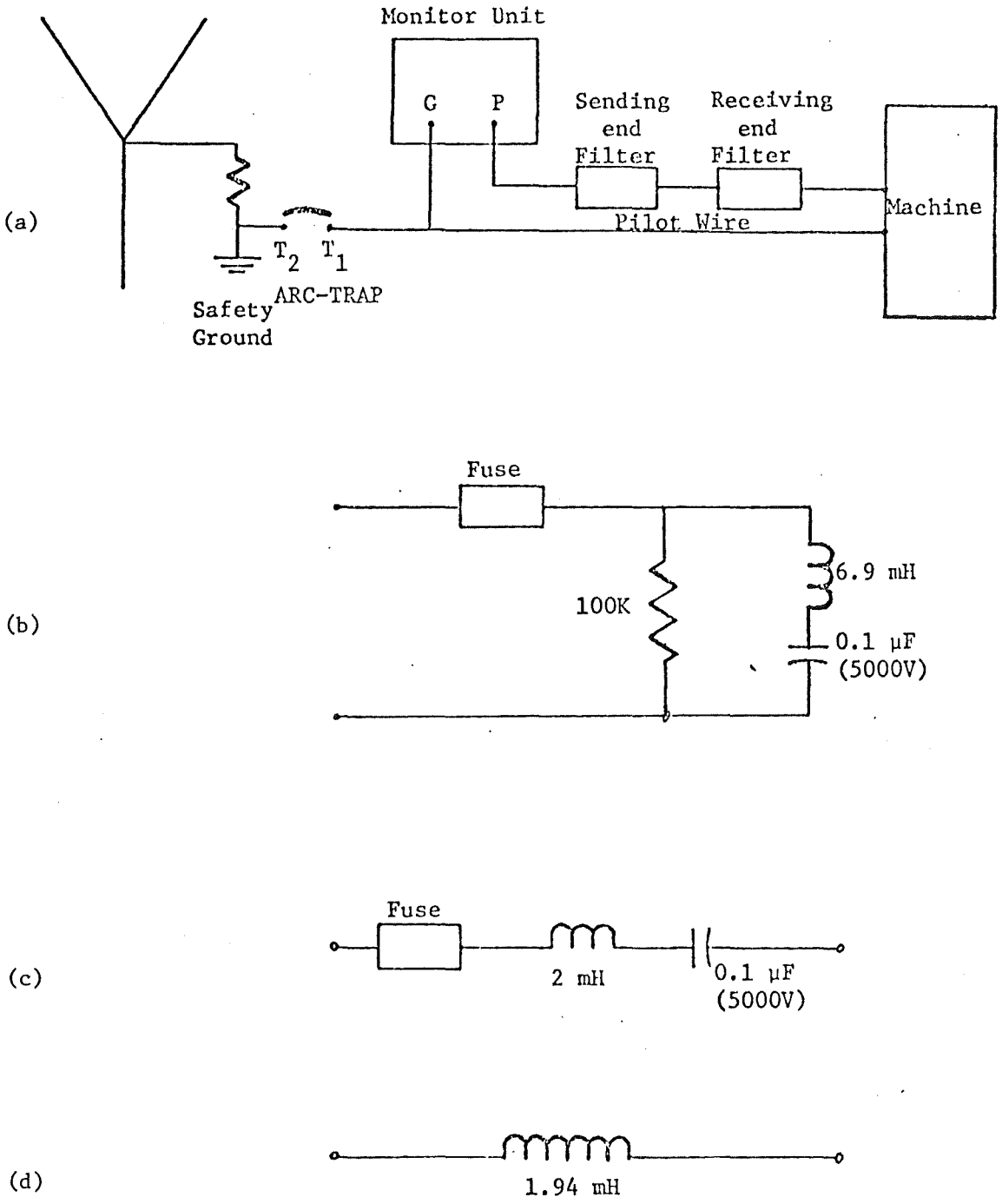


FIGURE 1.15. - FEMCO high-voltage ground-wire monitor. (a) Connection diagram; (b) Receiving end filter; (c) Sending and filter; (d) Arc-trap.

When the line inductance was increased by 1 mH (to simulate a long cable) a noticeable decrease in the sensitivity of the monitor was observed. In some instances the LED's indicating the tripping condition operated before the output relay had operated. This indicated that the monitor may have problems in monitoring very long lengths of cable. Also at higher lengths (and higher operating frequencies as the one used by the monitor) the cable can no longer be modeled as a lumped element and transmission line effects are to be taken into account. However, this is a subject of future investigation by WVU and any inferences at this stage may be rather premature.

The tripping relay took an average of 170 ms to operate when the ground wire was opened. When the supply power was shut off it took approximately 229 ms to trip.

At the time the high-voltage transient testing program was initiated, the monitor was not available for testing; hence no results could be obtained.

## 1.7 OVERALL CONCLUSIONS

Test results from ten of the commercially available ground wire monitors have been presented. Out of the ten monitors tested, four were dc, five audio-frequency, and one ac. Thus the manufacturers seem to be equally divided in their preference for the dc or audio-frequency option.

Of all the monitors tested, the primary weakness was found to be in the high-voltage transient performance. This could be substantially improved by employing high-power surge protection.

Two of the monitors operating around 4000 Hz (FEMCO and AMR) could have problems in monitoring long cable lengths (>1500 m, or 5000 ft) due to transmission line effects. However, this is an area of further research at WVU and any conclusions at this stage are rather premature.

# CHAPTER 2

# LOW-VOLTAGE GROUND-CHECK MONITORS

## 2.1 EVALUATION OF COMMERCIALLY AVAILABLE MONITORS

A program of evaluation and testing of low-voltage ground-check monitors was begun in 1972 as part of U. S. Bureau of Mines Grant G0122088. It was continued under Grant G0144137, and then transferred to Grant G0144138. Detailed information on the evaluation program and test results are given in references.

A total of 12 commercial monitors were evaluated during this program.* These monitors were developed by the following companies:

1) Eltron Corporation
2) Environmental Electronics Engineering, Inc.
3) Joy Manufacturing Co.
4) Ohio Brass Co.
5) Femco
6) Ensign Electric Division, Harvey Hubbell, Inc.
7) General Electric Co.
8) Control Products Corp.
9) Westinghouse
10) Continental Conveyor Corp.

Several other monitors were also evaluated, including one model developed at the Pittsburgh Safety and Mining Research Center and two developed at West Virginia University.

Seven monitors were evaluated during 1973-74, and the results of these evaluations are included in an annual report under Grant G0122088 (60). None of these monitors appeared to work in a completely satisfactory manner. Several of them worked moderately well in the laboratory, but field tests conducted by USBM-MSHA revealed an exceedingly high level of false trips and other problems. WVU then set up some criteria for monitor operation to be used as design goals. These were also included in the G0122088 Annual Report (60).

Six additional monitors were evaluated during the following two years, including revised units by EEEI and Femco. Most of these monitors worked considerably better than previously tested models, and the second-generation EEEI and Femco monitors had generally good-to-excellent capabilities. Although not tested by WVU, a second-generation Eltron monitor was built incorporating many of the WVU suggestions for circuit modifications. Monitors by these three manufacturers became some of the very first to win MSHA approval for use on low-voltage trailing cables. Test results on these monitors can be found in reports covering grant G0144138 (56,58).

No detailed evaluations of low-voltage monitors were carried out within the last two years of the grant. The research teams continued to act as a resource to the Bureau of Mines, MSHA, and manufacturers concerning monitor characteristics and requirements. MSHA's approval program operated successfully, and by now there are some 20 monitors approved for use, with several

---

*Reference to specific brands, equipment, or trade names in this report is made to facilitate understanding and does not imply endorsement by the Bureau of Mines.

more still being evaluated. Although perfection can never be achieved, the monitoring problem has been essentially solved by the combined efforts of manufacturers and the Federal government through MSHA and research supported by the Bureau of Mines. Further work in this area now centers on certain difficult monitoring situations for which effective solutions do not yet exist.

## 2.2 MODULAR MONITOR

Work on the modular monitor was initiated under USBM contract no. G0122088 and is described in the final report for that contract (60). The modular monitor was conceived as a method of selecting a monitor which, by simple substitution, would work in a particular location. At that time it was not apparent that any one ground check monitor could effectively monitor more than a few situations that normally arise.

Because of the considerable difference in approaches by the various manufacturers of monitors, and in ground circuit conditions, it was expected that several types of monitors would be required in order to monitor all conditions. Thus, the modular monitor was considered as one way of insuring that a satisfactory ground check monitor could be installed in any location without considerable knowledge of the ground circuit conditions or monitor types. By the simple expedient of substituting various modules, a technician could quickly arrive at a satisfactory ground check monitor.

In addition to the modular monitor, a systematic study was undertaken in order to further understand the relationships between monitor configurations and ground circuit conditions. It was anticipated that other monitor configurations might be discovered which would be useful under a greater variety of conditions or perhaps even monitor all conditions. A complete discussion is given in section 2.3.

### 2.2.1 Modular Monitor Main Frame

The modular monitor was designed so that the monitoring configuration could easily be changed. Thus, the basic monitor chassis contains only a power transformer, a fuse, and a switch as permanently attached components. All other components or modules are plugged into sockets. The general configuration is shown in figure 2.1. The simplest monitor would only require one monitor module and a relay, whereas more sophisticated monitors would require more modules. In one case, three monitor cards are required along with both power cards and a relay. The status indicator card is intended to be a diagnostic aid during field testing and practical use.

Connections to the power system are shown in figure 2.2. In addition to the main frame, several external components may be required. It should be noted that not all are required at any one time. The monitor configuration will determine which are required.

All pilot-type monitors were designed to use a machine mounted resistor of 50 ohms between the pilot and ground. This resistor was to be used for detecting pilot-to-ground wire shorts. Although detection of pilot-to-ground shorts is not required by MSHA, it is considered desirable.

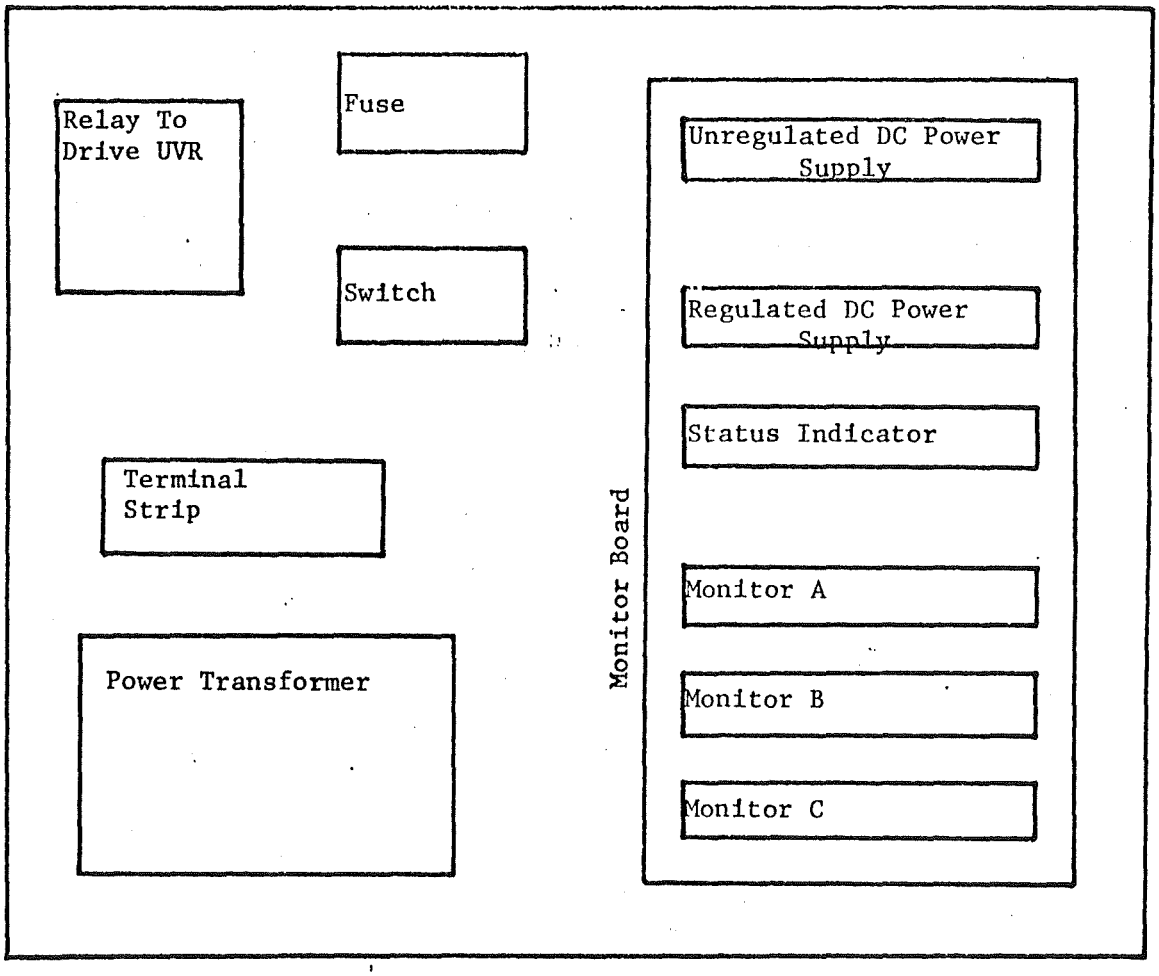


FIGURE 2.1. - Physical layout of the Modular Monitor main frame.

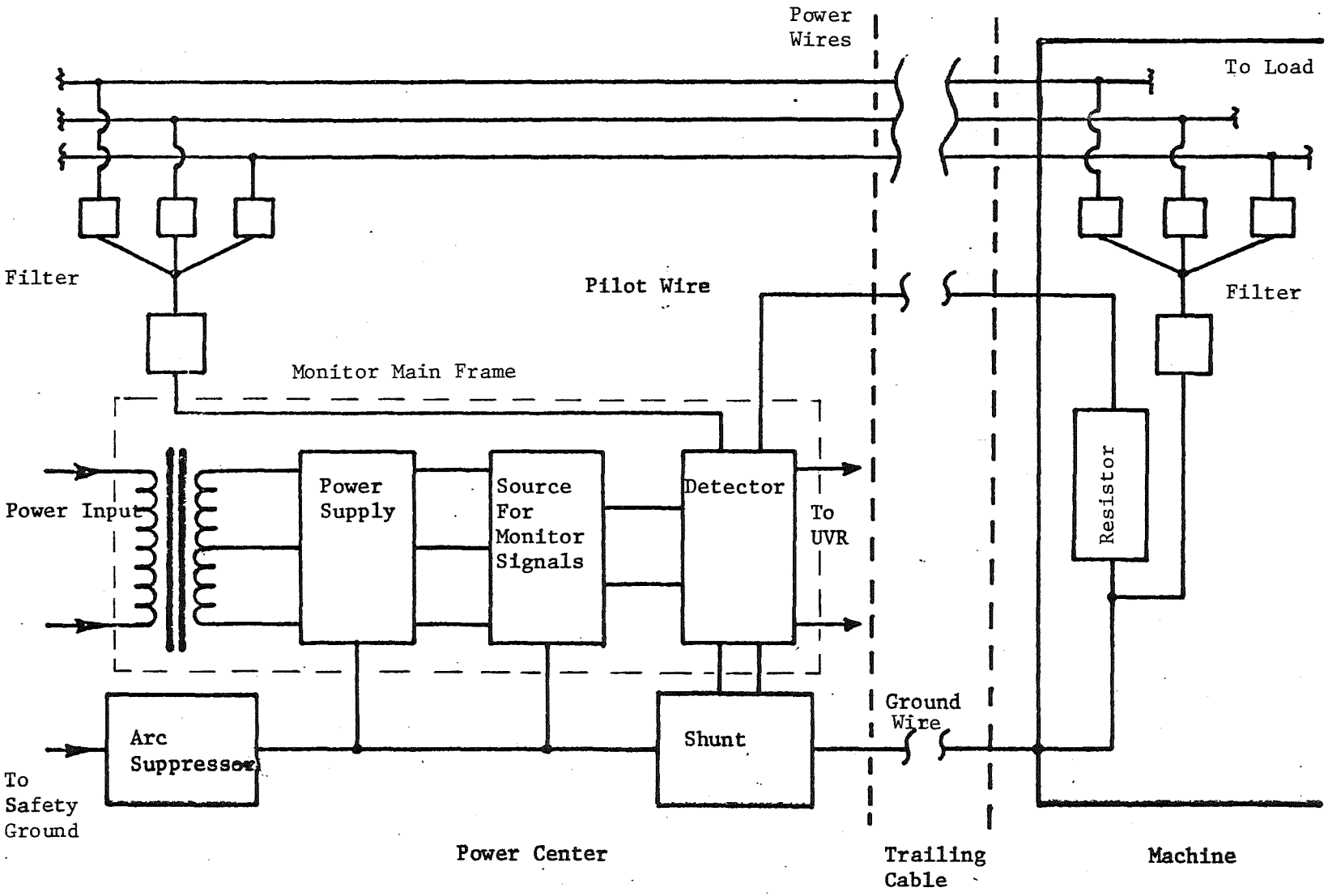


FIGURE 2.2. - Block diagram of the functions of the Modular Monitor.

A single resistance value was chosen since it is mounted inside the explosion proof housing of the mining machinery and is difficult to change. For the simple series relay monitors, the 50 ohm resistor chosen was a convenient value, but for the impedance measuring monitors, a lower value would be recommended.

Other components external to the monitor main frame may include filters for pilotless-audio frequency monitoring, an arc suppressor to isolate the ground wire from earth, and a ground wire shunt for shunt-type monitors. Any or all of these components may be included in a monitor configuration.

### 2.2.2 Monitor Modules

Several modules were constructed during the course of the project. From these two monitor modules were built and delivered to MSHA for acceptance tests. These two monitors are of the impedance measuring type, one using ac signals and the other dc signals. The circuit diagrams are shown in Appendix A1. Both of these monitors utilize a periodic self-testing cycle which provides for fail-safe operation using a minimum of redundant components. With the use of the 50 ohm resistor between pilot and ground at the machine, both units can detect a pilot to ground wire short. The dc monitor has passed MSHA laboratory tests but tests on the ac monitor have not been completed. Field testing has not been scheduled.

A number of advanced monitors were developed to show feasibility but fail-safe designs were not attempted. The frequency adaptive monitor and the synchronous detector-impedance monitor, which is similar in configuration to the Eltron-Ensign monitor, are the more advanced types. The frequency adaptive monitor features the ability to change frequency so as to only measure the resistive component of the loop impedance. Thus it automatically adapts to changes in the cable length. The second monitor uses a synchronous detector to separate the monitor signal from other signals. Thus, it can be used in the presence of considerable noise. As discussed later, the configuration has certain advantages for safety purposes. Both monitors can be used for pilotless monitoring. These monitors are discussed in more detail in a previous annual report (60).

### 2.2.3 Field Tests

The first field test installation was made at Eastern Associated Coal Company's Federal No. 2 mine on Miracle Run near Blacksville, West Virginia. The installation was made on a 152.4 m (500 ft) G-GC Cable suppling 480 volts, 3 phase to the main pump near the main shaft. The cable crosses the main haulage-way in the mine with the rectifier power cable immediately behind the ac power center supplying the pump. The ac and dc cables run parallel for a short distance.

Three monitor modules were field tested: ac series relay, dc series relay, and dc bridge resistance measurement. Both phases of ac and both polarities of dc were used. The results of the tests are shown in Table 2.1. Among other things, these results indicate the desirability of the modular approach to monitoring. In the case of the ac series relay, only one phase worked well. The dc series relay monitor worked satisfactorily, but the dc bridge resistance measurement monitor was inadequate, having a

TABLE 2.1. - Modular Monitor test results

Location Pump 152.4 m (500 ft)

| Module | In/Out | Date | Time | Counters Power | Counters Trip | Hours | #False Trips | Comments |
|---|---|---|---|---|---|---|---|---|
| Dc Series Relay | In | 11/4 | 8:30 p.m. | 168 | 387 | 175 | 0 | |
| | Out | 11/14 | 3:30 p.m. | 168 | 387 | | | |
| Dc Series Relay | In | 11/14 | 3:30 p.m. | 168 | 388 | - | - | Loose Power Fuse |
| Rev. Polarity | Out | 11/25 | 3:45 p.m. | 261 | 488 | | | |
| Ac Series Relay | In | 11/25 | 3:45 p.m. | 299 | 504 | - | - | Blown fuse in series with pilot |
| | Out | 12/4 | 11:30 p.m. | 300 | 506 | | | |
| Ac Series Relay | In | 12/4 | 1:30 p.m. | 300 | 512 | 166 | 16 | |
| Rev. Phase | Out | 12/11 | 9:30 p.m. | 300 | 528 | | | |
| Ac Series Relay | In | 12/11 | 9:30 p.m. | 300 | 529 | 99 | 0 | |
| Forward Phase | Out | 12/15 | 12:30 p.m. | 300 | 529 | | | |
| Dc Series Relay | In | 12/15 | 12:30 p.m. | 333 | 532 | 97 1/2 | 0 | |
| Switch Up | Out | 12/19 | 3:00 p.m. | 300 | 532 | | | |
| Dc Series Relay | In | 12/19 | 3:00 p.m. | 300 | 533 | 408 | 0 | Power system test in mine |
| Switch Down | Out | 1/5 | 3:00 p.m. | 301 | 534 | | | |
| Dc Bridge Resistance | In | 1/5 | 3:00 p.m. | 301 | 535 | 210 1/2 | 1553 | Not calibrated to drop-out at 3 Ω - drop out not known |
| Not Calibrated | Out | 1/14 | 9:30 p.m. | 302 | 2089 | | | |
| Dc Bridge Resistance | In | 1/14 | 9:30 p.m. | 302 | 2093 | 336 | 332 | Calibrated to 3 Ω |
| Calibrated | Out | 1/28 | 9:30 p.m. | 302 | 2425 | | | |

high rate of false trips. If any of the unsatisfactory approaches had been installed as a permanent monitor, it would need to be replaced, and conceivably, the replacement could be unsatisfactory also. With the modular approach, however, very little knowledge of the operating conditions is required to find a satisfactory monitor by trial and error.

It was anticipated that the nearby dc haulage track would interfere with the dc series relay monitors, but only the more sensitive dc resistance monitor was affected. It was also anticipated that the ac stray and induced currents would affect the ac monitors. This occurred on one phase direction only; the other being free of false trips. The monitor was removed after two months of testing.

Some decficiencies in the modular monitor package were noted during this field test. The most notable is the failure to provide an on-off switch for the monitor power supply. Other problems have been loose nuts, insufficient clearance, and other minor annoyances. A failure to provide an internal calibration resistor on the dc bridge module was remedied during the test period.

Practical modifications were made on the base unit when it was removed from the mine. These included remounting some components and adding an on-off-phase reversing switch.

Following these modifications, the monitor was installed on 14 April 1976 in the Robinson Run Mine near Shinnston, West Virginia. It is installed on one of two cables used to provide power to the coal slurry machine. This cable is approximately 150 m long, type G-GC with pilot wire and asymmetric grounds. A Femco Arc-Trap is installed on the cable. The monitor originally purchased by Consolidation Coal Company for this job gave a large number of false trips and has been bypassed.

The monitors tested at this installation are the same as those tested earlier. The results have been substantially the same. Only a few false trips were recorded in several hundred hours of operation with the series relay operations, and several false trips recorded with the more sensitive dc bridge resistance measurement.

The major restriction in both locations has been the lack of diode shunts approved by MSHA. Many of the more sophisticated monitor techniques developed in the West Virginia University Laboratory rely on diode shunts in the ground wire to detect monitor currents.

## 2.3 SYSTEMATIC STUDY OF GROUND-CHECK MONITORS

A systematic study of ground-check monitors was carried out in parallel with the laboratory work. The objective was to understand the relationships between the characteristics of the different monitor configurations and the requirements of mine conditions.

Monitor configurations may be classified a number of ways. For example, the classification scheme shown in figure 2.3 has been used extensively. There are five sets of descriptors for each monitor. Any monitor is specified by using one descriptor from each set. A complete discussion of the

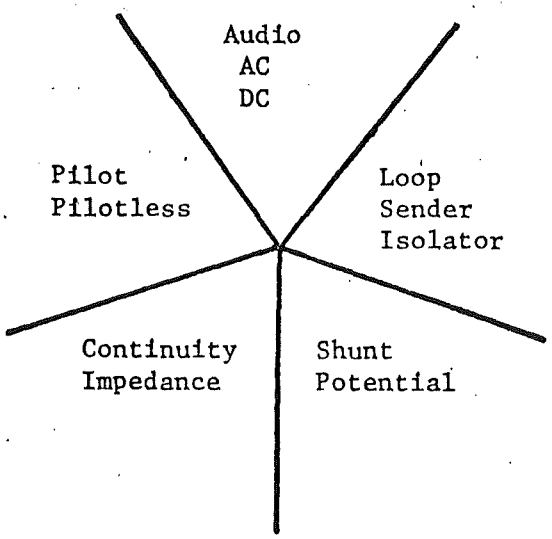


FIGURE 2.3. - Monitor classification breakdown. Any monitor can be classified by choosing one descriptor from each group.

descriptors and their characteristics is given in previous annual reports (56,57).

There are a total of 72 possible configurations that can be built as described by this method of taxonomy. As would be expected, some monitor configurations have better characteristics in some mine conditions than others. Following a study of characteristics of the various configurations and the requirements of the various mine conditions, it was concluded that 12 monitor types could satisfactorily monitor all mine conditions considered. These are the potential-impedance and shunt-continuity for the three signal sources: ac, dc, and audio. The audio monitors may be made for both pilot wire and pilotless situations. The ac and dc monitors are generally but not necessarily restricted to pilot wire situations. It is not clear, however, that the potential-continuity and shunt-impedance monitor types are substantially inferior. Many of the 24 monitor types were developed to some stage during the development of the modular monitor. Only two, however, both potential-impedance types, were carried all the way to submission to MSHA.

### 2.3.1 The Ultimate Monitoring Technique

Carrying the study of monitor characteristics still further, a single monitoring technique stands out. This study however, must be concerned with possible changes or restrictions in allowable machine grounding practices in the mines. Parallel paths, arc suppressors, impedance levels, cable couplers, and pilot wires all become subject to scrutiny.

It is recommended that pilot wires be eliminated. First, audio monitors make the pilot wire obsolete for monitoring. Second, a pilot-ground wire short can mask a broken ground beyond the short. Thus, if the pilot wire is used, the monitor should detect a pilot-ground wire short. Third, in many cables, the addition of the pilot wire caused the manufacturers to make the cable asymmetric. This causes an induced voltage between ends of the cable, and results in intermachine arcing. Arc suppressors must be added in series with the ground wire to eliminate the arcing. Audio monitors are probably the only practical method for monitoring without a pilot wire.

Arc suppressors should and can be eliminated. They are an unmonitored link to the safety ground and thus pose a potential safety hazard. An open arc suppressor would defeat all ground monitoring attempts.

Since many possible parallel paths exist between the machine frame and the safety ground connection, two choices are possible. First, measure the total ground connection impedance. This is allowable and is relatively safe. The second option is to measure the impedance of the ground wire. The second option is preferred since most other parallel paths are not reliable. In order to satisfy the second option for the potential type monitors, arc suppressors are often used to isolate the ground wire from the safety ground. As mentioned earlier, the arc suppressor presents a hazard in itself. The shunt type monitors do not require the arc suppressor, but with a normal configuration (the source between the ground wire and pilot/phase wire connection), the monitor is prone to false trips without an arc suppressor. One configuration, shown in figure 2.4, eliminates this problem by placing both the source and detector in the ground wire. Thus, in this configuration the ground wire

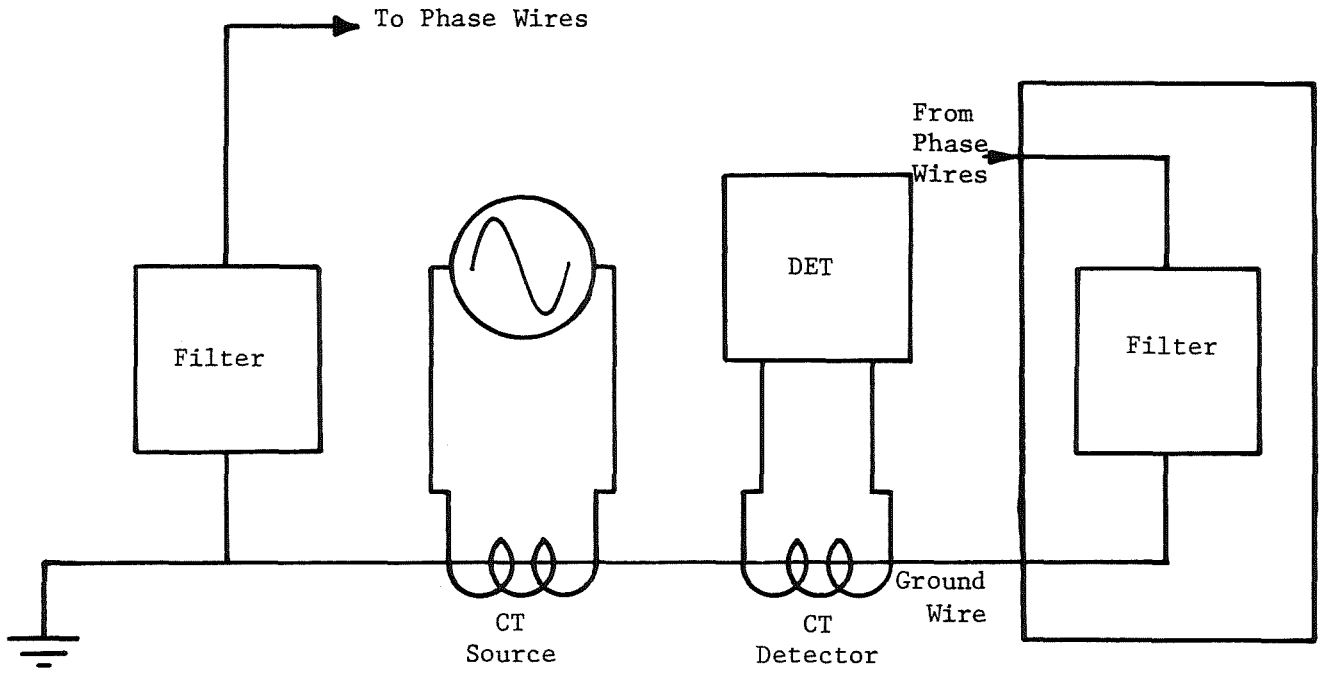


FIGURE 2.4. - Monitor configuration with both source and detector in ground wire.

must be monitored. This method has none of the drawbacks mentioned earlier.

Impedance levels should also be considered. If possible, only the lowest impedance levels should be accepted. A continuous but high impedance ground is little better than no ground wire at all. Thus, the ultimate monitor appears to be an audio-pilotless-impedance monitor with both source and detector in the ground wire. Unfortunately, this monitor is not available.

When cable couplers are used, the grounding circuit becomes the same as when multiple machine frames or control boxes are used. In these cases, parallel ground circuits occur. None of the present monitoring methods will work in this situation. A multipath monitor as discussed in the next section must be used. The cable coupler presents a special problem in that a selective filter cannot be used because of space limitations. It is therefore recommended that cable couplers either be eliminated or be isolated from earth and human contact.

## 2.4 MULTIPATH MONITOR

Now that there are several monitors accepted by MSHA for low voltage face equipment, attention is being turned toward high voltage monitoring and monitoring stationary equipment. In these cases, there are some extra problems. The biggest problems are larger transients and multiple branches with multiple machine frames tied to the ground wire. A typical example of a multiple machine frame system is shown in figure 2.5. Another type of multiple branch circuit is shown in figure 2.6.

In the case shown in figure 2.5, a monitor in the power center can check the continuity of the pilot-ground connection. Unfortunately, the electrical connection between the motor starter box and the ground wire cannot be checked. This can lead to serious shock hazards. Similarly, the parallel ground wire connections in Figure 2.6 cannot be checked with a serial type monitor.

A method is outlined in figure 2.7 to monitor the multiple connections. A monitor is placed in the power center which can distinguish between each of the selective isolators between pilot and ground connections. Thus, the monitor can determine the connection between pilot and ground at each load frame.

A number of approaches can be used with this basic configuration. The selective isolators could be passive devices or could be made active. Active isolators could be interrogated periodically or continuously at different frequencies or codes.

A block diagram of the system designed is shown in figure 2.8. This system uses passive filters at each machine frame. The voltage-controlled oscillator sends out audio frequency signals at the resonant frequency of each filter. As long as each filter has a good connection, it will pass its resonant frequency. A frequency, $f_o$, is generated to check for pilot-to-ground shorts and is also used as a fail-safe check in the detection circuitry. The coincidence detectors are used to verify that all the frequencies except $f_o$ are passed by the filters. Many fail-safe features are inherent in this

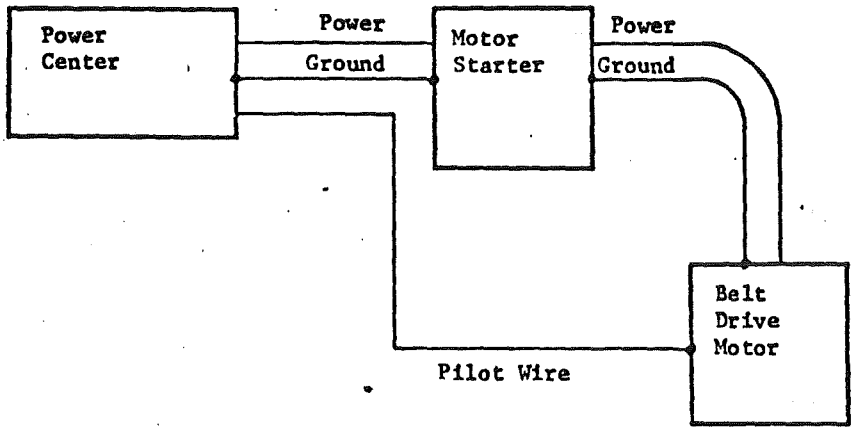


FIGURE 2.5. - A typical multiple machine frame system. The pilot wire is run separately to the second frame for monitoring purposes.

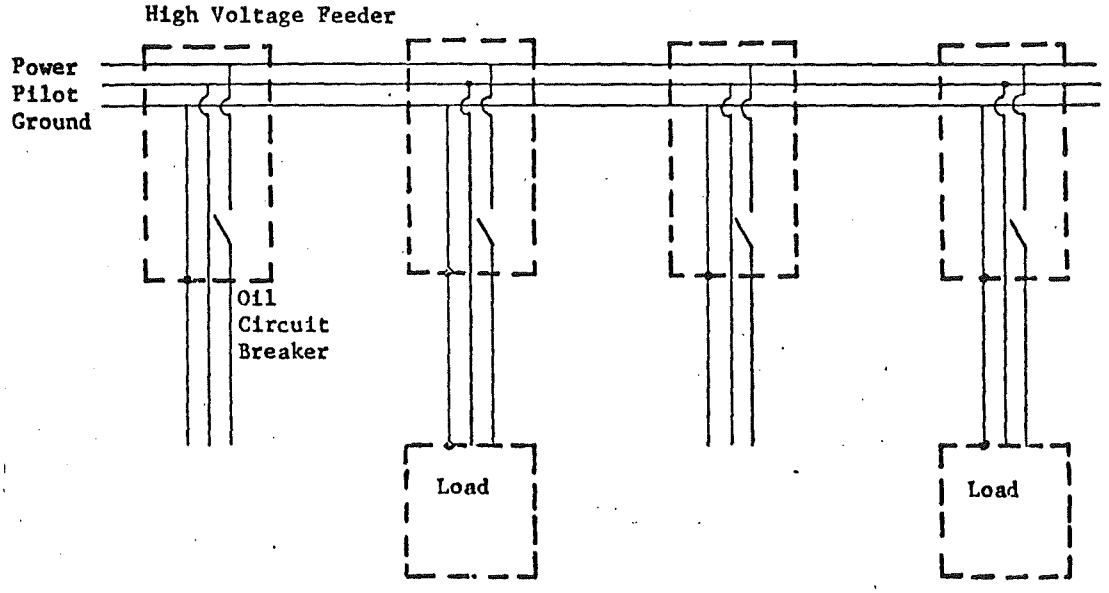


FIGURE 2.6. - A typical multiple branch system used in high voltage distribution.

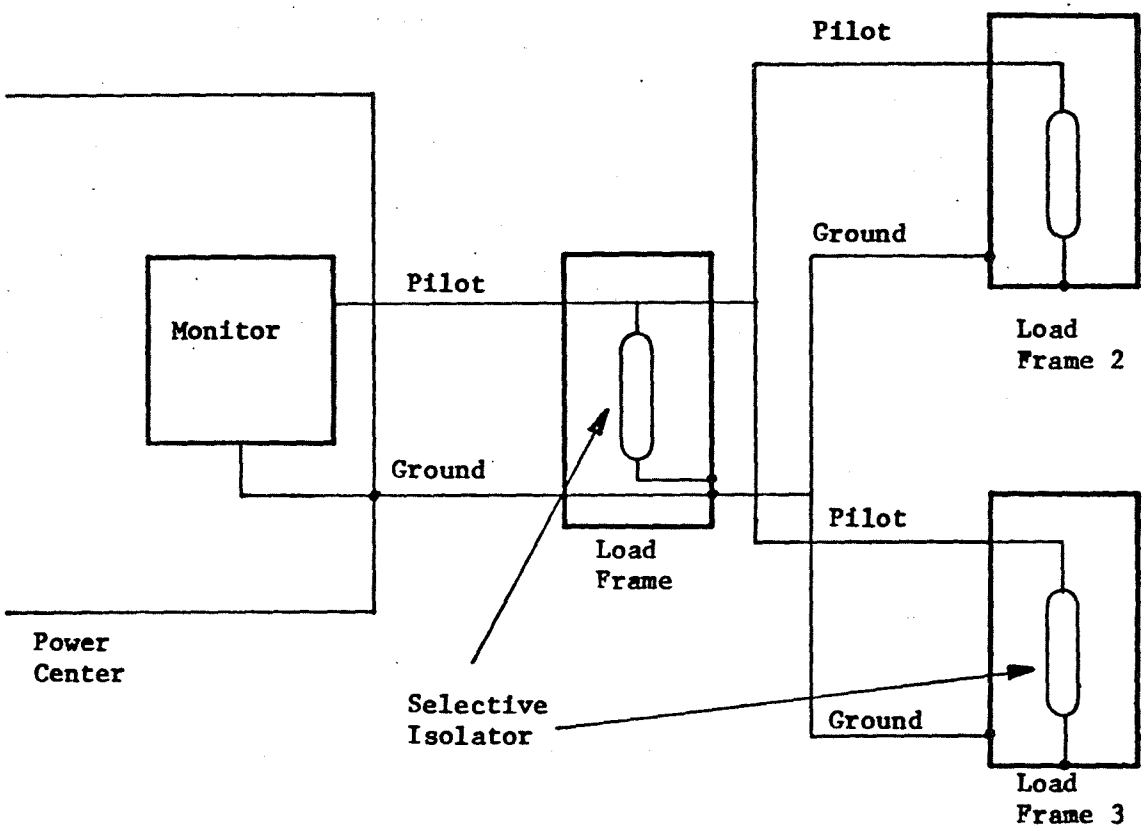


FIGUR E 2.7. - **Proposed method for monitoring multiple frame ground connections.**

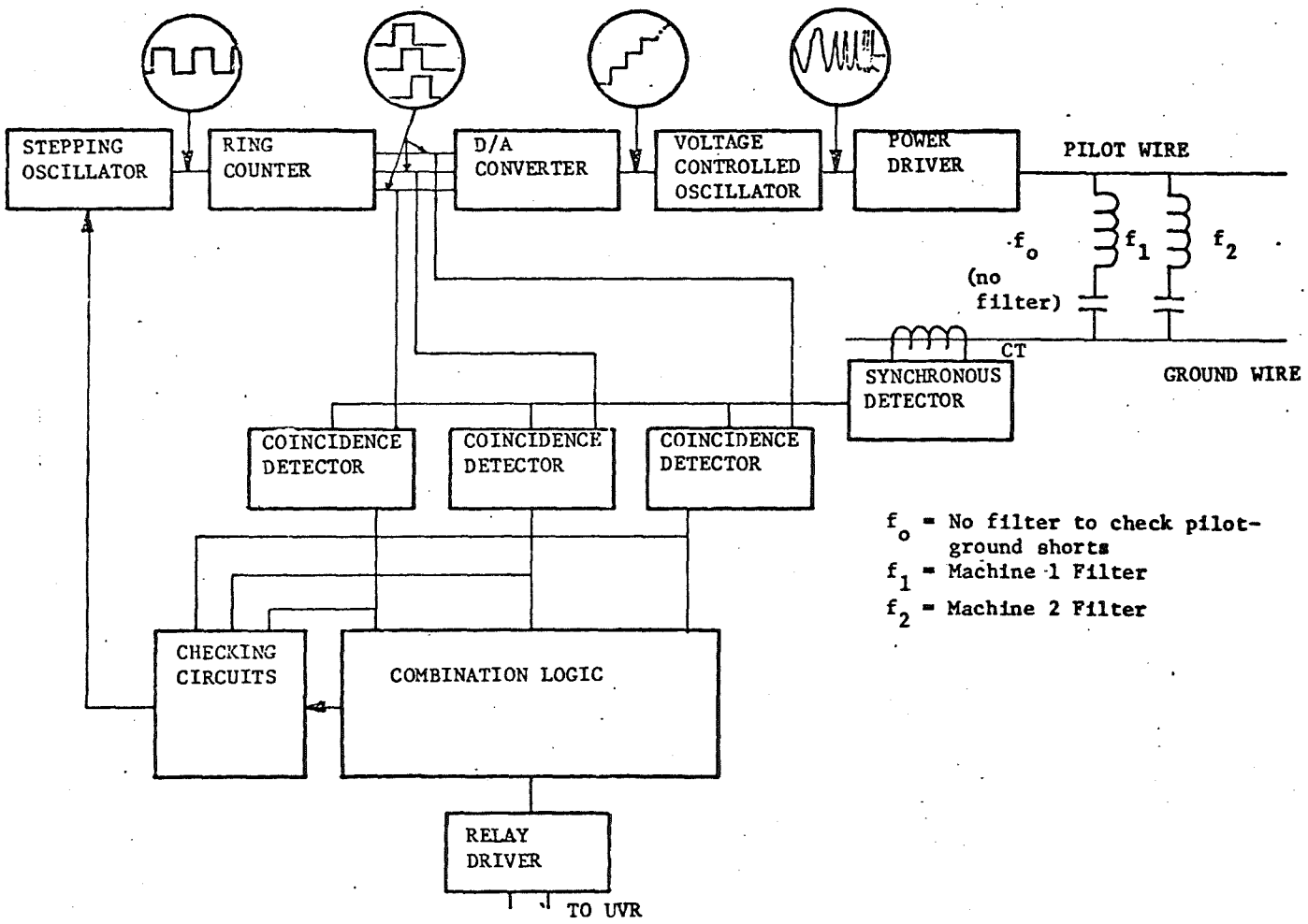


FIGURE 2.8. - Proposed design for a multiple circuit groundcheck monitor.

design. The combination logic is the most difficult to make fail-safe. Extra checking circuitry is necessary to verify correct operation. Feedback to the stepping oscillator circuit causes the ring counter to stop if a failure is detected either in the monitor or ground system. Indicator lights driven by the ring counter show which ground circuit or detector circuit failed. A more complete discussion is given in Appendix A2.

# CHAPTER 3

# MINE EQUIPMENT SHOCK HAZARD

## 3.1 ELECTRICAL GROUNDING SYSTEMS IN SURFACE COAL MINES

### 3.1.1 Introduction

The goal of this research task was to investigate several aspects of the resistance-grounded-neutral electrical systems found in surface coal mines. Several trips to operating mines were made to gather data on soil resistivity and machine resistance, as well as step and touch potentials around equipment. Theoretical studies were made on the impedance of earth electrodes under surge conditions, the results of which can be applied to the performance of mine equipment when struck by lightning. An analysis is included on the transfer of potential from one ground bed to another.

### 3.1.2 Ground System Functions

What purposes are served by a grounding system? The answer is fourfold and may be summarized as follows. First, it must limit potential gradients between conducting materials in a given area (23). When a phase conductor comes into contact with a machine frame, current flows through the equipment, which tends to become elevated in potential above that of the surrounding earth. If a man were to touch the machine while he was simultaneously connected to ground in some manner, his body would also tend to become elevated in potential, possibly to a lethal extent. Thus the grounding system should provide a low-resistance path for the fault current to return to the source. The maximum potential to which a man could be exposed when touching a machine frame is equal to the voltage drop along the ground conductor, as shown in figure 3.1 (21). This ground conductor may consist partially of trailing cable and partially of bare overhead conductors. In any case, the ground conductor should have low resistance so it can carry the maximum expected fault current without excessive voltage drop.

Second, the grounding system should limit the energy available at the fault location. Heavy arcing or sparking can ignite nearby combustible material. The air itself can become ionized, making it capable of carrying tremendous amounts of current. A high-energy fault can vaporize phase conductors, melt breakers and switchgear, or blow protective enclosures apart with explosive force (9). By controlling the maximum allowable fault current, the danger of fire is eliminated and equipment damage is reduced to a minimum.

Third, the control of over-voltages is essential. This condition may occur by accidental contact with a higher voltage system, or could result from transients due to resonance effects, intermittent ground faults, or switching surges (4). The maximum ratings for cable insulation, transformer windings, relay contactors, and so forth may be temporarily exceeded in these cases. This usually does not result in an immediate equipment breakdown, but component parts of the electrical system are successively over-stressed and weakened by repeated exposure. This leads to premature failures, reduced component life, and mysterious "nuisance trips" which can occur without apparent reason. By providing a path between the transformer neutral and ground, most of the sources of transient over-voltages can be reduced or possibly eliminated.

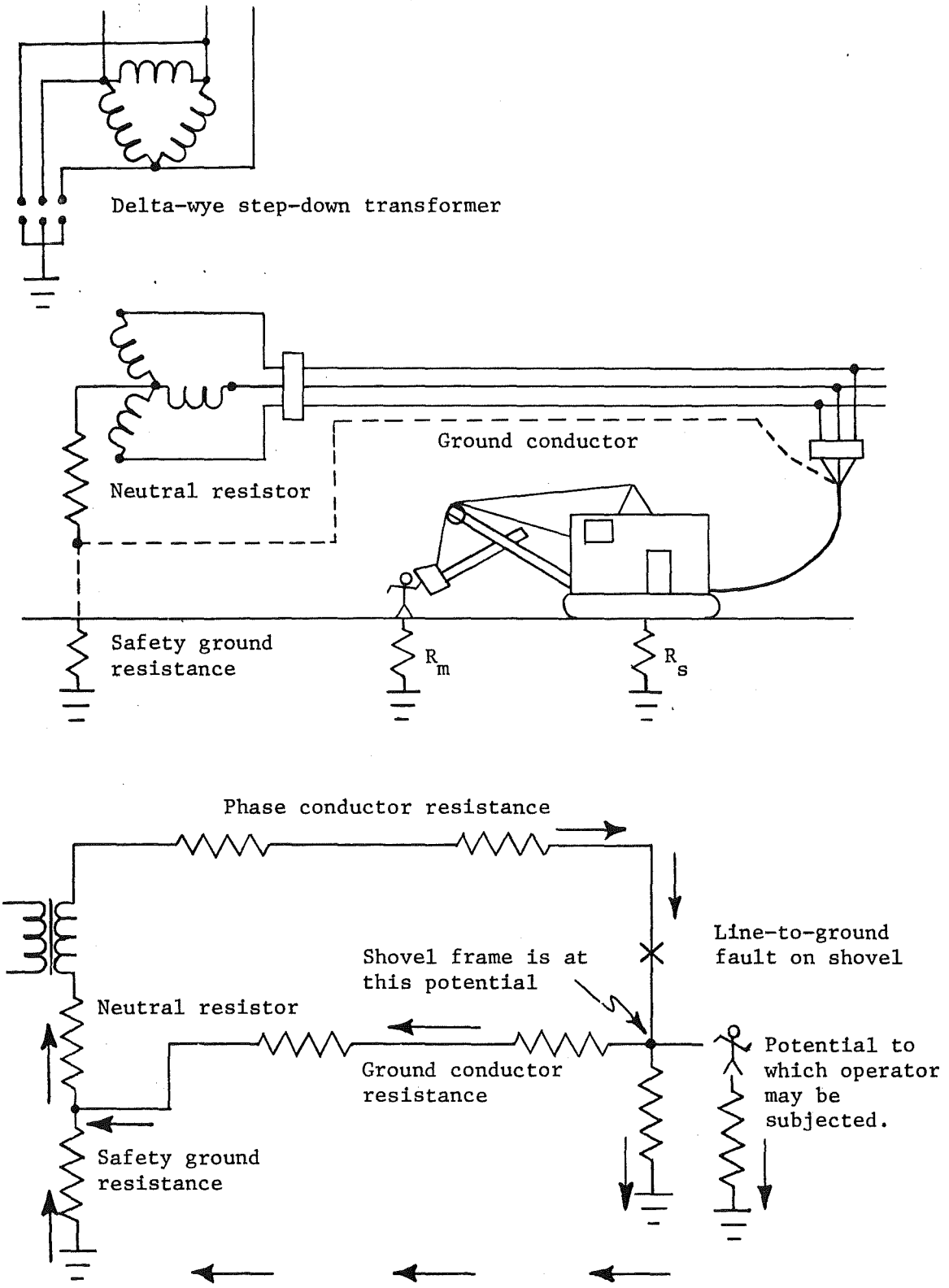


FIGURE 3.1. - Illustration of electric shock hazard (21)

Last of all, a grounding system should isolate defective areas by selective relaying of ground faults (30). The sensitivity and time delays of the protective circuitry should be adjusted so that a fault on one piece of equipment will cause the local breaker to sense the malfunction and quickly remove power only from the affected machine. If the relay coordination is not established correctly, back-up breakers may trip before the primary protection operates. Several large draglines or shovels may be needlessly shut down, and much time could be lost in an effort to locate the trouble spot. Thus the relaying system must be arranged so that, even at the lowest level of the power distribution chain, sufficient fault current can flow to enable the protective circuitry to sense it and take remedial action.

For use in mining applications it appears that the presently-used system, which might be described as a 'medium-resistance grounded system", is quite satisfactory. The use of series resistance in the line-to-neutral circuit is desirable because of its current-limiting properties. Most mine power systems are designed to limit the maximum fault current to either 25 or 50 amperes. This level of current is high enough to be sensed by protective circuitry but low enough to prevent lethal touch potentials on machine frames as long as ground conductors are intact (13). Short-lived transients and other excessive over-voltages are controlled by the earth connection (14). On ungrounded systems, transients caused by such conditions as resonance effects, intermittent ground faults, autotransformer connections, and switching surges have caused premature failure in many electrical components. Contact with a higher-voltage system, however, will result in a transfer of the higher system voltage to the phase conductors. This can occur when overhead distribution lines at several voltage levels cross over one another, or when transformer primary-to-secondary insulation breaks down. During the first line-to-ground fault, the other two phases may rise in potential up to full line-to-line value, which places an added stress of up to 1.73 times normal on the system insulation (14). The duration of this condition should be short, however, if the protective relaying is in proper working order. The medium-resistance grounded system, as currently applied in the mining industry, is an excellent performer. It serves to protect both men and machines, while providing selective relaying to promote system integrity.

### 3.1.3 Resistance of Large Machines

One facet of the research performed on ground systems by WVU has been an investigation into the contact resistance of large excavating machines as found in the mine. A dragline or drill would probably be perched on a bench above the highwall, while a shovel would usually operate from directly atop the coal seam.

Most large draglines rest upon a massive base, often called a "tub" which is circular in plan view, and serves to distribute the great weight of the dragline over a large surface area. This is ideal from one viewpoint, because this large contact surface between machine and earth probably means a low contact resistance. The contact resistance with respect to remote earth may be expressed as (47):

$$R_{\infty} = \frac{\rho}{4a} , \qquad (3.1)$$

where $R_{\infty}$ = contact resistance, in ohms

$\rho$ = soil resistivity, in ohm-meters (or ohm-feet)

and a = tub radius, in meters (or feet).

The use of this formula implies several approximations. First, the possible contact surface area provided by the dragline's bucket is neglected. Depending upon the length of the boom, this bucket may rest on the ground at a point several tens of meters (several hundred feet) from the center of the tub. Conversely, if the operator has just winched the bucket inward, in the process of filling it, the bucket may lie quite close to the tub. In any event, the ground contact surface of the bucket is much smaller than that of the tub. In any event, the ground contact surface of the bucket is much smaller than that of the tub. When the relatively small bucket size is combined with the wide variability in its possible location with respect to the tub, it seems sensible to omit its influence from calculations of contact resistance.

Second, this formula represents the dragline when it is resting upon its base or tub, but does not accurately reflect the shape of the surface in contact with the soil when the dragline is moving or "walking". Since the dragline tub is stationary most of the time, this is not a major consideration. While walking, the dragline's weight rests on its two large shoes, which are rectangular in plan view, and have a total surface contact area which ranges from 30-45% of the tub's contact area.

The contact resistance of a shovel or drill is more difficult to calculate because of the two (or more) crawler treads upon which these machines rest. The rectangular shape of the tread-soil interface cannot readily be analyzed. By modeling the crawler tread as an ellipsoidal electrode, its resistance with respect to remote earth may be given by (35):

$$R_{tr} = \frac{\rho}{\pi L} \ln \left( \frac{2L}{d} \right), \tag{3.2}$$

where $R_{tr}$ = tread contact resistance, in ohms

$\rho$ = soil resistivity, in ohm-meters (or ohm-feet)

L = tread length in contact with the ground, in meters (or feet)

and d is the diameter of the ideal ellipsoidal electrode. Its value can be assumed as:

$$d = \sqrt{wp}\ , \tag{3.3}$$

where d = equivalent diameter, in meters (or feet)

w = width of tread, in meters (or feet)

and p = penetration depth of tread into the soil, in meters (or feet).

Since a shovel will have two or more caterpillar treads, spaced a certain distance apart each tread will have an effect on the others, which can be expressed as "mutual resistance". For a typical loading shovel (which has only two treads):

$$R_{12} = R_1 + R_2 - 2\,R_m, \tag{3.4}$$

where $R_1$ and $R_2$ are the earth resistances of treads 1 and 2 with respect to remote earth,

$R_{12}$ is the direct resistance between treads 1 and 2,

and $R_m$ is the "mutual resistance".

For two parallel ellipsoidal electrodes (61):

$$R_{12} = \frac{2\rho}{\pi L} \ln \left\{ \frac{L^2}{sd} \left[ \sqrt{1 + \left( \frac{2s}{L} \right)^2} - 1 \right] \right\}, \tag{3.5}$$

where $R_{12}$ = resistance between treads, in ohms

$\rho$ = soil resistivity, in ohm-meters (or ohm-feet)

$L$ = tread length, in meters (or feet)

$s$ = center-to-center tread spacing, in meters (or feet)

and $d$ = equivalent tread diameter, in meters (or feet)

Since $R_1 = R_2 = R_{tr}$ from equation 3.2, then:

$$R_m = \frac{2 R_{tr} - R_{12}}{2} . \tag{3.6}$$

If we can assume that any current flow between the shovel and the earth will divide equally between the two treads, then the potential on the shovel frame is given as:

$$V = \frac{I}{2} (R_{tr} + R_m). \tag{3.7}$$

The resistance with respect to remote earth is equal to the voltage divided by the impressed current, or:

$$R_\infty = \frac{1}{2} (R_{tr} + R_m). \tag{3.8}$$

By substituting equation 3.6 into 3.7, it can be seen that the contact resistance of a shovel with two caterpillar treads is given as:

$$R_\infty = R_{tr} - \frac{1}{4} R_{12}, \tag{3.9}$$

where $R_\infty$ = shovel contact resistance, in ohms

$R_{tr}$ = contact resistance of a single tread, in ohms (given by equation 3.2)

and $R_{12}$ = resistance between the two treads, in ohms (given by equation 3.5).

As with the dragline, any effects on earth resistance caused by the dipper of the shovel resting on the ground have been ignored. The location of the dipper with respect to the axis formed by the shovel's tread is highly variable; as such, mathematical treatment becomes quite involved and is subject to gross approximations.

Figures 3.2 and 3.3 show the expected contact resistance for several different types of draglines operating on soil of various resistivities. The resistance values shown on the graphs were calculated using manufacturers' literature and formula 3.1. Figures 3.4 and 3.5 are similarly derived for electric loading shovels, using formulas 3.2, 3.5, and 3.9. If the resistivity of a particular soil does not fall within the range shown on the graphs, then the values shown on the x and y axes may both be multiplied by an appropriate constant.

To accurately measure the contact resistance of a piece of mining equipment, it must first be shut down and electrically isolated from the substation or switch house feeding it. This entails a loss of production at the mine and represents a considerable dollar cost to the operators. It was hoped that an alternative method of measuring contact resistance could be found. That is, if one could measure the soil resistivity in the vicinity of the machine, and then use the appropriate equations or graphs to find the resistance, a significant improvement over the present method would be achieved. With this in mind, several visits to working coal mines were planned.

### 3.1.4 Field Trip Measurements of Machine Resistance

During the week of 19 December 1977, a field trip was made to a major surface coal mine in the eastern United States. The purpose was to measure the contact resistance, or earth resistance, of large pieces of mining equipment. In addition, soil resistivity measurements were made in the vicinity of these machines in order that a comparison might be made between the measured values of resistance and theoretical values which can be obtained by the application of previously derived formulas.

The first machine to be tested was a very large dragline whose tub diameter was 30.5 m (100 ft). The walking shoes which measured 6.1 x 39.6 m (20 x 130 ft) each, were also resting on the ground, so their surface area was added to that of the tub, and the radius of a circle with the same total area was calculated. Two Wenner 4-probe arrays were used to measure soil resistivity along lines both parallel and perpendicular to the walking shoes of the dragline, which was about 1.9Ω. Field measurements, using the fall-of-potential method, gave values of 0.62Ω and 0.54Ω, respectively, for surveys conducted parallel and perpendicular to the walking shoes. The fall-of-potential plots are shown as figures 3.6 and 3.7. Unfortunately, it was not possible to disconnect the trailing cable ground conductors for this test, and the measured values are therefore suspect.

A second dragline was examined, and on this occasion the fall-of-potential measurements were made twice--first with the neutral (grounding conductors) connected, and then with the dragline completely isolated from the electrical power distribution system. When connected to the power system, parallel paths

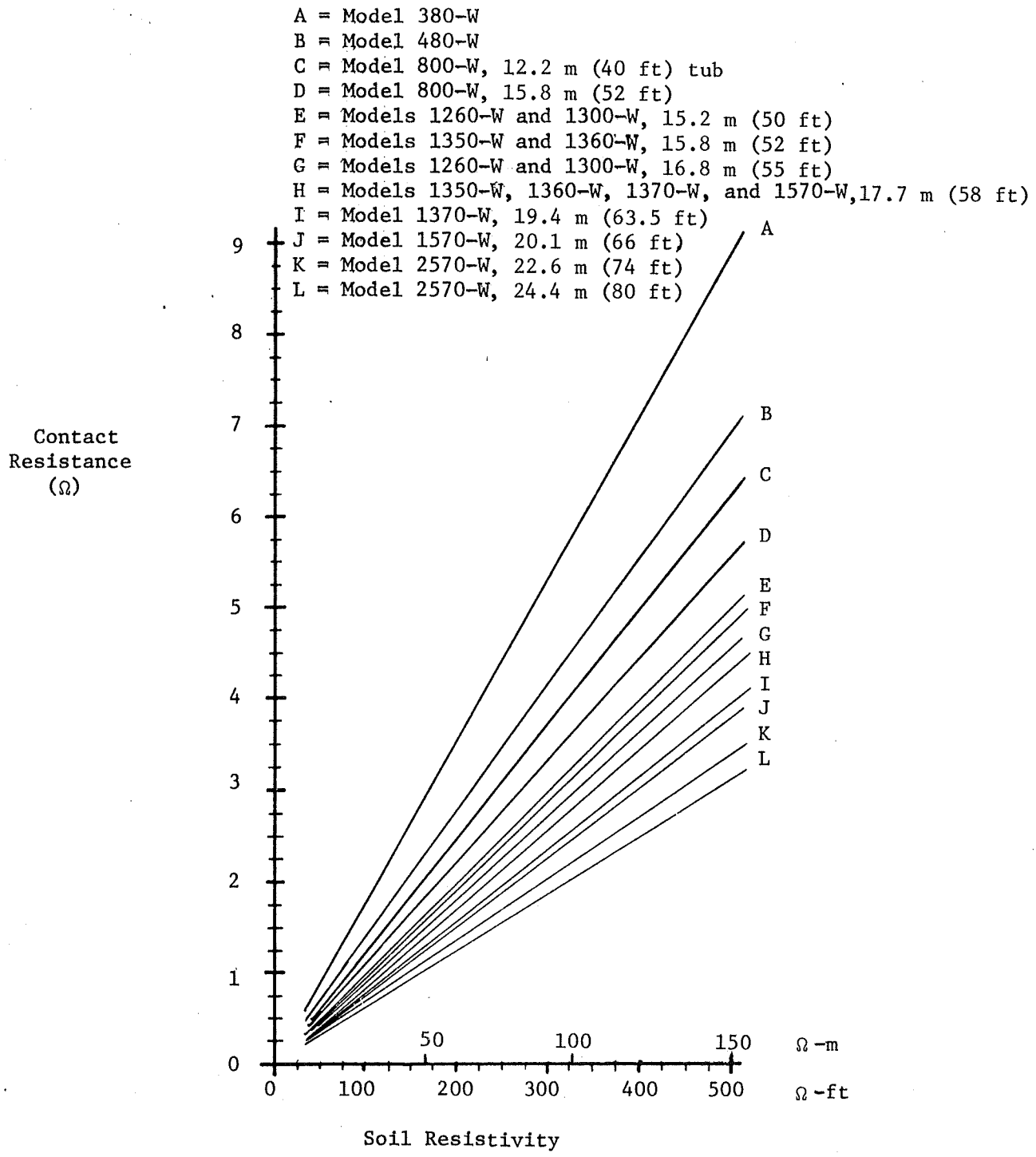


FIGURE 3.2. - Earth resistance as a function of soil resistivity for several models of Bucyrus-Erie Draglines.

A = Model 732
B = Model 736
C = Model 740
D = Model 752
E = Model 757

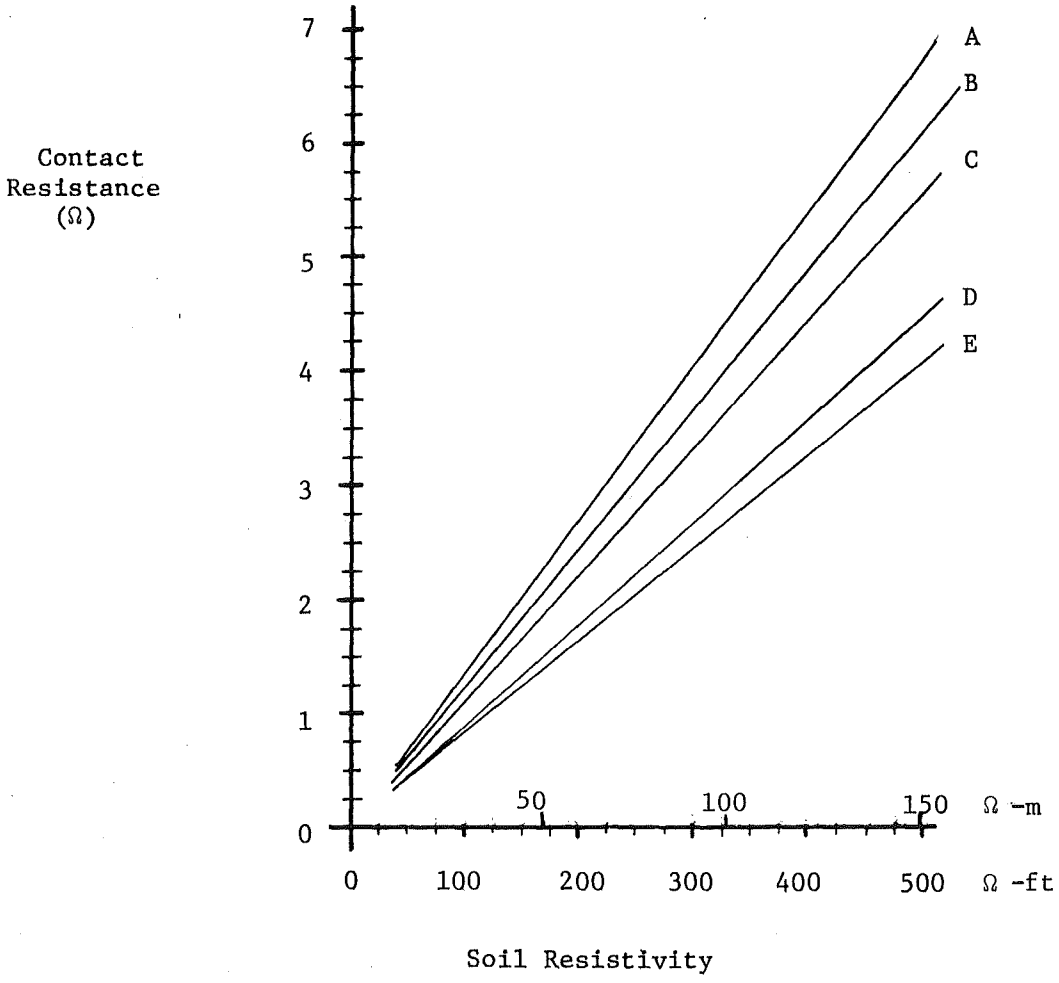


FIGURE 3.3. - Earth resistance as a function of soil resistivity for several models of Page Draglines.

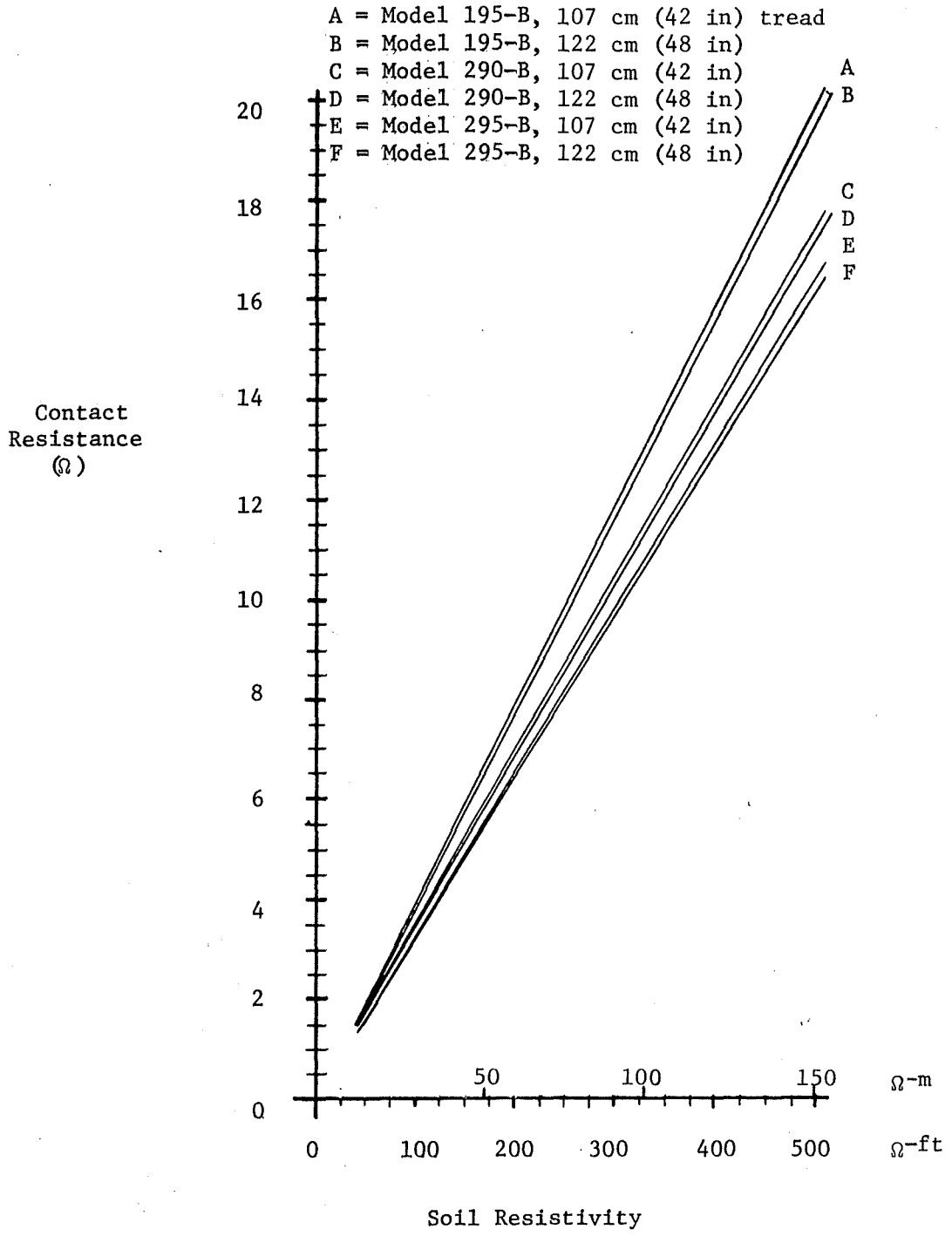


FIGURE 3.4. – Earth resistance as a function of soil resistivity for several models of Bucyrus-Erie Shovels (depth of tread penetration = 3.05 cm, 0.1 ft).

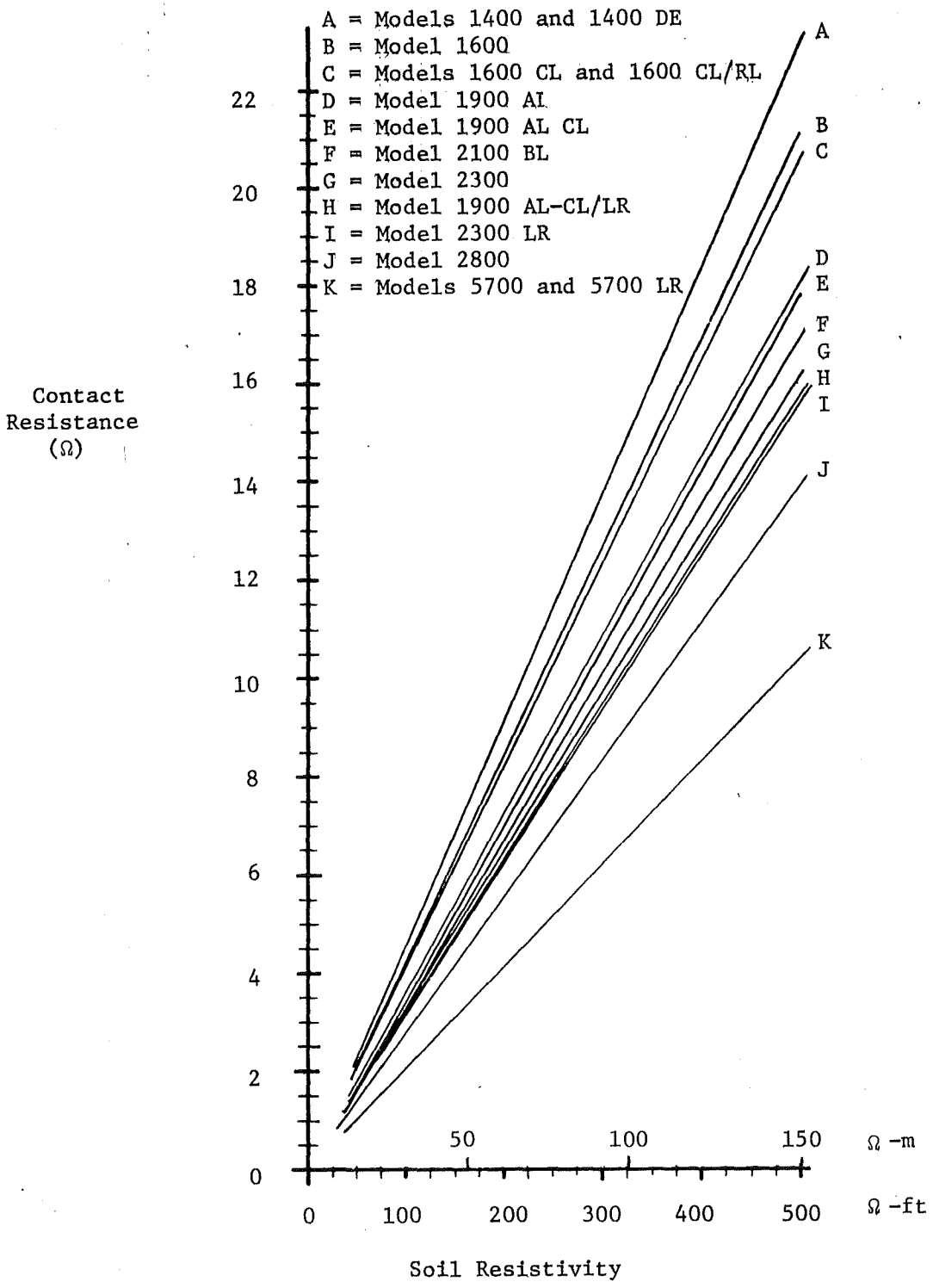


FIGURE 3.5. - Earth resistance as a function of soil resistivity for several models of P & H Shovels (depth of tread penetration = 3.05 cm, 0.1 ft)

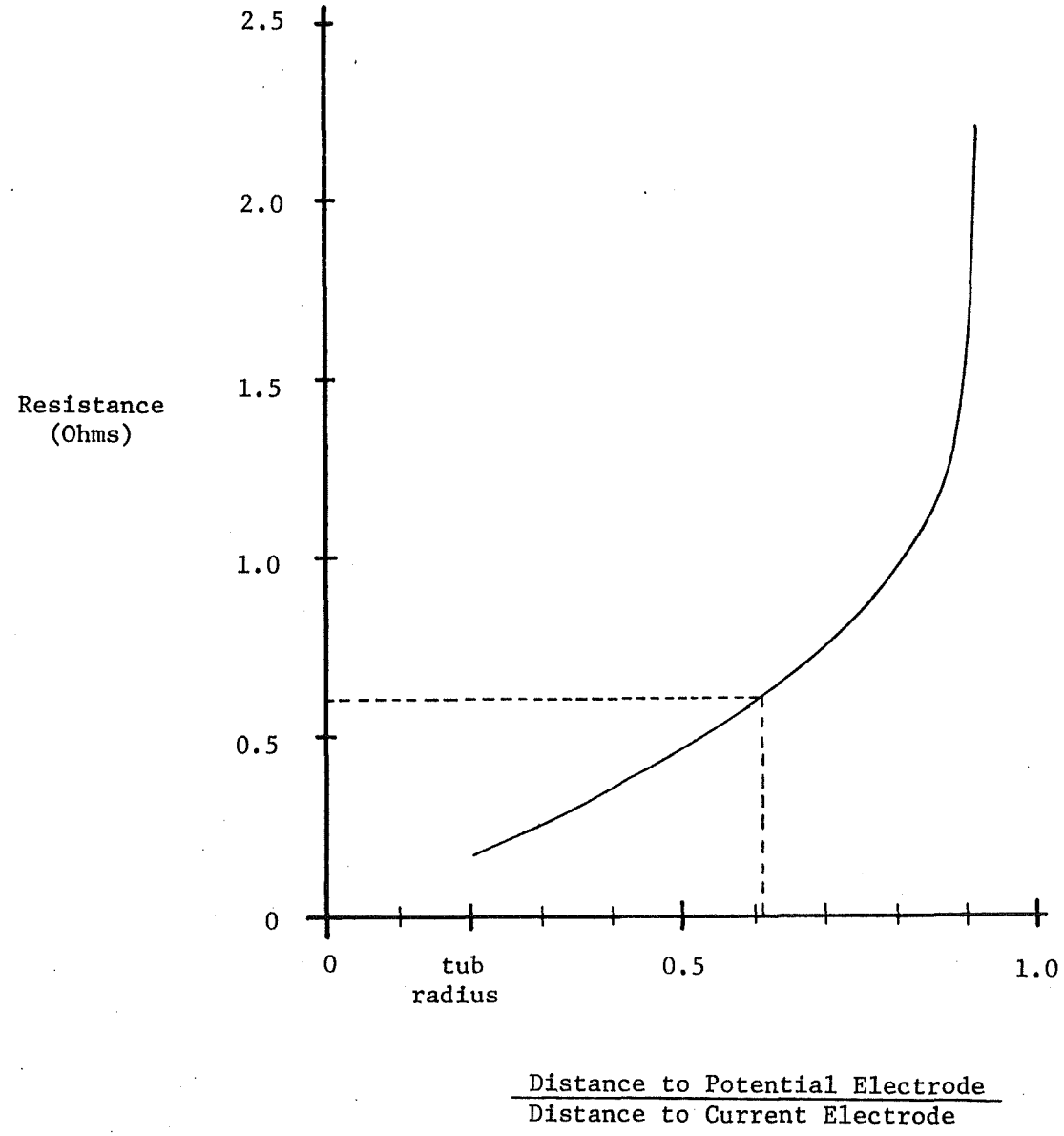


FIGURE 3.6. - Fall-of-potential resistance determination for B-E 4250-W Dragline connected to safety ground wire, traverse perpendicular to axis of feet.

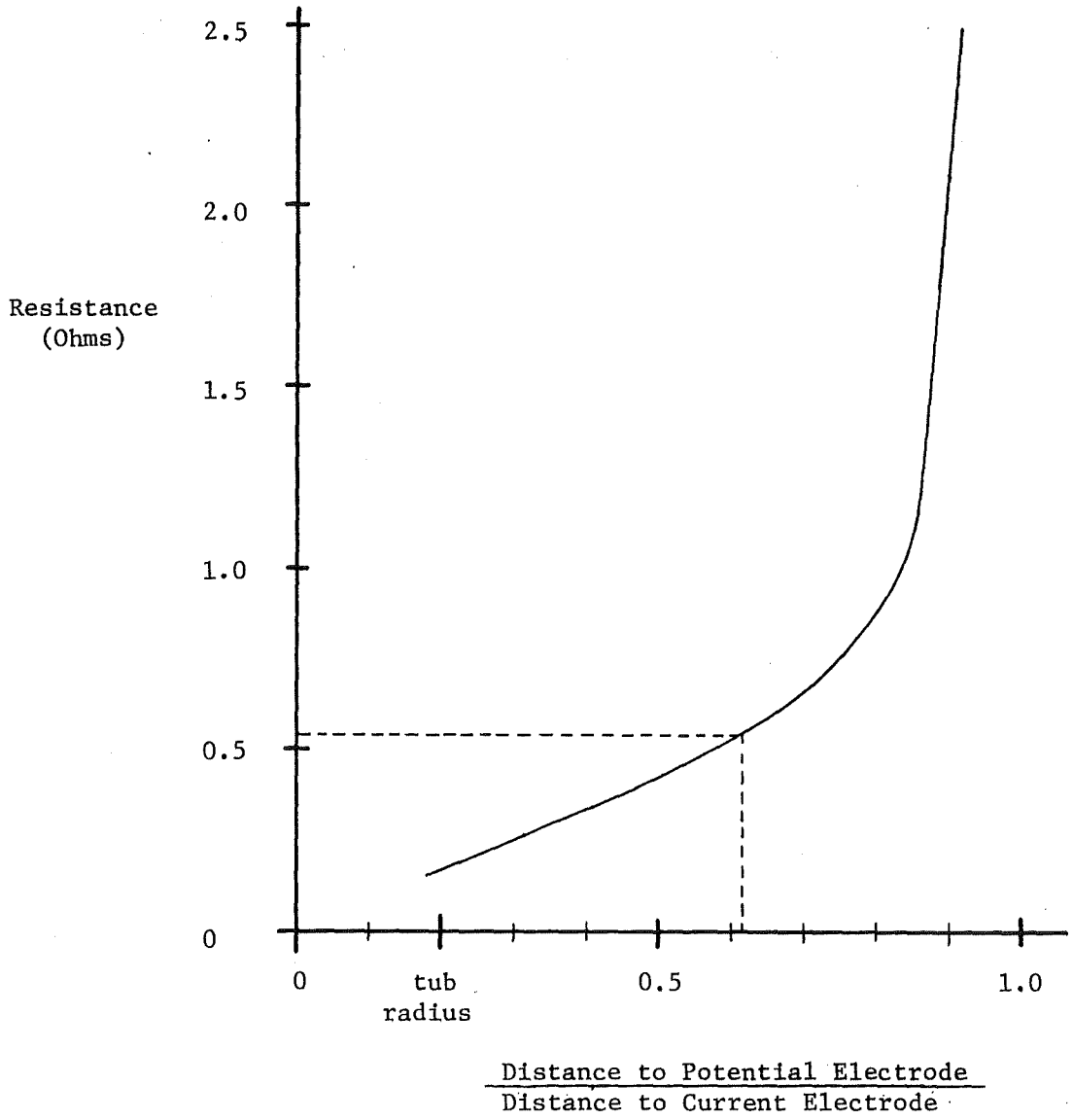


FIGURE 3.7. - Fall-of-potential resistance determination for B-E 4250 W Dragline connected to safety ground wire, traverse parallel to axis of feet.

exist whereby the current generated by the ground-test instrument can flow to earth via paths other than the frame of the machine under test. In this case, the safety ground grid at the substation as well as any additional machines connected to this ground grid will serve as alternate paths for the test current, thereby leading to erroneously low values of resistance. An apparent resistance of 0.63Ω was measured with the system connected, and a value of 1.4Ω was measured when the dragline was isolated from the system, as shown by figures 3.8 and 3.9. This machine also had its walking shoes resting on the earth, and an "equivalent radius" was again calculated. A resistivity survey was made using several different electrode spacings, and an average value found. Plugging these two numbers into the textbook equation, the theoretical resistance was determined to be 1.46Ω, compared to a measured value of 1.4Ω. The difference between these two numbers is less than 5%.

A third dragline was measured; in this instance the machine was isolated from the power system. The fall-of-potential measurement, illustrated in figure 3.10, yielded an earth resistance of 1.05Ω, while the calculated value of 1.73Ω is significantly higher. It is interesting to note that in this case, the resistivity survey showed the presence of a highly conductive surface layer immediately beneath the machine. If the resistivity value of this layer were to be used directly in the equation, then the theoretical resistance would be about 0.3Ω, which is also incorrect. It is difficult to say whether the discrepancy between measurement and theory is due to problems in interpreting resistivity data or to shortcomings in the theoretical development.

At this same mine several shovels were also tested to determine their ground resistance and compare measured data with theoretical values calculated from formulas. A fall-of-potential survey, shown by figure 3.11, gave a resistance value of 5.75Ω for the first shovel, which was isolated from the power system and was sitting on a 152 cm (60 in) seam of coal. Using the average resistivity figure derived from a resistivity survey and plugging this number into the theoretical equations, a value of 29.1Ω, or 6 times the measured value, was obtained. It should be noted that the coal seam itself has a very low conductivity. If it is assumed that the test current flows in the soil layer immediately beneath the coal, then the theory yields a resistance value of 14.6Ω, which is 3 times the measured value. However, underlying soil layers having even lower resistivity are present, and if these are taken into account, then a resistance of 9.7Ω is obtained, still almost twice the measured value.

A second shovel was measured, and this time data was taken with the trailing cable grounding conductors both connected and disconnected from the power system. With the shovel isolated, the earth resistance was 7.9Ω, while this reading fell to 1.3Ω when the machine was attached to the remainder of the power system. The fall-of-potential plots are graphed in figure 3.12. Calculations using the average soil resistivity and textbook formulas gave a value of 5.2Ω, which is about 2/3 of that measured with the machine isolated. The resistivity survey revealed a multi-layered earth beneath the machine, with high-resistivity layers alternating with low-resistivity layers. If it is assumed that all the test current flowed in the surface layer, which was highly conductive, then theory predicts a resistance of 0.4Ω, which is much lower than the measured value.

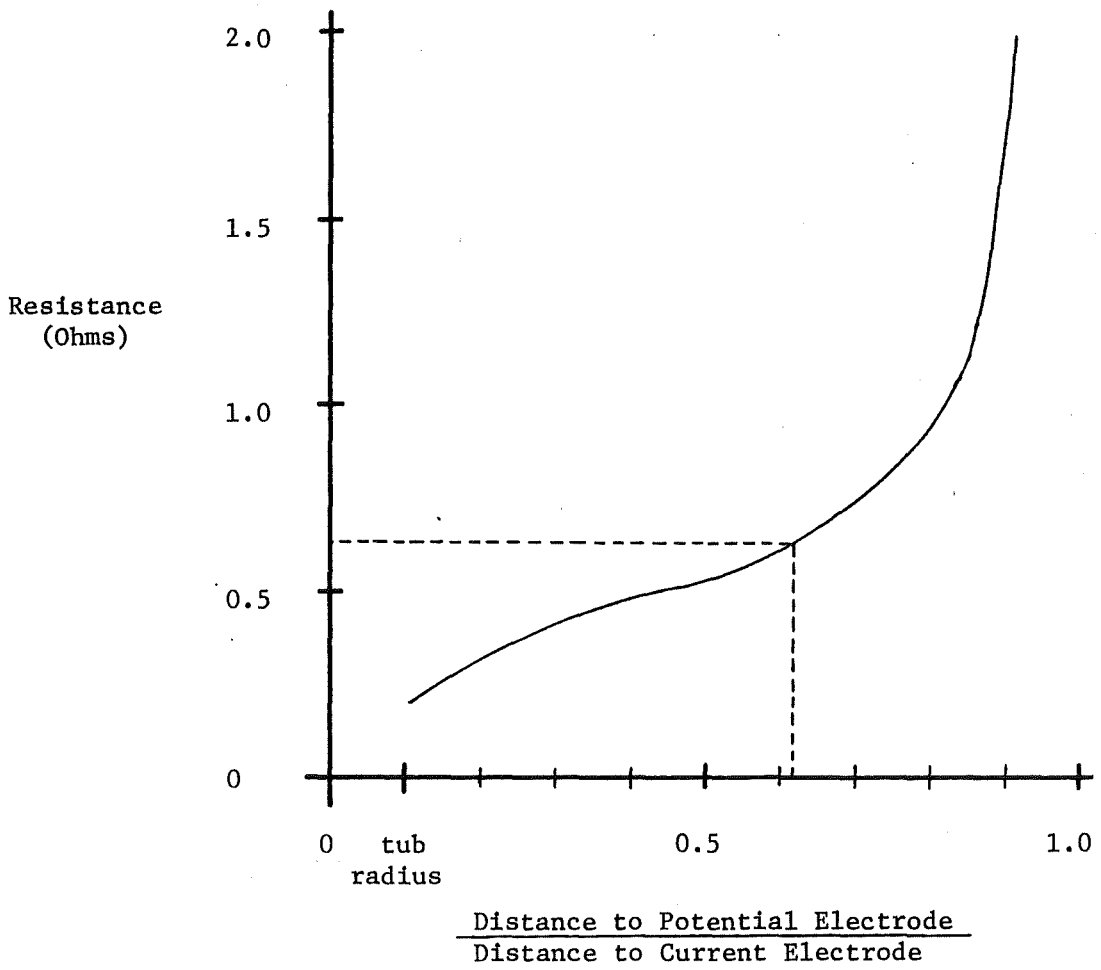


FIGURE 3.8. - Fall-of-potential resistance determination for Marion 7800 Dragline connected to safety ground wire, traverse perpendicular to axis of feet.

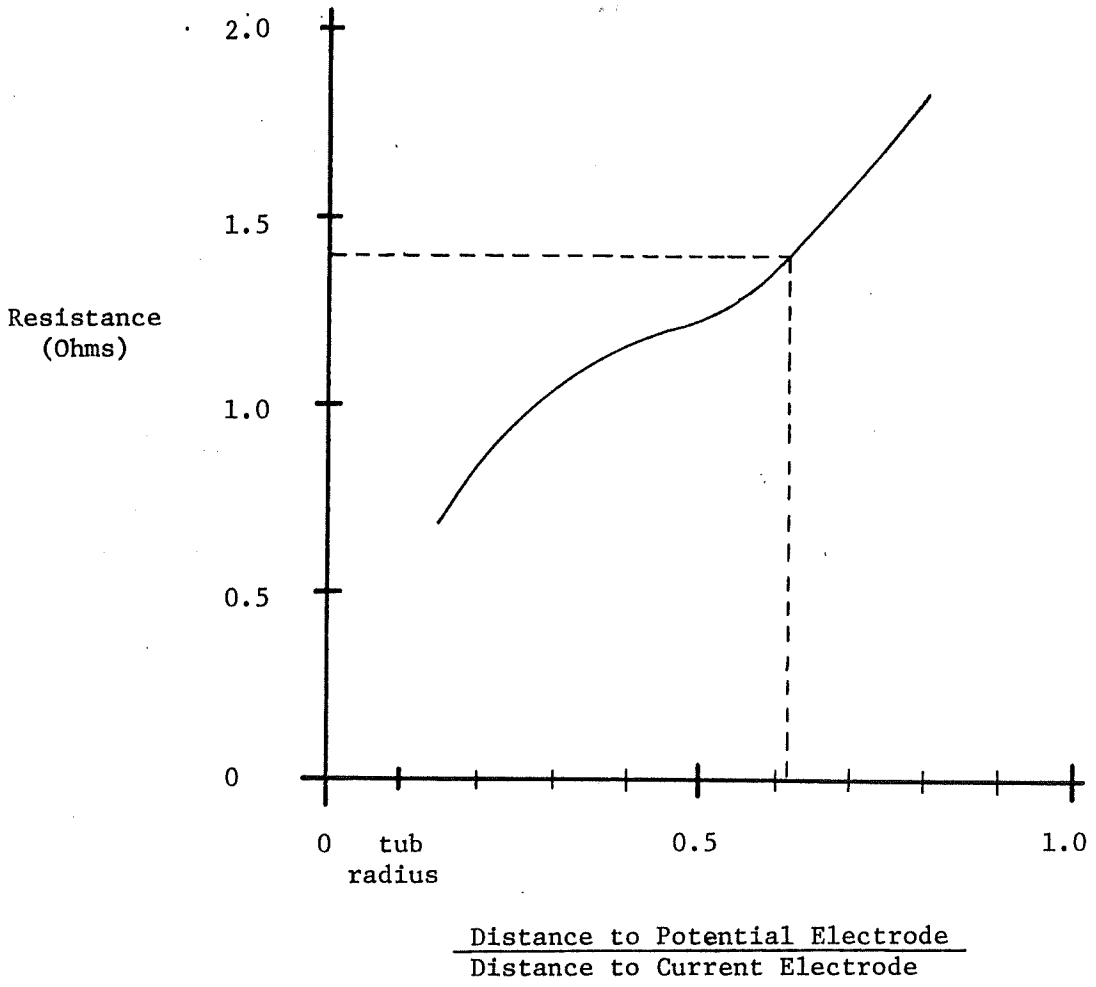


FIGURE 3.9. - Fall-of-potential resistance determination for Marion 7800 Dragline disconnected from safety ground wire, traverse perpendicular to axis of feet.

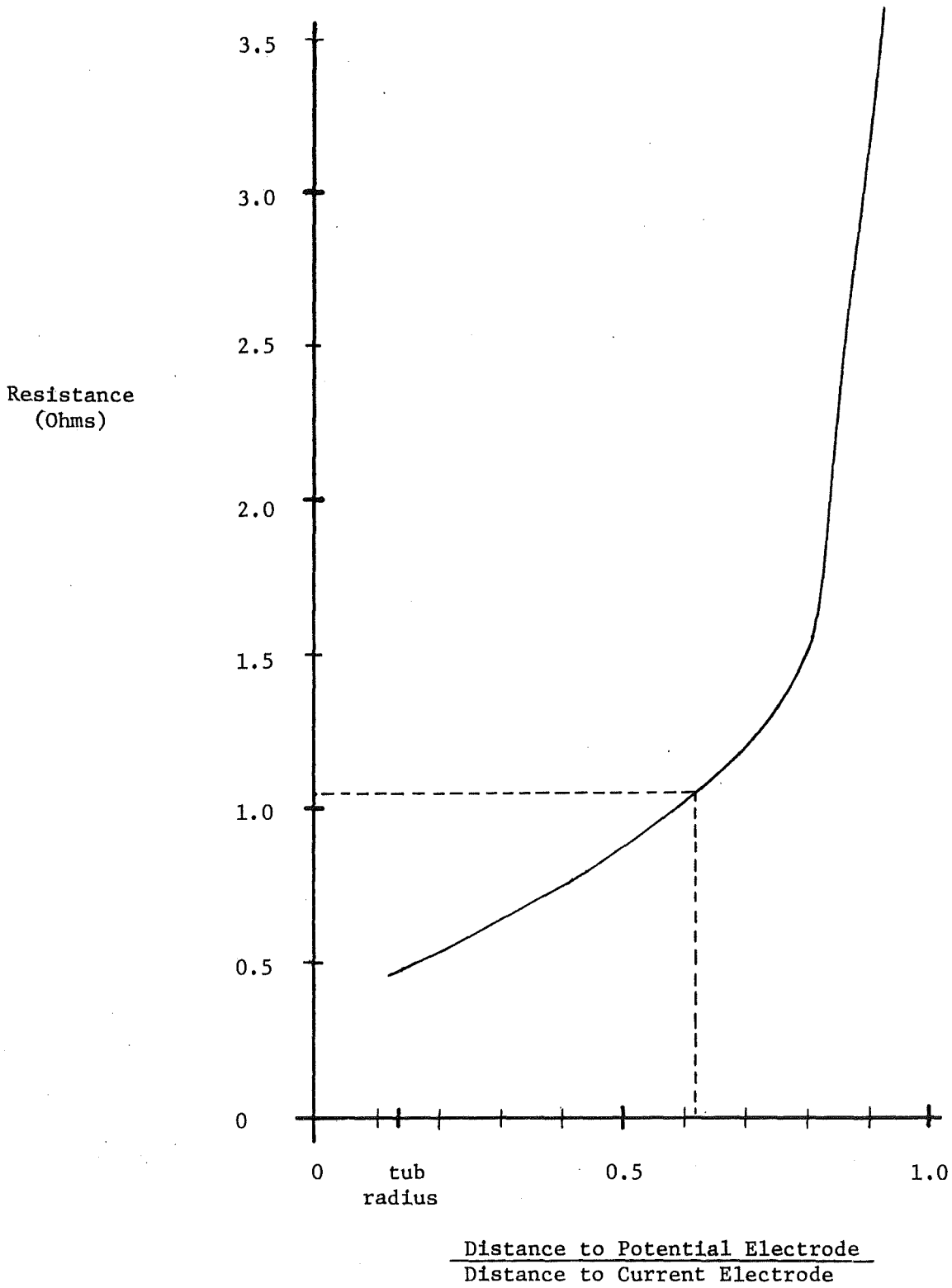


FIGURE 3.10. - Fall-of-potential resistance determination for B-E 500 W Dragline disconnected from safety ground wire, traverse 45° off axis of feet.

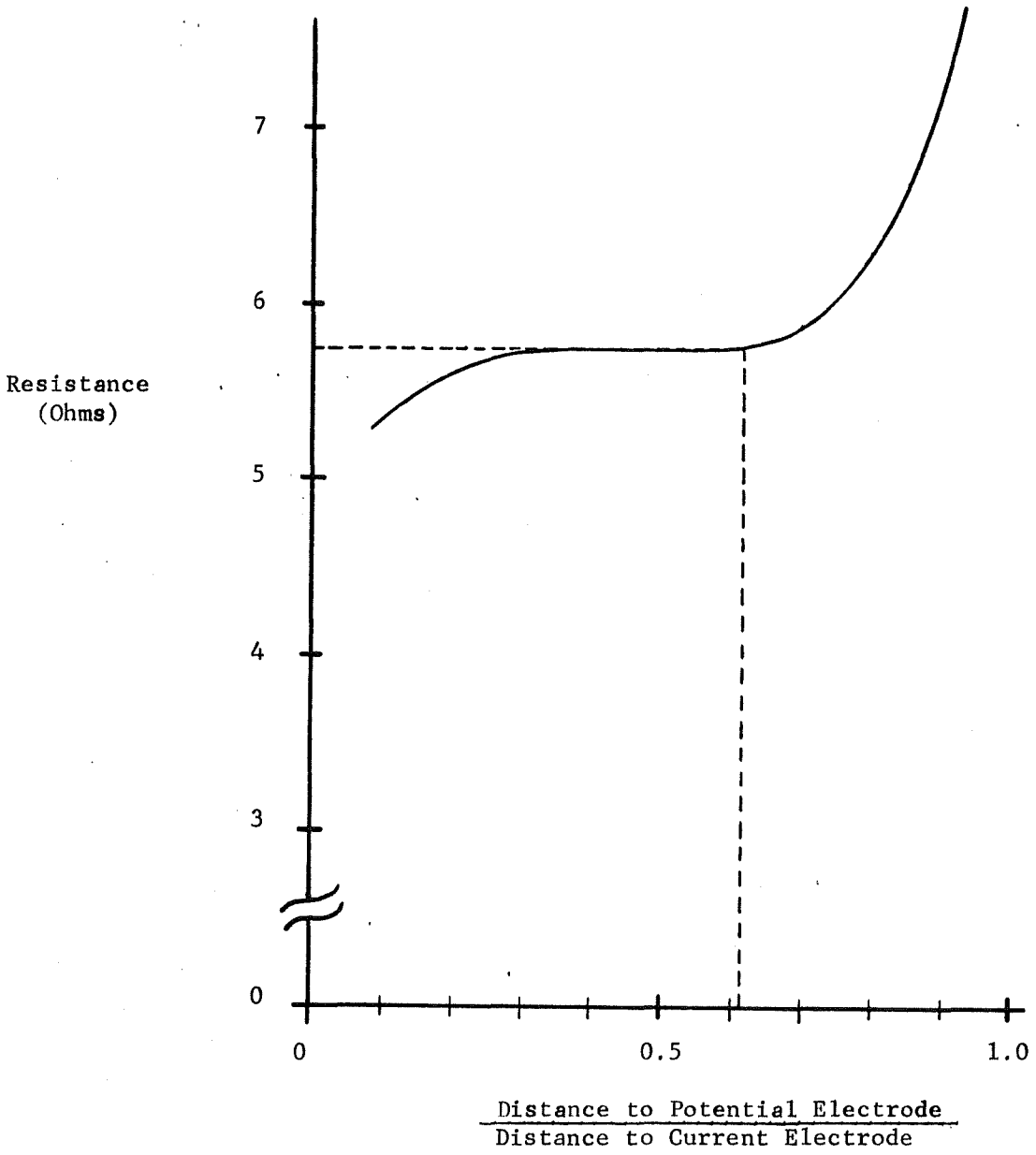


FIGURE 3.11. - Fall-of-potential resistance determination of Marion III-M Shovel disconnected from safety ground wire, traverse directly to rear.

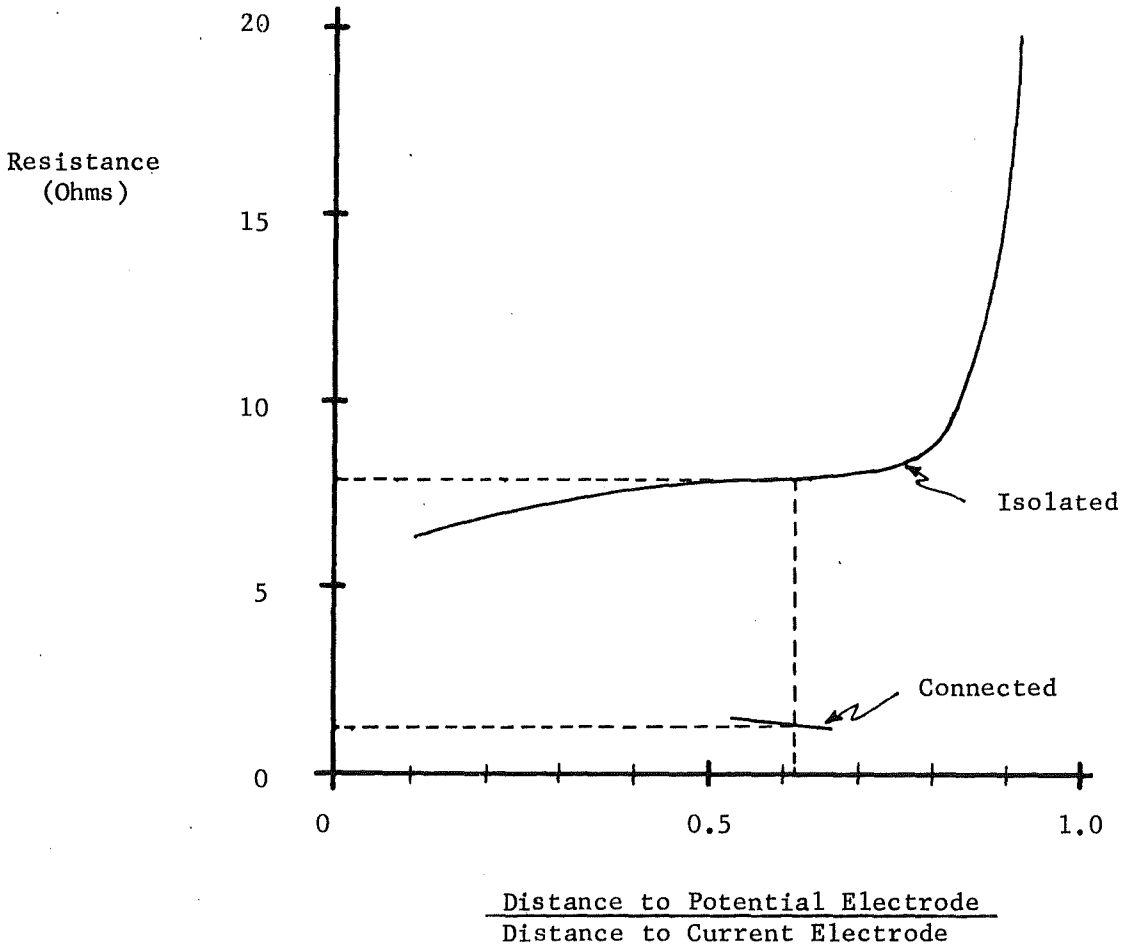


FIGURE 3.12. - Fall-of-potential resistance determinations for B-E 190-B Shovel with safety ground connected and disconnected, traverse directly to rear.

Two large drills, used for making blast-holes in the overburden were also checked. These drills are crawler-mounted and therefore an analysis similar to that used for shovels is appropriate. Again, fall-of-potential measurements were made with the system connected to the machines and also with the drills isolated completely. The first drill measured 4.05Ω earth resistance when isolated, and 1.74Ω when attached to the safety ground grid, as shown by figure 3.13. Theoretical calculations yielded a value of 54.3Ω, which is off by an order of magnitude. As usual, a Wenner 4-probe survey was used to find an average soil resistivity for insertion into the textbook equations. The second drill, which was quite similar to the first, measured 4.8Ω earth resistance when isolated and 1.6Ω when parallel paths were present. Figure 3.14 shows the fall-of-potential plot. Calculations from theory yielded 8.9Ω, which differs from the measurement almost by a factor of 2.

Figure 3.15 is the graph obtained from fall-of-potential measurements made on a large stripping shovel which was sitting on coal and was mounted on eight crawler treads. Because of the orientation of the machine with respect to the pit, the line of electrodes used to make the measurements was parallel to the axis of the crawlers and ran quite close to the shovel's bucket. Although very large in size (34.4 $m^3$, or 45 $yd^3$), the bucket was suspended above the coal seam except for two teeth on the lip of the bucket which were in contact with the coal. The shovel resistance was measured at 8.21Ω, and the presence of the bucket does not seem to have adversely affected the measurement. In contrast with this result, the initial effort to measure the resistance of this shovel consisted of a line of electrodes driven on the opposite side of the machine, parallel with the axis of the treads, and also parallel to the shovel's trailing cable, which ran nearby. Instrument readings did not indicate the usual fall of potential, but remained at essentially the same value, independent of the potential electrode positioning. This apparent isopotential could have been caused by current leakage through the trailing cable into the earth, although mine personnel stated that the machine had been operating satisfactorily. An attempt to calculate the expected shovel resistance by use of equations was not made. The theoretical considerations inherent when dealing with two separate treads are simple when compared to an analysis involving 8 treads.

In a separate but related experiment, the resistance of two sled-mounted junction boxes was measured. Each junction box was directly attached to a length of trailing cable which was laid out on the ground adjacent to the box. The resistance of each box was first measured with the grounding conductors in the trailing cable connected to the junction box; then the grounding conductors were disconnected and the resistance measured again. It was hoped that the effect of capacitive coupling to earth could be seen by the difference (if any) in the two resistance measurements. The first junction box showed negligible change in resistance, while the second box showed a change of about 3%. The fall-of-potential plots are given in figures 3.16 and 3.17. Thus it would seem that coupling between the earth and the grounding conductors or phase conductor shields in a trailing cable can vary to a large extent, presumably depending upon the condition of the cable insulation and jacket.

During the week of 4 June 1978 a second trip was made into the field for the purpose of collecting data. Earth resistance and soil resistivity surveys were made on two electric shovels in a further attempt to verify the applicability of certain formulas (equations 3.2, 3.5, and 3.9) in the calculation of

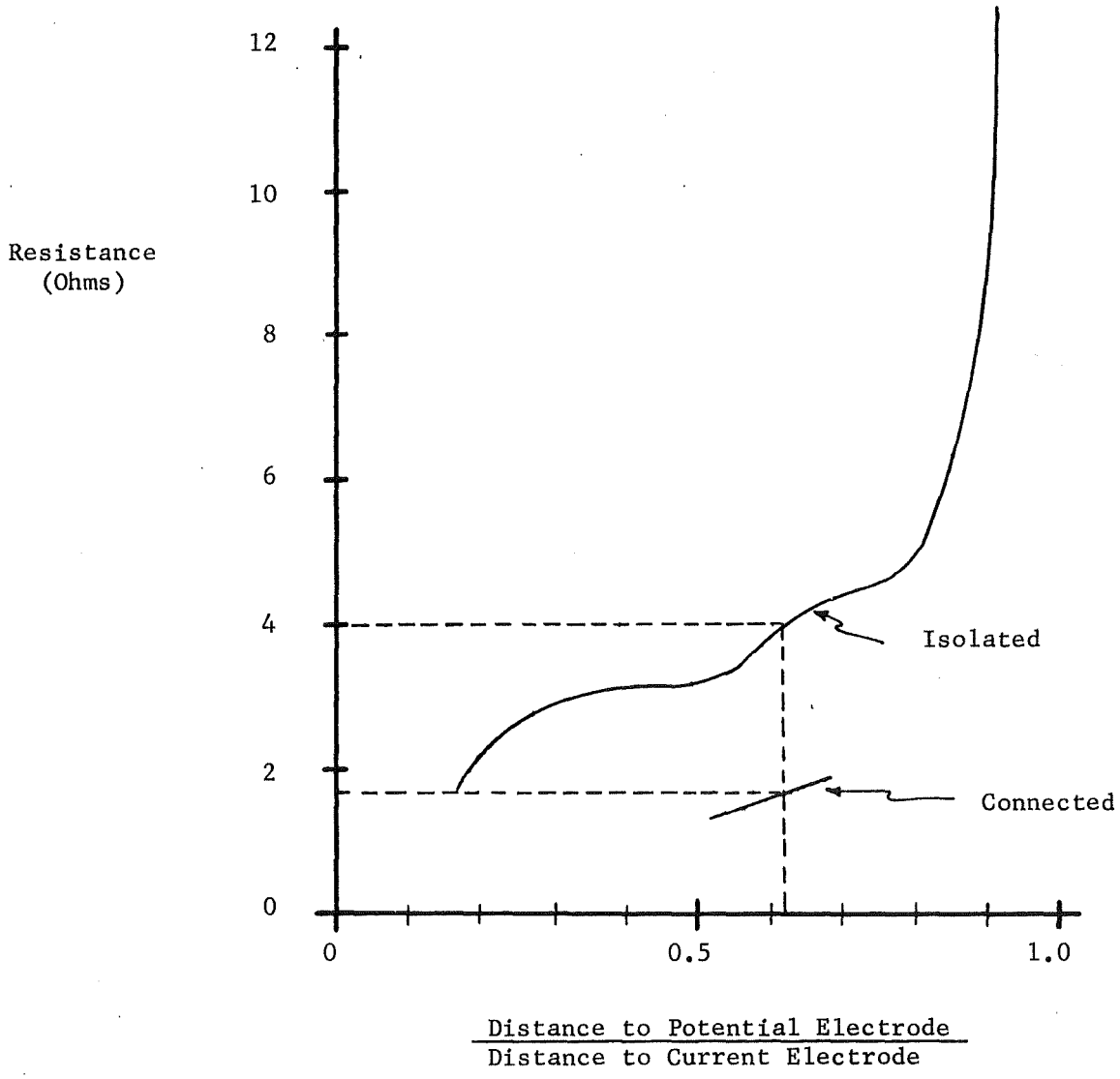


FIGURE 3.13. - Fall-of-potential resistance determinations for B-E 61-R Drill with safety ground disconnected and connected, traverse perpendicular to direction of travel.

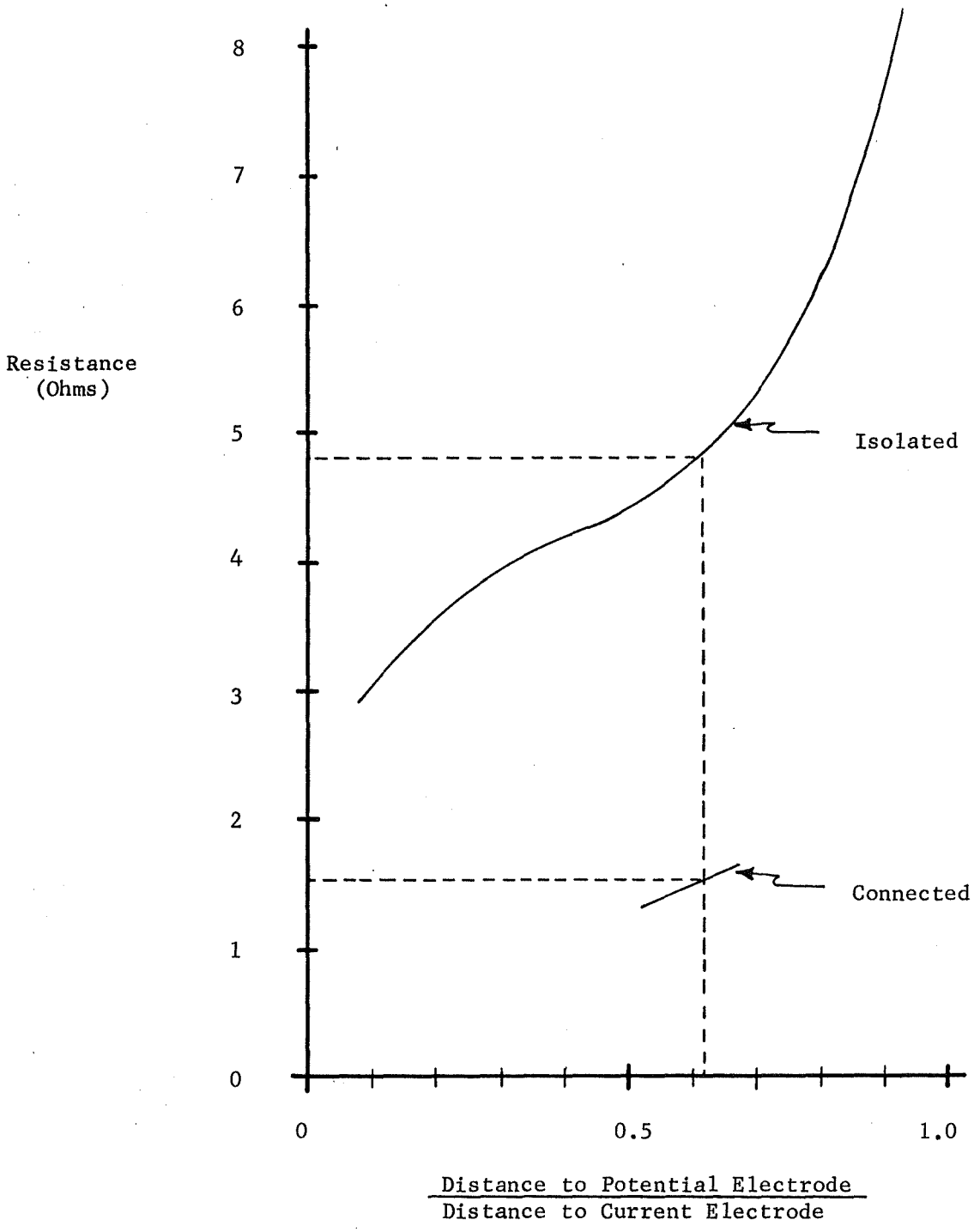


FIGURE 3.14. - Fall-of-potential resistance determinations for B-E 60-R Drill with safety ground connected and disconnected, traverse perpendicular to direction of travel.

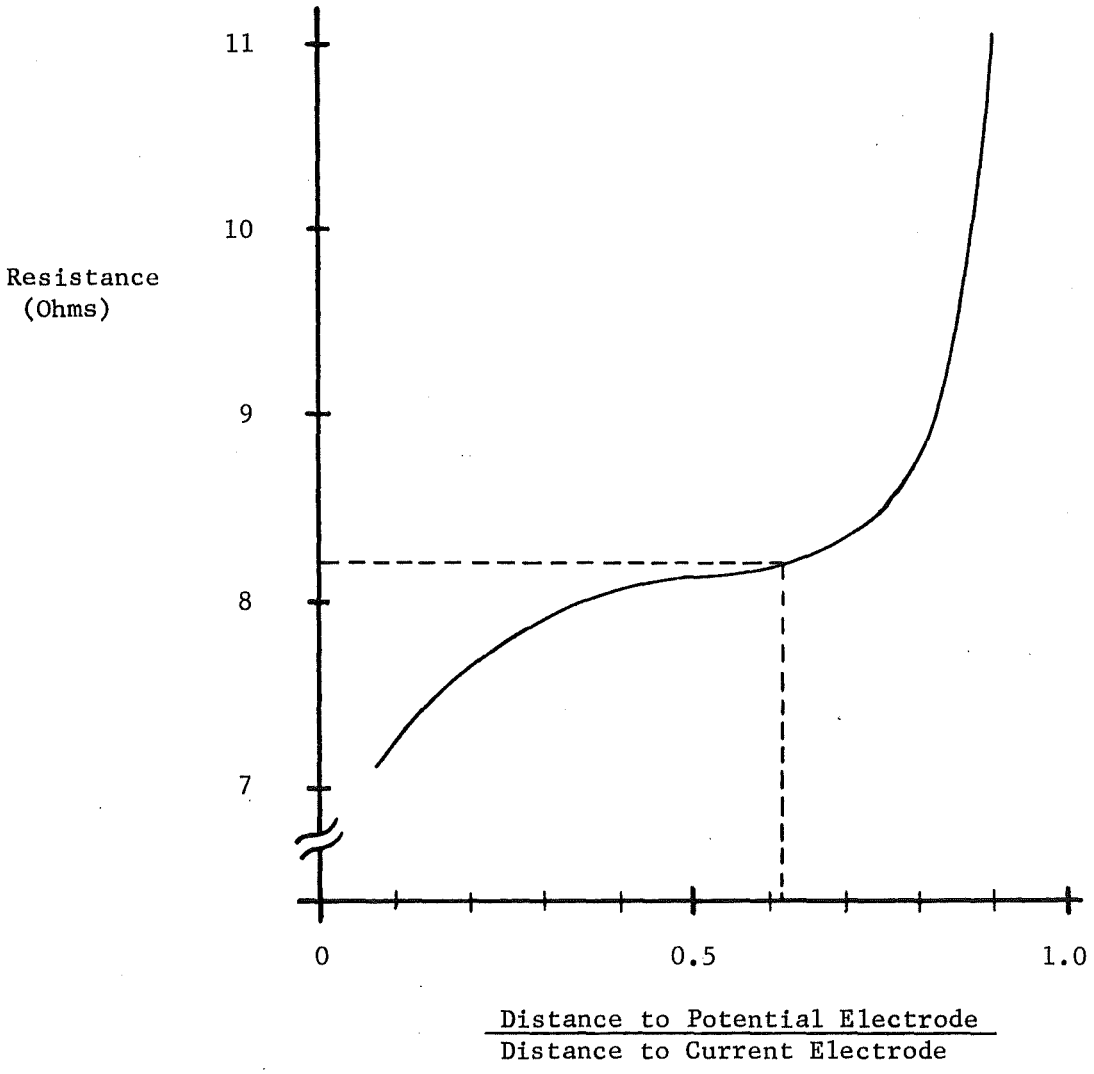


FIGURE 3.15. - Fall-of-potential resistance determination for Marion 5561 Shovel with safety ground disconnected, traverse parallel to direction of travel.

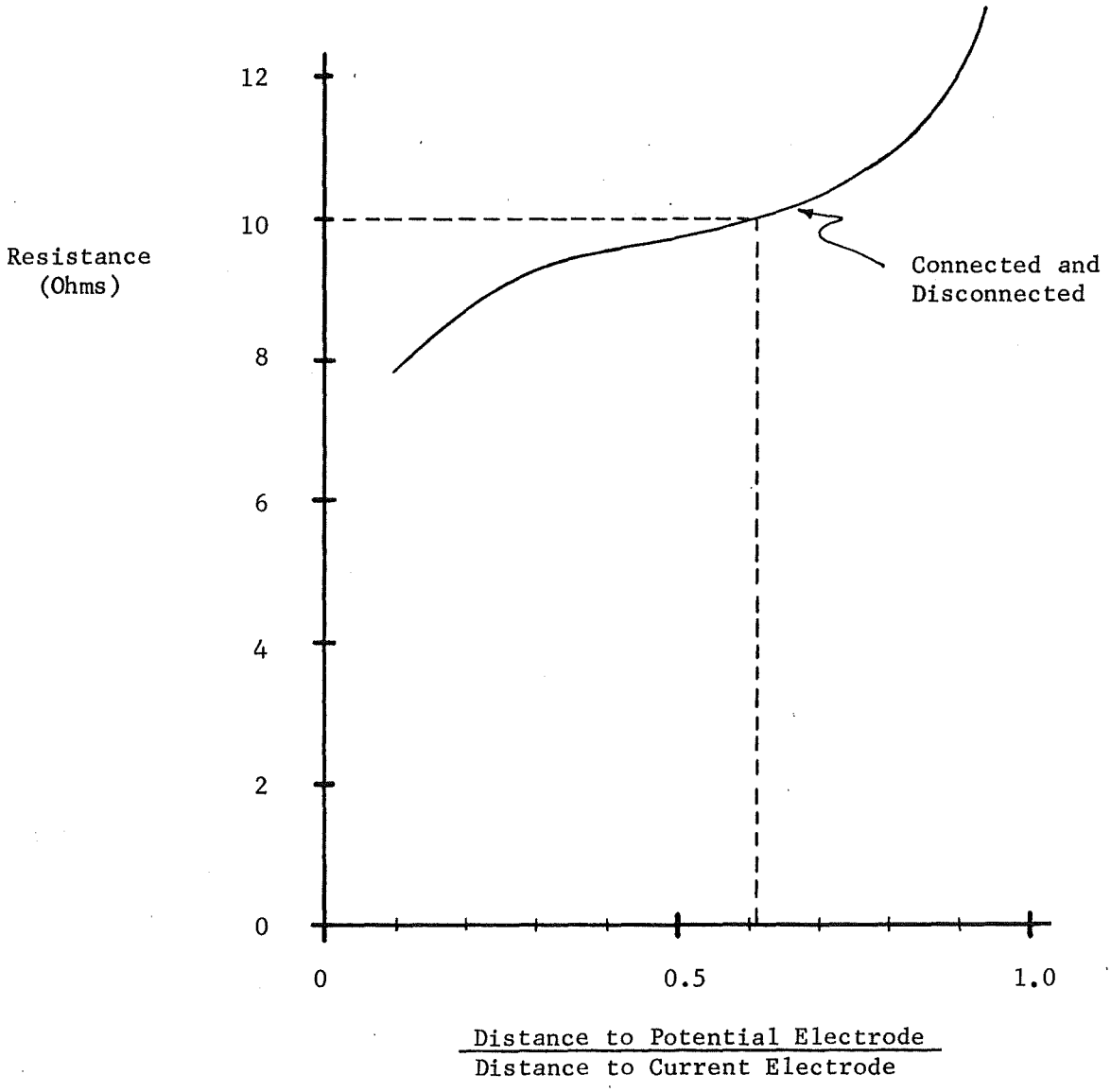


FIGURE 3.16. - Fall-of-potential resistance determination for Skid-Mounted Junction Box connected and disconnected from trailing cable (Box "A").

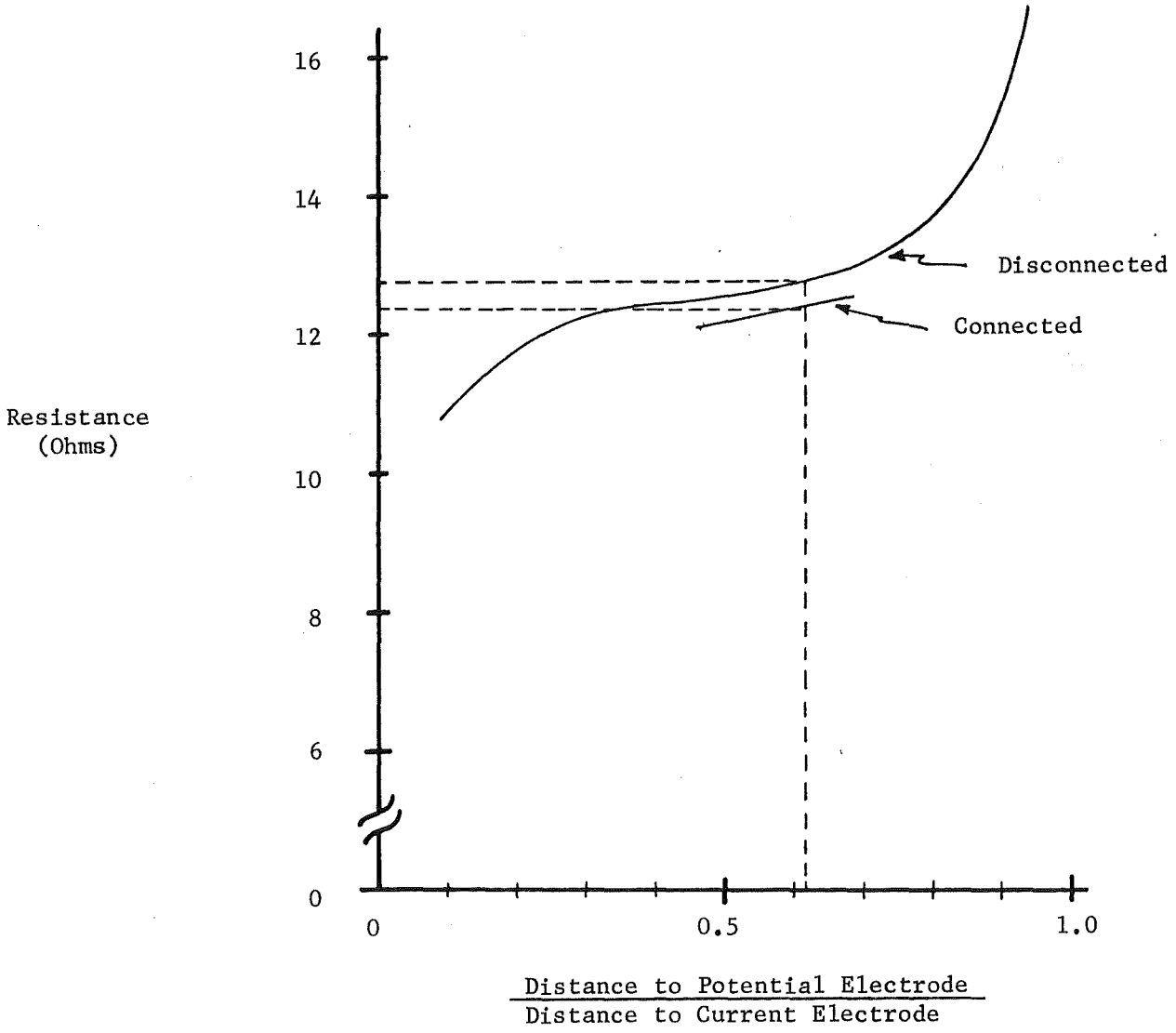


FIGURE 3.17. - Fall-of-potential resistance determination for Skid-Mounted Junction Box connected and disconnected from trailing cable (Box "B").

shovel resistance.

The first shovel measured was being erected near a surface substation, and was ideally situated for the convenience of the field crew. Unfortunately the test instrument carried by the investigators developed a serious malfunction shortly after being set up, and the ideal field conditions quickly deteriorated. After borrowing a manually-operated instrument from the regional office of MSHA, a second attempt was made to perform experiments on this shovel. However, during the time which had elapsed while another instrument was being secured, the shovel had been moved from its previous location atop the soil and was now sitting almost entirely on a series of huge wooden cribs. The cribs were quite moist, however, and proved to have a resistivity of 147.5 Ω-m (484 Ω-ft), while the soil was even more conductive, with a resistivity of 29.9 Ω-m (98 Ω-ft).

Although the shovel rested almost entirely on the wooden cribs, it is reasonable to assume that current flowing through the shovel frame to earth must also flow in the soil. An analysis of the fall-of-potential plot, shown in figure 3.18, yielded a resistance value of 4.78Ω. Using just the soil resistivity value in the equation gives a result of 3.53Ω, while the value of resistivity for the wood alone yields 17.43Ω. As can be seen, the true resistance value lies between the limits found by using either resistivity figure alone.

A second shovel was also measured, this one sitting on an undisturbed rocky overburden near a substation. Three resistivity readings were taken, using the 4-probe Wenner array at electrode spacings of 0.6, 1.5, and 3 m (2, 5, and 10 ft). The average resistivity value was calculated, and plugging this figure into the equation yielded an earth resistance of 4.43Ω. The measured value of 4.72Ω, shown in figure 3.19, differs from the calculated value by less than 7%. It should be noted in this case that all three resistivity values obtained from the Wenner arrays were relatively close to each other.

Figure 3.20 is a graph of the fall-of-potential survey performed on a vertical-mast rotary drill used for boring blastholes in the overburden. The earth resistance is 13.23Ω. Since the drill contact surface was composed of 4 large circular jacks in addition to the normal pair of crawler treads, the equation derived for use with shovels is inappropriate and no calculated resistance could be derived.

Table 3.1 summarizes the results of resistance measurements made on the surface equipment described above. Note that all the values are below 15Ω, with the draglines being less than 2Ω, while all the shovels fall below 10Ω. The field tests show that it is not presently possible to get an accurate indication of earth resistance simply by measuring the physical size of the contact area, measuring the soil resistivity, and then plugging these numbers into an equation. For the draglines which were examined, it appears that use of an equation can yield values which agree with field measurements within about ±50%, which is not overly impressive. However, the equation used is relatively simple. For shovels or drills mounted on two caterpillar treads, agreement between equation and field measurement is poor. The presence of two separate contact surfaces (the treads) leads to an analysis which is much more complex and subject to approximations. The wide discrepancy in the results suggests that the equation is of limited validity. Therefore, earth

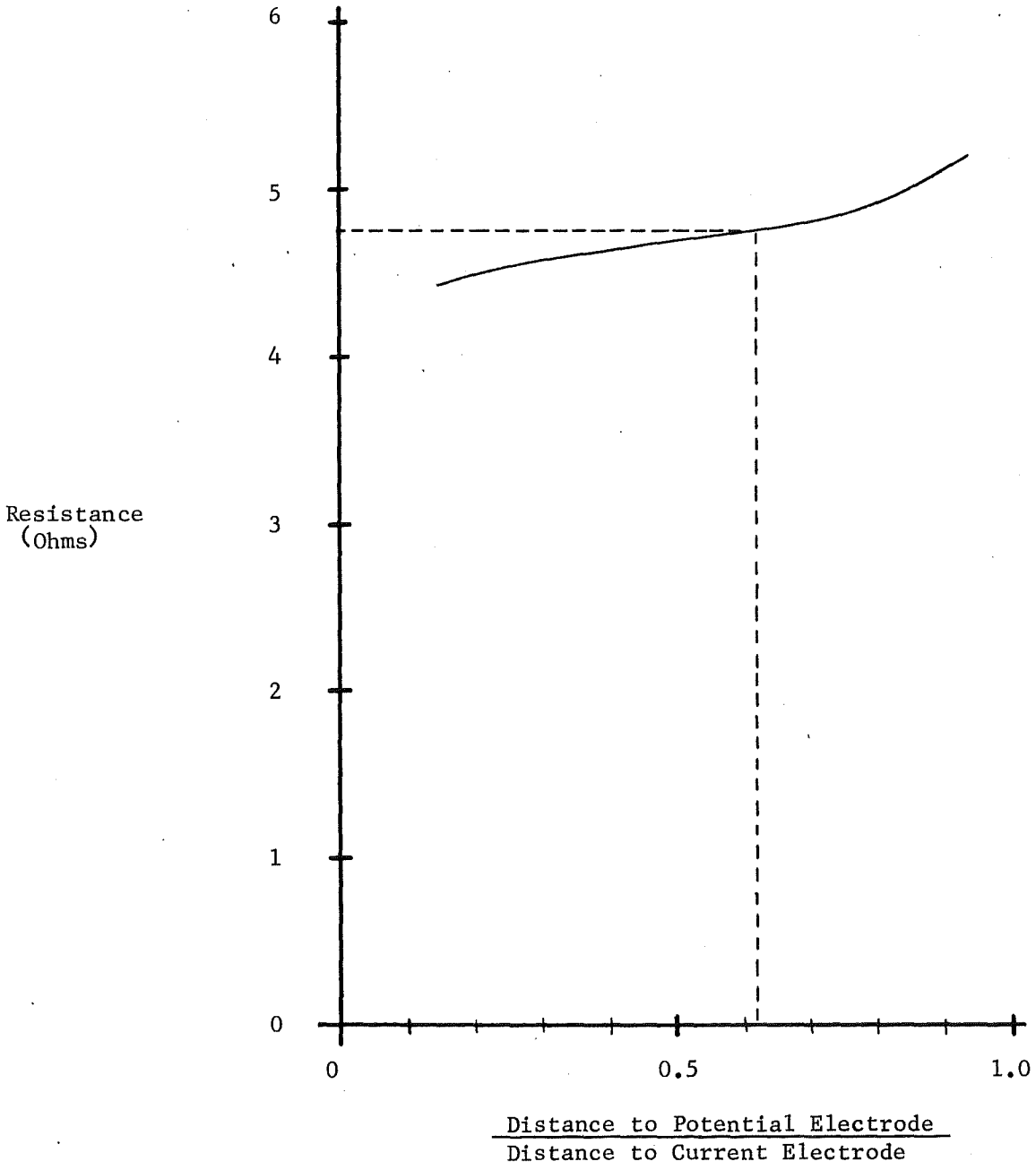


FIGURE 3.18. - Fall-of-potential resistance determination for B-E 191 Shovel disconnected from safety ground, traverse parallel to direction of travel.

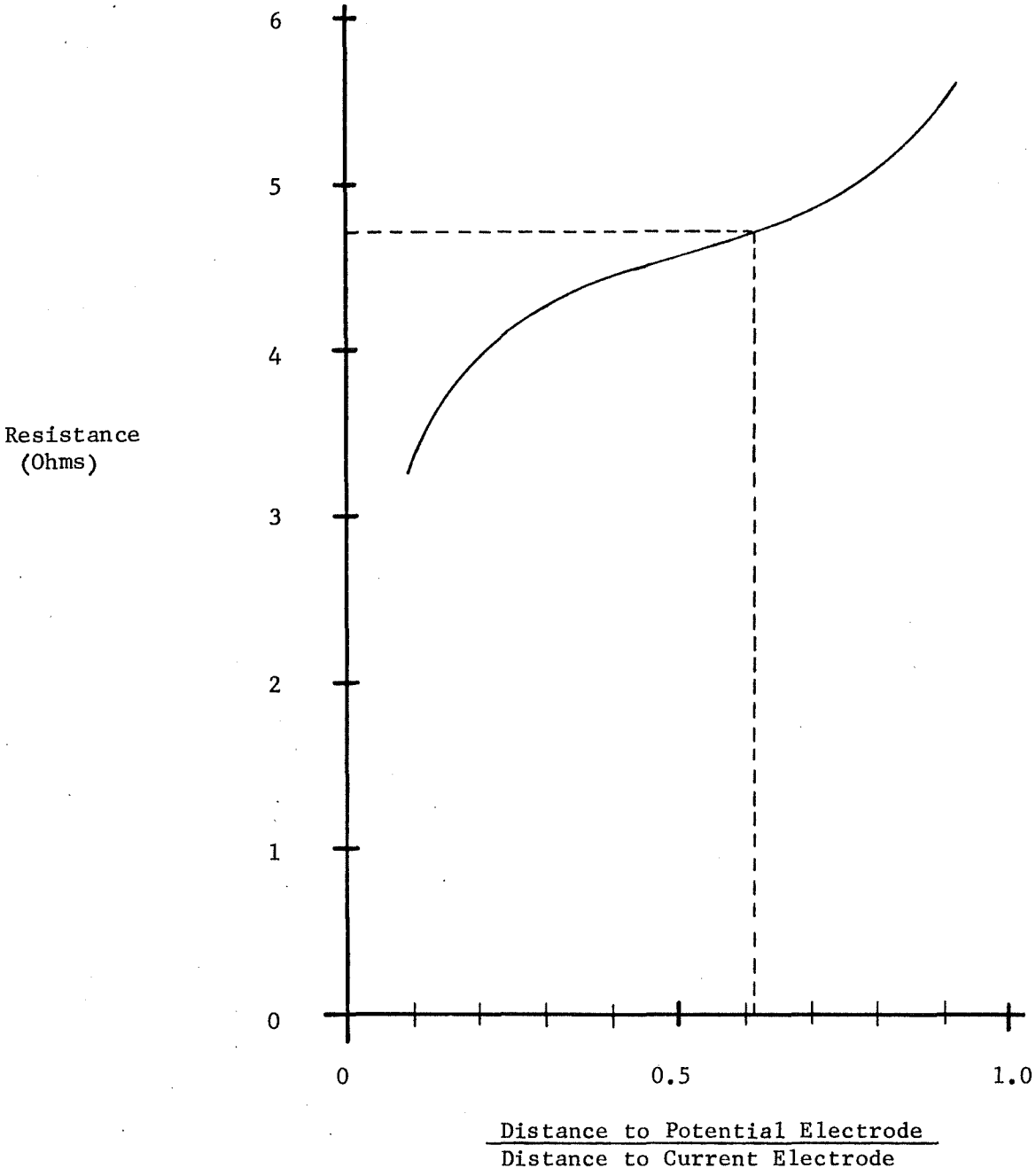


FIGURE 3.19. – Fall-of-potential resistance determination for B-E 280-B Shovel disconnected from safety ground, traverse 45° from direction of travel.

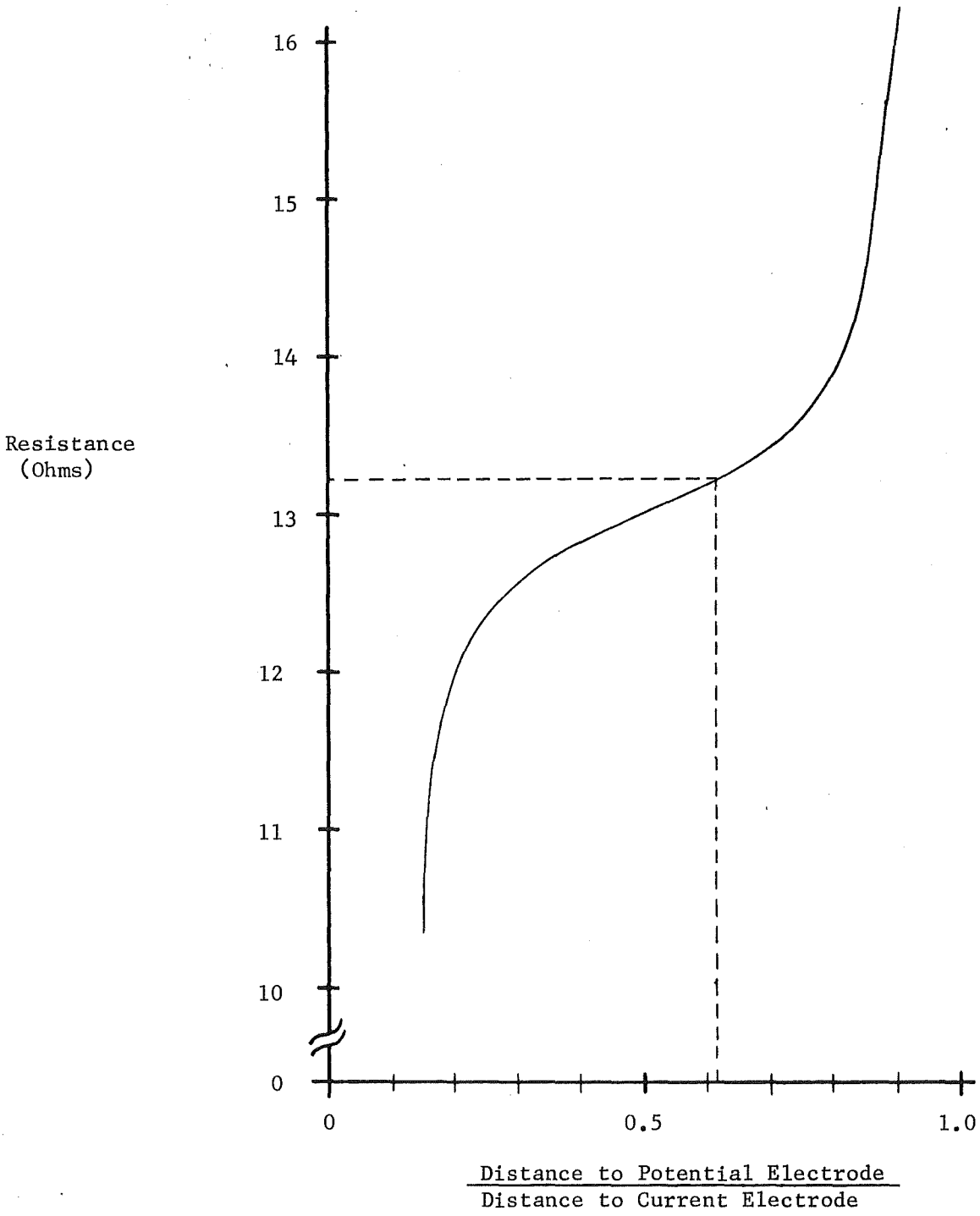


FIGURE 3.20. – Fall-of-potential resistance determination for Joy R-15 Drill disconnected from safety ground, traverse parallel to direction of travel.

TABLE 3.1. - Resistance values for several pieces of mining equipment

| Machine | Contact Area, $ft^2$ | Contact Area, $m^2$ | Measured Resistance, ohms | Calculated Resistance, ohms* |
|---|---|---|---|---|
| Marion 7800 Dragline . . . | 1520 | 141.2 | 1.4 | 1.8 |
| B-E 500-W Dragline . . . . | 804 | 74.7 | 1.05 | 1.73 |
| Marion 111-M Shovel . . . | 96 | 8.9 | 5.75 | 14.0 |
| B-E 190-B Shovel . . . . . | 152 | 125.9 | 7.9 | 5.8 |
| B-E 280-B Shovel . . . . . | 198 | 18.4 | 4.72 | 3.39 |
| B-E 191 Shovel . . . . . | 115 | 10.7 | 4.78 | 2.22 |
| Marion 5561 Shovel . . . . | 448 | 41.6 | 8.21 | -- |
| B-E 61-R Drill . . . . . | 152 | 14.1 | 4.05 | 14.5 |
| B-E 60-R Drill . . . . . | 152 | 14.1 | 4.8 | 9.8 |
| Joy R-15 Drill . . . . . | 86 | 8.0 | 13.23 | -- |

* For treads, $\bar{p}$ = p measured at spacing "a" $\simeq$ 1.5 x tread length

resistance should always be made via direct connection to the machine in question, even though this is more difficult and may lead to a loss in production.

### 3.1.5 Surge Impedance of Electrodes

A general conclusion which can be reached after a study of the literature is that the impedance of an earth electrode subjected to large-amplitude surges will be equal to or less than its 60 Hz resistance (10, 52).

The major cause of this phenomenon is breakdown of the soil surrounding the electrode under the stress of intense electric fields (40). In this manner the apparent physical size of the electrode increases to the dimensions of the soil volume in which breakdown has occurred, as shown in figure 3.21. In addition to breakdown within the soil volume, electrode resistance may be reduced due to the formation of streamers radiating horizontally along the surface of the ground (10).

Because lightning or transient surges have steep wavefronts, the character of a ground rod or electrode presumably will appear different as viewed by these high frequency waves than it would in the presence of power frequency currents. Tests have shown that soil resistivity decreases with frequency but figure 3.22 reveals that this effect is not pronounced (46). Since lightning is basically a current impulse of tremendous amplitude, perhaps it is the peak current magnitude which determines electrode behavior rather than the spectral content of the stroke. Independent tests by a number of experimenters all show that the surge impedance ($Z_o$) of a ground electrode is less than or equal to its resistance (R) under steady-state conditions (10, 52). This decrease in resistance was thought to arise from electric discharges which short-circuited higher-resistance portions of the soil. Therefore a series of laboratory demonstrations was carried out using a smooth hollow sphere as an earth electrode and measuring the current flow into the sphere for various impressed voltages (40). The ratio of voltage to current was assumed to be the electrode resistance. Several pointed projections were then added to the sphere and the tests repeated. As the length of the points was increased, the surge resistance dropped steadily, as shown in figure 3.23. It seems that an electrode design which leads to the development of high electric field intensities will yield the lowest surge impedance.

Similar studies on rod electrodes gave essentially the same results. In each case, oscillographic records were made of voltage and current versus time, from which graphs of voltage versus current (resistance) were drawn (47). Figure 3.24 shows the results for a small rod electrode in point contact with plastic clay. The initial resistance is about the same as that found when the electrode was measured using a "Megger", but after some time lag the voltage reached a level where the surrounding soil broke down and the effective resistance fell markedly. The input waveform used was a 1.5 x 40 μs impulse. The field strength required to produce soil breakdown varies widely, depending upon the composition and moisture content of the soil, but tests have yielded figures in the range from 1-40 kV/cm (2, 8, 10, 40)

Much effort has been spent to determine the expected surge impedance of an earth electrode if its steady-state resistance is known. In general it has been found that a low-resistance earth electrode will exhibit a somewhat lower

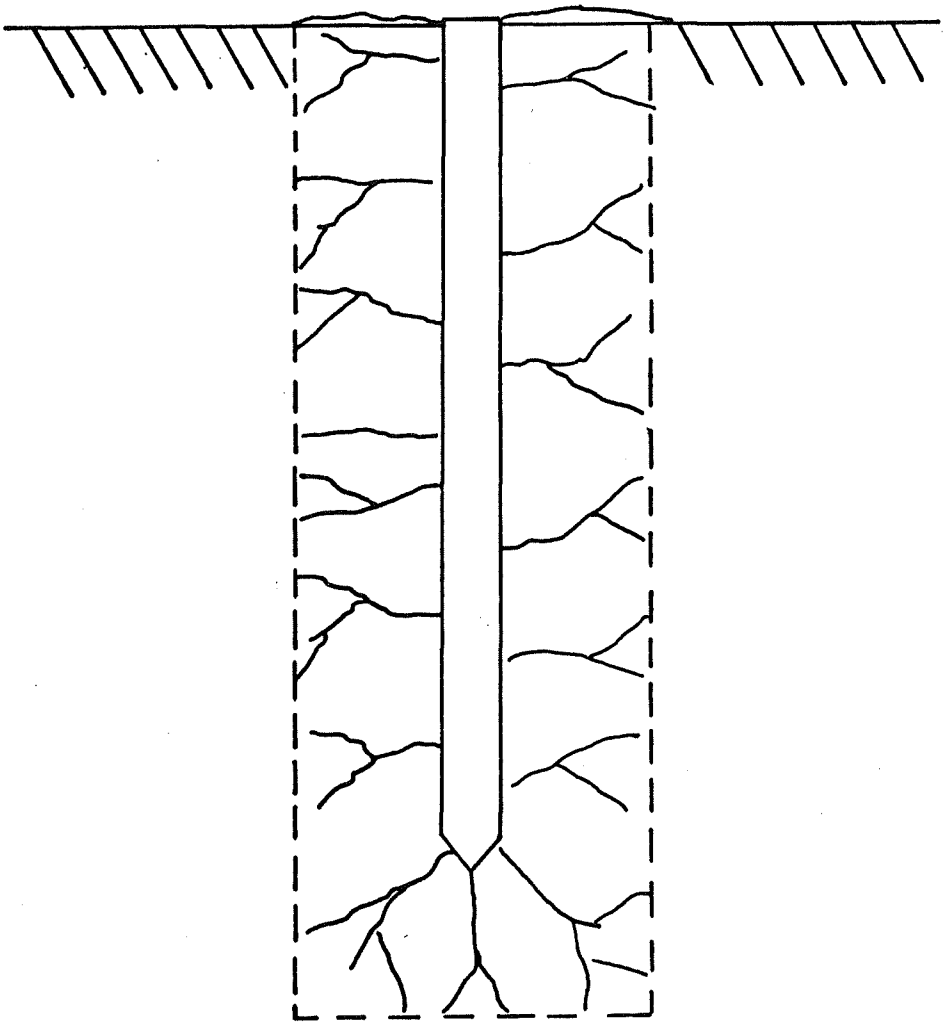

FIGURE 3.21. - Increase in effective size of earth electrode under surge conditions due to breakdown of surrounding soil (3).

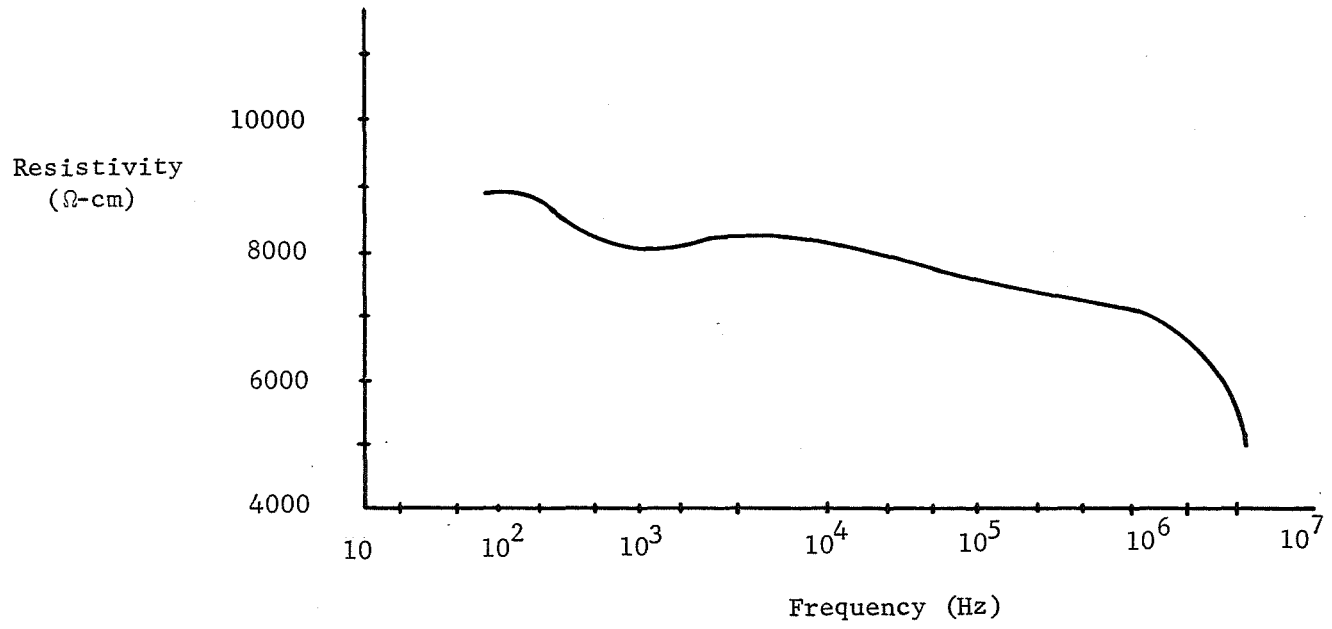


FIGURE 3.22. - Variation of soil resistivity with test frequency (46).

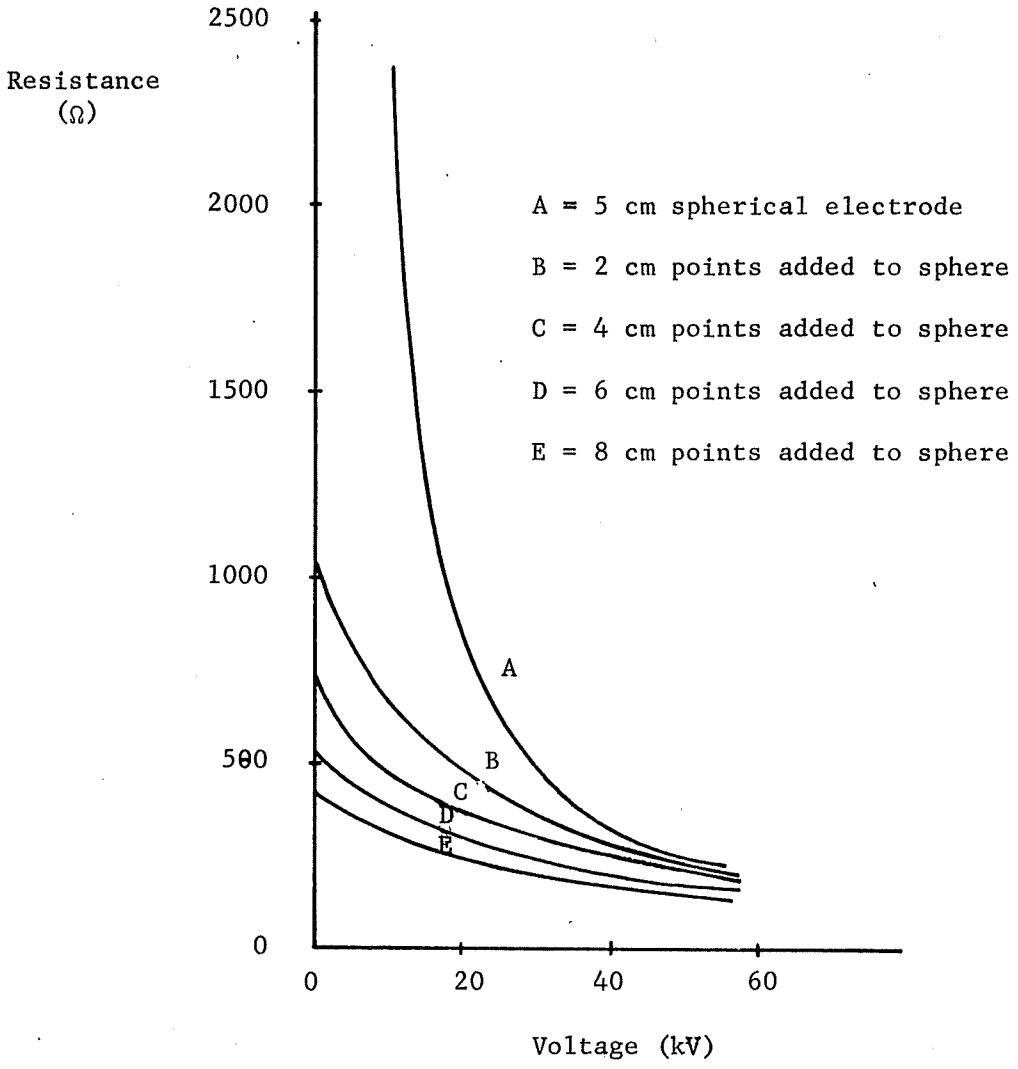


FIGURE 3.23. - Effect of electrode shape on surge impedance (40).

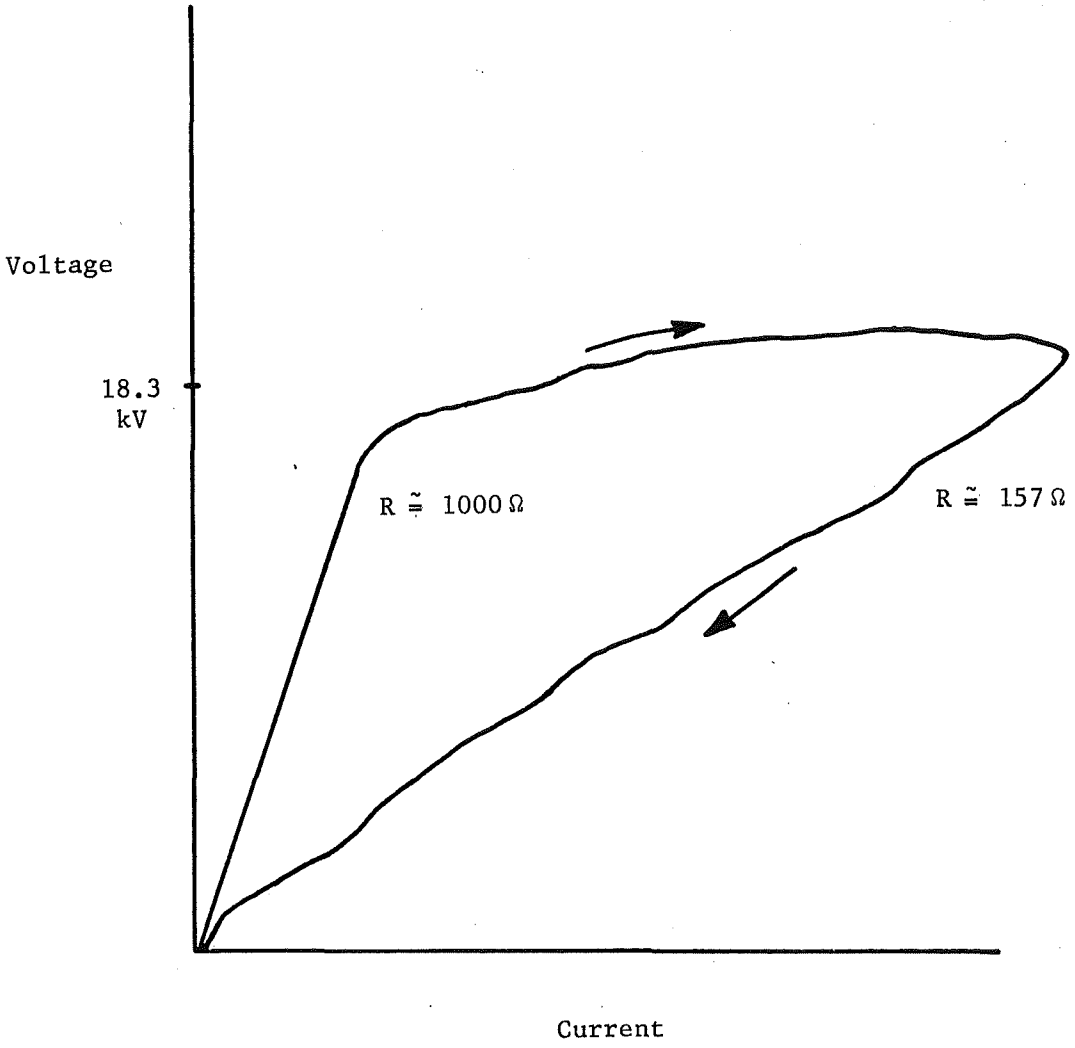


FIGURE 3.24. - Variation in apparent resistance of earth electrode under surge conditions (10).

value of surge impedance, while a high-resistance electrode will have a surge impedance which can be only a small fraction of its normal resistance (3, 54). When subjected to a lightning-induced current surge, high-resistance electrodes develop correspondingly higher voltages and potential gradients, thereby leading to more pronounced decreases in their apparent resistance. This effect is shown in figure 3.25, which illustrates the ratio of impulse impedance to 60 Hz resistance for four different rod electrodes subjected to various magnitudes of impulse current. The rod with the highest steady-state resistance showed the greatest fall in resistance under impulse conditions, while the rod with the lowest initial resistance showed the smallest decrease. The range in resistance values at steady-state was from 13.75Ω to 149Ω, while the spread of impulse impedance values was from 10Ω to 30Ω. The tendency for high-resistance grounds to break down more dramatically under impulse conditions has the effect of bringing closer together the surge impedance of high and low-resistance grounds.

If lightning should strike the mast of a drill or the boom on a shovel or dragline, there are several paths to ground for the surge current. The shortest path would be directly through the machine/earth contact interface. The other path would be back along the metallic ground conductors to the safety ground bed. Typical resistance values for machinery which is commonly found in most surface coal mines have previously been listed as Table 3.1. It is possible that, if a machine were struck by lightning, the surge impedance would be even lower than the resistance value shown in the Table. Since the approximate surge impedance of a trailing cable is 50Ω, it is likely that current from a lightning stroke would flow to earth through the machine frame.

### 3.1.6 Mapping of Potential Gradients Around Machines

Table 3.2 shows some typical lightning-stroke parameters gathered by researchers during years of work in countries throughout the world. Assuming that a 20kA lightning-stroke were to hit an electric shovel and go to earth through the machine/soil interface, and that the machine's surge impedance was 5Ω, then a potential of 100kV would be impressed on the machine frame. The flow of current through the soil underlying the shovel would produce a potential field on the surface of the earth surrounding the machine. A large surface-mine complex in the Midwest was visited to map potential gradients around equipment.

### 3.1.7 Potential Maps From Field Trip Results

Figure 3.26 shows an actual map of the surface potentials around a Bucyrus-Erie 280-B loading shovel. The machine was first disconnected from the substation, and a small test current was circulated between the machine frame and a driven rod located 61 m (200 ft) away. The voltage on the shovel frame (and the bucket) was normalized to 1.0, and the numbers on the contour lines represent the potential between the machine frame and that point on the earth's surface. Because the shovel's counterweight overhangs the treads by several feet, a person standing on the earth while touching the rear of the shovel could in this instance be exposed to 80% of the frame potential, which would amount to 80kV in the previously-mentioned example. The potential gradients are particularly steep near the bucket and near the crawler treads, especially at the corners. It is possible that a person standing on the earth while touching the machine could be severely shocked. High step potentials would

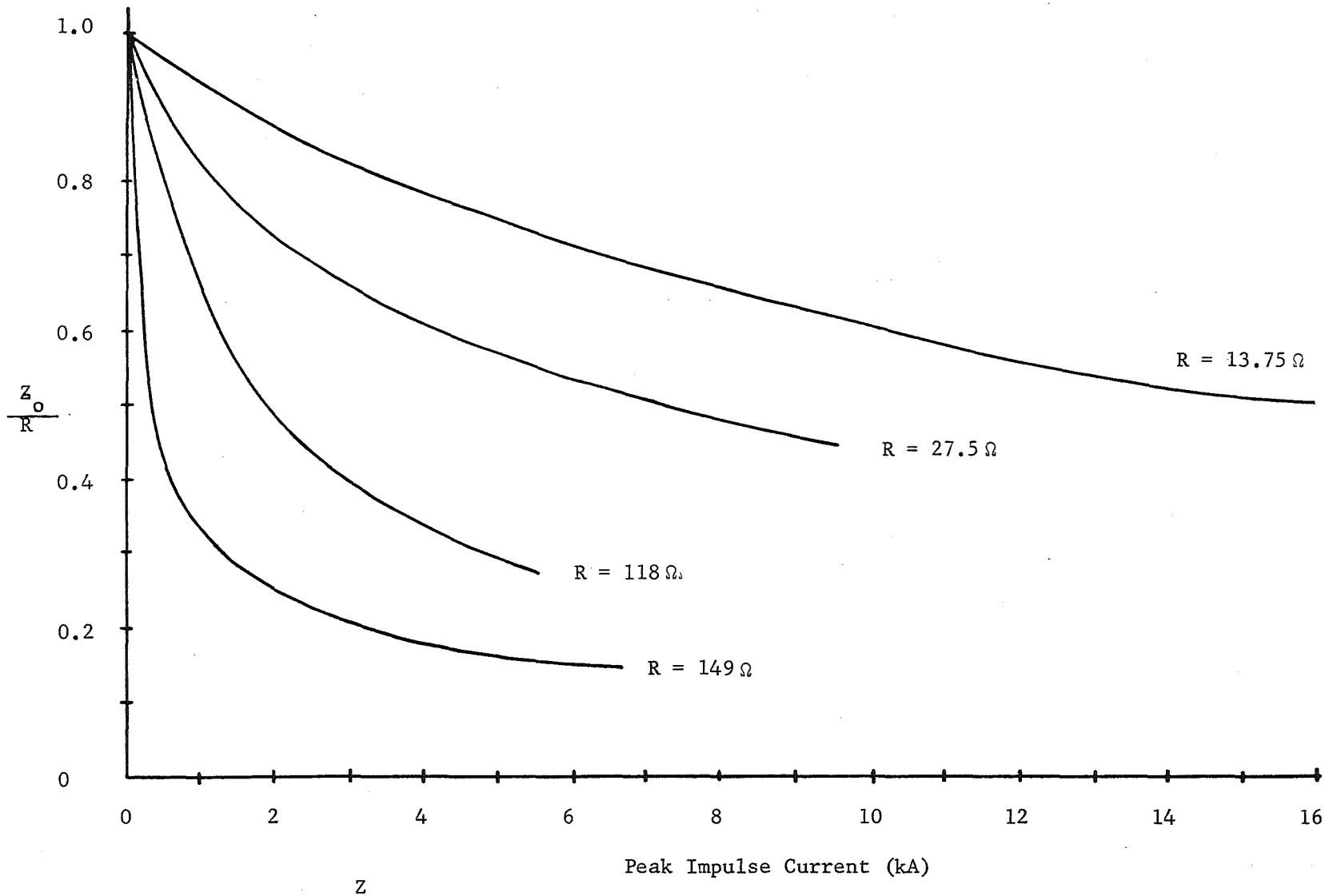


FIGURE 3.25. - Variation in $\frac{Z_o}{R}$ ratio as a function of current for several rod electrodes (3).

TABLE 3.2. - Lightning parameters (54)

| Parameters | Values | | |
|---|---|---|---|
| | Minimum | Average | Maximum |
| Return Stroke: | | | |
| Propagation velocity, m/s | $2 \times 10^7$ | $5 \times 10^7$ | $14 \times 10^7$ |
| Current rise, kA/μs | < 1 | 10 | < 80 |
| Time to peak current, μs | < 1 | 2 | 30 |
| Peak current, kA | - | 10-20 | 110 |
| Decay time to half of peak current, μs | 10 | 40 | 250 |
| Charge transferred, C | 0.2 | 2.5 | 20 |
| Lightning Flash: | | | |
| Number of strokes per flash | 1 | 3-4 | 26 |
| Time interval between strokes, ms | 3 | 40 | 100 |
| Duration of flash, s | 0.01 | 0.2 | 2 |
| Total charge transferred, C | 3 | 25 | 90 |

Crawler Treads = 1.4 x 6.7 m (4.5 x 22 ft)
Bucket = 3.05 x 3.05 m (10 x 10 ft)

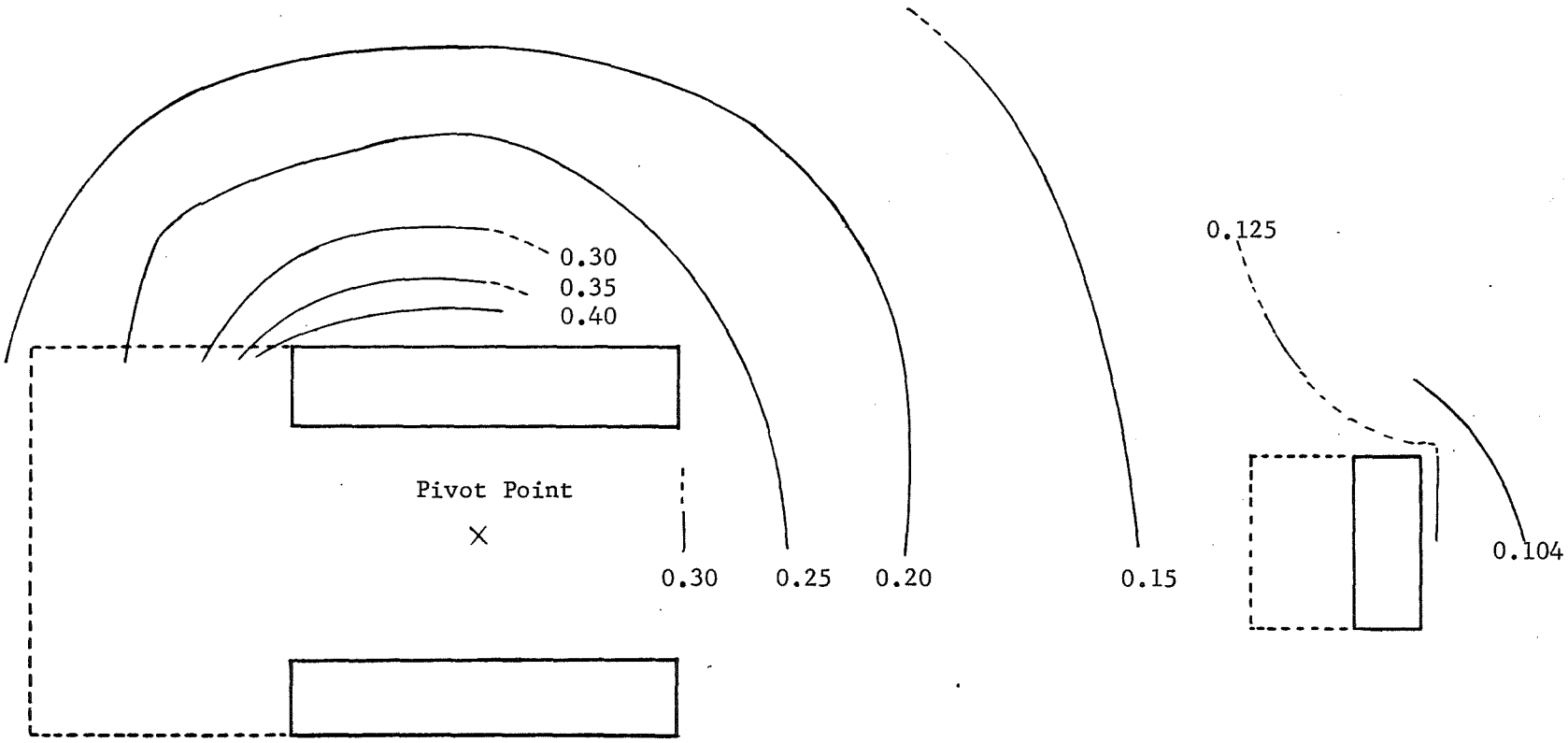


FIGURE 3.26. - Potential gradient survey around a loading shovel, with voltages in per unit of frame potential.

also exist in the area surrounding the shovel, even at distances of 25 feet or more. Thirty meters (100 ft) from the machine, the potential gradient would be better than 325 volts per meter (100V/ft).

Figure 3.27 shows an abbreviated potential survey made around another loading shovel. As in the previous figure, the potential drops off sharply along a line extending from the ends of the crawler tread, while the gradients are more gradual in the direction perpendicular to the tread. A potential map around a vertical-mast drill rig is shown in figure 3.28. The shape of the equipotential lines seems to indicate that the four large circular jacks are supporting a lot of the drill's weight. Some of the equipotential contour lines seem to pass beneath the crawler tread, which would show that portions of the tread were not in contact with the mine floor.

A visit was made to MSHA headquarters in Washington, DC, to examine Federal accident reports on electrical fatalities in surface-mine environments. Records were found on 90 deaths which had occurred since 1969. A complete review of these records failed to produce any direct evidence of electrocution caused by lightning striking a machine, although several accidents were described where the cause of death was undetermined.

In some cases, malfunctions can lead to elevated frame potentials, but several steps can be taken to minimize the likelihood of electrocution. Persons in contact with the ground should not sit, touch, or lean against any piece of equipment. To facilitate getting on and off the machine, hand rails and steps should be constructed of non-conducting material, or should be well-insulated from the machine frame if made of metal.

If the metallic ground conductor leading from the machine frame back to the safety ground bed at the substation should become open, then the equipment could become elevated to a dangerous potential in the event of a phase-to-ground fault. This situation is unlikely in mines which use trailing cable for the entire span between substation and machine, but is quite possible if overhead distribution lines are used to connect substations to switch houses. With an open ground conductor, the neutral grounding resistor is placed in series with the machine's contact resistance, and the frame voltage is then proportional to the contact resistance. Federal records show that a man was electrocuted in a limestone quarry in 1977 when he came in contact with a 2300 V shovel with a line-to-ground fault while the ground system was disrupted. The use of reliable high-voltage ground-check monitors will provide protection in cases such as this.

### 3.1.8 Transfer of Potential Between Ground Beds

The transfer of potential from the substation ground bed to the safety ground bed can endanger mine personnel in the same manner as was discussed earlier, that is by elevating the frames of machinery connected to the ground bed to some voltage above ground. The substation ground bed can normally be expected to handle primary faults as well as lightning and other surges coming into the substation via the overhead lines. Common practice therefore dictates that the safety ground bed be physically separated from the substation ground bed by a distance of 8 m (25 ft), or even 15 m (50 ft). The following example will show that this is perhaps not the best solution.

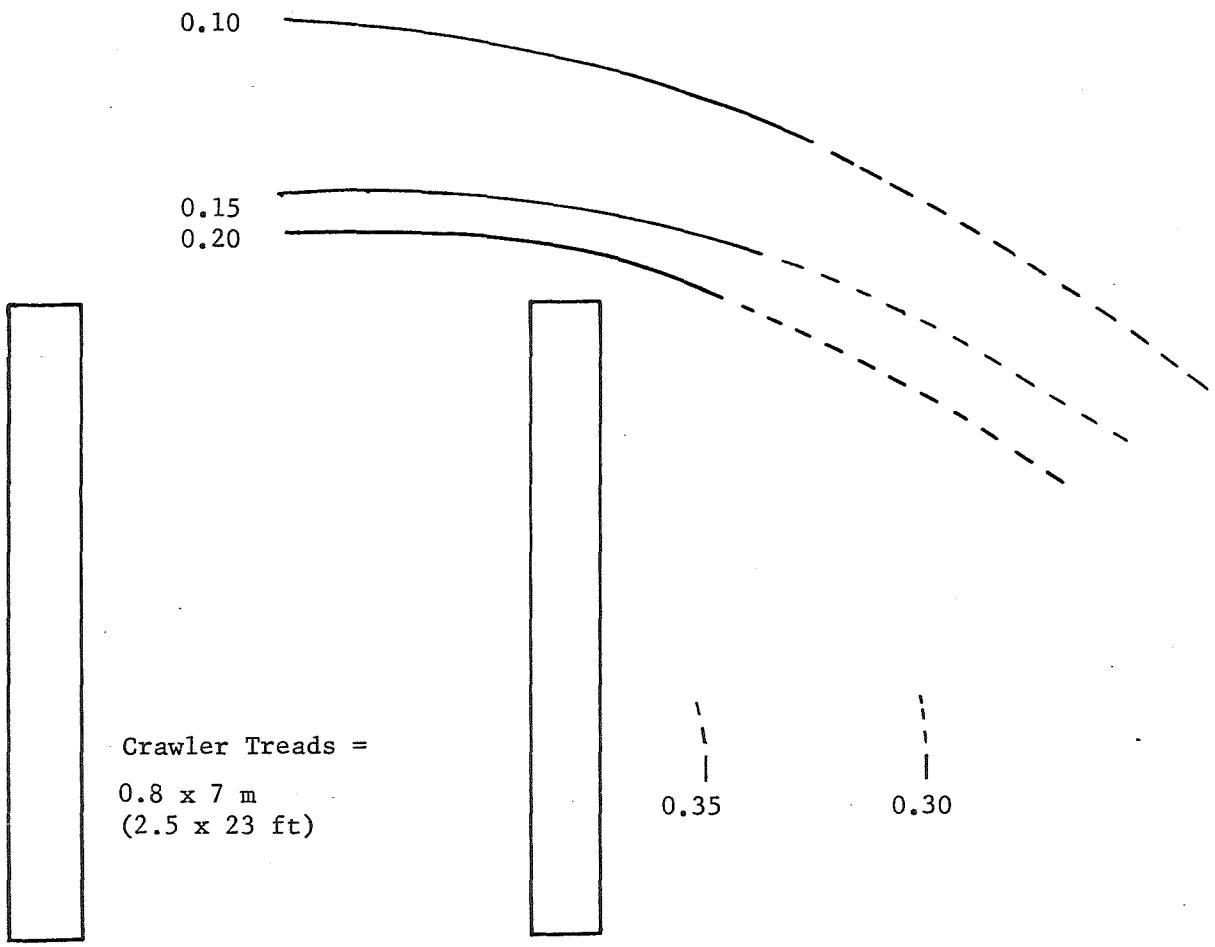


FIGURE 3.27. - Potential gradient survey around a loading shovel, with voltages in per unit of frame potential.

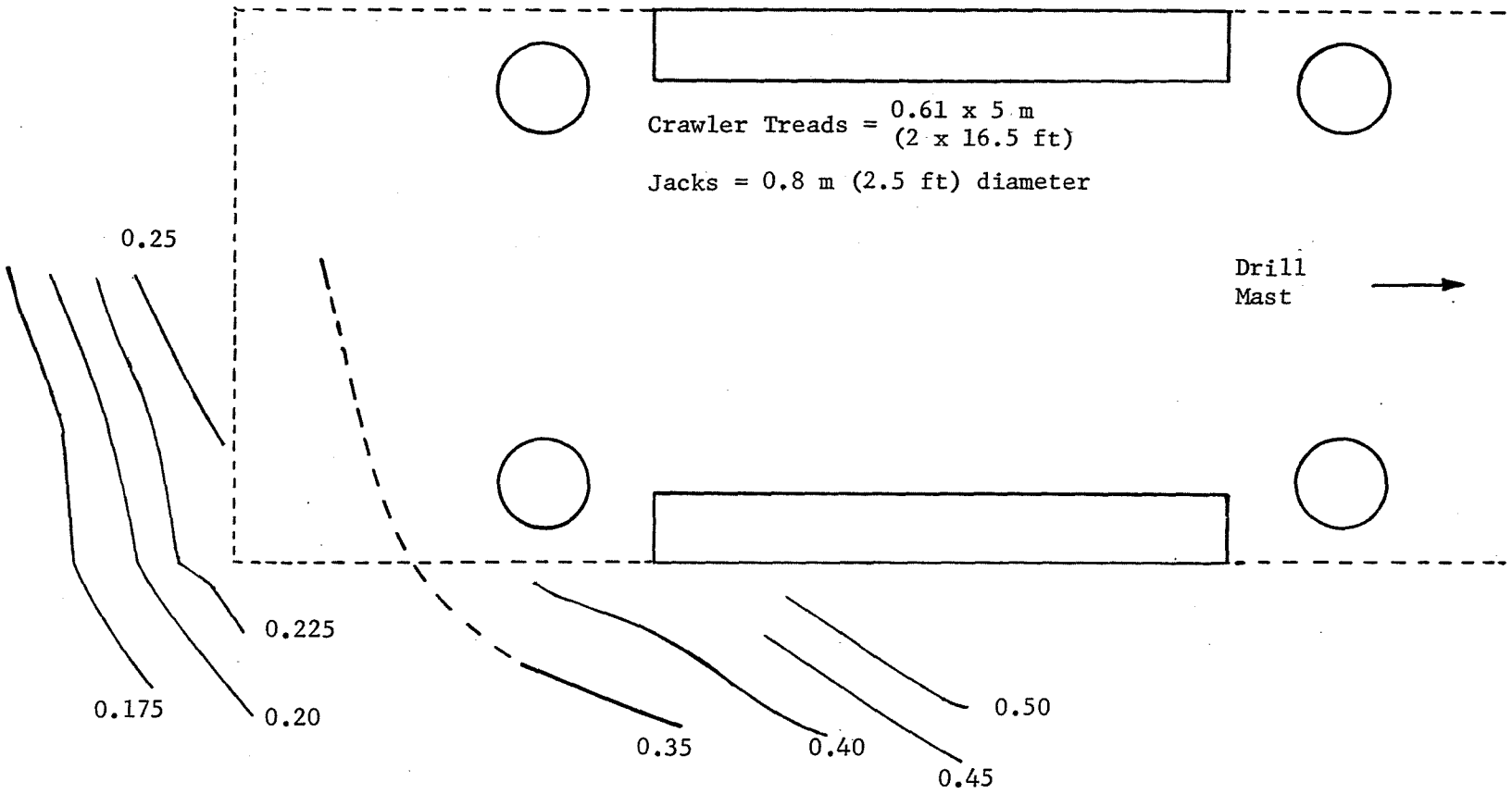


FIGURE 3.28. - Potential gradient survey around a Blast-hole Drill, with voltages in per unit of frame potential.

For the sake of simplicity it will be assumed that the substation ground bed consists of a single driven rod, 6.1 m (20 ft) long and 5 cm (2 in) in diameter. When immersed in soil whose resistivity is about 30 Ω-m (100 Ω-ft), this rod will show a resistance of just under 5Ω. Assuming that a primary fault causes 2000 A to flow into the ground bed, the rod is thereby elevated to a potential of 10,000 V with respect to "true ground". Figures 3.29 and 3.30 show the voltage profile on the surface of the earth surrounding the electrode. The shape of the profile depends upon the length-to-radius ratio of the electrode. Neutral-resistor grounding systems are designed so that, under fault conditions, the allowable potential in the circuit external to the resistor is 100 V or less. Now, if the induced potential on the safety ground bed is also to be limited to 100 V, then figure 3.30 shows that the separation distance between the two beds must be in excess of 90 m (300 ft).

Clearly, no "magic number" can be specified for the separation distance between substation and safety ground beds which will insure that hazardous potentials are not transferred from one to the other. The design of the substation ground bed, the soil resistivity, and the exposed magnitude of fault current are all parameters which will affect the necessary distance of separation between ground beds.

It may be possible, in surface mining environments, to eliminate the safety ground bed, relying instead on the machinery/soil contact surfaces to provide the necessary earth connection. All the advantages of the resistance-grounded-neutral system would be retained, without the added expense of installing a safety ground bed. In systems which use overhead lines for part of the secondary distribution, fault current would be forced to flow through machine frames in the event of a phase-to-earth fault. However, it should be noted that some fault current may flow through the machine frame even if the safety ground bed were in use. Adequate protective circuitry used in conjunction with ground-check monitors would be essential if the safety ground bed were eliminated.

## 3.2 MEASUREMENT OF POTENTIAL GRADIENTS

### 3.2.1 Introduction

Along with the research just described, a substantial effort was made to develop equipment and techniques for making effective field determinations of surface potential gradients near metallic objects in contact with the earth (earth electrodes). Instrumentation was designed and constructed, computer gradient plotting techniques were researched, and several field trials of the system were carried out. Each of these steps is covered in detail below, and a complete circuit description and operations manual for the equipment is included as Appendix B to this report.

### 3.2.2 Construction of the Gradient Plotter

#### 3.2.2.1 Wheel Assembly Construction

Figure 3.31 is an isometric sketch of the wheel assembly for the gradient plotter. The aluminum wheel which makes actual contact with the ground is 0.91 m (3 ft) in circumference and is 1.27 cm (½ in) thick. It has 30 equally spaced

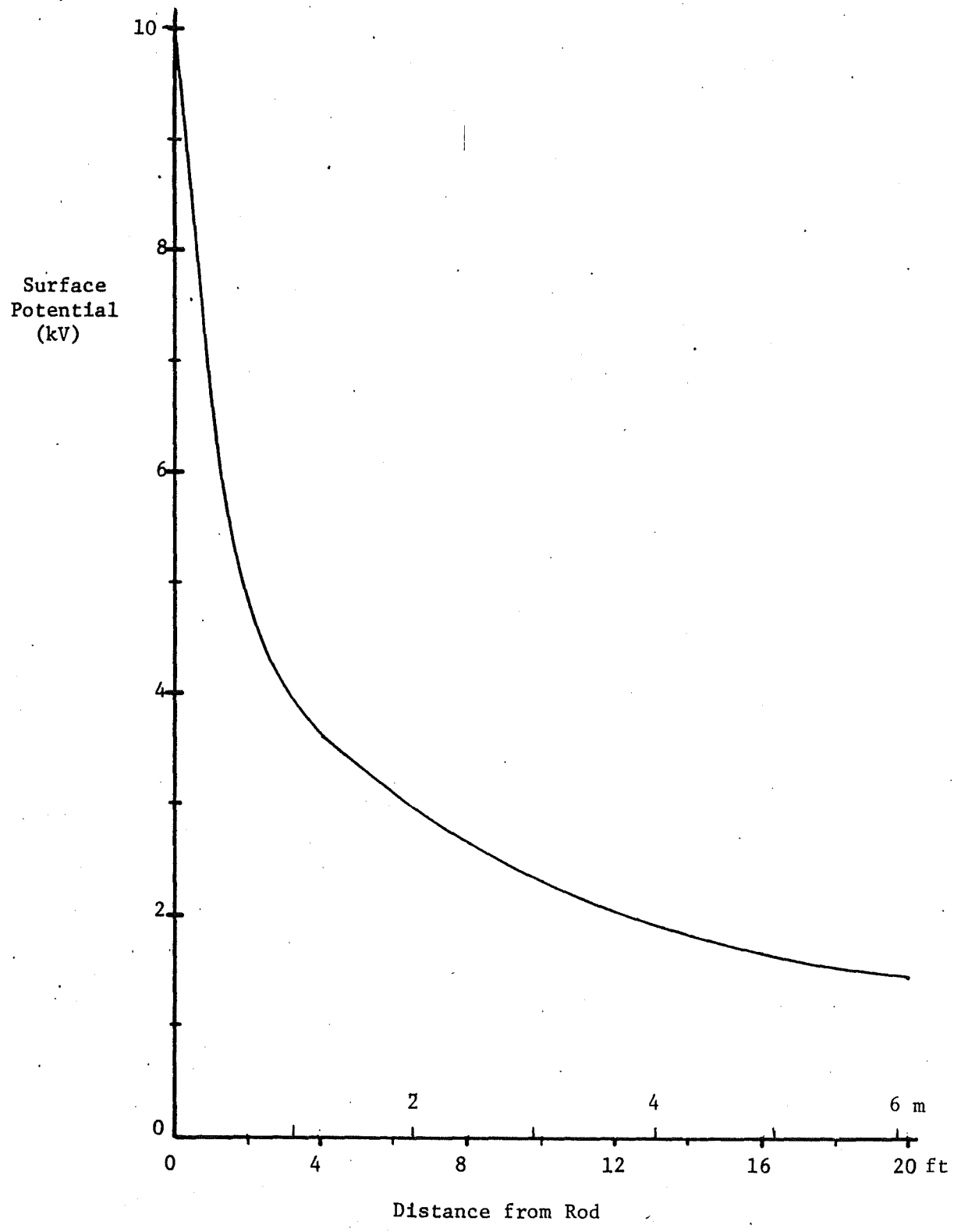


FIGURE 3.29. - Surface potential profile near the substation ground rod.

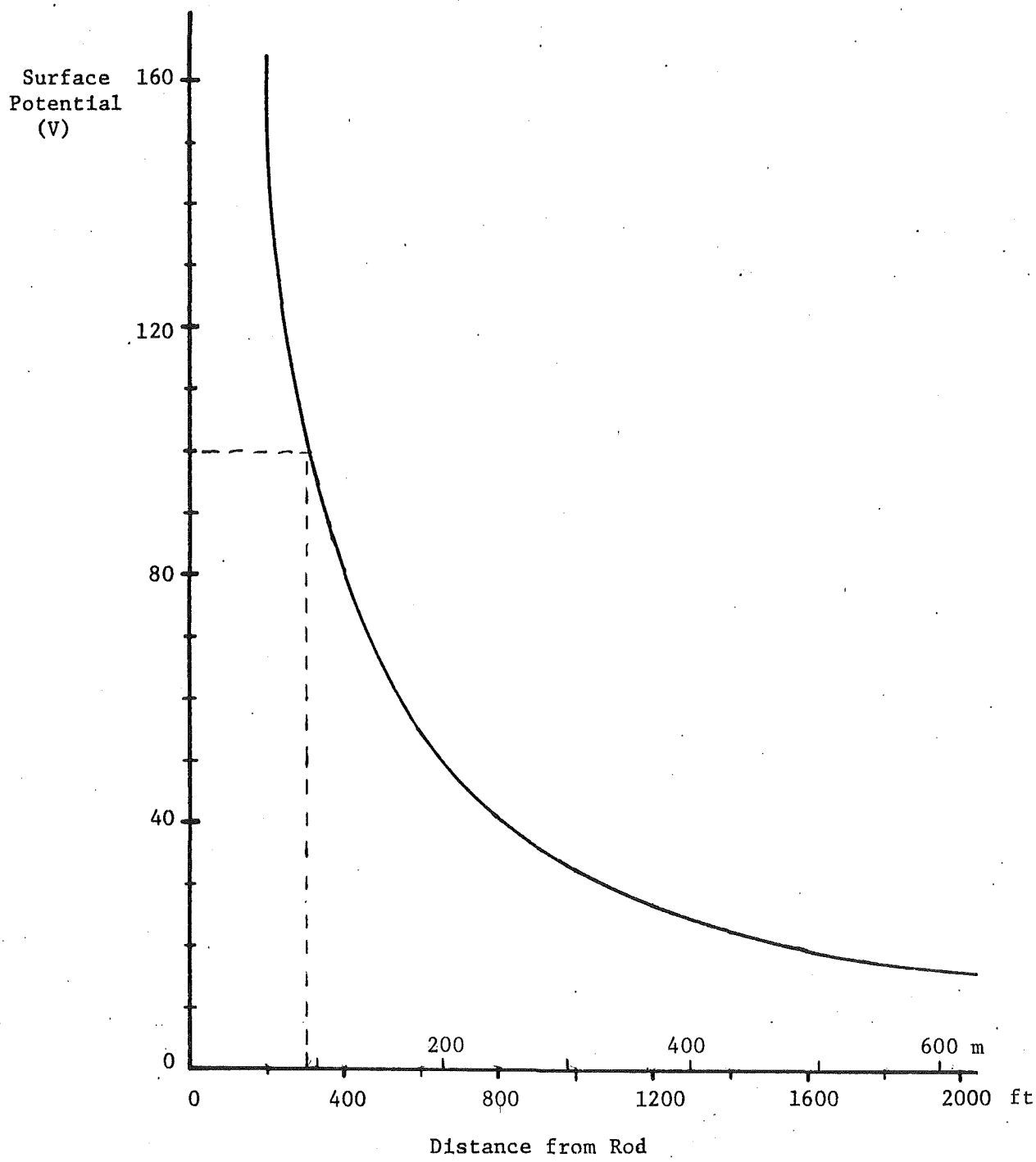


FIGURE 3.30. - Expanded potential profile around substation ground rod.

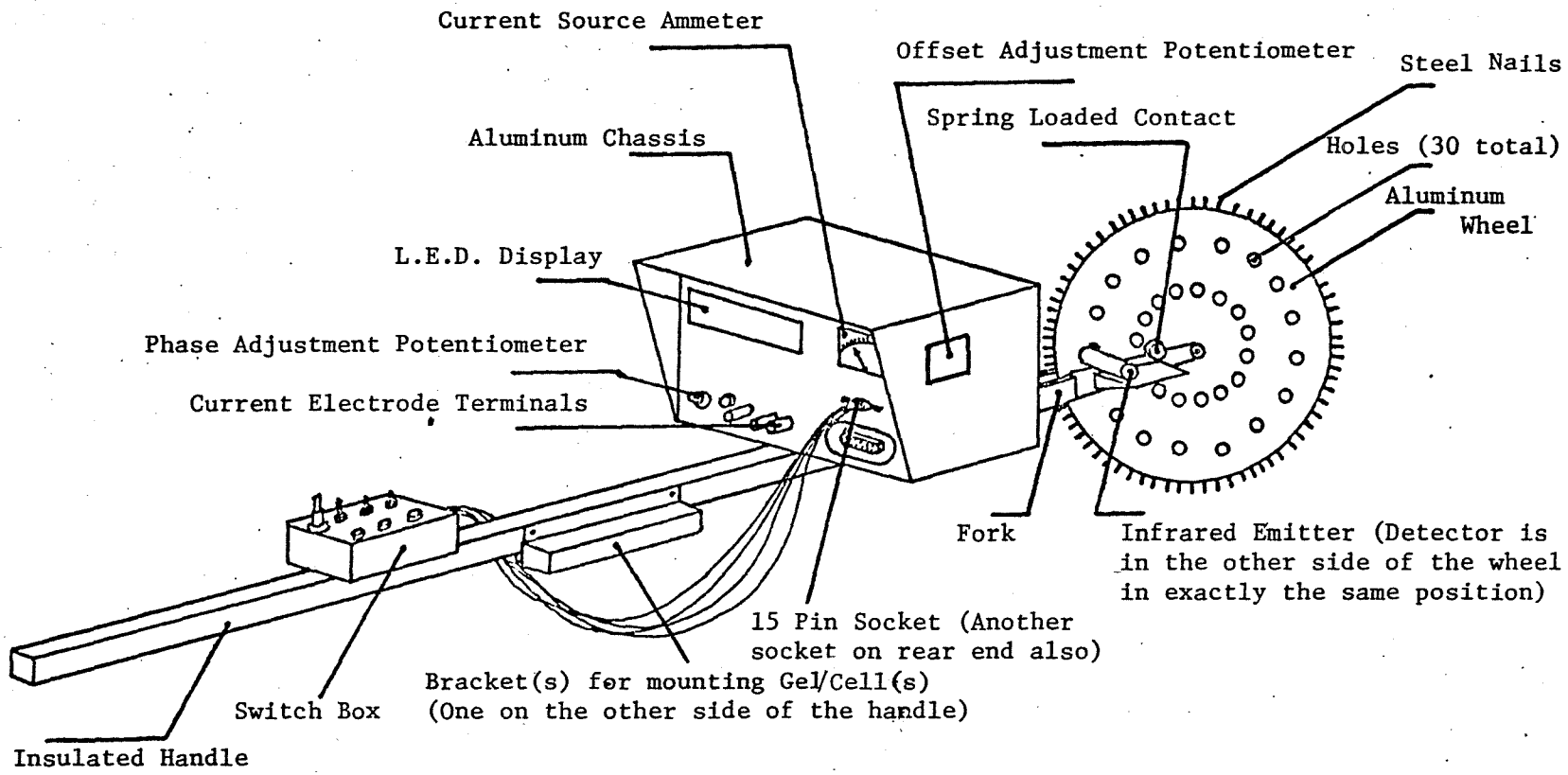


FIGURE 3.31. - Isometric sketch of the wheel assembly.

holes drilled circumferentially at a distance 10.2 cm (4 in) from the center. The circular arc obtained by the radial projections through adjacent holes is 3 cm (0.1 ft).

An infrared emitter and infrared detector are mounted on either side of the wheel in teflon pieces. Figure 3.32 shows how they are actually mounted. One end of each teflon piece is hollowed out into a concave surface, and on each surface the emitter and detector are fixed by means of adhesive. Electrical leads are taken out of the other end of the teflon pieces. The teflon pieces are mounted inside spring loaded sockets so that the concave surfaces are flush with the wheel surfaces. This does not hamper the wheel movement since teflon is self-lubricating. All extraneous infrared light is thus cut-off and the infrared device is made very sensitive. The infrared emitter and infrared detector are mounted at the same radial distance of 10.2 cm (4 in) from the wheel center as the 30 holes, so that when each hole comes in line with the emitter and detector an infrared signal is transmitted from the emitter to detector and an impulse is generated which corresponds to 3 cm (0.1 ft). A series of impulses is generated as the wheel is rolled along. These are fed into a counter circuit for display as well as for conversion into an analog signal for feeding to the X input of an X-Y recorder.

Steel nails are driven along the wheel rim projecting 0.32 cm (1/8 in) from the rim. This insures better contact between the wheel and earth, especially when the surface is grassy. It may be recalled that the voltage signal is actually transmitted to the detecting circuit through the aluminum wheel which acts as the conducting medium.

The wheel is linked to a well-insulated handle through a fork, and provides smooth motion as it is pushed along. The handle is well-insulated to avoid any possibility of a parallel current path through the operator's body (which will introduce measurement errors). A spring loaded electrical contact grazes the surface of a circular copper strip which is screwed onto the wheel to insure better contact. This improves electrical conductivity between the wheel and the detecting circuit.

The electronic circuitry is housed inside a lightweight aluminum chassis with an overall dimension of 25 cm x 15 cm x 18 cm (10 in x 6 in x 7 in), and is mounted on the lower end of the wheel handle. Incoming and outgoing terminations, L.E.D. Distance Display Unit, testpoints, phase adjustment potentiometer and the current source ammeter are mounted on the chassis at convenient locations.

The circuit control buttons, switches, and current magnitude potentiometer, are mounted on a smaller box at the upper end of the handle within easy reach of the operator. The connections between this box and the main chassis are done with single core multi-stranded wires. Wires of different colors are selected for different terminations so that they can be easily identified with a wiring drawing. At the chassis end, the wires are terminated in a 15-pin plug-in type socket, which can be easily pulled out of or inserted into a 15-pin plug where all wiring from the printed circuits terminate. The circuitry inside the chassis can therefore be easily isolated when required in order to carry out laboratory tests or repairs.

Two 12-volt Gel/Cells* mounted adjacent to the chassis supply power to the complete circuit. Each Gel/Cell has a continuous capacity of 1.5 ampere hours

---

* References to specific brands, equipment, or trade names in this report is made facilitate understanding and does not imply endorsement by the Bureau of Mines.

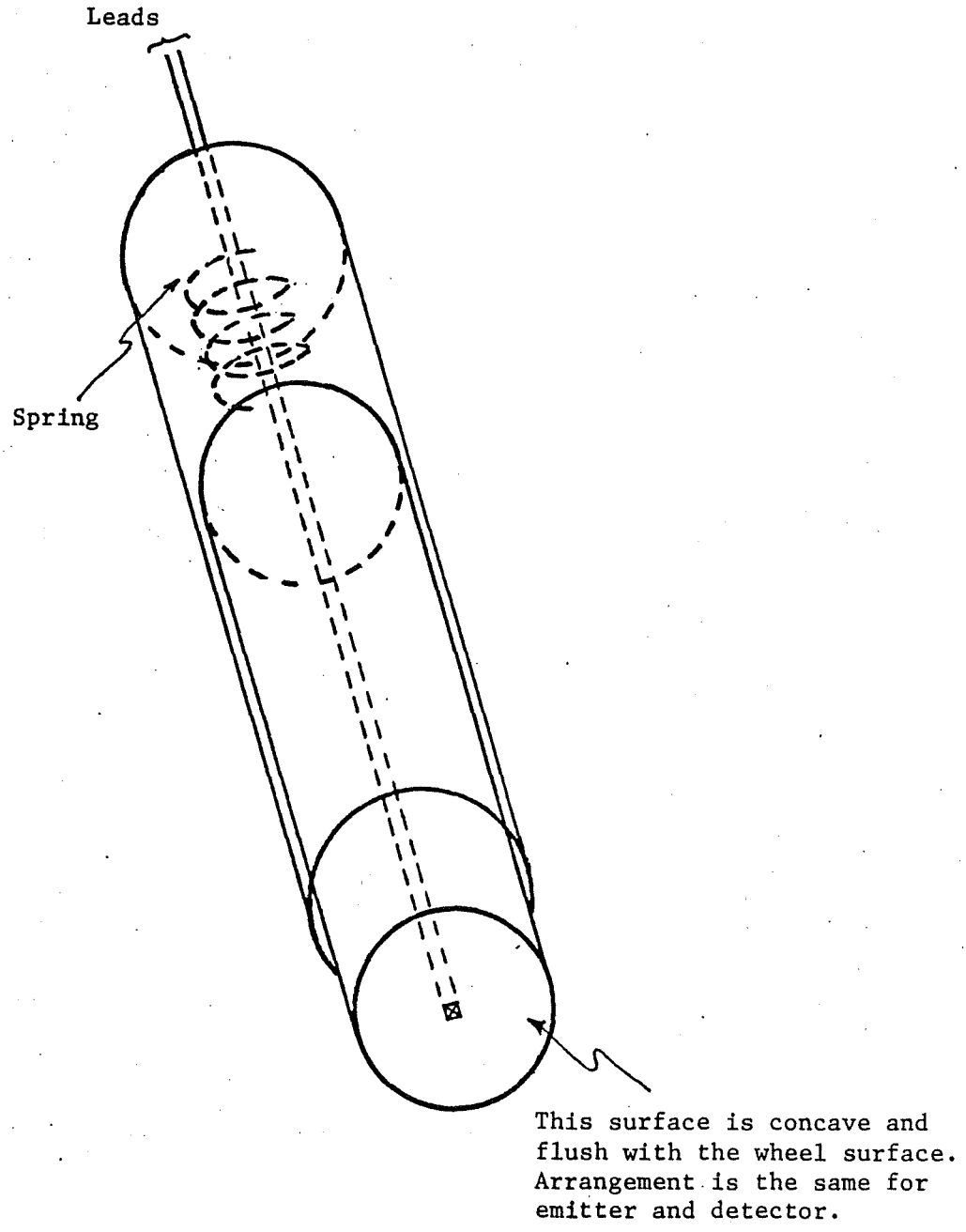


FIGURE 3.32. - Mounting arrangement of infrared emitter and detector.

and with the total current consumption of the circuitry being 250 mA, the batteries will have a 6-hour cycle when fully charged. This is more than sufficient for one experimental run.

The complete wheel unit weighs 23 pounds.

3.2.2.2 Required Accessories

Two reels of special non-kinking cable with high resistance insulation are required for injecting a current signal between the reference electrode and auxiliary electrode. They rest on the crossbars of two alloy steel rods, 1.27 cm (½ in) in diameter and 0.6 m (2 ft) long, driven into the earth. One of the rods is tied to the machine (around which the field distribution is desired). The other rod is the auxiliary electrode. Electrical connections to the electrodes from the cables is accomplished through the reel itself.

A 76 m (250 ft), 4 conductor shielded cable, transmits the voltage and distance signals from the wheeled electrode to the X-Y Recorder.

The X-Y Recorder is servo-operated, with an adjustable full-scale range of 1 volt to 10 volts for both X and Y inputs. Standard graph paper can be used for plotting.

3.2.2.3 Constant Current Source Design

Figure 3.33 is the block schematic of the constant current source. A 11 Hz square wave voltage signal is generated and fed through a potentiometer into a voltage-controlled current source circuit. The output is a current signal whose magnitude is constant over a wide range of loads and is adjustable by varying the input potentiometer. This output is fed to the ground resistance. A metering circuit monitors the output current and generates a proportional signal for feeding a microammeter calibrated to a full scale reading of 100 mA.

3.2.2.4 Distance Measurement Unit

Figure 3.34 is the block schematic of the distance measuring unit. An infrared emitter generates a signal which is picked-up by an infrared detector when the wheel holes are in line with the emitter/detector. The 2 V impulses are fed to a Schmitt Trigger circuit which generates 5 V pulses. This is fed to an UP-DOWN switching circuit whose outputs are fed to the input stage of an UP-DOWN binary counting chain as well as to the input stage of an UP-DOWN B.C.D. counting chain. The 10 most significant bits of the binary counting chain output are fed to a digital-to-analog converter for generating the X input signal to the X-Y plotter. The 16 bit output of the B.C.D. counting chain is input to a set of four 7 segment drivers whose outputs are connected to four 7 segment LED displays. The display is normally off and can be turned on by depressing a push-button connected to appropriate points in the circuit. A one decimal display accuracy is obtained.

3.2.2.5 Voltage Detecting Unit

Figure 3.35 is the block schematic of the voltage detecting unit.

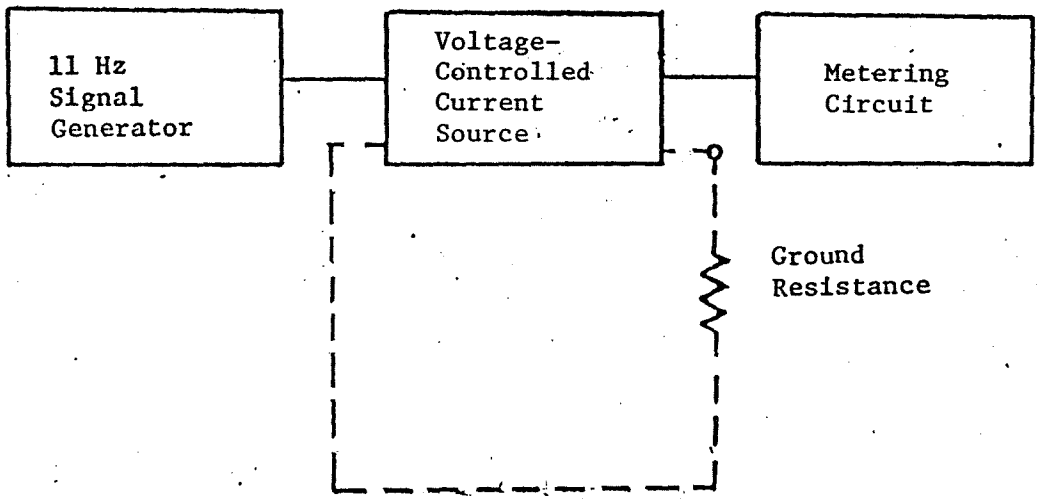


FIGURE 3.33. – Block schematic of constant current source.

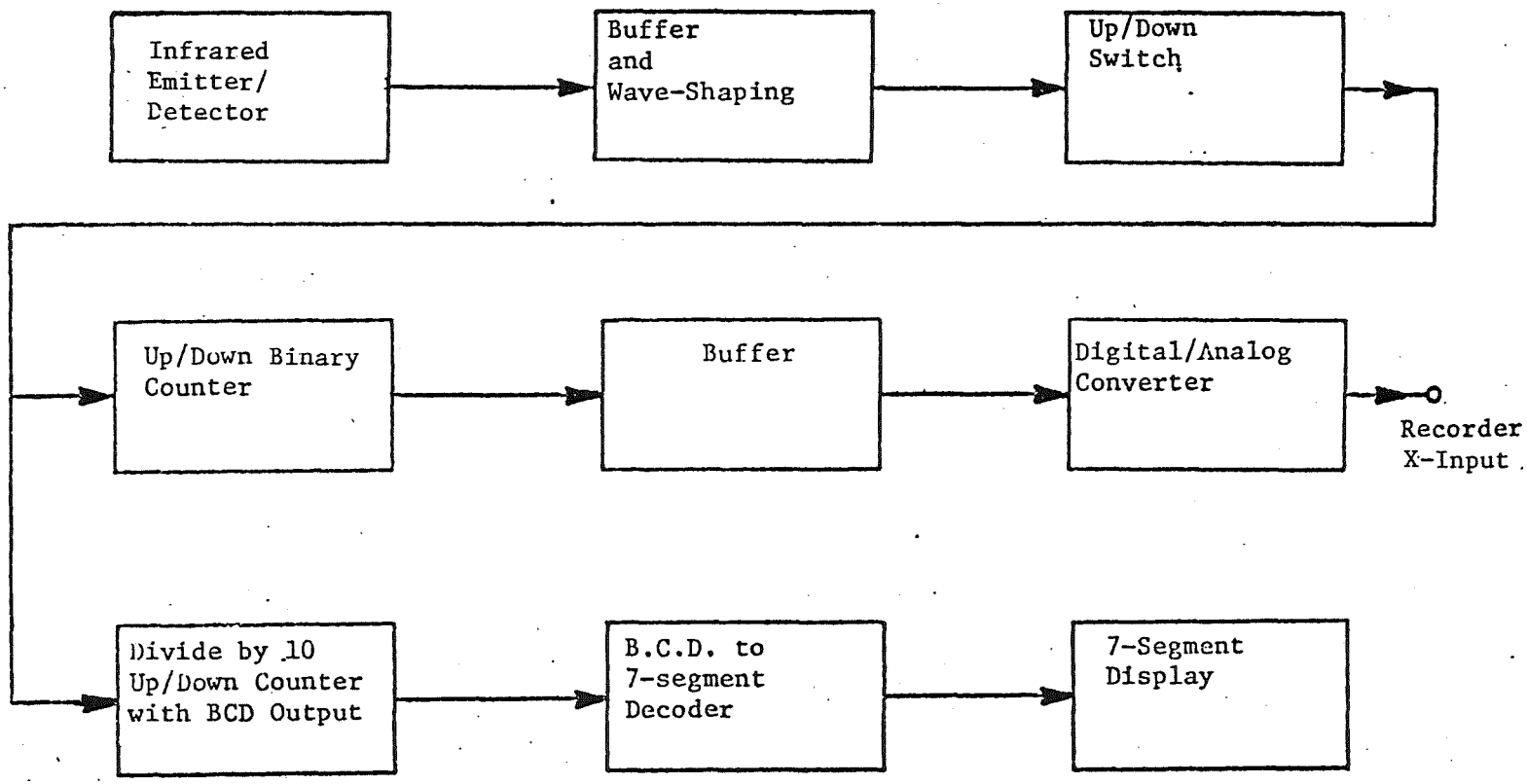


FIGURE 3.34. - Block schematic of distance measuring unit.

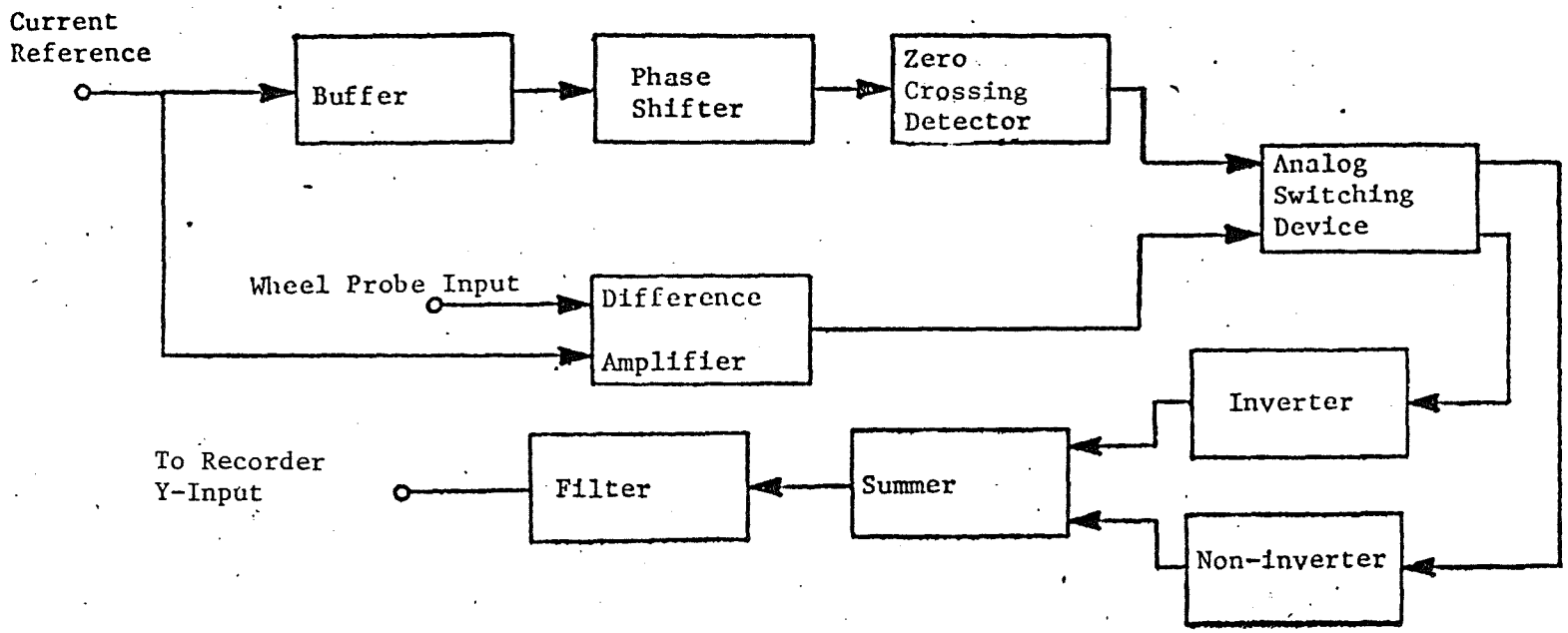


FIGURE 3.35. – Block schematic of the voltage detecting unit.

Synchronous detection is used to detect and filter only the voltages corresponding to the injected-current signal. The injected current signal is also fed simultaneously to the input of a buffer as well as to the input of a difference amplifier. The buffer output goes through a phase-shifting circuit to the input of a zero crossing detector. The phase shifter brings the reference signal and the detected signal in phase, while the zero crossing detector generates two square wave signals that are 180 degrees out-of-phase with each other. The signals are fed into an analog switching device.

The detected signal from the wheel probe is fed to the inverting input of the difference amplifier. The current reference signal is fed to the non-inverting input. The difference amplifier output is therefore proportional to the difference of the two input signals, and proportional to the difference of potential between the reference electrode and the wheel. This signal is also fed to the analog switching device. The detected signal is chopped at a rate determined by the frequency of the two signals from the zero crossing detector. The analog switch output consists of two halves of the input signal, the positive half and the negative half. The negative half is inverted and the two signals are summed and fed to a low-pass-filter whose output is a dc signal corresponding to the 11 Hz signal. This is fed to the Y input of the recorder.

### 3.2.3 Contour Mapping

#### 3.2.3.1 Hand Plotted Contours

Consider figure 3.36 in which the object of study is shown as a square and dotted lines indicate the radial traverses made with the potential gradient plotter. Each radial traverse gives a fall-of-potential plot, which can be used to extrapolate voltage profiles for a typical potential rise of the object. A typical voltage profile is shown in figure 3.37 to illustrate hand plotting. A', B',.....,J' are the voltages for which contours are desired. A, B, .....,J are the corresponding distances from the object, along a particular traverse. A set of voltage profiles along various radial traverses could be sectionalized at the voltage levels A', B', ....,J' and the corresponding distances from the object read off. A contour plot of voltage A around the object is obtained by joining the corresponding A's which reflect the distances from the object. A similar procedure is repeated to obtain contours corresponding to B', C',...,J'. The accuracy of the plot improves as the number of traverses increases.

#### 3.2.3.2 Wolf-Contour Package (65)

The Wolf Contour Package is a software Fortran Language Computer Program which has been successfully tried in the past (56) to obtain potential contours with input data based on theoretical calculations. The input data is actually processed by a series of CALL subroutines. These CALLING sequences result in the generation of output data which can be directly stored on tape. The tape data can be fed into a Calcomp Plotter whose output is a plot of equipotential contours. The CALLING routines include a wide range of options and some of the important ones are listed below.

1. Contour levels can be specified at any value desired.

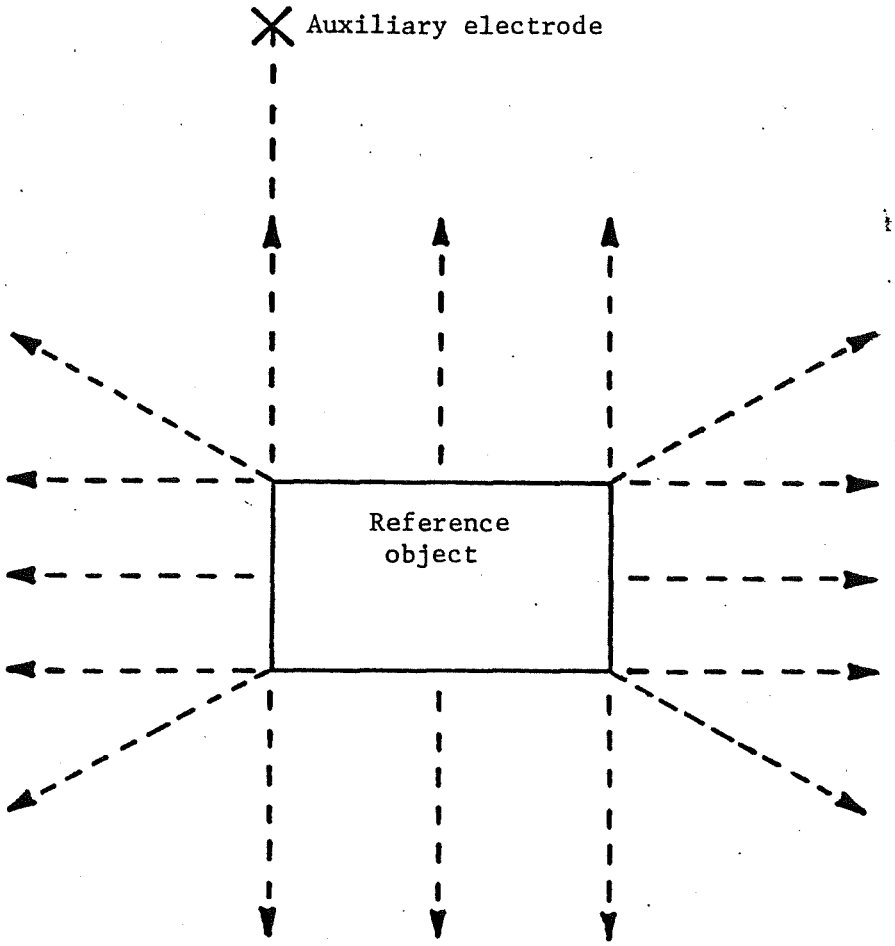


FIGURE 3.36. - Illustration of radial traverses around the object under study to obtain fall-of-potential curves.

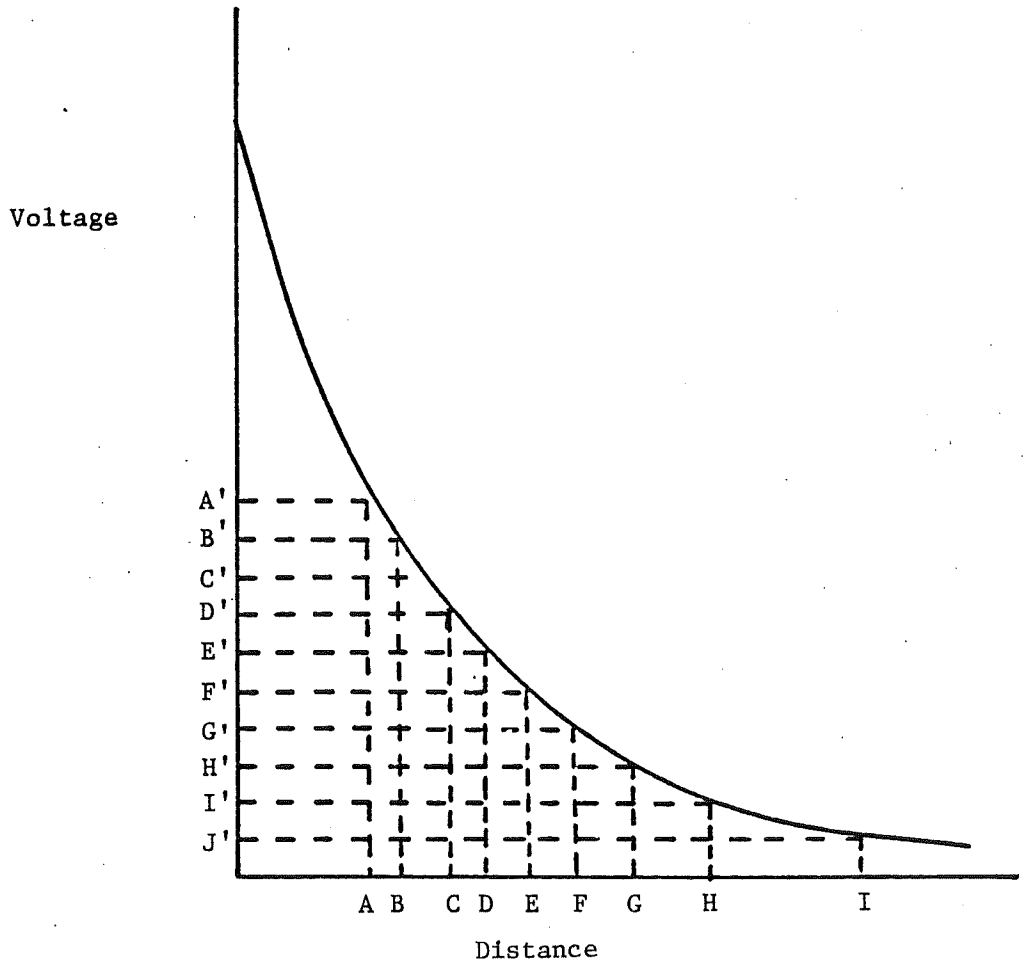


FIGURE 3.37. - Typical voltage profile to illustrate hand plotting.

2. Different types of contour lines such as multiple lines, dashed lines and lines with tick marks can be specified.

3. Undefined points are acceptable.

4. Data smoothing is possible

5. Data dump can be made available.

The Wolf Package in association with the Calcomp Plotter can also generate contours with input data from the potential gradient plotter. The following conditions must be met to obtain accurate and well defined plots.

1. The input data must be in a well-defined square or rectangular matrix array with points on the array clearly defined.

2. The plotting options must be clearly specified.

Comments explaining the applications of the various subroutines are available in the Wolf-Contour Manual.

### 3.2.4 Field Tests Conducted Using the Gradient Plotter

#### 3.2.4.1 Description of Field Tests

The WVU experimental ground bed was chosen as the location to conduct preliminary field tests with the potential gradient plotter. At the time of its installation, this ground bed was considered a good location for experimental studies on soil resistivity characteristics and ground-bed resistance. It was presumed that the soil composition was quite uniform in that area. There was no prior knowledge about the presence of any underground objects. Figure 3.38 shows the location of the experimental ground bed. Five steel rods 1.27 cm (½ in) in diameter were driven 2.4 m (8 ft) into the ground. Four of the rods formed the corners of a square. The fifth rod was driven at a point lying on the extension of one side. Bare copper conductors running 23 cm (9 in) below the ground when tied to the ground rods with brass clamps enabled formation of a low-resistance ground bed.

#### 3.2.4.2 Field Test #1

Figure 3.39 shows the radial traverses made with the potential gradient plotter and also the location of the auxiliary electrode at a distance of 45.7 m (150 ft) from the ground bed.

Figure 3.40 **b** shows voltage profiles obtained along traverses 4 to 7 for an injected current of 20 mA. The readings were recorded on an X-Y plotter. The following observations could be made from the profiles.

1. The profile along traverse #1 (figure 3.40 a) reveals a low gradient near the ground bed and a steep gradient near the auxiliary electrode. The profile between the electrodes is itself very unusual and not the fall-of-potential profile one would normally expect. The Y output also appears to be noisy.

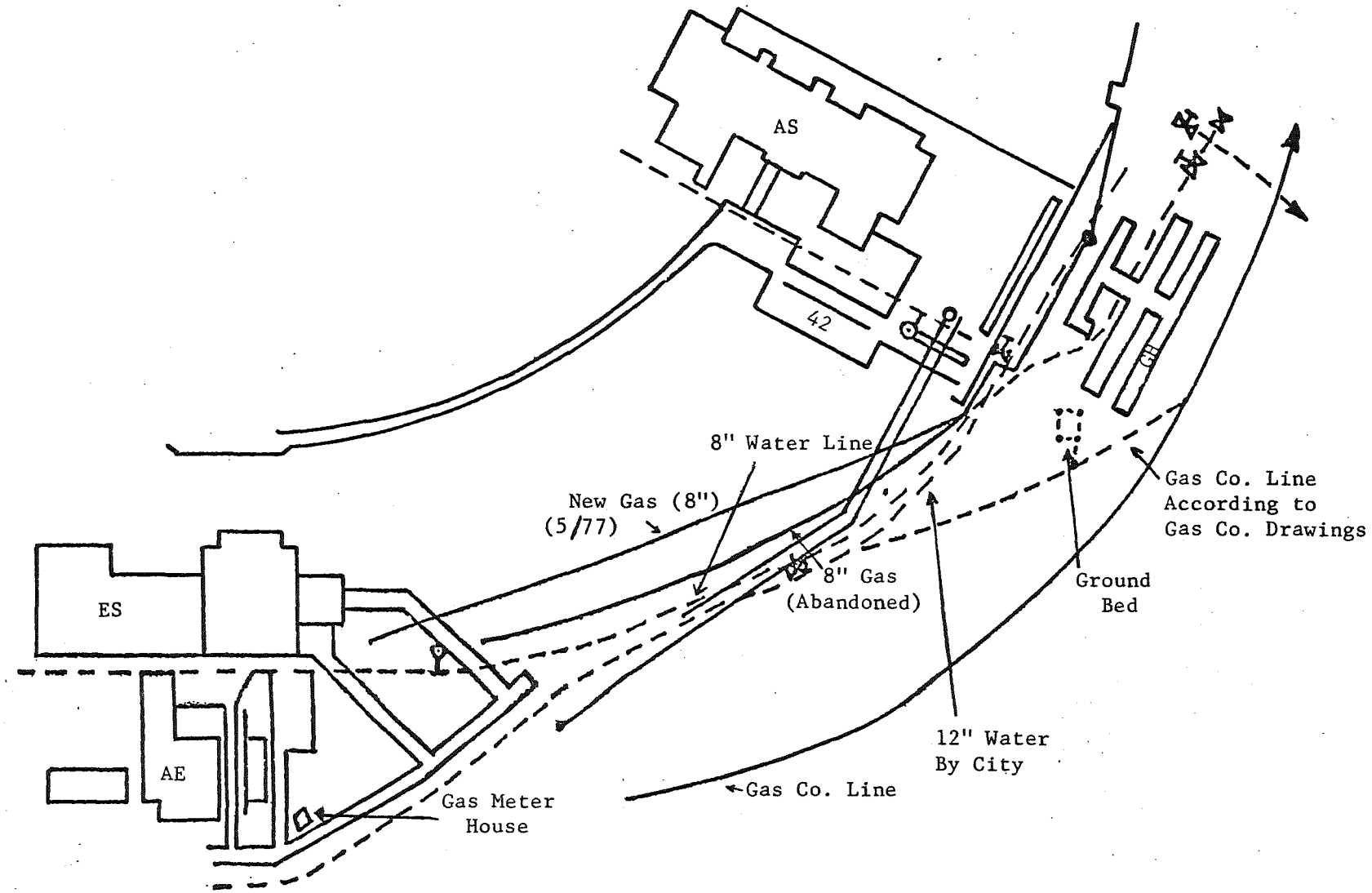


FIGURE 3.38. - Portion of Evansdale Utility Plans with the ground bed added.
(Courtesy: W.V.U. Physical Plant).

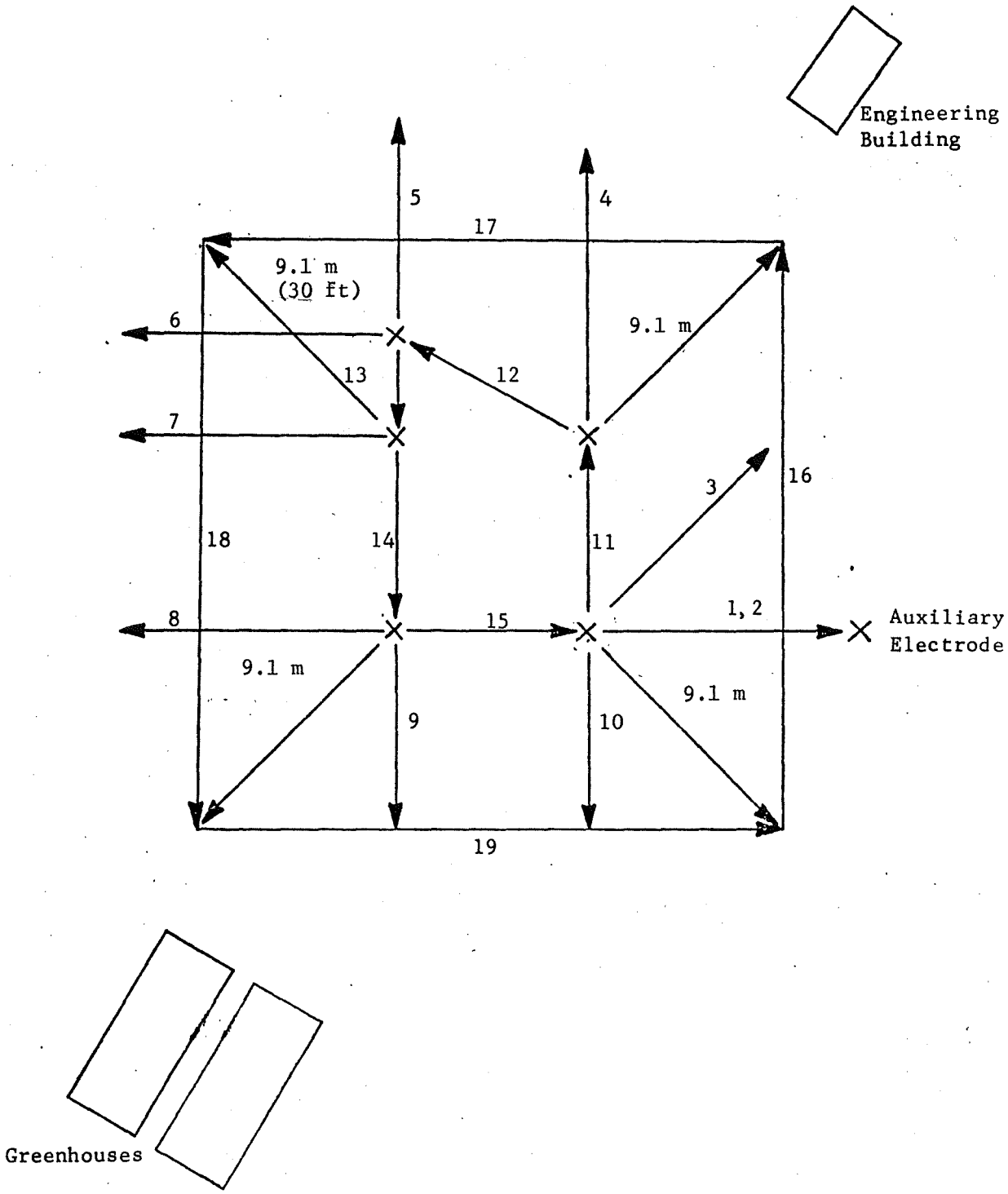


FIGURE 3.39. - Radial traverses made during field test #1.

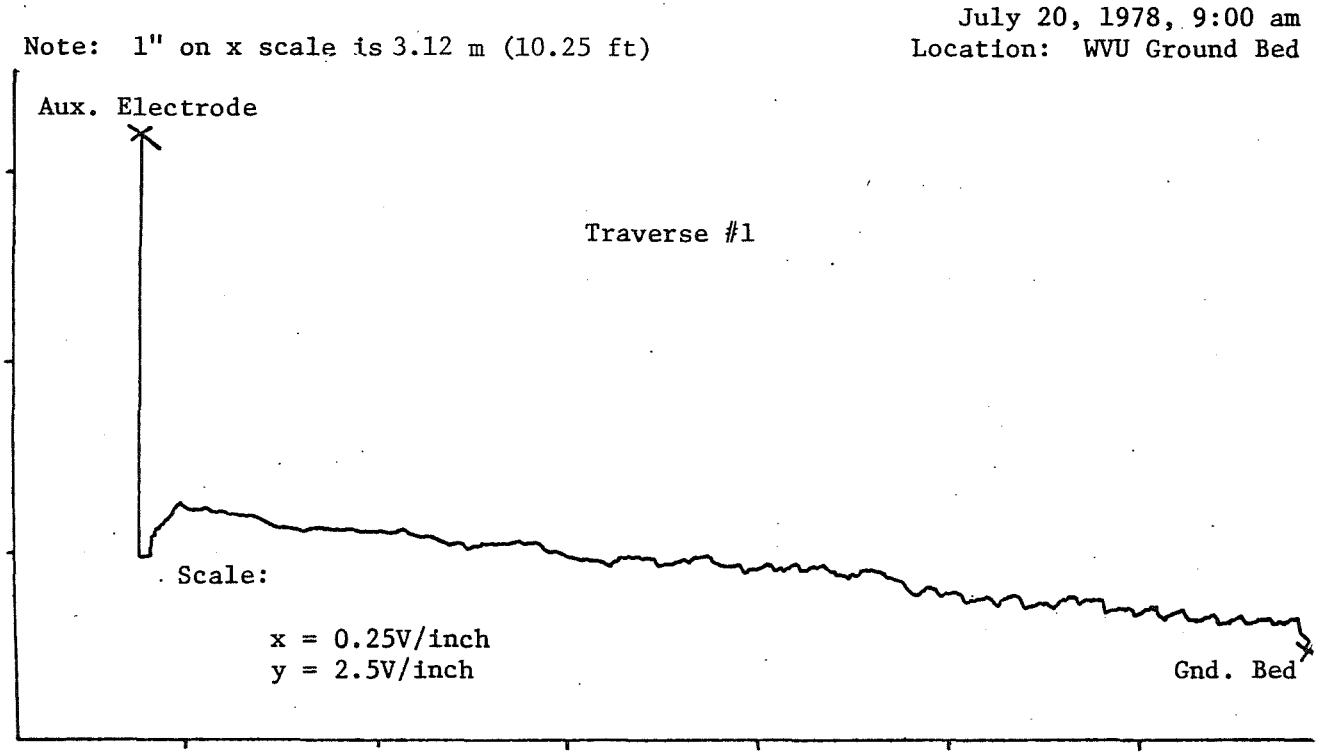


FIGURE 3.40 a. - Field test #1.

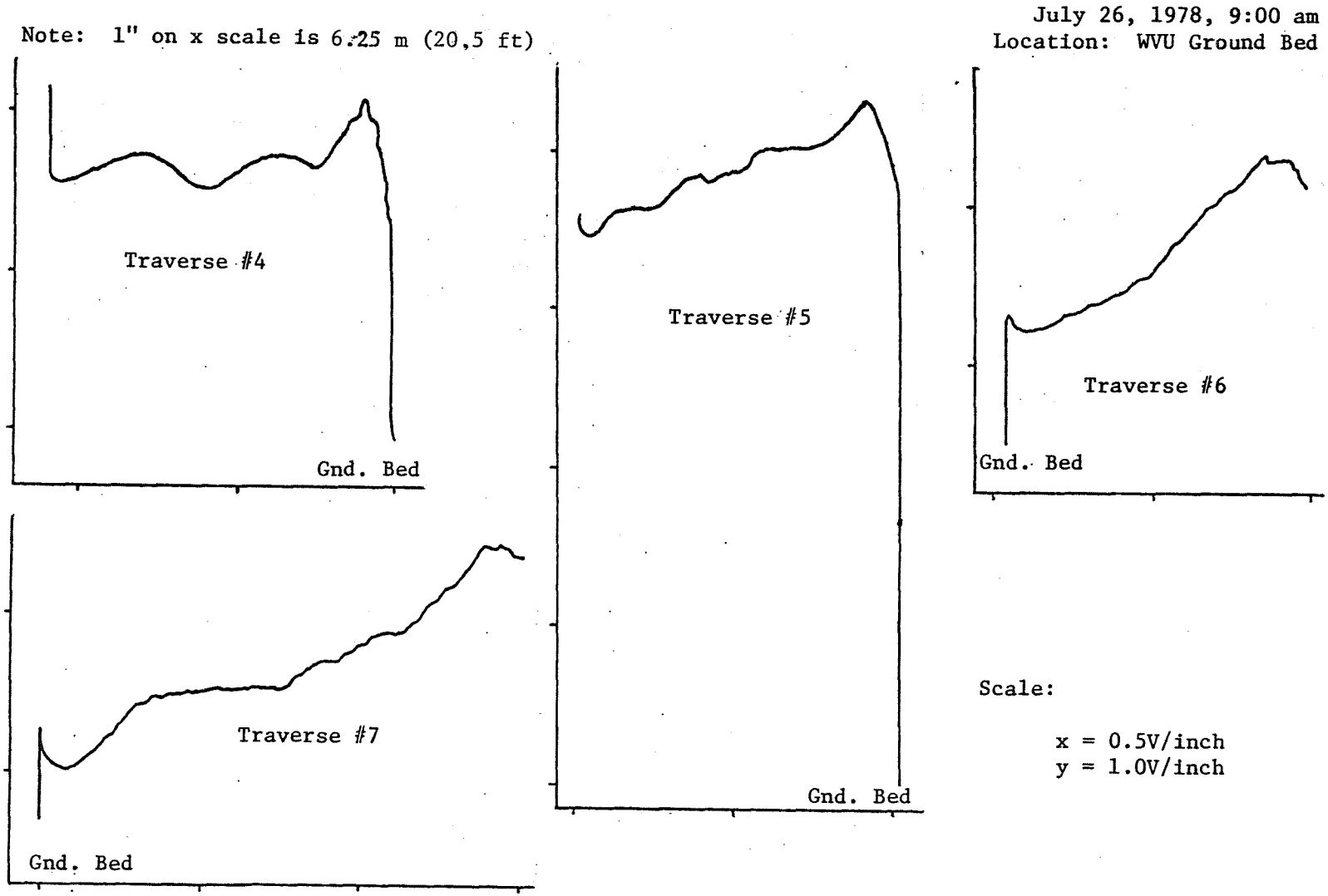


FIGURE 3.40 b. - Field test #1.

2. The profile along traverse #4 shows a steep gradient at the ground rod, and some unusual voltage variations. Voltage peaks and dips are evident.

3. The profile along traverse #5 shows a steep gradient at the ground rod and a gradual drop in the voltage as the distance from the ground rod increases.

4. Another unusual profile was obtained along traverse #7. A steep gradient at the ground rod is followed by a relatively flat portion after which there is a voltage dip.

After investigating the condition of the ground bed and also the sub-surface conditions the following observations and conclusions were made:

1. The five ground rods were not tied to each other. Each ground rod behaved as an isolated point electrode. Point electrodes result in a higher earth electrode resistance and hence a higher potential gradient and a higher voltage rise in its vicinity compared to a low-resistance ground bed. That explains the steep gradient and the high voltage rise near each ground rod.

2. The voltage peaks and dips suggested the possibility of buried objects in the vicinity of the ground bed. A field survey of that area was made to determine the location of the ground bed relative to the surrounding objects. The utility plan of that area was obtained from the WVU Physical Plant. The two plans were combined into one drawing as shown in figure 3.38. This showed that a buried pipe was running under the ground bed whose potential was probably being raised by the potential of the ground rods.

3. The potential distribution around each ground rod might have also been affected by the presence of adjacent rods, and also by the presence of the bare copper conductor lying disconnected between the ground rods.

4. Mutual interaction between the buried pipe and ground bed could also have affected the potential distribution.

It was definitely felt that another set of tests should be conducted after insuring that the ground rods were properly interconnected.

3.2.4.3 Field Test #2

Another field test was conducted a few days later after first insuring that the ground rods were properly tied together. Figure 3.41 shows the traverses made.

The ground-bed resistance was first checked by making a fall-of-potential measurement with a Bison-meter. It was found to be 5.17 ohms.

An X-Y plotter was again used, powered with the output of a thyristor inverter whose dc input came from a car battery. Except for occassional

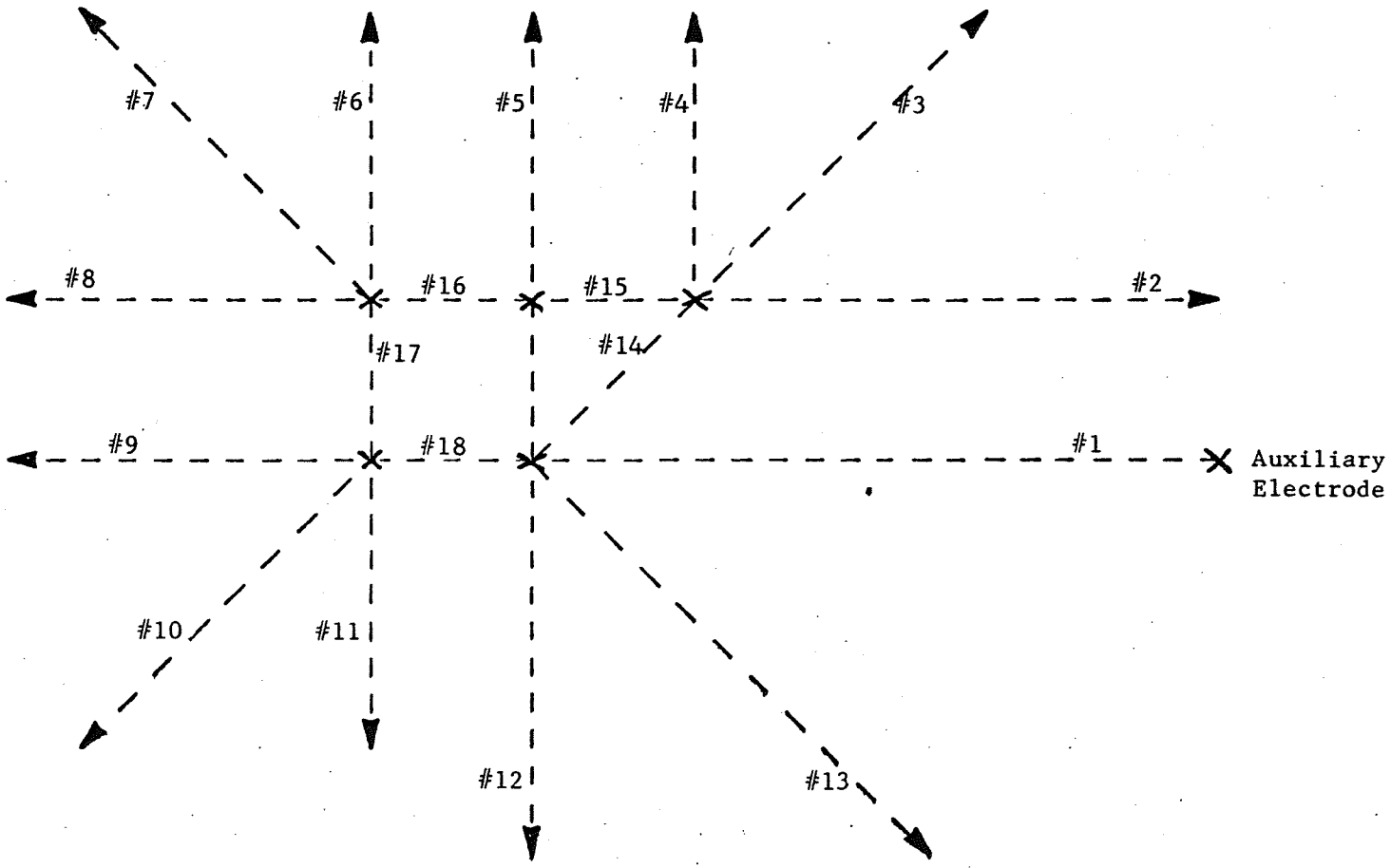


FIGURE 3.41. - Radial traverses made during field test #2.

malfunctioning of the recorder servo system, a set of readings were obtained and are shown in figures 3.42 a and b. Based on these profiles a rough hand plotted contour was attempted and is shown in figure 3.42 c. From this hand plot and the voltage profiles the following observations could be made:

1. The gradients and the potential rise of the ground bed have considerably reduced as compared to the profiles obtained with field test #1.

2. Some areas of high gradients (shown with dotted circles) were observed.

3. Contours A,B,C,D appear to close upon themselves only at a very large distance which again strongly indicates the presence of the buried pipe. One possibility is that the pipe is at or near potential of the ground bed and is reflected on the ground surface as a lower isopotential along a radial traverse shown by the dotted line. Contours A to D close at a large distance (possibly at the end of the pipe).

There were certain areas (marked X) where readings were not taken and only extrapolations were made to obtain contours. It was felt that another set of readings should be taken to get more data at these points and to verify the accuracy of the readings previously obtained.

3.2.4.4 Field Test #3

This field test, conducted a few days after field test #2 yielded a set of readings along the traverses shown in figure 3.43. A fall-of-potential reading with the Bison meter yielded a resistance of 4.13 ohms. This lower value is probably due to rainfall the previous night which may have lowered the resistivity.

Traverse #1 (marked in asterisk) resulted in a fall-of-potential curve shown in figure 3.44 a. The mid-portion was not flat but sloping.

The auxiliary electrode was moved further away from the ground bed (traverse #1A) and resulted in a fall-of-potential profile whose mid-portion has a very small slope, as seen from figure 3.44 b.

The voltage profiles along the other traverses are shown in figures 3.44 c to e.

Figure 3.45 is field map obtained from the above profiles. More information could be extracted from this map since longer traverses were made and spread more uniformly around the ground bed. The following observations were made from the field map:

1. The contours near the ground bed have the same shape as was obtained from field test #2.

2. Contours of .1 V, .2 V, .3 V, and .4 V confirms the presence of the buried pipe (as indicated from the results of field test #2).

Note: 1V on x scale = 6.25 m (20.5 ft)

July 29, 1978, 2:00 p.m.
Location: WVU Ground Bed

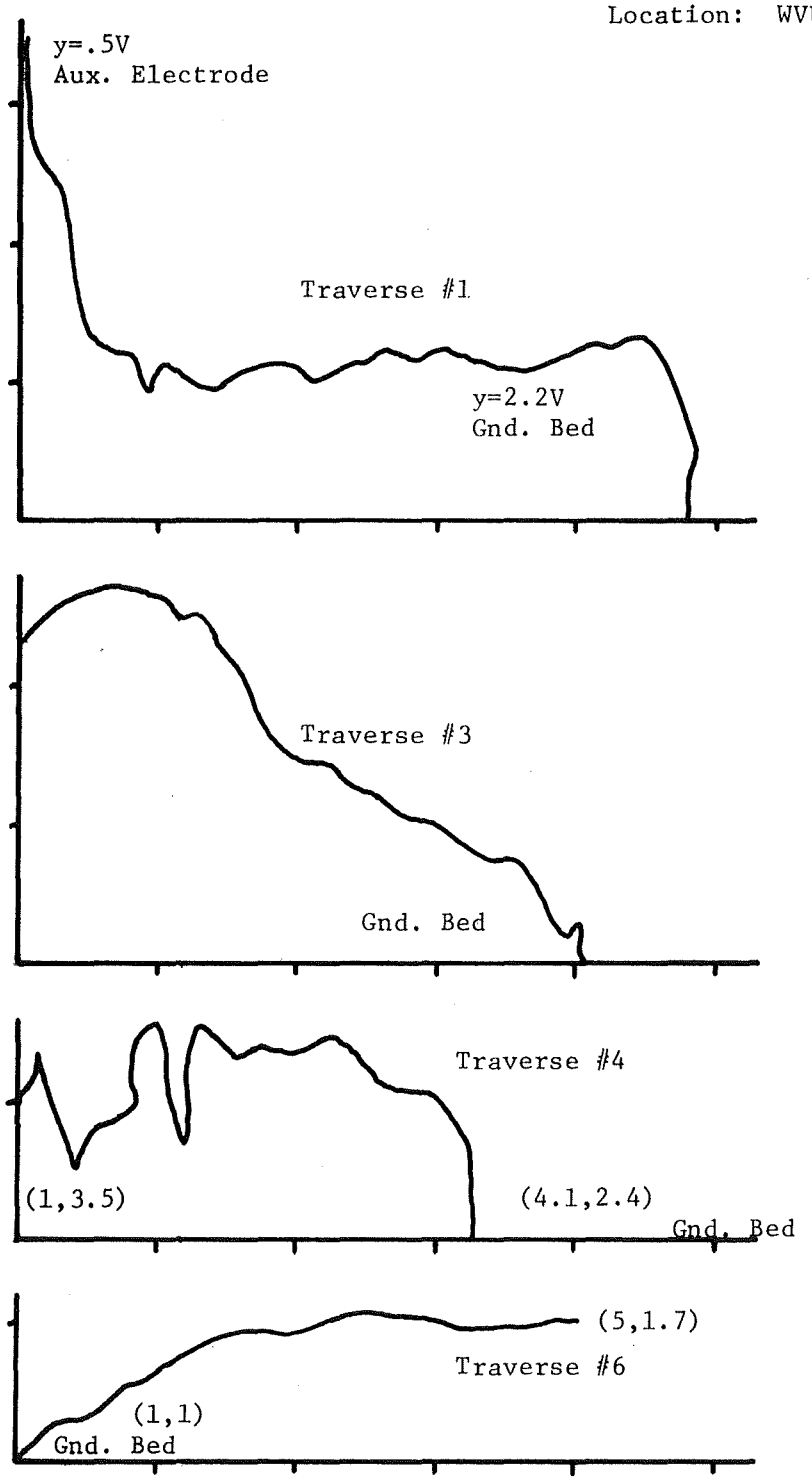


Scale: (Traverse 3, 4, 6)

x = 0.5V/.75 inch
y = 1.0V/.75 inch

Scale: (Traverse 1)

x = 1V/.75 inch
y = 1V/.75 inch

FIGURE 3.42 a. - Field test #2.

Note: 1V on x scale is 6.25 m (20.5 ft)

July 29, 1978, 2:00 p.m.
Location: WVU Ground Bed

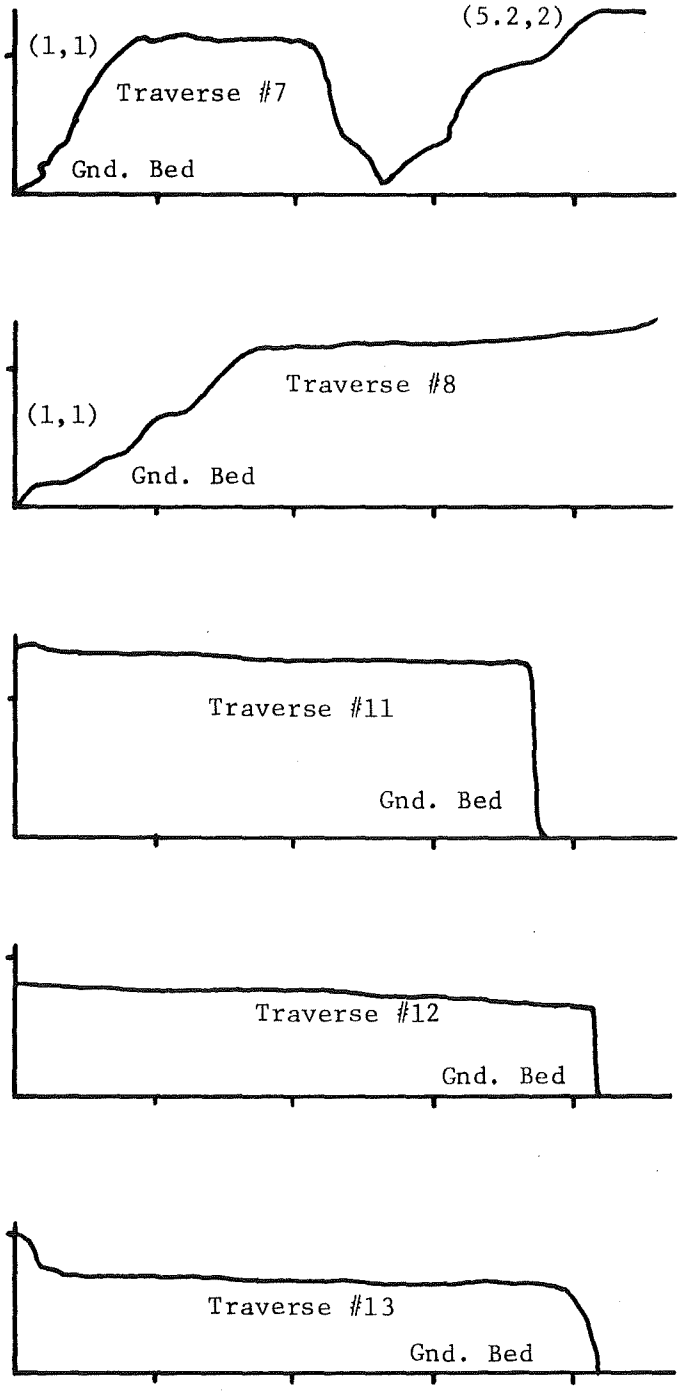


Scale: x = 0.5V/.75 inch
y = 1.0V/.75 inch

FIGURE 3.42 b. - Field test #2.

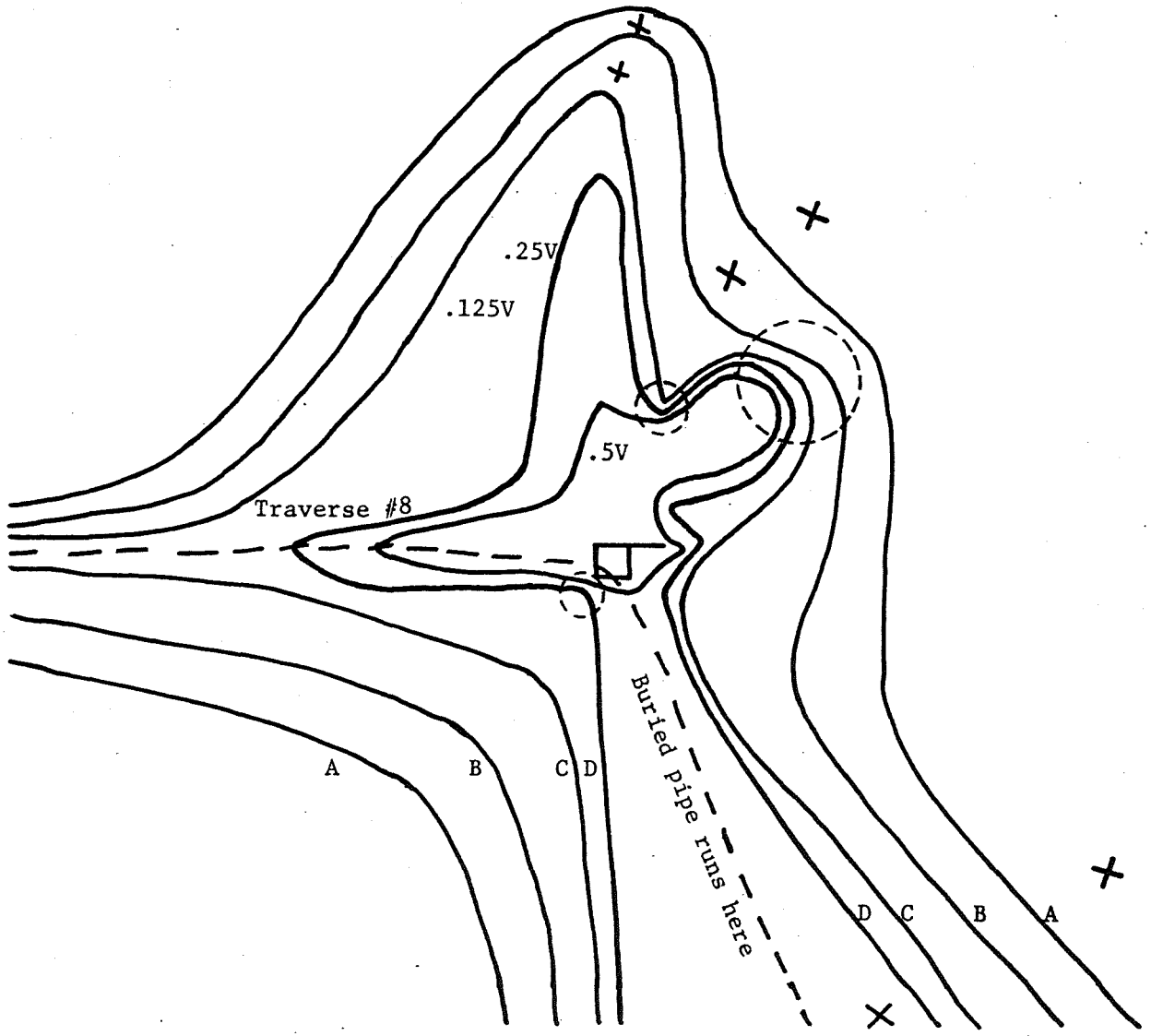


FIGURE 3.42 c . - Rough hand-plotted contour constructed from data obtained from field test #2.

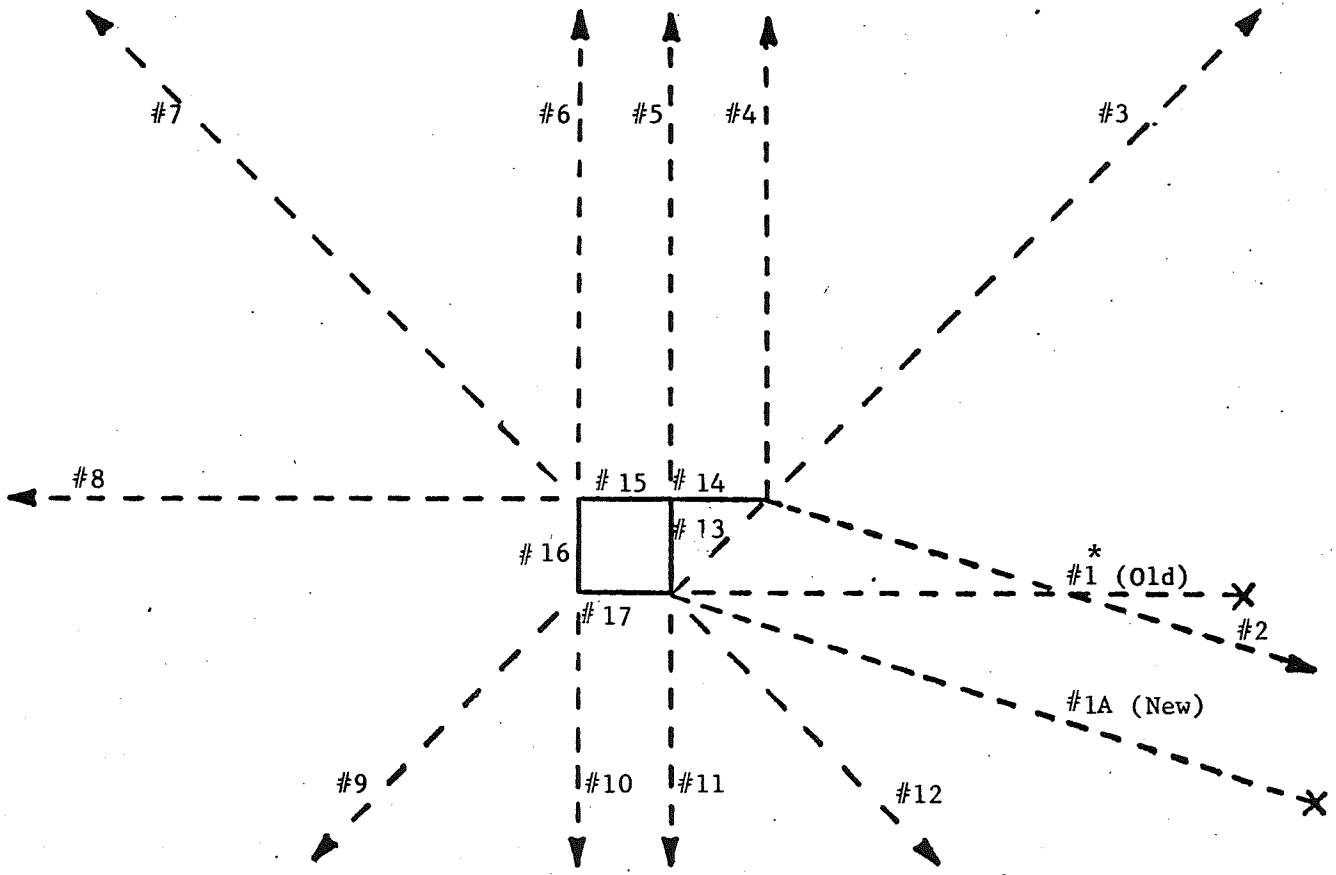


FIGURE 3.43. - Radial traverses made during field test #3.
(August 1, 1978 1:30 PM to 5:00 PM).

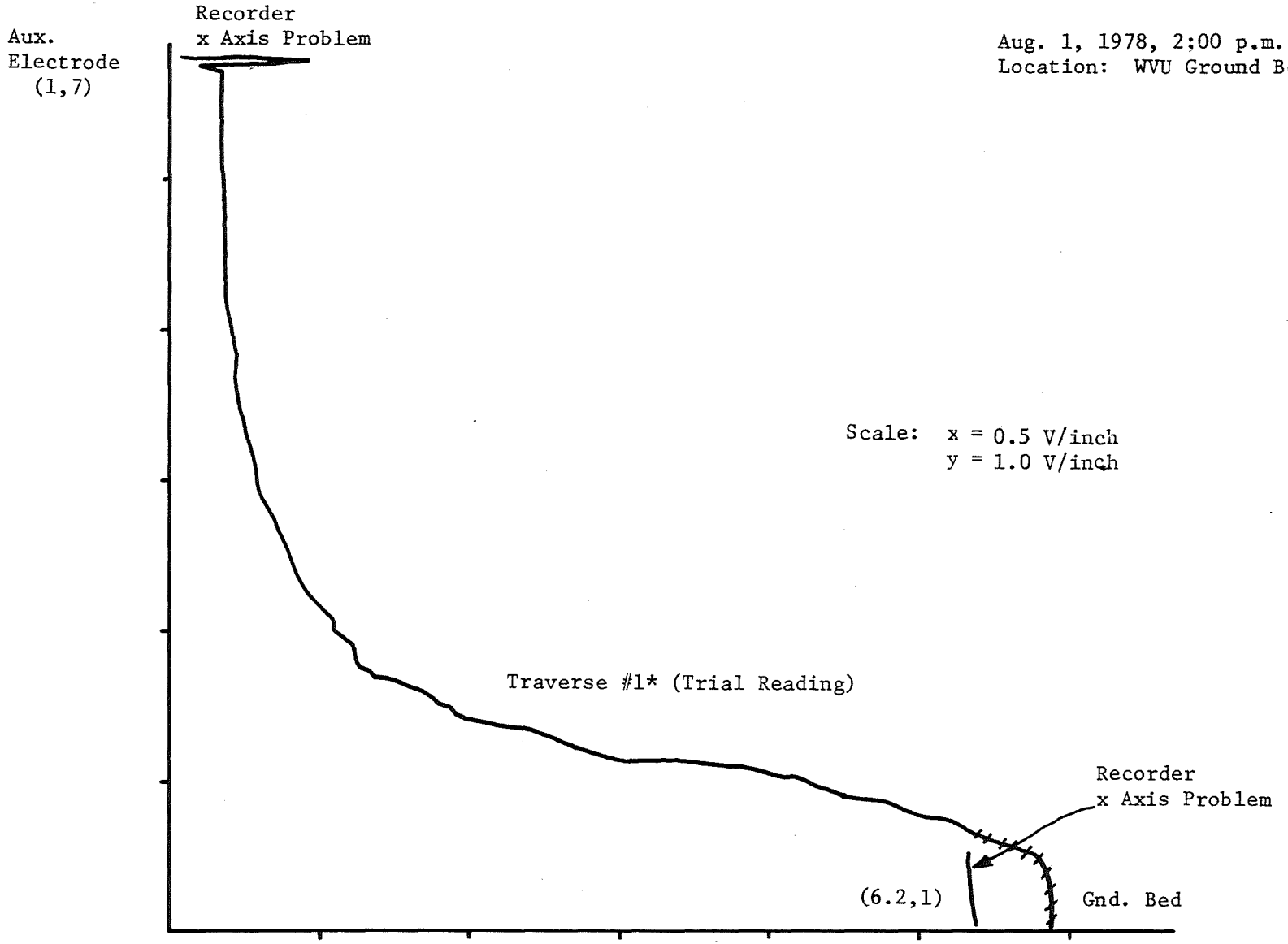


FIGURE 3.44 a. - Field test #3.

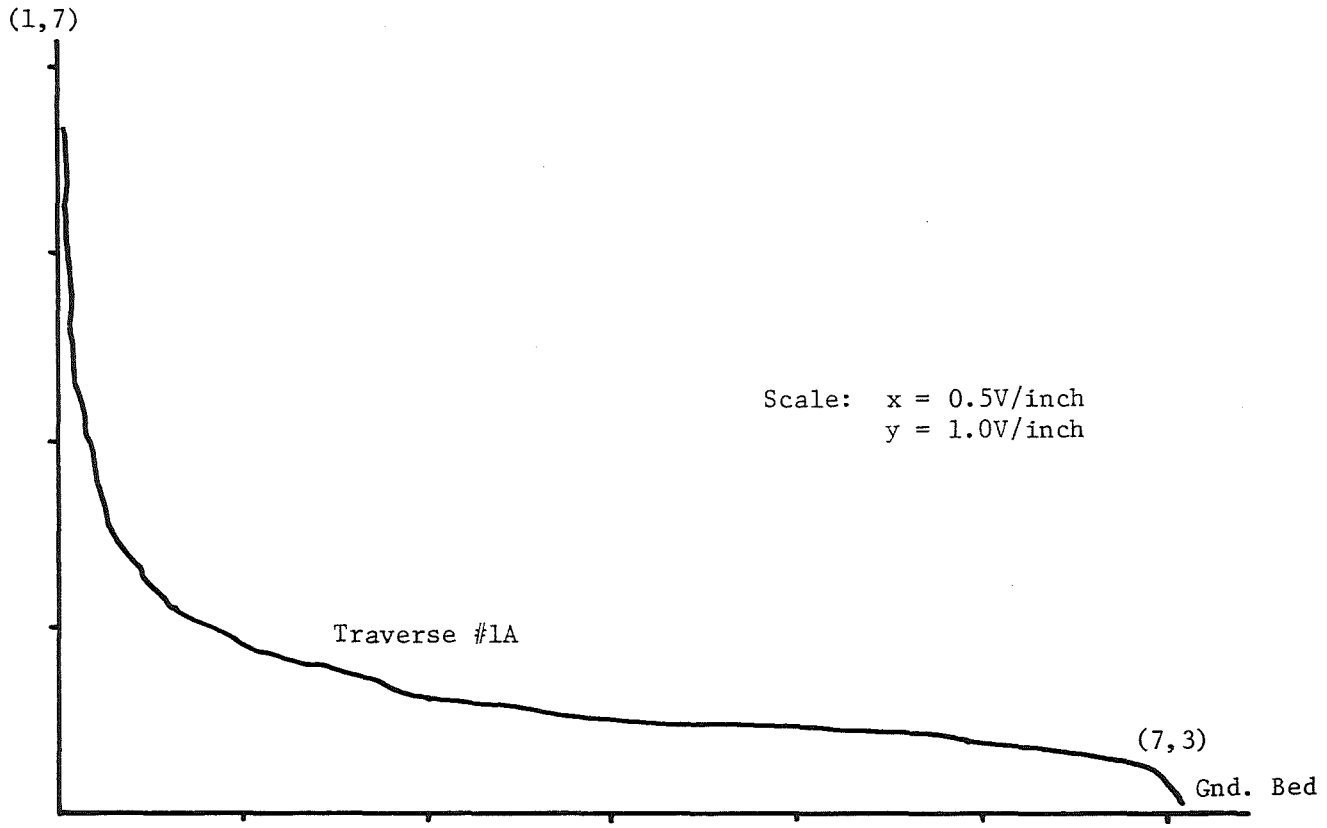


FIGURE 3.44 b. - Field test #3.

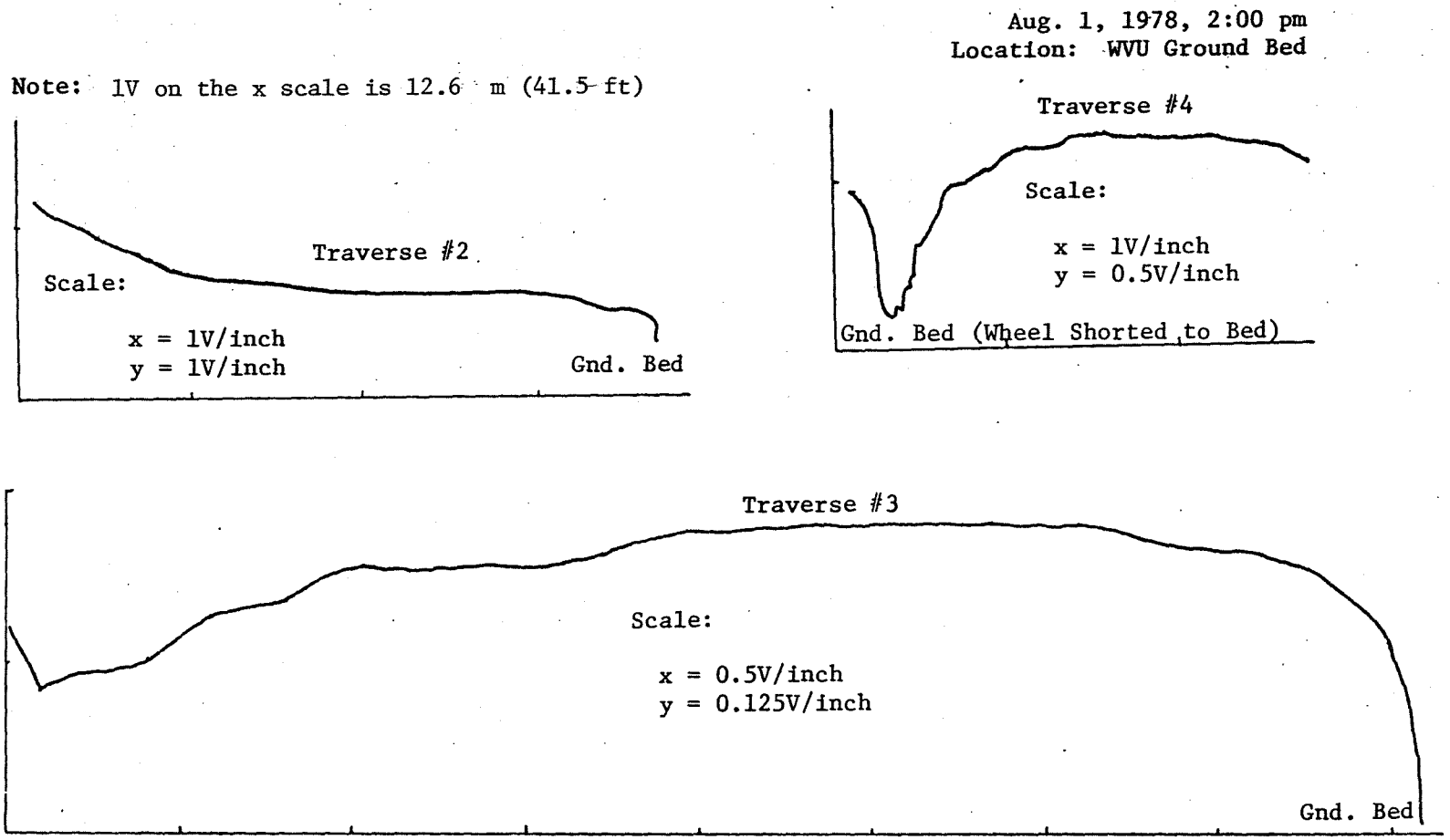


FIGURE 3.44 c. - Field test #3.

Note: 1V on the x scale is 12.6 m (41.5 ft)

Aug. 1, 1978, 2:00 p.m.
Location: WVU Ground Bed

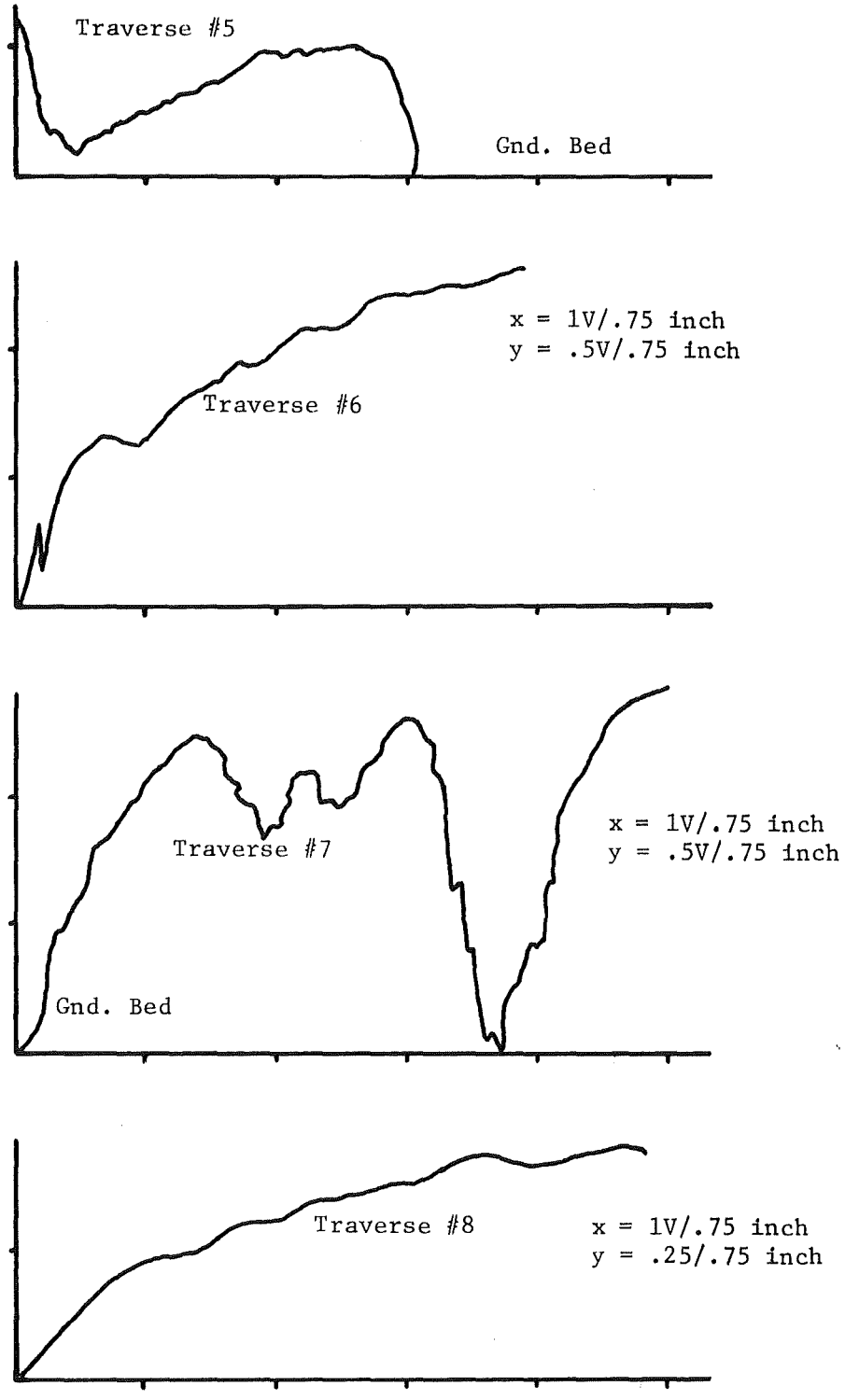


FIGURE 3.44 d. - Field test #3.

Note: 1V on the x scale is 12.6 m (41.5 ft)

Aug. 1, 1978, 2:00 p.m.
Location: WVU Ground Bed

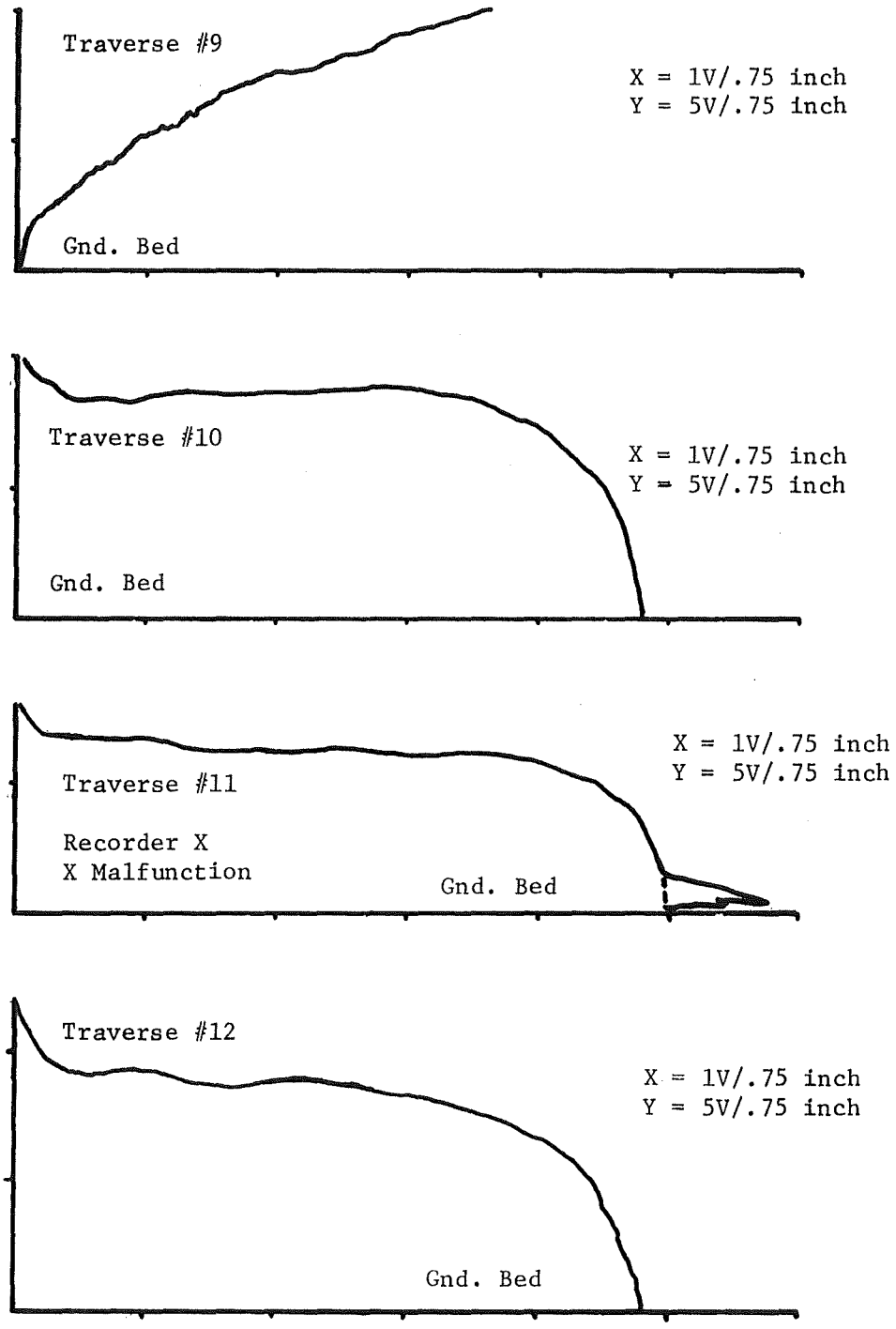


FIGURE 3.44 e. - Field test #3.

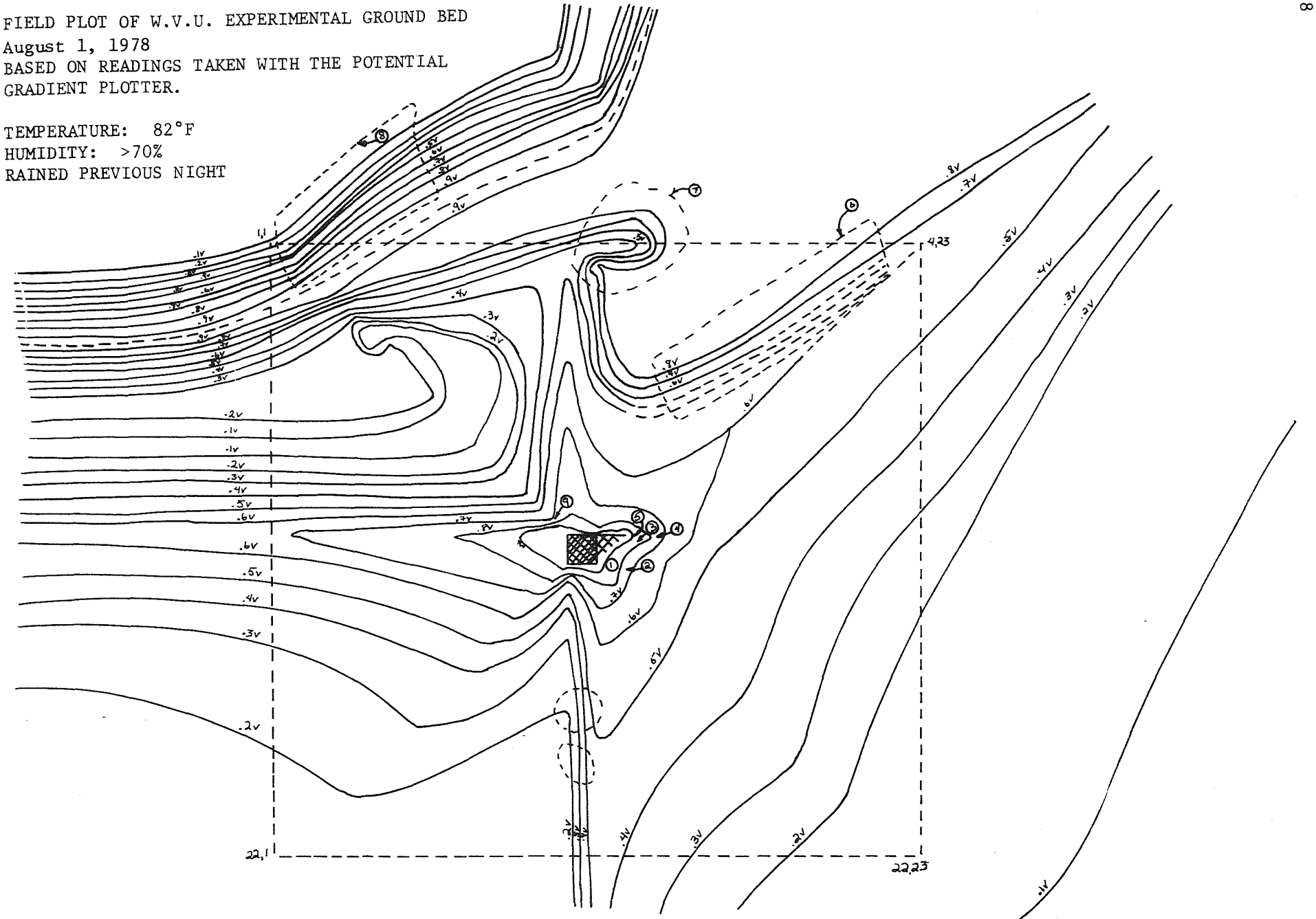


FIGURE 3.45. - Field map constructed from data obtained from field test #3.

3. Points not clearly defined in test #2 have now been measured and strongly suggest the possibility of some other underground object being raised to the ground bed potential. This has been shown as object B in the figure 3.45.

### 3.2.5 Comparison of Field Test and Theoretical Results

Reference 56 contains a description of the theoretical procedure to obtain a computer calculated field plot of the WVU experimental ground bed using the Gauss-Jordan Elimination Method. The earth is assumed homogeneous and the input data consists of the radius of the rods, depth of the rods, number of rods, the relative X and Y co-ordinates of each rod, and the voltage applied to each rod. Figure 3.46 shows the computer calculated field map using the Wolf Contour Package.

The field map shows the potential contours to be almost circular near each ground rod and radiate uniformly outward. At large distances from the ground bed the contours encircle the entire ground bed and gradually assume a circular shape.

There are considerable differences in the field maps obtained from theoretical and experimental studies. The experimental results differ from the theoretical results due to the following reasons:

1. The earth is neither uniform nor is it homogeneous.

2. The theoretical solution does not reflect the effects of buried objects. It is simply a solution to the Laplace equation for a given set of boundary values.

It can be concluded that a theoretical analysis is no doubt a good starting point to study the field distribution, but should be supplemented by a more detailed experimental investigation to gather data on areas of steep gradients, isopotentials, and how effective a ground system really is as a low-resistance path for fault currents.

## 3.3 ALTERNATIVE GROUND ARRANGEMENTS

### 3.3.1 Introduction

Whereas the present grounding practice of establishing a separate safety-ground for underground mines provides a high degree of protection, the possibility exists that alternate grounding arrangements may provide better protection for surface coal mines. Surface mines tend to have only a few pieces of heavy equipment, and considerable exposure to lightning. The following pages discuss possible alternatives to the safety ground bed system. To put the safety problem in perspective, it is necessary to first review the purpose of a ground system; then to look at alternatives which are available in order to determine the system best-suited for surface coal mine usage.

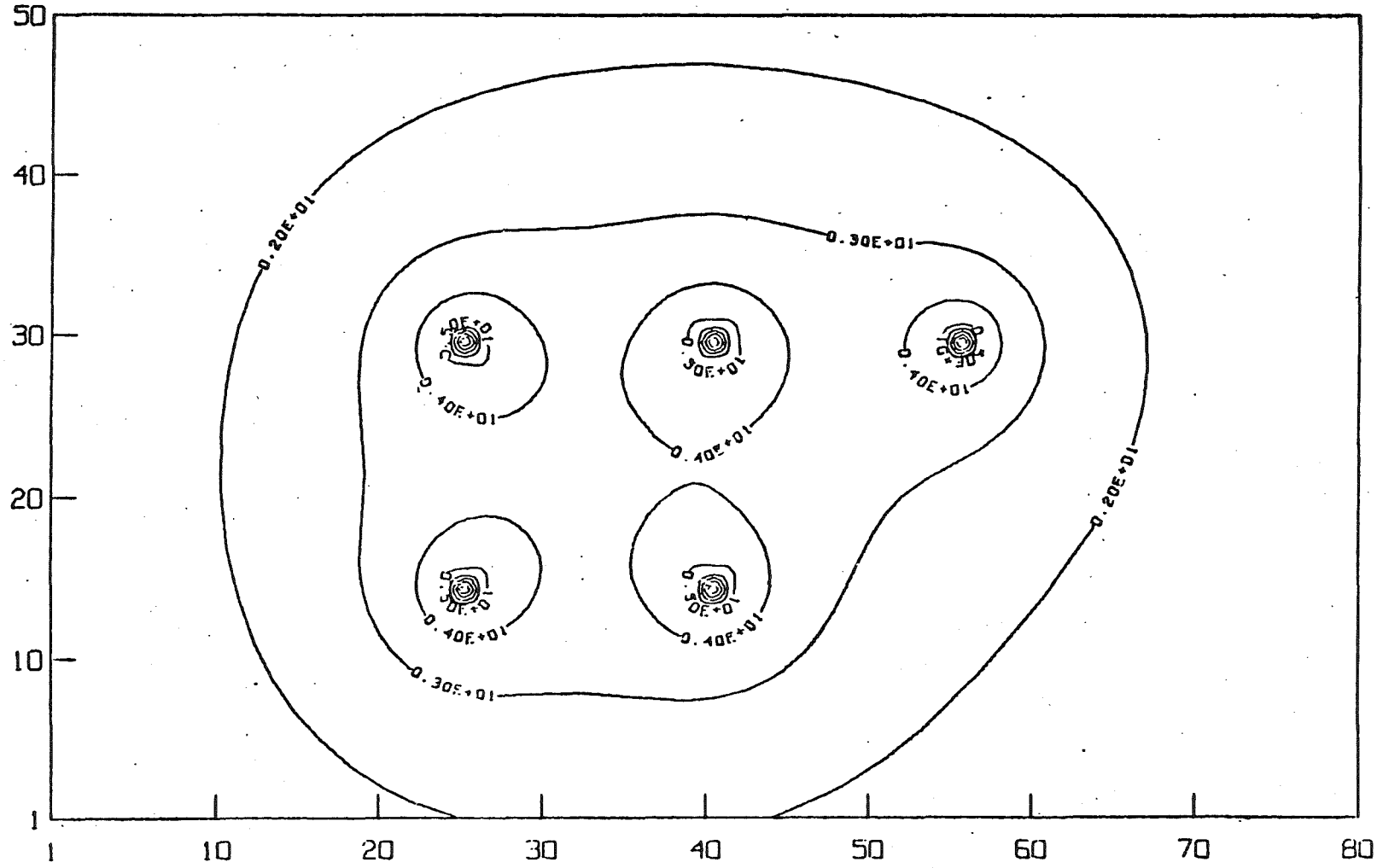


FIGURE 3.46. – Computer-calculated field map for the WVU Experimental Ground Bed (arbitray distance scale) based on theoretical calculations.

### 3.3.2 Purposes of a Grounding System

Since the major functions performed by a grounding system were discussed in some detail at the beginning of Chapter 3, only a brief summary will be included here. First, potential gradients between conducting materials must be limited to values which are not hazardous to personnel who may come into contact with exposed metal surfaces (23). Next, the amount of energy available at a fault must be restricted, both to minimize equipment damage and to rule out the danger of fire or explosion in hazardous atmospheres (9). Third, an earth connection to the system neutral point helps to control over-voltages (transients) which may otherwise cause a premature breakdown in the electrical equipment due to repeated over-stressing of key components (4). Finally, the grounding system should permit the effective isolation of offending sections of the power distribution network by the selective relaying of faults (30).

### 3.3.3 Types of Grounding

Several different grounding philosophies have been propounded and utilized by various groups in the electrical industry, each with its own advantages and disadvantages (14). These methods for power system grounding are discussed below.

1. Ungrounded Neutral. The "ungrounded" system was probably the first to be used because of its simplicity. In this system there are no intentional ground connections whatsoever. However, a truly ungrounded system cannot exist since any current-carrying conductor may be coupled to ground via numerous paths including motor windings and the distributed capacitance of the wiring itself (41). The first line-to-ground fault on such a system will have little apparent effect (15), but the two ungrounded phases will rise to full line-to-line voltage with respect to ground. There is no way for current from a single fault to find a complete circuit back to the source, so its magnitude will be very small or nil. Very low fault current means no flash hazard and no equipment damage. Circuit operation continues normally with no interruption of power, which is an important consideration in industries where downtime is critical (64). The first fault is often hard to locate because its effects are negligible. Often no repair effort is made until a second fault occurs, with is concomitant hazards of arcing, heavy current flow, and equipment damage. Since the entire system is "floating", there is no control of transient over-voltages. Except for the problem of accidental contact with a higher-voltage system, all the other over-voltage sources mentioned previously are enhanced by the distributed capacitance to ground (14).

2. Solidly-Grounded Neutral. In contrast to the ungrounded system, the solidly-grounded neutral system has its neutral point tied directly to earth. The first ground fault produces a substantial current flow which may be quickly sensed by protective circuitry, thereby shutting down the bad section. Transients are controlled since the system now has its neutral solidly referenced to ground. The hazards of this system are due to the magnitude of the fault current. Detection equipment must be sensitive enough to detect low-level fault

currents (such as arcing faults) and yet fast enough to disconnect short-circuits before significant damage can be done.

3. Low-Resistance-Grounded Neutral. This system is established by inserting a resistor between the system neutral point and ground. The resistance is sized so that ground fault currents are limited to about 400 A (14). Transients are controlled by the earth connection, and ample fault current is available for actuating protective relays. The flash hazard is not as serious as in the solidly-grounded neutral system, but a current flow of several hundred amperes can still do considerable damage.

4. High-Resistance-Grounded Neutral. This arrangement is also characterized by a resistor which is placed between the system neutral point and ground, but the value of resistance is higher and is sized according to the system voltage level. Where the line-to-neutral potential is 1000 V or less, the neutral grounding resistor must limit the fault current to 25 A or less; for systems where the line-to-neutral potential is above 1000 V, the voltage drop in the grounding circuit external to the resistor must be limited to 100 V or less under fault conditions (59). With this system, sensitive relay circuitry can detect faults on the order of 15 A, providing fault isolation and facilitating quick location of the trouble spot (13). The level of fault current is low enough that the dangers of arcing and flashover are practically eliminated, and the ground connection serves to limit the amplitude of transient over-voltages.

From the foregoing discussion, it seems that the "high-resistance-grounded neutral system" is the only choice for use in surface coal mines. The current limiting provided by this arrangement protects mine personnel from step and touch potentials which could prove to be fatal if other types of grounding were utilized. In addition, equipment damage caused by excessive fault current or by transient over-voltages is minimized or eliminated.

The problem is now reduced to deciding how to best achieve the earth connection which will function as the grounding point for the neutral resistor.

### 3.3.4 Typical Surface Mine Power Distribution

Figure 3.47 illustrates the type of power distribution which can be found in today's surface coal mines. Power from the utility is transformed to the utilization level in one or more substations located at strategic points on the mine property. Depending upon the size of the shovels or draglines in use at the mine, the secondary line-to-line voltage may be 4160 V, 7200 V, or 13.2 kV. All the metallic enclosures inside the substation (surge capacitors, lightning arrestors, etc.) are connected to the "substation ground bed". On the secondary side of the transformer, the neutral point (either direct or derived) is connected through the neutral grounding resistor

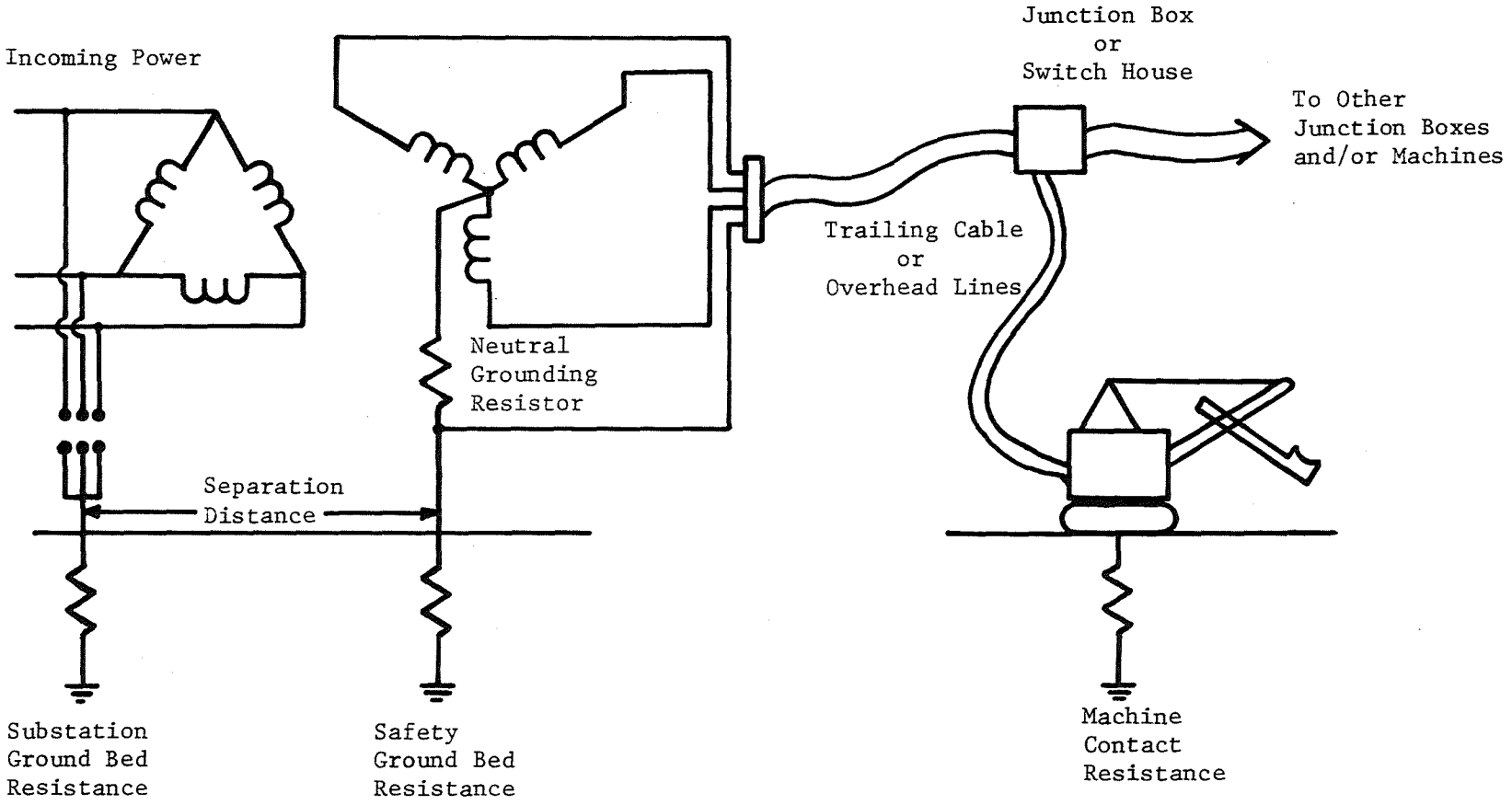


FIGURE 3.47. - Simplified representation of surface coal mine power system.

to a separate earth terminal known as the "safety ground bed". Normal practice is to locate the safety ground bed about 8 m (25 ft) away from the substation ground bed, although a separation distance of 15 m (50 ft) sometimes used.

A metallic conductor joins the safety ground bed to the frames of all equipment (shovels, draglines, drills, etc.) powered from the secondary of the transformer. This conductor may be part of a trailing cable or may be carried as an overhead conductor if pole lines are used. The metal frame of each piece of electrically-powered mining equipment is thus solidly tied to the safety ground bed. This safety ground bed is usually established somewhere near the substation, and may consist of one or more driven rods, or may be a buried mesh or grid of interconnected conductors. This type of ground bed has several advantages:

1. It can be located in a safe spot where it is unlikely to be run over by a bulldozer or be disrupted in some manner.

2. It can be made fairly large in size and extent (if necessary) in order to obtain a low value of earth resistance. A value of 5Ω or less is generally considered to be acceptable.

3. Because the bed is permanent, its resistance value is fairly constant (except for some seasonal variations) and can be readily measured by straightforward techniques such as the fall-of-potential method.

### 3.3.5 The Problem with Transfer of Potential

This kind of ground bed has one important disadvantage: its close proximity to the substation ground bed. The substation ground bed is called upon, from time to time, to carry currents which may reach several thousands of amperes. This could occur during a primary fault, lightning surge, or other system malfunction. As illustrated in figure 3.47, the substation ground bed does not make absolutely perfect contact with the soil in which it is buried, but has a small value of resistance, which may be 5Ω or less. When conducting current, there will be a voltage drop associated with the flow of this current through the ground bed resistance. The soil surrounding the electrode will therefore not be at zero potential. There will be a potential "hill" associated with the substation ground bed - the highest voltage will be that of the ground electrode itself, while the potential will progressively decrease as one moves farther and farther away from the bed. Now, if the safety ground bed is located somewhere on the potential "hill" associated with the substation ground bed, then it will likewise be raised in potential. This "transferred potential" will also appear on the frame of each mining machine connected to the safety ground bed.

An example can be used to illustrate this point. Let the substation ground bed consist of a single driven rod, 6.1 m (20 ft) long and 5 cm (2 in) in diameter, when immersed in a soil whose resistivity is 30.5Ω-m (100 Ω-ft), this rod will have an earth resistance of just under 5Ω. The formula for the earth resistance of a single rod is (48):

$$R = \frac{\rho}{2\pi\ell} \ln \left( \frac{2\ell}{a} \right) \tag{3.10}$$

where R = earth resistance of the rod, in ohms
$\rho$ = earth resistivity, in ohm-meters (or ohm-feet).
$\ell$ = rod length, in meters (or feet)
a = rod radius, in meters (or feet)
and ln = natural logarithm.

Now, the potential at a point on the earth's surface at a distance r from the rod may be calculated from (4):

$$V = \frac{\rho I}{4\pi\ell} \ln \left[ \frac{\sqrt{\ell^2+r^2}+\ell}{\sqrt{\ell^2+r^2}-\ell} \right] \tag{3.11}$$

where V = voltage on the earth's surface at a distance r, in volts
I = current carried by the rod, in amperes
r = distance from ground rod, in meters (or feet)

and the other parameters have been previously defined.

If the substation ground bed carries a fault current of 2000 amperes, then the potential on the ground rod will be 10,000 volts. The voltage profile at the surface of the earth surrounding the electrode is shown in figure 3.48, while the potential somewhat farther from the ground rod is drawn in figure 3.49. If it is decided to limit the transferred potential at the safety ground bed to 100 volts, then the safety ground bed must be located about 91 m (300 ft) away from the substation ground bed. The potential value of 100 volts was chosen as a criterion because Federal law requires that neutral-resistor grounding systems be designed so that the maximum potential in the circuit external to the grounding resistor (during a fault) is 100 volts or less (59). Obviously, the numbers used in this example are purely arbitrary, and different values for the various parameters could easily be chosen and justified. However, the purpose of the exercise was to point out that it is probably not a good idea to locate the safety ground bed in close proximity to the substation ground bed.

If the substation bed was subjected to a lightning surge, then a nearby safety ground bed would be raised to a very high potential for a short length of time. However, because of the waveform of a lightning impulse (very fast rise time and short duration), it is possible that very little of this transferred potential would propagate through the trailing cable to the frames of equipment connected to the safety ground bed (6). In contrast, the time required to clear primary faults is sufficiently long that there could easily be a transfer of potential from the substation ground bed to the safety ground bed.

One solution to this problem might be to move the safety ground bed much farther away from the substation ground bed, thereby reducing the

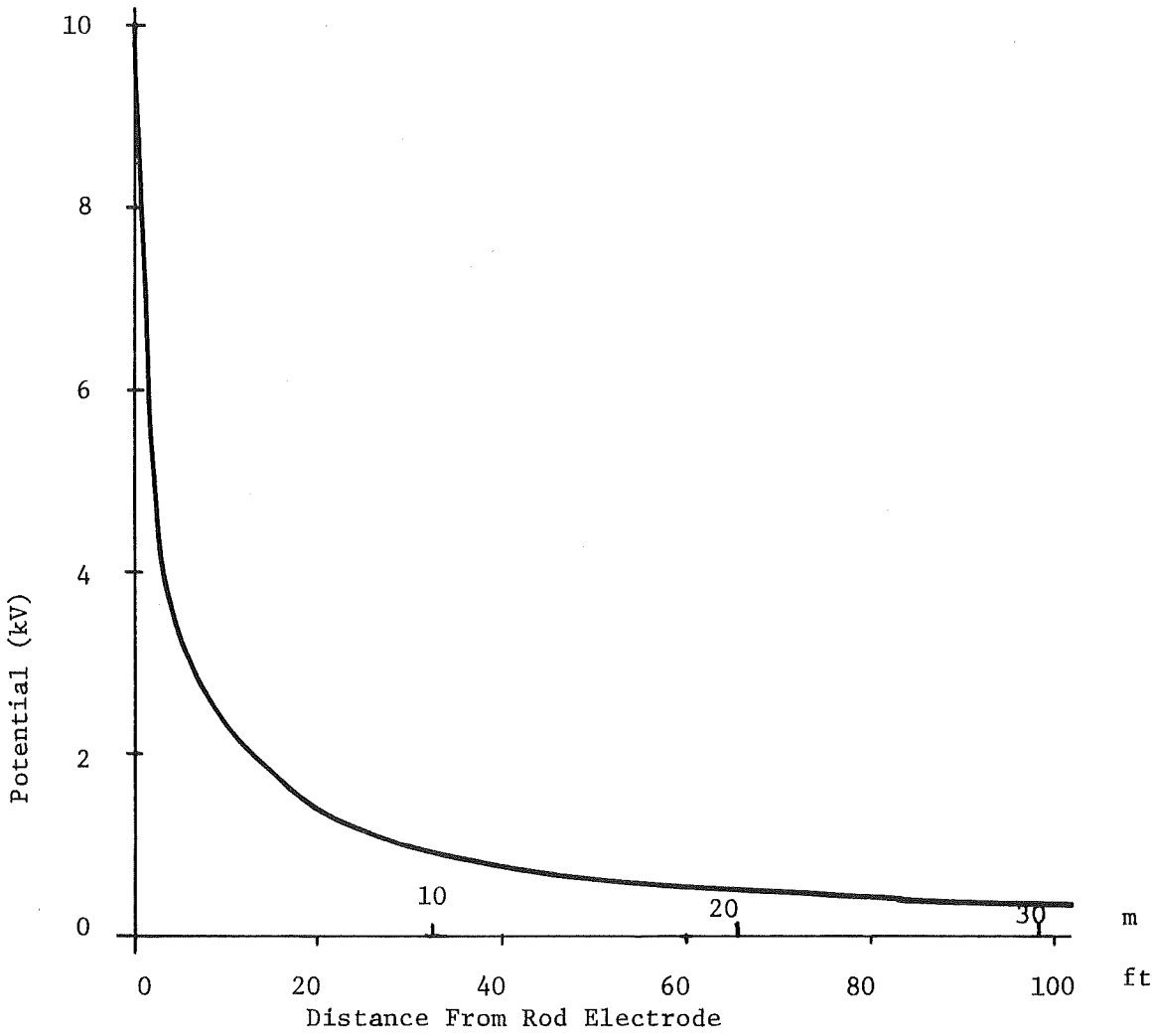


FIGURE 3.48. - Potential on the earth's surface near a current-carrying electrode.

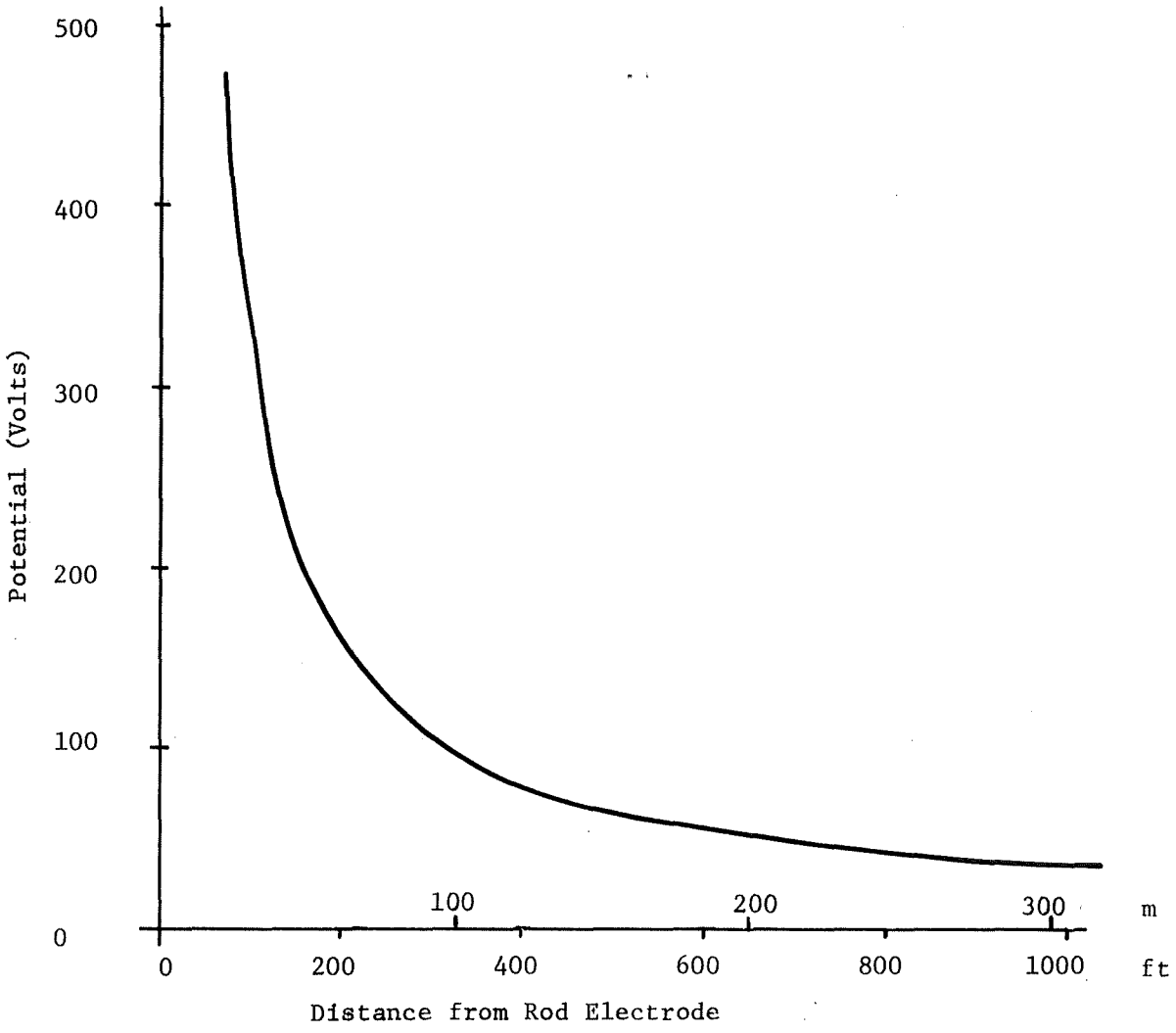


FIGURE 3.49. - Potential on the earth's surface at a distance from a current-carrying electrode.

magnitude of any transferred potential. Unfortunately, unless the maximum primary fault current and the substation ground-bed resistance are both known before hand, it is impossible to determine the separation distance which is necessary to prevent the transfer of hazardous potentials. In addition, the required separation distance might be unrealistically large.

### 3.3.6 Using the Mining Machinery as a Ground Bed

Most of the equipment used in surface mining (draglines, shovels, drills) is quite large in size, and is supported either on caterpillar-type treads or on a circular base called a tub. These machines are also quite heavy, and the combination of size and weight may result in a machine-earth interface whose resistance is quite low - in effect, a ground bed. Table 3.3 shows the measured values of earth resistance for different types of electrically-powered equipment used in open-pit copper mines and surface coal mines (5). The resistance values in the Table range from less than 1Ω to 86Ω, although all the machinery used in surface coal mining had a measured resistance of less than 14Ω. Because a surface substation generally supplies power to several pieces of portable or mobile equipment at one time, the "safety ground bed" would be composed of the parallel combination of several machine contact resistances, leading to a lower value of resistance. These mining machines are usually operated at locations which are well removed several hundred meters from the substation which supplies their power, thereby greatly decreasing the hazard of transferred potential. In addition, the expense of building a safety ground bed is eliminated if machine frame contact surfaces are used to replace the safety bed.

The major disadvantage of this kind of system is that the resistance of such a "safety ground bed" could vary widely, depending upon the number and size of the machines powered from a single substation, and the conductivity of the soil in the area where the machines are working.

### 3.3.7 Driving a Ground Rod Near Each Mining Machine

Perhaps it would be possible to drive a ground rod near each machine and use this rod as a safety ground bed. If the soil resistivity near a shovel or dragline is known, then the formula given earlier (equation 3.10) can be used to determine the earth resistance for a ground rod of any size. Similarly, if a specific value of earth resistance is desired, this formula will yield the dimensions of the electrode which is required. The soil resistivity near most of the coal mining equipment shown in Table 3.3 was measured using the Wenner 4-probe technique, and the average values of resistivity are shown in Table 3.4. The length of ground rod required to give an earth resistance of either 5Ω or 15Ω when situated in this type of soil was then calculated, and the results are also displayed in the table. In each case a rod diameter of 5 cm (2 in) was assumed. The earth resistance value is that due to the rod alone, and does not include the effect of the machine contact resistance, which would be in parallel with the ground rod. Note that a parallel combination of ground rod and machine frame will NOT yield a net resistance such as would be predicted from circuit theory. The mutual resistance between two closely-spaced electrodes will be large enough that the parallel combination of the two will yield a net resistance only slightly lower in value than the smaller of the two individual resistances.

TABLE 3.3. - Measured resistance values for various types of surface mining equipment (5)

| Type of Mine | Machine | Weight | | Contact Area, | | Resistance, Ω |
|---|---|---|---|---|---|---|
| | | (X 1000 lb) | Tonnes | $ft^2$ | $m^2$ | |
| Open-pit Metal | Drill 1 | 75 | 31 | 48 | 4.5 | 86 |
| | Shovel 1 | 380 | 172 | 90 | 8.4 | 18.2 |
| | Shovel 2 | 380 | 172 | 90 | 8.4 | 60.4 |
| | Shovel 3 | 405 | 184 | 90 | 8.4 | 39 |
| | Shovel 4 | 500 | 227 | 107 | 9.9 | 4.25 |
| | Shovel 5 | 950 | 431 | 140 | 13.0 | 21 |
| | Shovel 6 | 379 | 172 | 147 | 13.7 | 4.5 |
| | Shovel 7 | 379 | 172 | 147 | 13.7 | 10.2 |
| | Shovel 8 | 379 | 172 | 147 | 13.7 | 8.1 |
| | Shovel 9 | 379 | 172 | 147 | 13.7 | 5.3 |
| | Shovel 10 | 580 | 263 | 155 | 14.4 | 13.5 |
| | Shovel 11 | 580 | 263 | 155 | 14.4 | 7.5 |
| | Shovel 12 | 975 | 442 | 158 | 14.7 | 8 |
| | Shovel 13 | 972 | 441 | 163 | 15.1 | 29 |
| | Shovel 14 | 915 | 415 | 166 | 15.4 | 5 |
| | Shovel 15 | 915 | 415 | 166 | 15.4 | 34.8 |
| | Dragline 1 | 1,600 | 726 | 1,018 | 94.6 | 0.9 |
| Surface Coal | Drill 2 | - | - | 152 | 14.1 | 4.05 |
| | Drill 3 | - | - | 152 | 14.1 | 4.8 |
| | Drill 4 | - | - | 86 | 8.0 | 13.23 |
| | Shovel 16 | - | - | 96 | 8.9 | 5.75 |
| | Shovel 17 | - | - | 152 | 14.1 | 7.9 |
| | Shovel 18 | - | - | 115 | 10.7 | 4.78 |
| | Shovel 19 | 960 | 435 | 198 | 18.4 | 4.72 |
| | Dragline 2 | - | - | 1,520 | 141.2 | 1.4 |
| | Dragline 3 | 1,271 | 577 | 804 | 74.7 | 1.05 |

TABLE 3.4. - Rod lengths necessary to achieve a resistance of 5Ω or 15Ω when driven in soils with resistivity similar to that which was measured in actual coal mines

| Machine | Contact Area, | | Earth Resistance, | Soil Resistivity, | | 5Ω Rod Length, | | 15Ω Rod Length, | |
|---|---|---|---|---|---|---|---|---|---|
| | $ft^2$ | $m^2$ | Ω | Ω-ft | Ω-m | ft | m | ft | m |
| Drill 3 | 152 | 14.1 | 4.8 | 239 | 72.8 | 55 | 16.8 | 15 | 4.6 |
| Drill 4 | 86 | 8.0 | 13.23 | 373 | 113.7 | 92 | 28.0 | 26 | 7.9 |
| Shovel 16 | 96 | 8.9 | 5.75 | 656 | 199.9 | 175 | 53.3 | 50 | 15.2 |
| Shovel 17 | 152 | 14.1 | 7.9 | 140 | 42.7 | 30 | 9.1 | 8 | 2.4 |
| Shovel 18 | 115 | 10.7 | 4.78 | 46 | 14.0 | 8 | 2.4 | 2 | 0.6 |
| Shovel 19 | 198 | 18.4 | 4.72 | 126 | 38.4 | 26 | 7.9 | 7 | 2.1 |
| Dragline 2 | 1520 | 141.2 | 1.4 | 161 | 49.1 | 35 | 10.7 | 10 | 3.0 |
| Dragline 3 | 804 | 74.7 | 1.05 | 111 | 33.8 | 23 | 7.0 | 6 | 1.8 |

Looking at Table 3.4 it can be seen that Shovel 16 was located in an area of low soil conductivity, and a rod 15 m (50 ft) long would be required achieve a resistance of 15Ω. Rod lengths which are considerably shorter will suffice in all other cases, with the necessary size ranging from 0.6 m (2 ft) to 7.9 m (26 ft). Figure 3.50 is a graph which enables one to determine how long a ground rod should be to achieve an earth resistance of either 5Ω or 15Ω when driven in soils whose resistivity is 305 Ω-m (1000 Ω-ft) or less. This figure is drawn for rods which are only 5 cm (2 in) in diameter, while figure 3.51 shows the outcome when the same type of analysis was made for a borehole casing 30.5 cm (12 in) in diameter. Comparing the two figures, it can be seen that a six-fold increase in the diameter of the rod decreases the earth resistance by about 20%. In any event, if the soil resistivity is fairly high, a very long ground rod or borehole casing must be used in order to achieve a satisfactorily low value of earth resistance.

### 3.3.8 Safety Ground Bed Tied Directly to Substation Ground Bed

At the present time there are no Federal regulations which require the use of a separate "safety ground bed" for substations supplying power to surface coal mines. It would seem feasible therefore to simply tie the bottom end of the neutral grounding resistor to the substation ground bed, which is normally quite extensive, and presumably has a low value of earth resistance.

Any potential appearing on this "unified ground bed" would now be transferred directly to the frames of all equipment powered from the substation. That is, by tying the substation ground bed solidly to the safety ground bed, the coefficient of coupling between these two beds is now equal to unity.

If mine operators were to start using this type of grounding system, perhaps they could be convinced to install a single ground bed at each substation which was large enough to provide a very low value of earth resistance, such as 1Ω or less. The potential which is transferred from a 5Ω station ground bed to a safety ground bed located only 7.6 m (25 ft) away may be higher than the potential which appears directly on a "unified ground bed" whose resistance is only 1Ω.

### 3.3.9 Conditions Which May Lead to Hazardous Potentials on Machine Frames

Four different situations were examined which may lead to the appearance of dangerous voltages on the frames of mining equipment. These are:

1. Transfer of Potential
2. Lightning Striking a Machine
3. Secondary Phase-to-Earth Fault
4. Secondary Phase-to-Neutral Fault with Open Ground Conductor

Problems caused by transferred potential were covered earlier in this text, and the remaining three topics will now be considered.

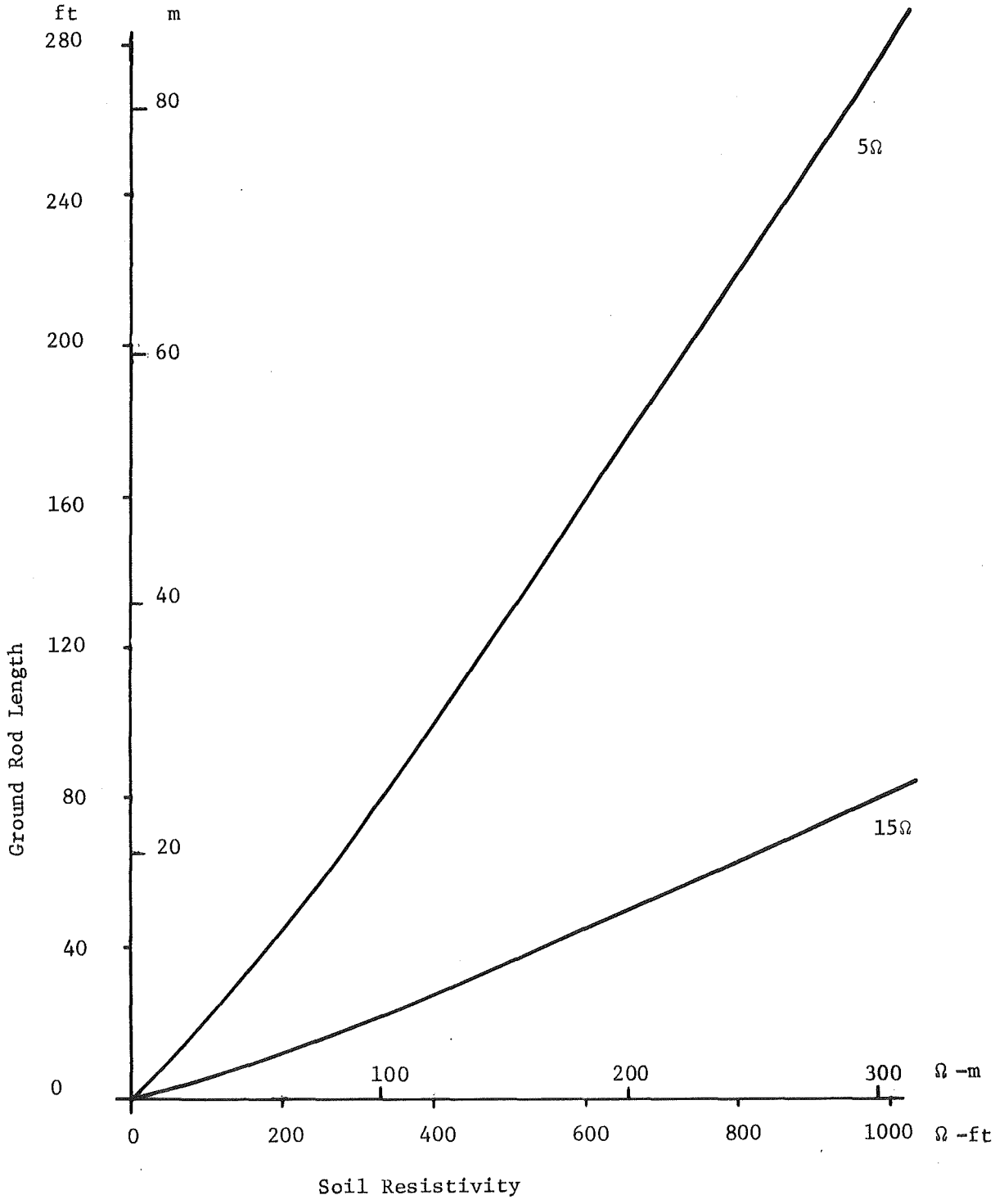


FIGURE 3.50. - Length of Ground Rod (5 cm, or 2 in diameter) required to achieve earth resistance of 5Ω or 15Ω.

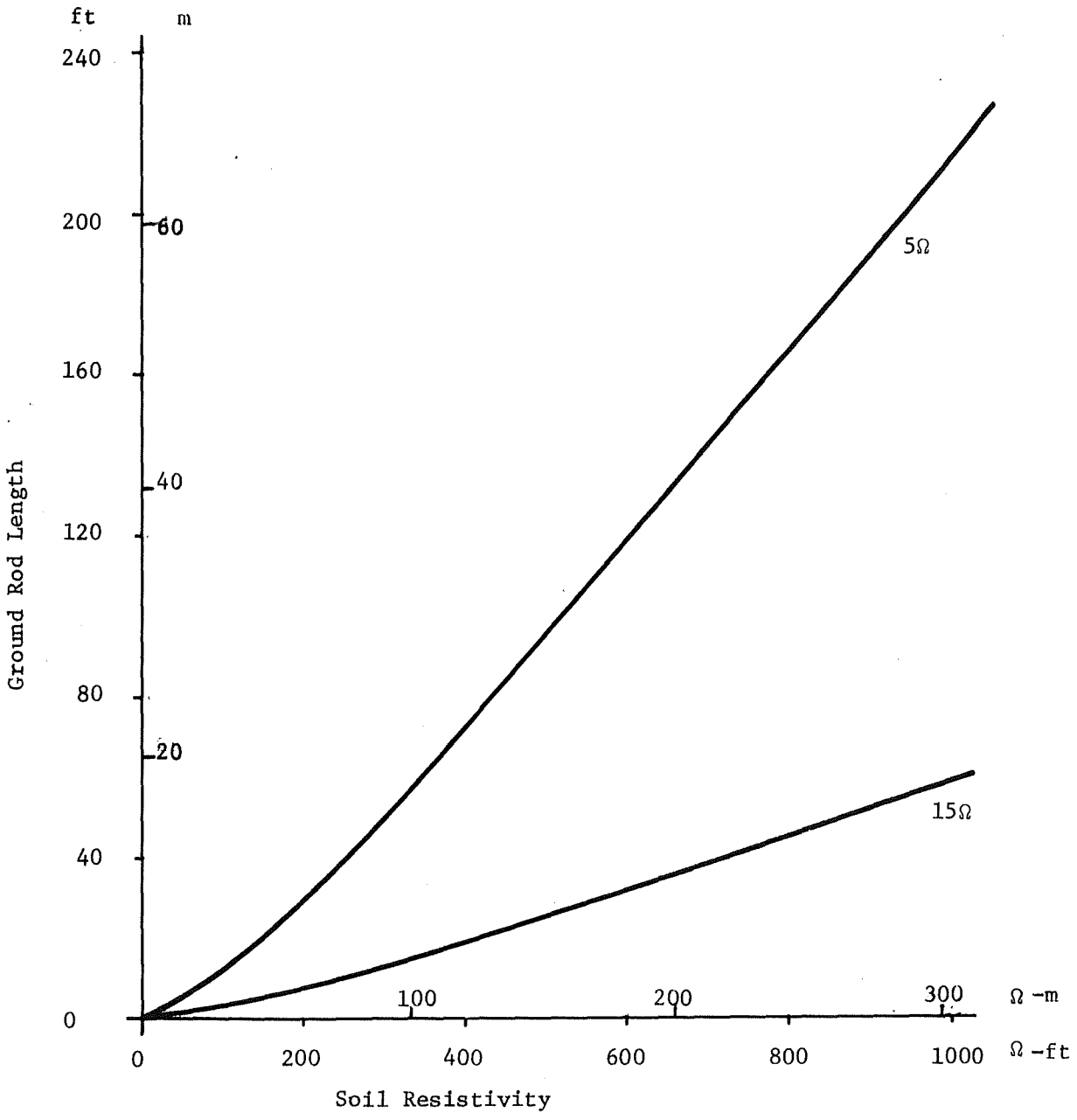


FIGURE 3.51. - Length of Ground Rod (30.5 cm, or 1 ft diameter) required to achieve earth resistance of 5Ω or 15Ω.

### 3.3.10 Lightning Striking a Machine

One does not normally think of a dragline or shovel as an earth electrode, but it is likely that, in the event of a lightning stroke to the boom or mast of a large piece of surface mining equipment, the machine would temporarily act as a fairly effective lightning rod. A study of the literature indicates that the impedance of an earth electrode under surge conditions will be equal to or less than its steady-state resistance (10, 52). The major cause of this phenomenon is the breakdown of the soil surrounding the electrode under the stress of intense electric fields (40). Electrode resistance may also be reduced due to the formation of streamers radiating horizontally along the surface of the ground (10)

If lightning should strike a surface-mining machine, there are several paths which the surge current can follow to earth. The shortest path would be directly through the machine frame/soil interface, while another path would be back along the ground conductors to the safety ground bed, a locally-driven ground rod, or the frame of another machine. Table 3.3, which appeared earlier in this report, shows the results of earth resistance measurements made on electrically-powered surface mining equipment. All of the contact resistance values found in surface coal mines were below 15Ω, while 2/3 of the machines measured in open-pit metal mines had an earth resistance of 25Ω or less. From the previous analysis one could assume that, under surge conditions, the impulse impedance of any unit of equipment would be less than the resistance figure given in the table. Since the approximate surge impedance of a trailing cable is 50Ω and overhead lines are about 400Ω, it is likely that current from a lightning stroke would flow to ground via the machine/earth contact surface.

The lightning waveform is characterized by a very fast rise time, on the order of 1 to 2 microseconds (54), and therefore somewhat resembles an RF signal whose frequency is around 250 kHz. There will be some voltage drop across the machine itself due to the L di/dt term, but the series inductance of a drill mast or dragline boom is small because of the large cross-sectional area of such structures.

In the event of a lightning strike to a piece of mining equipment, hazardous step and touch potentials will exist at and around the machine for a short period of time, no matter what type of grounding method is used. An examination of all available MSHA reports on surface mine electrical fatalities over the last 7 years failed to produce any direct evidence of electrocution caused by the mechanism just reviewed. However, several accidents were described where the cause of death was undetermined, and lightning was suggested as one of a number of possible explanations.

### 3.3.11 Phase-to-Earth Fault on Secondary Distribution

Many surface coal mines use shielded trailing cable to span the entire distance from substation to machine, and phase-to-earth faults would therefore be unlikely to occur. However, open-pit metal mines often use overhead lines to transmit power around the mine perimeter and down the benches. At strategic locations the overhead lines then terminate at switch-houses, from which the power is carried to machinery via trailing

cables. These overhead lines may run for 1600 m (1 mile) or more, and phase-to-earth faults are possible.

Figure 3.52 illustrates the circuit configuration for a phase-to-earth fault in mining environments where each of the four previously discussed methods of neutral grounding is used. If a machine frame is used as the only ground connection, then all the fault current will flow through the frame, while the alternative techniques (safety ground bed, unified ground bed, and locally-driven rod) will provide a parallel path for the fault current, which may yield a lower touch potential at the machine. In any event, there will be a potential on the frame of the machine no matter what type of grounding system is used, although its value will depend upon the ratio of the various resistances.

### 3.3.12 Phase-to-Neutral Fault with Open Ground Conductor on Secondary Distribution

If the ground conductor(s) leading from the machine frame back to the transformer neutral should open, then machine frames could become elevated to a dangerous potential in the event of a phase-to-neutral fault near the machine. This situation is unlikely to occur in mines which use trailing cable for the entire span between substation and machine, but is quite possible if overhead distribution lines are used to connect substations to switch-houses or junction boxes. This situation is illustrated in figure 3.53 for a mine power system using a traditional safety ground bed or unified ground bed. If there is only one machine connected to the transformer secondary, then the safety ground bed resistance is placed in series with the machine frame contact resistance, and the touch potential on the machine is determined by the resulting voltage-divider network. If several machines are connected, see figure 3.53 (b), then fault current may flow downward through the frame of the faulted equipment and return to neutral via the frame of another machine as well as the safety ground bed. In this manner, a problem on one machine may cause a hazardous condition to exist on several other machines.

Figure 3.54 illustrates a phase-to-neutral fault on a power system where the machine frame itself is used as the earth connection. If there is only one machine connected to the transformer secondary, then (theoretically) no fault current would flow in the event of a phase-to-neutral fault at the machine, if the ground conductor was open. However, it is likely that a small leakage current would exist because of capacitive coupling between the earth and the components of the power distribution system such as trailing cables, switch-houses, transformers, etc. If several pieces of equipment are powered from the same transformer, as shown by figure 3.54 (b), then fault current can flow through the earth from one machine to another and thence back to the neutral point. Again, the frames of both machines are elevated in potential.

A power system utilizing ground rods driven near each piece of operating equipment is drawn in figure 3.55. As before, a phase-to-neutral fault at the machine frame occurs in combination with an open ground conductor. If the transformer load consists of a single machine, then the fault circuit will be completed via capacitive coupling. For two or more machines supplied

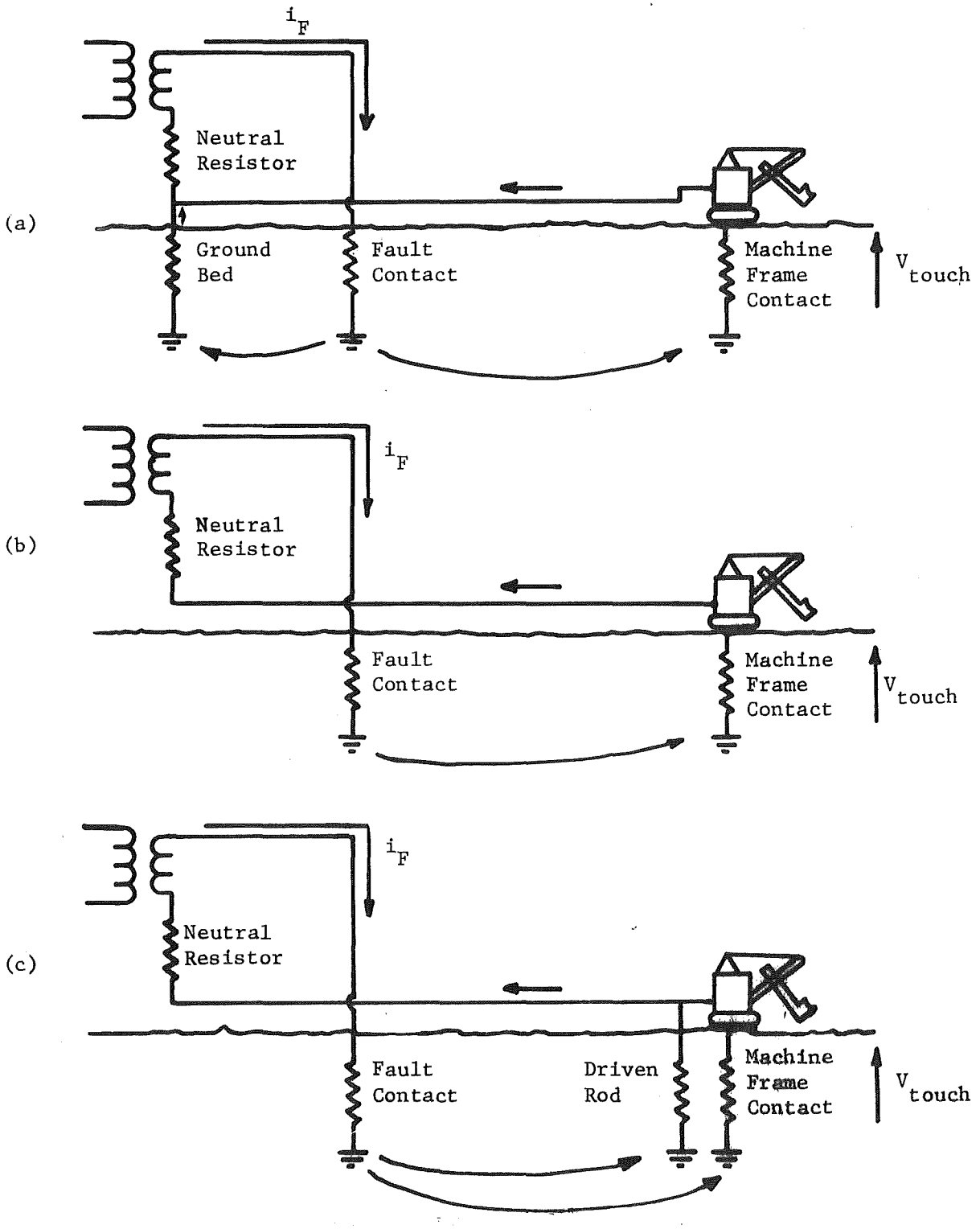


FIGURE 3.52. - Phase-to-earth fault on secondary distribution.

(a) Safety ground bed; (b) Machine frame as ground;
(c) Locally-driven rod as ground.

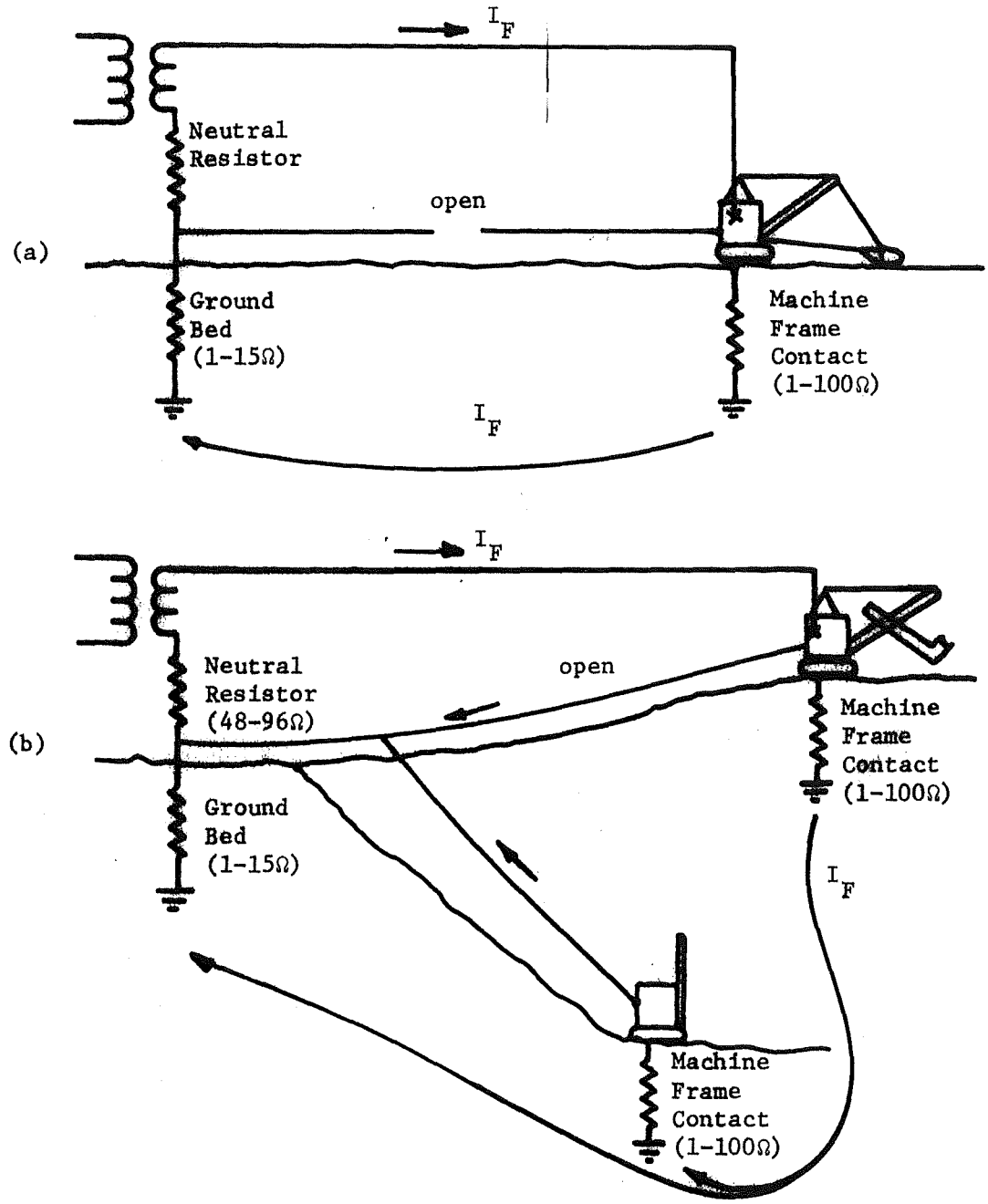


FIGURE 3.53. - Phase-to-netural fault at the machine, with open ground conductor, using safety ground bed or unified ground bed;

(a) Single machine on secondary;
(b) Several machines on secondary.

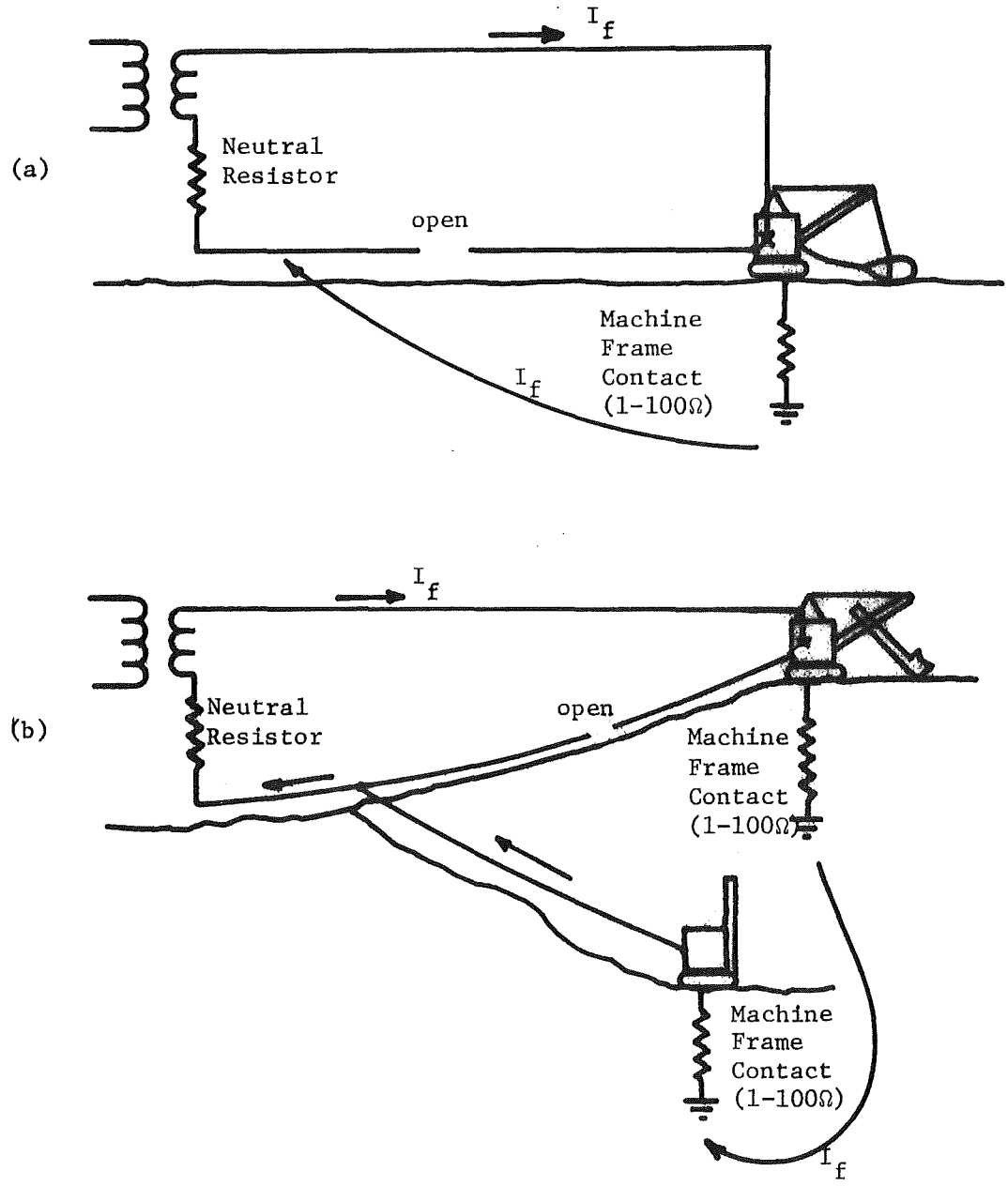


FIGURE 3.54. - Phase-to-neutral fault at the machine, with open ground conductor, using machine frame ground;

(a) Single machine on secondary;
(b) Several machines on secondary.

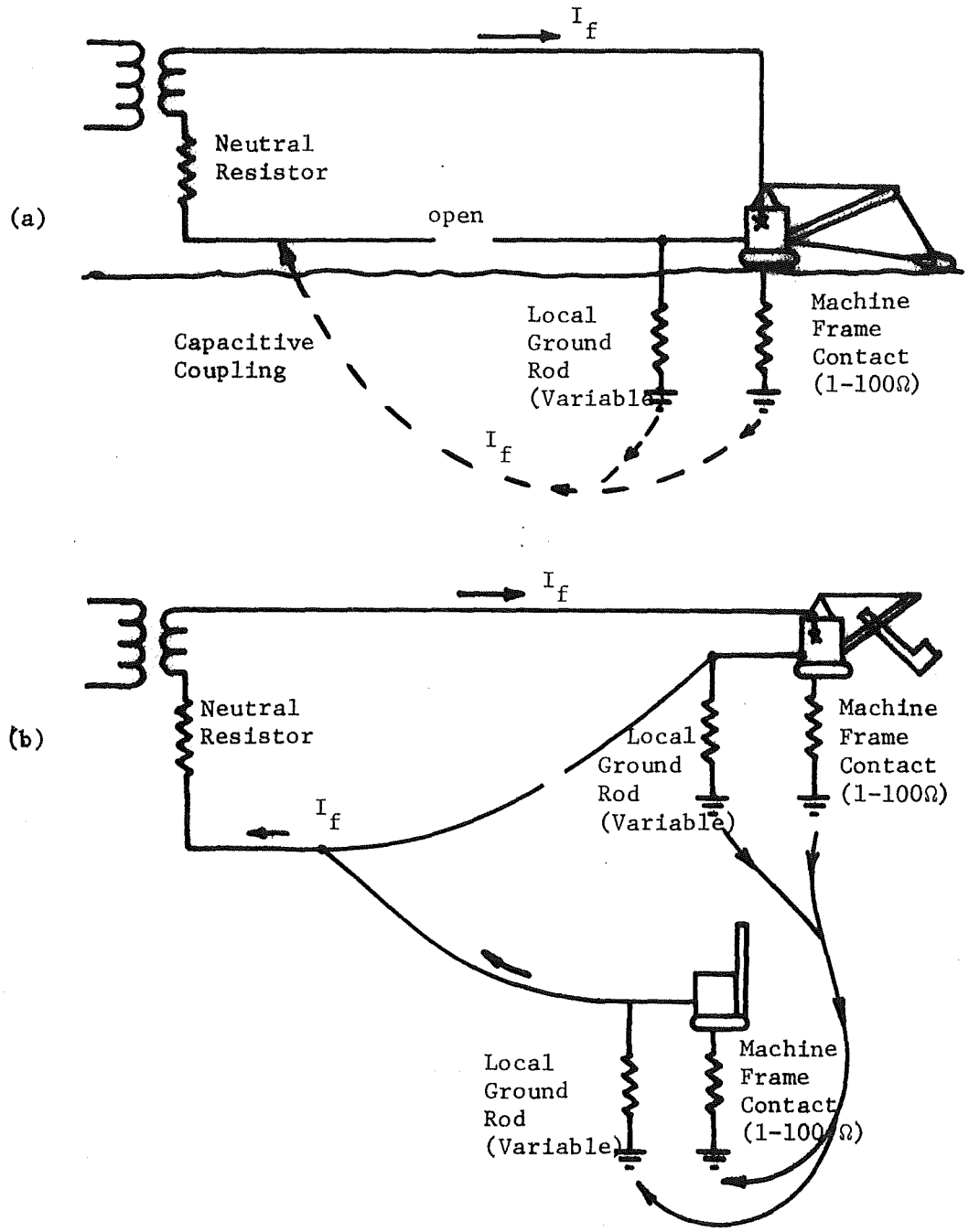


FIGURE 3.55. - Phase-to-neutral fault at the machine, with open ground conductor, using Locally-driven ground rods;

(a) Single machine on secondary,
(b) Several machines on secondary.

from a common point, the flow of fault current may be such that each piece of equipment will have its frame elevated above ground potential.

### 3.3.13 Fulfilling the Purposes of a Grounding System

As described earlier in this section, the four major functions of a grounding system are:

1. Limiting potential gradients.
2. Limiting the energy available at a fault.
3. Control of over-voltages.
4. Isolation of faulted sections of a power system.

All of the alternative grounding systems discussed herein utilize a series resistance between the transformer neutral point and the grounding conductors in order to limit the maximum current (and energy) during faults involving ground or neutral. Each type of grounding system also incorporates a solid connection to earth at some point between the substation and the load, which serves to control the maximum amplitude of transients and other over-voltage conditions. Isolation and detection of faults can be achieved through the proper selection and co-ordination of protective relays. Phase-overcurrent relays will trip in case of line-to-line faults, while factors involving ground or neutral can be detected in a variety of ways. For instance, a potential transformer in parallel with the neutral resistor will work effectively, even if the neutral resistor should open. A current transformer may be used in series with the neutral resistor, or may be connected residually with the phase-overcurrent relays. A balanced-flux or "window" current transformer monitoring the three phase conductors will detect unbalanced conditions such as would exist during a ground fault. Ground-check monitors may be used to insure the integrity of the grounding conductors.

The remaining criteria is the limitation of potential gradients, which is most important from the standpoint of personnel safety. If fault current flows through a machine frame into the underlying earth, then the frame of that equipment will become elevated above zero volts, and a "potential hill" will exist around that machine, with the machine frame sitting at the highest potential (the top of the potential hill). A man touching the machine while standing on the earth may receive a shock, as could a person who was walking near the machine if he bridged a large potential difference with his feet. Therefore, workers who are in contact with the earth should never sit, touch, or lean against any piece of equipment, even though it may appear to be grounded. To facilitate getting on and off a machine, hand-rails and steps should be constructed from non-conducting material, or should be insulated from the machine frame if made of metal.

### 3.3.14 Exposure Voltage and Exposure Time

The four grounding methods which have been discussed differ from each other in terms of the possible voltage level to which a worker may be exposed

and the probable time for which the hazardous condition may exist. A comparison on this basis therefore seems justified.

Machine frame grounding provides the best isolation from primary faults and from lightning strikes to the primary distribution because of the physical separation between the substation and the machines. In the event of a phase-to-earth fault on the secondary, all of the fault current must flow through one or more machine frames to return to neutral. The magnitude of the fault current will depend largely upon the resistance of the phase-to-earth contact, but will be less than the allowable value for which the neutral resistor was sized (usually 25 or 50 amperes). If the current is 40% or more of the design value, then the protective relays will quickly trip, but a low-level current may persist for many seconds. Such a low-level current could give rise to dangerous touch or step potentials near the machines. However, if the secondary distribution system uses shielded trailing cables exclusively, a phase-to-earth fault is highly unlikely. A phase-to-neutral fault at the machine could lead to dangerous frame potentials on several machines if the ground conductor was open. However, ground-check monitors should prevent the operation of a circuit with an open ground. If the monitor failed, then relays designed to detect an imbalance in phase currents would have to act, with the time of exposure to shock hazard being determined by the magnitude of the fault current and the time-dial settings on the relays.

A local ground bed provides essentially the same degree of isolation from primary faults as does machine frame grounding. During a secondary phase-to-earth fault, current will divide between the local ground bed and the machine frame in inverse proportion to their resistances. As discussed in the preceeding paragraph, the magnitude of this fault current may be so low that it will persist for a long time before tripping a breaker, but may still cause hazardous frame potentials. In the event of a phase-to-neutral fault at the machine, hazardous voltages could appear on the frames of several pieces of equipment should the ground conductor become open. As before, ground-check monitors should prevent this from happening. In general, local grounding is roughly equivalent to machine frame grounding in terms of performance. However, to construct a local ground bed whose earth resistance is similar to that of a large dragline or shovel (1-15Ω) could be a major undertaking.

The method of grounding presently used throughout the industry consists of a separate "safety ground bed" usually established in close proximity to the substation and its ground bed. Primary faults and lightning strokes will be coupled into the secondary distribution because the two ground beds are relatively close together, and the degree of coupling is proportional to the mutual reistance between the two beds. If there is a secondary phase-to-earth fault, current will flow through the machine frame(s) and the safety ground bed proportional to their conductances. Depending upon the magnitude of the fault resistance, this current amplitude may be small enough that the clearing time will be rather long, although it is possible that the accompanying frame voltages will be high. A phase-to-neutral fault at the machine, simultaneous with an open ground conductor, may lead to hazardous frame potentials, with exposure time dependent upon the current magnitude and relay settings.

The "unified ground bed" consists of a single bed which serves as both the substation and the safety ground connection. In this arrangement, coupling from the primary to the secondary side of the ground system is 100%, and any potential appearing at the ground bed due to primary faults or lightning will be directly coupled to the secondary. For lightning, the time of exposure is very short, on the order of microseconds, while fault-clearing time can range from several cycles to a second or more. In both cases there is a possibility that large potentials may appear on machine frames. The performance of the unified ground bed, in the event of a phase-to-earth fault or a phase-to-neutral machine fault with an open ground conductor, is similar to that of the safety ground bed discussed above.

Several surface coal mines have recently been plagued by the frequent destruction of their high-voltage ground-check monitors. It appears that, when lightning strikes a machine, the surge propagates back to the substation via the grounding conductors on the trailing cable. Once inside the ground check monitor, the surge voltage is sufficient to arc from the safety ground bed connection to the case of the monitor (which is at the potential of the substation ground bed) destroying or damaging the monitor in the process. With a unified ground bed, this problem would not exist because of the common ground. With machine frame grounding or local grounding, the situation would be similar to that which now exists using a safety ground bed.

No matter what type of grounding strategy is adopted, dangerous step and touch potentials will exist when lightning strikes a machine. The majority of the surge current from the stroke will flow to earth directly through the machine frame contact resistance, and the current amplitude may be on the order of 10,000 amperes (23). Fortunately, the exposure time will be quite short, probably less than 200 microseconds.

### 3.3.15 Summary and Recommendations

It appears that the use of ground rods driven near each piece of mining machinery, or the use of the machine frame contact surface as an earth connection, may be superior to the more traditional "safety ground bed" and the "unified ground bed" in preventing the unwanted transfer of potential between a surface substation and the frames of equipment powered from the substation. The four alternative grounding methods seem to be roughly equivalent in performance when dealing with fault conditions on the secondary distribution, or when handling lightning strokes to the machines. However, the practicality and feasibility of driving ground rods near each piece of equipment and achieving a satisfactorily low value of earth resistance remains to be proven. In addition, the variability in the contact resistance of a machine sitting on the earth may be such that Federal officials would be reluctant to approve this mode of grounding in lieu of the traditional "safety ground bed".

It is very difficult to make definitive recommendations on grounding practice in view of the wide variability in current magnitudes and exposure times. However, the concept of local grounding (driving ground rods near each machine) seems to be quite impractical. Machine frame grounding is easy to do, since it requires no work at all, but the variability of the

earth resistance value thus achieved renders this arrangement suspect. The "unified ground bed" performs about as well as the safety ground bed, except for increased coupling from primary to secondary. If this property of the "unified ground bed" is not looked upon as a liability, then it should be used by the surface mining industry because of its simplicity and reduced cost when compared with the traditional safety ground bed.

# CHAPTER 4

# GROUND BED STUDIES

## 4.1 RESISTIVITY MEASUREMENTS

The resistance of a ground bed can be calculated from the number of electrodes in the bed, their size and separation, and the earth resistivity. All these factors except the earth resistivity are easily measured. Considerable effort was expended during the contract period to examine the existing methods, to refine and extend them, and to develop new methods of making resistivity measurements.

### 4.1.1 Existing Measurement Techniques

There are three common methods of measuring resistivity: the Wenner array, the Schlumberger array, and dipole array. A study of these three methods indicated that the Wenner array was the most applicable (57). Further investigation of resistivity methods centered around this method (56). Resistivity profiling and resistivity mapping techniques were investigated and field-tested. Profiling methods, as developed by Orellana and Mooney (38), proved to be the only reliable source of variation with depth. The alternative of examining borehole corings is not attractive due to the unavoidable disturbance of the cored material and the high cost and limited availability of the method. Resistivity mapping proved useful for finding ground bed sites and determining horizontal resistivity variations.

### 4.1.2 Modelling Work

To quantitatively study the Wenner array in horizontally layered earth (that is, bedding planes parallel to the surface of the earth), a conductive-rubber model was constructed. A number of technologies had to be mastered to successfully use the model. These included obtaining a high contrast in resistivities of adjacent layers of rubber, techniques of pointing the electrodes, and methods of analytically accounting for the finite size of the model (57). Although none of the three problem areas was trivial, the last area required the most original research. The concept of a "correction factor" was introduced to allow for the boundaries of the model. Correction factors were computed numerically for a variety of possible electrode locations (56-57).

### 4.1.3 Field Work

The Bison Earth Resistivity meter was purchased to do resistivity soundings and mappings (as well as resistance measurements, which will be discussed below). Resistivity mappings were done in several locations (57). Resistivity soundings were done both on the finite rubber model and in the field. The methods of Orellana and Mooney (38) were used to find multilayer approximations to the resistivity sounding data. Several problems with these methods became apparent only through their use: 1) the high degree of uncertainty in the layer thicknesses and resistivities, 2) the practical difficulty of obtaining the proper size of log-log paper to use the scale, and 3) the lack of uniqueness in the solution. The principal use of this curve-matching method has been in geophysical prospecting, where it may have

greater success. For determining resistivity values for ground-bed resistance prediction, it seems to have limited usefulness.

4.1.4 Development of New Methods

Current resistivity measurement methods used for ground-bed resistance prediction were borrowed from geophysics. When applied to ground-bed design, there are some understandable deficiencies. The Wenner array, for example, has the advantages of extreme simplicity and accuracy in homogeneous earth. Existing methods for interpreting the measurement in non-homogeneous earth are well-documented, if inexact. None of these advantages offset the fact that the measured resistivity, in non-homogeneous earth, does not correspond to the effective resistivity of any electrode. (The effective resistivity is the value which, used in the electrode resistance formula, gives the measured electrode resistance). The effective resistivity for a hemisphere of radius 's' is given by

$$\rho = 2\pi s R_{\infty} \tag{4.1}$$

where $R_{\infty}$ = the measured resistance.

The effective resistivity can only be calculated for a specific model of the earth. The simplest such model is that of two horizontal layers of different resistivities: a top layer of resistivity $\rho_1$ and thickness 't', and a bottom layer of resistivity $\rho_2$ and infinite thickness. For this case, the effective resistivity for a small hemisphere (s<<t) can be shown to be

$$\rho = \rho_1 \left[1 + 2 \sum_{n=1}^{\infty} \frac{K^n}{[1 + (2nt/s)^2]^{\frac{1}{2}}}\right] \tag{4.2}$$

where

$$K = \frac{\rho_2 - \rho_1}{\rho_2 + \rho_1} . \tag{4.3}$$

Keller and Frischknecht (24) have calculated the resistivity measured by the Wenner array for this case. With an interelectrode spacing 'a':

$$\rho = \rho_1 \left[1 + 4 \sum_{n=1}^{\infty} \frac{K^n}{[1 + 2nt/a)^2]^{\frac{1}{2}}} - 2 \sum_{n=1}^{\infty} \frac{K^n}{[1 + (nt/a)^2]^{\frac{1}{2}}}\right] \tag{4.4}$$

A measurement scheme has been found which provides a better estimate of the effective resistivity. This arrangement is shown in figure 4.1. Using an outer electrode spacing equal to the hemisphere radius yields a measured resistivity of:

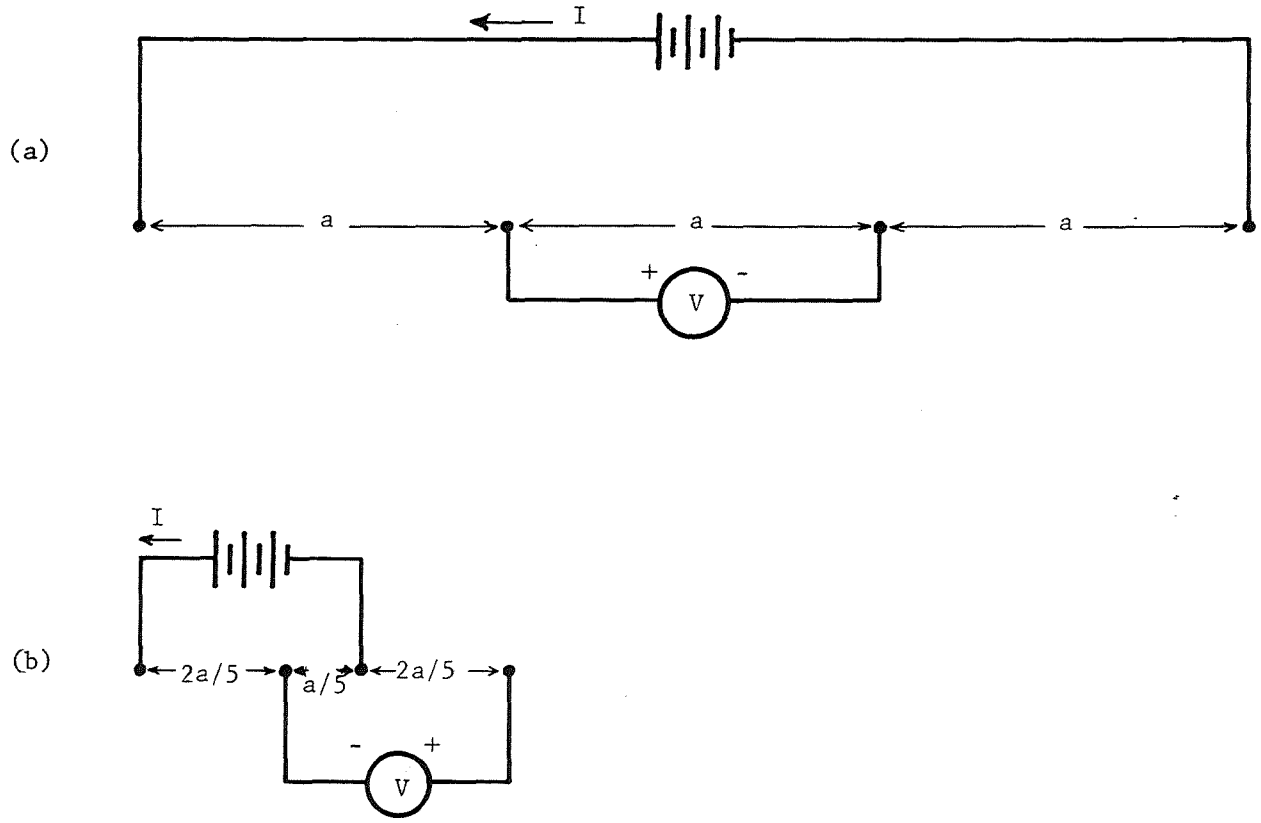


FIGURE 4.1. - Resistivity measurement methods. (a) Wenner Array; (b) Hill Array.

$$\rho = \rho_1 \left[1 + 2 \sum_{n=1}^{\infty} \frac{K^n}{[1 + (2nt/s)^2]^{1/2}} + 10 \sum_{n=1}^{\infty} \frac{K^n}{[1 + (20nt/s)^2]^{1/2}} \right.$$

$$\left. - 10 \sum_{n=1}^{\infty} \frac{K^n}{[1 + (10nt/s)^2]^{1/2}} \right]. \qquad (4.5)$$

The last two summations nearly cancel for $s \ll t$. This method shows promise for use in ground-bed design even where $s \approx t$. Future research will hopefully find the limitations of this method and find other methods more applicable to different electrodes.

### 4.1.5 Summary

Resistivity methods for ground-bed design have been thoroughly evaluated during the contract period. These methods have been field-tested and analytically examined. Extension of current methods has been done in the important area of finite modelling. Work was initiated at the end of the contract period to develop totally new methods of measuring earth resistivity that would be more applicable to ground-bed design.

## 4.2 RESISTANCE MEASUREMENTS

Four methods of determining ground-bed resistance were examined during the contract period: 1) two-point, 2) triangulation, 3) ratio, and 4) fall-of-potential. While all four methods proved workable under some circumstances, none but the fall-of-potential was found adequate for measuring the resistance of extensive, low-resistance ground beds. Becuase analysis showed the inherent problems with the other methods, only this last technique was used experimentally.

### 4.2.1 Analysis of the State-of-the-Art

The fall-of-potential method has been analyzed elsewhere in great detail, most notably by Tagg (48-49). He studied two problems of interest: location of the center of a large ground bed, and potential induced on the ground bed by the auxiliary current electrode. Unfortunately, both analyses appear incorrect. Neither one includes the large effect of the redistribution of ground bed current due to the presence of the current electrode. This effect makes the first analysis invalid for any ground bed large enough to require such treatment; it makes the "more exact" results of the second analysis less accurate than the usual approximation. During the contract period, both analyses were scrutinized and the second was revised. The first seems to be without hope of rectification.

### 4.2.2 Resistance of Earth Electrodes

Serious study of resistance measurement of ground beds required an examination of the resistance formulae, so that a logical criterion for evaluating the measurement techniques could be developed. In all cases, valid equations for the self-resistance of electrodes existed in the

literature (though some choices had to be made between alternate expressions). Mutual resistance formulae were more difficult to extract. Sufficient analysis existed in the literature to produce these expressions, but they appeared nowhere explicitly. Even the simplest expression for the mutual resistance of a hemisphere and point source had to be obtained from extending the analysis of an electrostatic analogy (56). Expressions for the mutual resistance between rods and between dragline tubs were obtained in a similar way. Although most of the work was done considering the earth as a homogeneous medium, self- and mutual-resistance expressions for the rod (or borehole casing) in horizontally layered earth were also desired. These results are all summarized in Tables 4.1 and 4.2.

### 4.2.3 Modelling Work

Early in the contract period, an ambitious program began to construct a three-dimensional finite-element model of the earth. The project was soon terminated with very limited success. There are theoretical and practical problems which caused this early abandonment. The major theoretical problem is that ground-bed resistance calculations fall in a class of potential theory known as "exterior Dirichlet" problems: the only boundary condition on the potential is at a point infinitely far away. This requires the use of either a very extensive model or an inversion scheme. The extensive model is tedious to construct and computationally slow (and therefore expensive). The inversion scheme removes all physical correlation between the model and the actual region of earth.

Practical difficulties were myriad: obtaining the required amount of input data was nearly impossible; putting the required data into a computer-acceptable form was a herculean task, even with an automatic mesh-generating scheme. Compounding these problems was a software difficulty. The only available finite-element modelling program was a poorly supported version of NASTRAN. This version of NASTRAN had an inoperative plotter package and from the little documentation available, error analysis was impossible.

Despite these difficulties, a mesh generation program was written to create input cards; in inversion scheme (Kelvin) was successfully implemented and some test cases done. The results are contained in reference 56 .

### 4.2.4 Field Work

The fall-of-potential method was used several hundred times to find the resistance of a variety of electrodes, from short, single rods to large structures tens of square meters in area (hundreds of square feet). Meters used have been three- and four-terminal, hand-crank and battery-powered, with a wide frequency range. The nearly universal success of the method in the field shows the fall-of-potential's basic soundness. The results appear in references (56), (57), and (58). (Theoretical problems with the potential-electrode location had to be corrected in some measurement situations; details are in the next section).

### 4.2.5 Development of New Techniques

Measuring the resistance of a ground bed is straight-forward where the

TABLE 4.1. - Self and mutual resistances of various electrodes

| Electrode Type | Resistance | Mutual Resistance |
|---|---|---|
| Hemisphere | $\frac{\rho}{2\pi a}$ | $\frac{\rho}{2\pi r}$ |
| Disc or Drag-line Tub | $\frac{\rho}{4a}$ | $\frac{\rho}{2\pi a} \sin^{-1} \frac{a}{r}$ |
| Ring of Wire | $\frac{\rho}{\pi \ell} \ell n \frac{4\ell}{\pi a}$ | $\frac{2\rho}{\pi} \cdot \frac{F(i)}{\ell+2\pi r}$ <br> $i = \frac{2\sqrt{\ell r}}{\ell+2\pi r}$ <br> $F(i) = \int_0^{\pi/2} (1-i^2 \sin^2\psi)^{-1/2} d\psi$ |
| Rod or Bore-hole Casing (homogeneous earth) | $\frac{\rho}{2\pi\ell} \ell n \frac{2\ell}{d}$ | $\frac{\ell}{2\pi\ell} \sinh^{-1} \frac{\ell}{r}$ |
| Rod or Bore-hole Casing (layered earth) | Use above formulae with: <br> $\frac{1}{\rho} = \sum_{j=0}^{n} \frac{C_j}{\rho_j}$ <br> $C_j = (1-y_{j+1}^2)^{1/2} - \sum_{k=0}^{k=j-1} C_k$ <br> $C_0 = (1-h_h^2)^{1/2}$ <br> $Y_j = 1 - \frac{1}{\ell} \sum_{k=0}^{k=j} h_k$ | |

TABLE 4.2. - Symbols used in Table 4.1

| Symbol | Explanation |
|---|---|
| a | Electrode radius |
| c | Weighting coefficient |
| h | Layer thickness |
| i | Argument of elliptic integral |
| j,k | Indices of summations |
| $\ell$ | Electrode length |
| r | Circle radius (ring of wire)<br>or<br>Separation (rod electrode) |
| y | Weighted, normalized layer thickness |
| F | Elliptic integral |
| $\pi$ | 3.14159... |
| $\rho$ | (Without subscript) resistivity<br>(With subscript) layer resistivity |

current-return electrode can be located far from the bed. If the ground bed is extensive, or the terrain unfavorable, such that this condition can not be met, the fall-of-potential method must be modified. Two effects occur: the potential due to the ground bed does not fall off exactly with the reciprocal of distance close to the bed, and the current distribution of the bed is altered by the current-return electrode.

The fall-of-potential method was improved to account for the potential distribution of the ground bed by two very different methods. For those electrodes or groups of electrodes which yielded to analysis of their potential functions the method was altered by re-positioning the potential electrode. These analyzable electrodes included the large hemisphere (57), the rod (56), small groups of rods (56), and the dragline tub (58).

For other, more complex shapes of ground beds, a variation on the fall-of-potential method was created and dubbed the "29° Rule". In this method, the potential electrode, the ground bed center, and the current electrode are the vertices of an isosceles triangle. The base (the line connecting current and potential electrodes) is half the length of either of the other two triangle sides. The angle opposite the base is then $2 \sin^{-1} (1/4) = 29°$. This method compensates for variation in the potential function of the ground bed by placing the potential electrode as far from the bed as possible, where the variations from theory are less severe. Error analysis of the 29° rule compared with the usual fall-of-potential method showed that it was always superior (56).

### 4.2.6 Summary

A thorough study of the state of the art of resistance measurements showed that the major measurement problems were then not dealt with. A major theoretical and field effort to resolve these problems was undertaken and considerable progress made. Measurement of the resistance of a variety of electrodes can now be done with confidence, at least in relatively homogeneous soil.

## 4.3 GROUND BED DESIGN

When work began in the area of ground-bed design, little practical literature existed for the engineer with given design constraints. The principal thrust of ground-bed design work was to fill in this void by providing specific guidelines. Conventional analysis and topologies were to be used initially, with concern for optimum design coming later.

### 4.3.1 Basic Considerations

Mutual-resistance effects greatly complicate the resistance calculation of any ground bed containing more than one earth electrode. For a coal-mine safety ground bed, the low resistance requirement (usually 5 ohms) results in multiple-rod beds in all but the most fortuitous (low-restivity) sites. These mutual-resistance effects mean that the resistance of the bed is a function of the separation between rods, as well as the individual rod resistances. Thus a bed made with two rods, each with 14 ohm resistance, will have a resistance between 7 and 14 ohms, depending on the separation

between rods. Complexity of the calculations increases dramatically with the total number of rods because in general, a matrix, whose rank is equal to the number of rods, must be inverted. Resistivity of the earth is a major variable in determining the resistance of an electrode configuration, because it varies over several orders of magnitude. The earth near the ground bed has a greater effect on the resistance than does soil far away, so that resistivity measurements near the site are imperative. Only through resistivity sounding and mapping can a good site be chosen and the ground-bed resistance predicted.

### 4.3.2 Development of Guidelines

Using the basic guidelines previously developed, a guide for ground-bed construction was written. The guide provided a straight-forward way of estimating the resistivity variation at the chosen site such that an appropriate resistivity value could be used in the design tables. Once the appropriate value was determined, one of a variety of permissible bed designs, listed in tables, could be chosen. The permissible designs ranged from those requiring a large area with few rods, to many rods in a small area.

The entire guide was written in a 'cookbook' fashion. Although many subtle problems (from frost penetration to anistropies) are dealt with by the procedures, no deep understanding of these phenomena is necessary. Likewise, very little calculating is required to use the guide.

### 4.3.3 Recent Developments

The guidelines, as developed, had two major deficiencies: they only covered rodbeds, and the only rodbeds covered were those of conventional design. Both defects were attacked in subsequent research and writing. The major electrode to be included by the research was the borehole casing. A procedure was developed to build a ground bed using a combination of rods and a borehole casing (48). The procedure is intended for the common instance where an existing borehole casing is not quite adequate for providing a low-resistance ground.

Optimum rod configurations to provide minimum resistance with a given number of rods in a given area were also studied (48). This study showed that many common rod arrangements made poor use of the constituent rods, and that simple modification to the rod configuration could yield resistance decreases of up to 25%.

### 4.3.4 Summary

Ground-bed design was approached from a comprehensive basis, from exploiting conventional design to creating new optimum configurations. Work was done to provide easy access to current ground-bed technology, as well as advancing the state of the art.

## 4.4 GROUND BED CONSTRUCTION WORKSHOP

The work of WVU in codification of ground bed construction and measurement techniques was reported in detail in the 1974-75 Annual Report (57)

which included guides in the Appendices. These guides were written to provide practical information on construction and measurement in a form which would be readable by most of the industry people directly involved. These guides were well-received by the limited audience which saw them. It was finally decided to modify them somewhat and to publish the construction guide as a separate document. U.S. Bureau of Mines IC 8767 became available early in 1978, and has been very well received (26). In order to further disseminate this information, a series of Ground Bed Construction Workshops was held under the USBM Technology Transfer Program. The workshop was held four times at the Pittsburgh Mining and Safety Research Center at Bruceton, PA, May 2, May 3, June 27, and June 28, 1978.

WVU participated heavily in the workshop, being responsible for approximately two-thirds of the lecture material, field measurements, and analysis. The lecturers were Wils L. Cooley, Associate Professor of Electrical Engineering, West Virginia University, Principal Investigator; and Herman W. Hill, Jr., Graduate Research Assistant, West Virginia University. The workshop developer and third lecturer was Roger L. King, Electrical Engineer, U.S. Bureau of Mines, Technical Project Officer. Table 4.3 indicates the agenda of the workshop.

The four workshops were attended by approximately 90 persons. Plans are indefinite, but it may be offered several more times at different locations.

## 4.5 CORROSION OF EARTH ELECTRODES

### 4.5.1 Introduction

Corrosion studies on earth electrodes were begun in September 1975, and have continued until the end of the grant period. Several aspects of corrosion were investigated, the most important being to evaluate the corrosion resistance of various materials which could be used for earth electrodes. A considerable effort was also expended to find a method of detecting corrosion damage which does not require removal of the electrode from the earth.

The study of corrosion was prompted by the experiences of several mines in which ground beds and equipment in contact with earth were found to be severely damaged by electrolytic corrosion. Figure 4.2 shows a photograph of the remains of a 2.44 m (8 ft) ground rod removed from the safety ground-bed of one such mine. As reported in annual report 1975-76 (56). such corrosion is the result of chemical reactions at the electrode surfaces driven by the presence of stray dc current from electric haulage track. The severity of the corrosion problem is dependent on many factors, many of which are covered in Chapter 5 of this report.

### 4.5.2 Field Measurements of dc Ground Current

Several measurements were made in the field to confirm that dc current does flow in the safety ground, and that it can be correlated with haulage activity. A possible corrosion current path can be described involving a typical, low voltage power distribution system for underground coal mine operations.

TABLE 4.3. - Agenda for Ground Bed Construction Workshop

| Time | Subject & Speaker |
|---|---|
| 8:15 | Registration |
| 8:30 | Introduction, Norman Hanna, Acting Research Director, Pittsburgh Mining and Safety Research Center |
| 8:40 | Why Build a Ground Bed?, Dr. Wils L. Cooley, Associate Professor of Electrical Engineering, West Virginia University |
| 8:55 | Ground Bed Resistance, Dr. Wils L. Cooley, Associate Professor of Electrical Engineering, West Virginia University |
| 9:10 | Touch and Step Potentials, Herman W. Hill, Jr., Graduate Research Assistant, Department of Engineering, West Virginia University |
| 9:40 | Resistivity Measurement Procedures, Roger L. King, Electrical Engineer, Pittsburgh Mining and Safety Research Center |
| 9:55 | Resistance Measurement Procedures, Herman W. Hill, Jr., Graduate Research Assistant, Department of Engineering, West Virginia University |
| 10:10 | Break |
| 10:30 | Ground Bed Design Principles, Herman W. Hill, Jr., Graduate Research Assistant, Department of Engineering, West Virginia University |
| 10:50 | Design and Installation of Ground Bed, Roger L. King, Electrical Engineer, Pittsburgh Mining and Safety Research Center |
| 11:20 | Ground Bed Resistance Measurement, Dr. Wils L. Cooley, Associate Professor of Electrical Engineering, West Virginia University |
| 12:00 | Lunch |
| 1:30 | Field Measurements, Group Participation |
| 2:45 | Workshop Calculations, Group Participation |
| 3:45 | Wrap-Up |

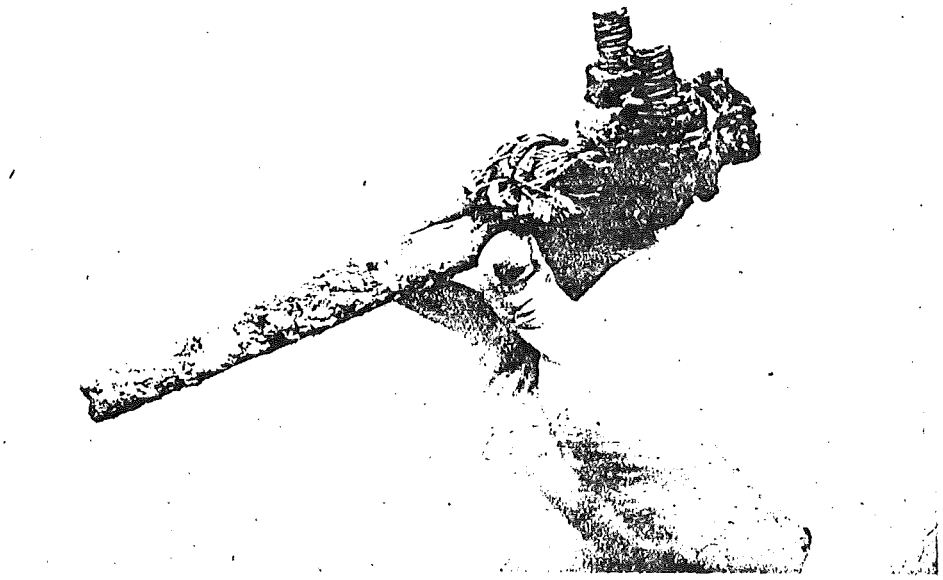

FIGURE 4.2. - Severed ground rod due to corrosion.

At the substation, depending on available power, approximately 38 kV is brought to the primary side of a delta-wye connected transformer (see figure 4.3). Lightning arresters are located at the primary side and grounded through a system ground. On the secondary side approximately 7.2 kV is taken underground via the bore hole. By law the center of the wye is grounded through a resistor so as to limit ground fault current to not more than 25 amperes (55). This ground is termed the safety ground. The earth side of the resistor is carried into the mine along with three-phase power and attached to all machine frames. It should be noted that most machines are in intimate contact with earth during mine operations.

For ease of operation most underground mines use a dc haulage system to transport men and coal into and out of the mine. The mine trolley system uses rectified dc. The trolley wire above carries the current away from the rectifier while the track itself is used as the return current path. In some trolley systems the negative side of the rectifier is also grounded. A problem arises in using the rail itself as a current conductor. To simplify installation, the rail joints are not welded; however, rail bonding is used to insure a good electrical connection. Rail bonds consist of a 4/0 copper stranded wire tack-welded to each rail (see figure 4.4). Through the course of events rail bonds become broken, worn, or in some cases may not be present at all. Disconnected rail bonds introduce a resistance in the return current path allowing for some current to flow via the ground back to the rectifier (see figure 4.3). Once the current enters the ground a number of possible routes are available. One such route prompting ground bed corrosion will be described. Remembering that all mine machinery comes in contact with the earth, one possible route would be from the rail to a mine machine, down through the safety ground bed via the safety ground wire and back to the rectifier (see figure 4.3).

In the described circuit the safety ground bed becomes anodic, thus making it susceptible to corrosion. To make matters worse, ground leakage current, both ac and dc, tends to circulate in the ground system adding to the ground bed corrosion problem (31). These leakage currents could be due to: 1) imbalances in the three-phase system, 2) electrolytic cells set up by different metallic ground beds connected together, 3) telluric induced currents (32), or 4) mild non-clearing faults during operations (see figure 4.5). Whatever the cause, the fact remains that these currents are present and flowing in the ground system.

Bruceton, Pennsylvania is the home of a USBM test center. At this particular facility testing of dc track haulage equipment is done using a circular, above-ground dc trolley system. This system provides a perfect location for measuring leakage current.

The Bruceton trolley system is representative of a corrosion circuit previously described (see figure 4.3). Three-phase ac power is rectified providing 300 V dc to run a resistive controlled locomotive. Current is passed from the rectifier to an above-ground trolley wire and returned via the rail (see figure 4.6). Railbonds were non-existent, suggesting the possibility of large leakage currents. The safety or system ground bed was connected to the negative side of the rectifier and to the rectifier's metal case. Ground-bed resistance on the day of the test was approximately

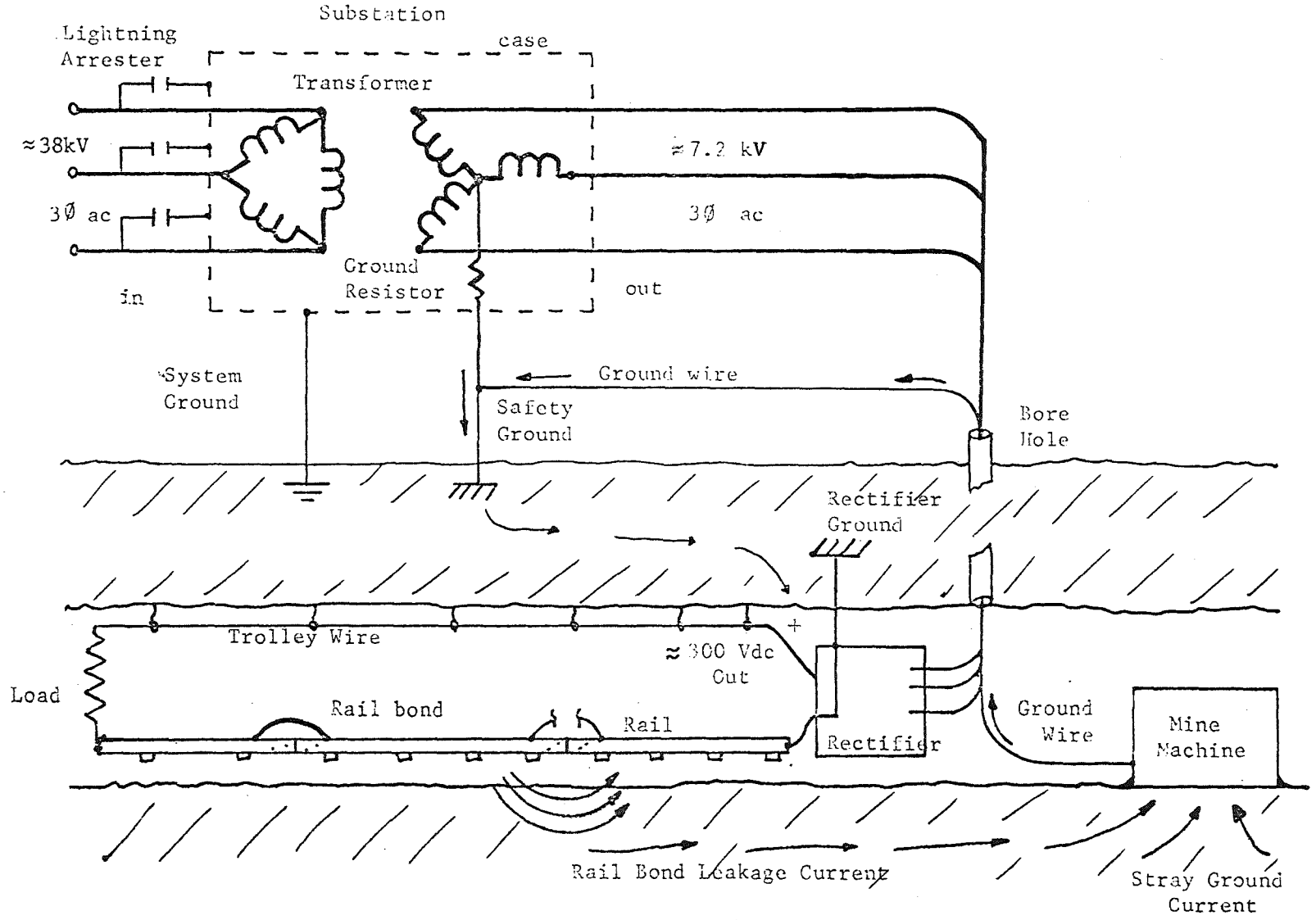


FIGURE 4.3. - Possible corrosion current path for underground mine power systems.

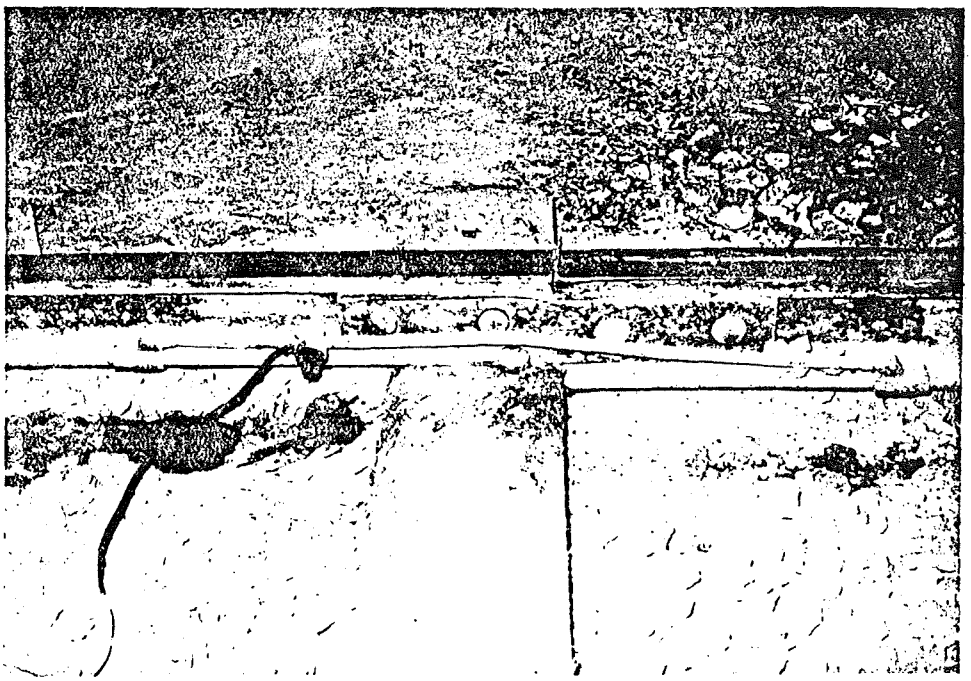

FIGURE 4.4. - Dc electrical haulage rail bond.

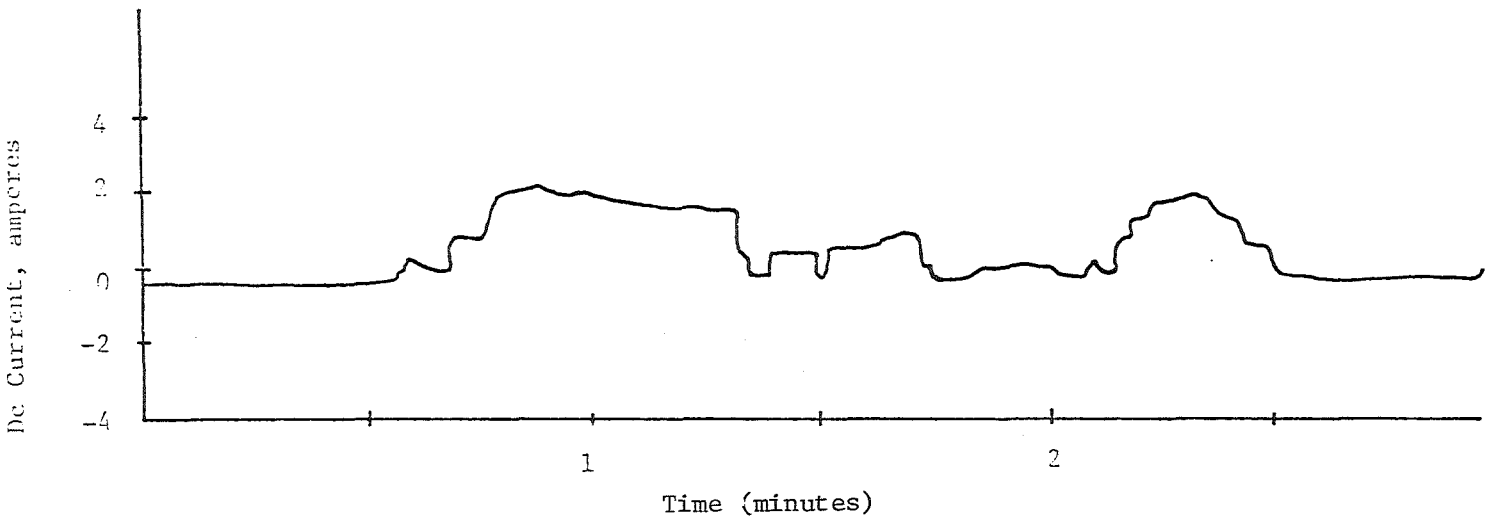


FIGURE 4.5. - Dc offset of a 0.4 ampere (p-p) ac ground current, recorded by Penn State, 1975.

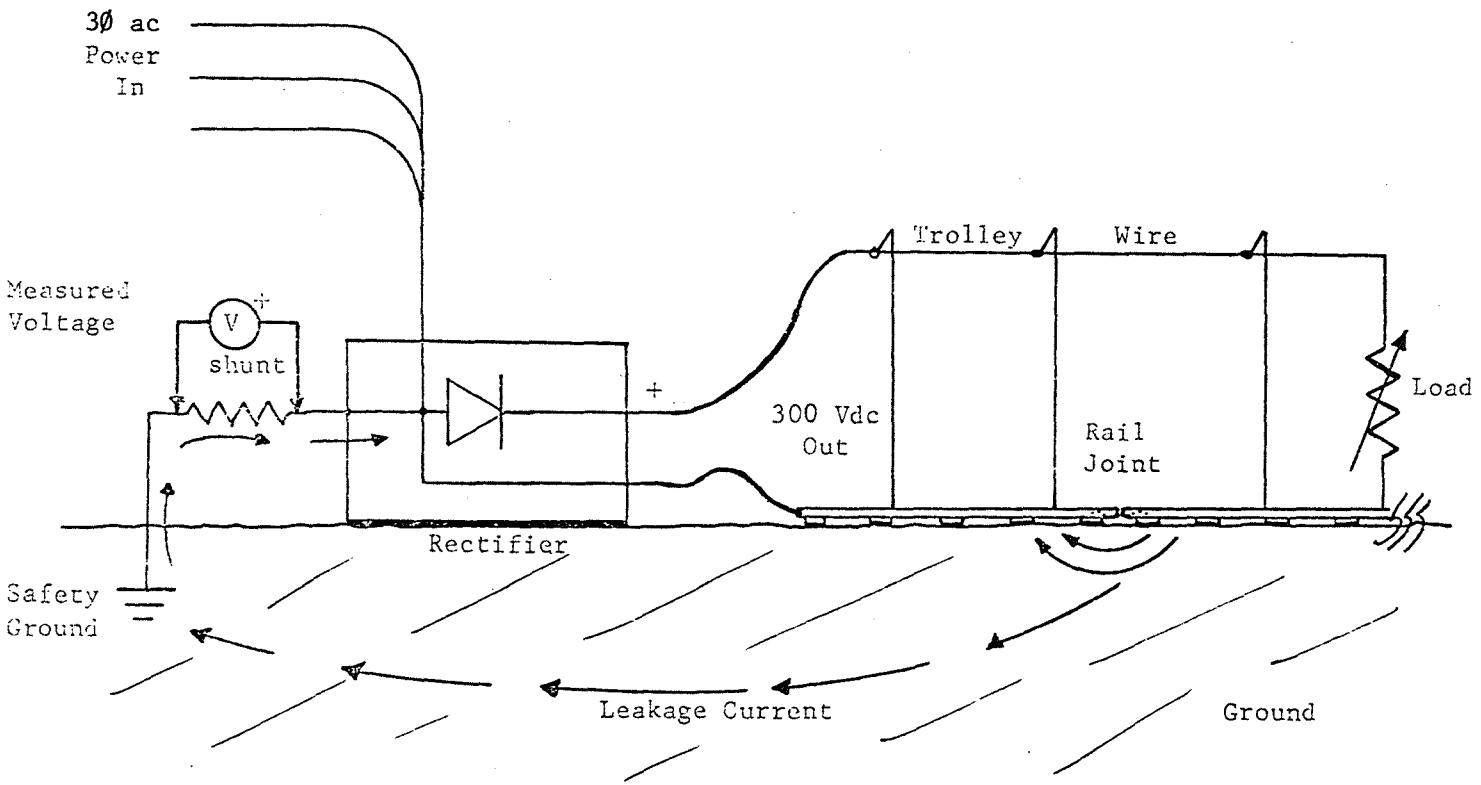


FIGURE 4.6. - Test trolley schematic, Bruceton, Pennsylvania.

3.8 ohms, obtained by the three-electrode method.

With power removed, a series shunt was placed in the ground wire and current was measured as a corresponding voltage drop. Ground current was monitored as the train traveled the oval track. Ground current was recorded using a Simpson Multicorder* with an external pre-amplifier. The trolley rectifier circuit was equipped with a dc ammeter; however, this meter was not working during the test.

Leakage current in the ground was proportional to the quantity of current used by the trolley locomotive. Quantity of current was judged by the volume of rectifier noise generated. Leakage currents ranged from 0 to 2 amperes depending on the amount of current drawn from the rectifier (see figure 4.7). Contrary to the ground bed corrosion circuit of figure 4.3, all leakage current passed from the ground bed to the rectifier. Current flow in this direction suggests corrosion of the rail joints.

Even though no evidence of severe corrosion existed at Bruceton's test track, this experiment proved that substantial currents circulate in the dc rail haulage system. The direction of leakage current at Bruceton can be attributed to the absence of additional system grounds. Given the right conditions in a mine environment, a ground bed corrosion circuit is very possible.

### 4.5.3 Ground Rod Evaluation

In order to effectively evaluate a large number of ground rods in a short period of time, a simulated ground bed was proposed. This approach allowed experimental conditions to be carefully controlled. The details of the test facility have been covered in the 1975-76 Annual Report (56).

Tests consisted of placing electrode samples approximately 30 cm (1 ft) long in the center of the soil box. A 20 volt, 25 ampere dc power supply was used to impress current from the sample electrode (anode) to the copper wire surrounding the box perimeter (cathode). A circuit of this nature could also be described as cathodic protection of the copper wire. A precision shunt (10 A, 50 mV) was placed in series to record the current as a corresponding voltage drop.

The soil was watered and salted prior to testing and remained covered with plastic throughout each test. Each rod was cleaned and weighed prior to current passage. Duration of current passage ranged from days to weeks depending on the rate of corrosion. At the conclusion of each test the rod was carefully removed and examined for corrosion. Corrosion products were removed and each rod was scrubbed with a commerical cleanser and nylon brush. No attempt was made to remove tightly bound corrosion products. After thorough cleansing the rod was dried and weighed (36). Rods tested in this manner included:

1.27 cm (1/2") Copperweld$^{R}$ Rod*

---

* Reference to specific brands, equipment, or trade names in this report is made to facilitate understanding and does not imply endorsement by the Bureau of Mines.

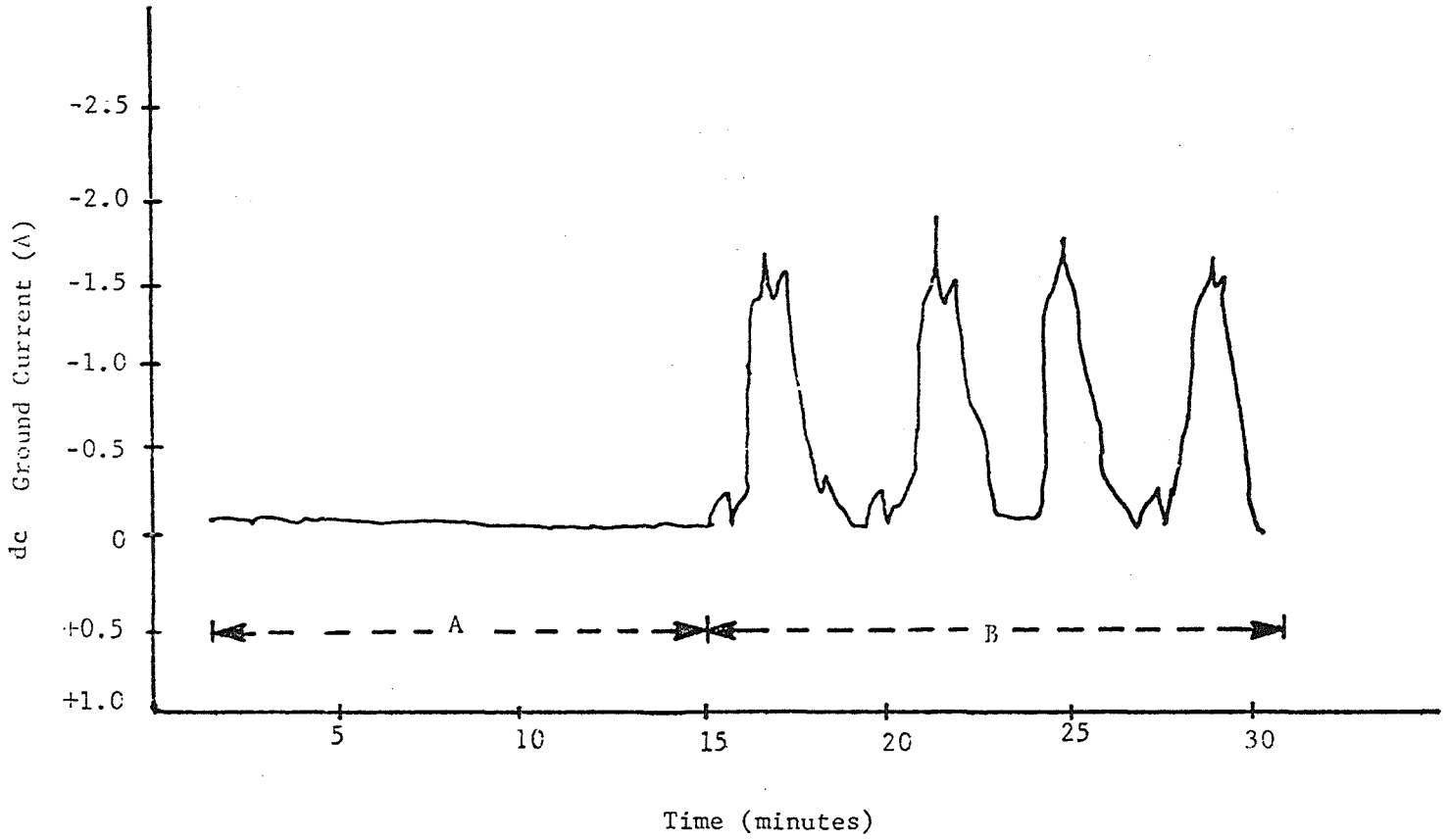


FIGURE 4.7. - Leakage current, Bruceton, Pennsylvania test track, 7 September 1977. (A), Locomotive stopped; (B), locomotive moving.

1.59 cm (5/8") Steel Reinforcing Rod (Rebar)

1.59 cm (5/8") Stainless Steel Rod (#304)

1.59 cm (5/8") Galvanized Steel Rod

1.27 cm (1/2") SiCrFe Rod, Duriron$^{R}$*

1.27 cm (1/2") Graphite Rod

4/0 Stranded Al Wire

(Although tests on the first two electrodes were reported in the 1976-77 Annual Report, results are repeated here for completeness).

Three specialized electrodes were tested: Rebar in concrete, graphite with coke breeze backfill, and X-it$^{R}$ Rod*. Rebar in concrete consisted of a steel reinforcing rod backfilled with concrete (see figure 4.8). This combination is suggested in recent literature to be a possible solution to low-resistance grounding (11). The concrete-steel electrode was left idle in moist soil for one week to allow moisture migration into the porous concrete, thus decreasing concrete resistivity (34).

Graphite surrounded by coke breeze is recognized as a standard installation method (7). Coke breeze provides lower contact resistance and increased chlorine gas ventilation. This test electrode consisted of a graphite rod backfilled with a rather granular coke breeze.

X-it Rod has recently bloomed as an answer to low-resistance earth grounding (66). X-it Rods consist of type K copper or galvanized tubing, 5.4 cm (2 1/8 in) in diameter, capped at both ends and filled with salt and a special hydrophilic substance. Four holes appear at the top and bottom of each rod; instructions request that the top holes always remain above ground, uncovered. A sample X-it Rod was obtained from X-it Rod Corporation of Beaumont, California. This custom-designed rod duplicated every aspect of a standard X-it Rod except length. Due to the 30.5 cm (1 ft) depth of the simulated ground beds the sample X-it rod was reduced in length to 45.7 cm (18 in) (see figure 4.9). Further communications with X-it Rod president, C. J. Reinmuller, provided instructions for installation and use of the miniature rod to insure maximum efficiency. Installation procedure required the X-it rod to be submerged in water for 10-15 seconds followed by hanging it in air until water ceased to drip; this method, normally unnecessary, insured adequate moisture inside the rod for the brief test period. The X-it rod was placed into the soil, making sure that the top holes were always exposed to the atmosphere. A period of 2 1/2 weeks passed with the X-it rod unconnected, allowing the inside electrolyte to stabilize. During the 18-day preparation period contact resistance readings were obtained to evaluate the

---

* Reference to specific brands, equipment, or trade names in this report is made to facilitate understanding and does not imply endorsement by the Bureau of Mines.

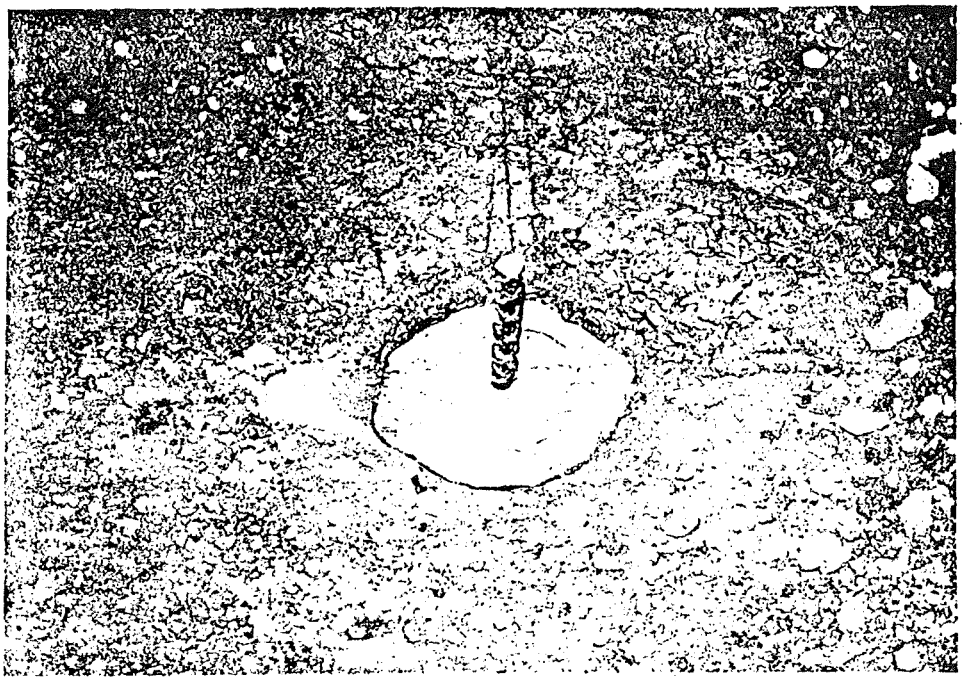

FIGURE 4.8. - Concrete encased, steel reinforcing rod used as a ground electrode.

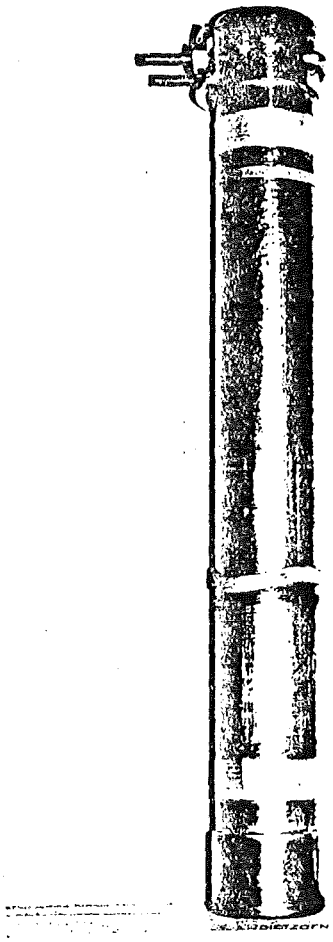

FIGURE 4.9. - Custom-designed X-it$^{R}$ Rod used for corrosion test.

electrode's stability. Current passage was started when contact resistance reached an equilibrium.

4.5.4 Data Collection

An accurate time record of current passed through each anode was captured by one of two chart recorders. The current passed at any given time is proportional to the corrosion rate. In order to determine total corrosion rate as a weight loss, however, it was necessary to calculate the total charge passed. This was done using a numerical integration program written for the HP-97. The results appear in Table 4.4.

From the calculated charge expressed in Ampere-Hour and the electrode's weight loss, a corresponding corrosion rate (gm/A-hr) is given. By calculating the surface area, S, of each electrode,

$$S = 2(\pi)rl + 2(\pi)\ r^2, \qquad (4.6)$$

charge density is expressed in A-hr/cm$^2$ (see Table 4.4). Observations were made before, during, and after each rod test. A brief description of each rod tested and corresponding observations follow.

Copperweld Rod - A 2.44 m ( 8 ft) Copperweld rod was purchased from a local coal mine supply service and cut into 30.5 cm (1 ft) sections for experimentation. The rod used showed no visible signs of corrosion activity prior to testing. The Copperweld rod was driven 22.2 cm (8 3/4 in) into the test soil and connected to the dc supply with a standard ground-rod connector. The soil remained moist for the duration of the test. During current passage green copper oxide ($Cu_2O$) appeared at the base of the exposed rod. Current passage continued for 45 days ranging from 0 to 4 amperes (see figure 4.10). At 31 1/2 days into the test the rod grew thin near the soil surface; some time shortly thereafter the rod severed at the soil surface, leaving a portion of rod buried below ground (see figure 4.11). After separation the original circuit was no longer intact; however, the exposed section lay touching the soil causing current flow to continue. Upon removal, the below-soil section was covered with a black, carbonaceous, grease-like substance. After scrubbing, the rod showed a very fine wire-like narrowing where final separation occurred. The buried section showed numerous pits and general deterioration (see figure 4.11). Including both sections, rod length after corrosion was 30.2 cm (11 7/8 in).

Steel Reinforcing Rod (Rebar) - Steel reinforcing rods were purchased from a local construction supply company and cut to a 30.5 cm (1 ft) length for experimentation. Before testing some corrosion (iron oxide) was noted on the rod's surface. The test rod was driven 18.4 cm (7 1/4 in) below the soil surface and current was passed for seven days. Current values ranged from 0.5 to 4 amperes. During current injection a black, carbonaceous substance appeared at the exposed rod's base. At the test's conclusion, a circular iron deposit surrounded the steel rod. Soil remained moist throughout the experimental period. Upon removal a black, carbonaceous, grease-like substance clung to the rod; after cleansing, the rod showed localized corrosion near the soil surface with extensive pitting elsewhere (see figure 4.12).

TABLE 4.4. - Ground rod current passage results

| Rod | Period, Days | Charge, A-hr | Wt Loss, gm | Corrosion Rate, gm/A-hr | | Charge Density, A-hr/cm$^2$ |
|---|---|---|---|---|---|---|
| | | | | Measured | Theoretical | |
| Copperweld$^R$ | 45 | 107.9 | 143.7 | 1.33 | 0.7 | 0.87 |
| Steel Rebar | 7 | 110.8 | 69.8 | 0.63 | 0.7 | 0.71 |
| Steel Rebar in concrete | 14 | 129.5 | 94.9 | 0.73 | 0.7 | 0.83 |
| Graphite in soil | 2 | 126.8 | 21.5 | 0.17 | - | 1.00 |
| Graphite in coke | 7 | 222.8 | 7.75 | 0.03 | - | 1.76 |
| Duriron$^R$ (SiCrFe) | 4 | 297.2 | 55.0 | 0.19 | - | 3.45 |
| Galvanized Steel | 8 | 467.5 | 207.8 | 0.44 | 0.7 | 3.00 |
| X-it$^R$ | 14 | 470.7 | 570.0 | 1.21 | 1.19 | 0.57 |
| Al Wire, 4/0 | 8 | 88.8 | 51.3 | 0.58 | 0.34 | 0.40 |
| Stainless Steel | 8 | 404.11 | 124.4 | 0.31 | 0.65 | 2.59 |

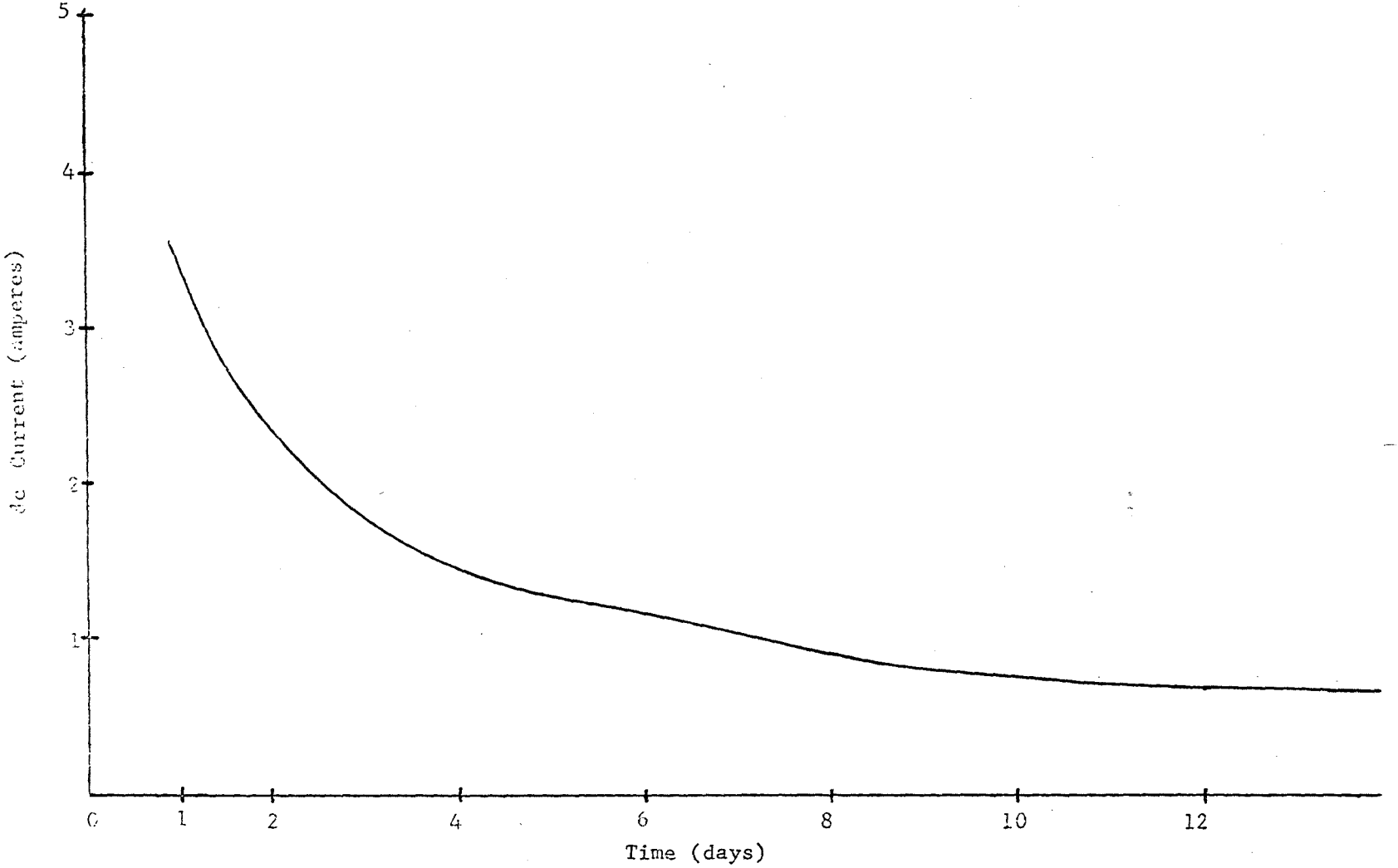


FIGURE 4.10. - Current passage versus time for a standard Copperweld Ground Rod.

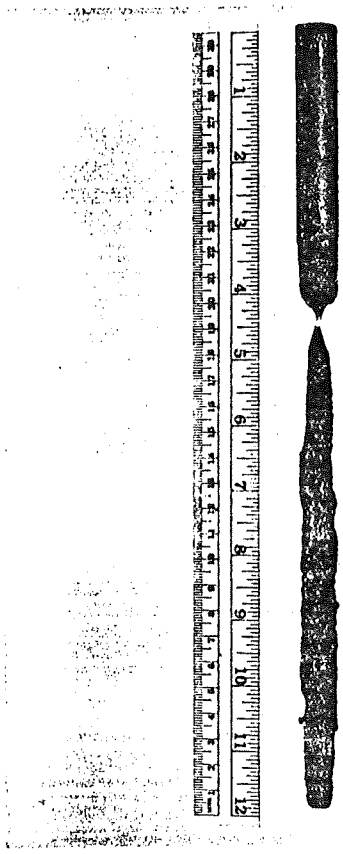

FIGURE 4.11. - Copperweld$^{R}$ Rod after corrosion test.

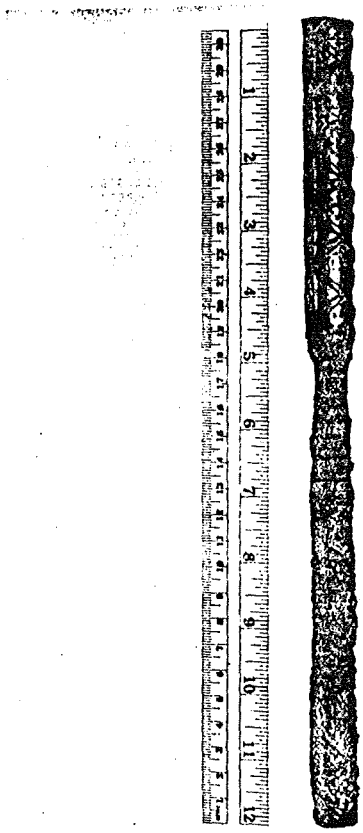

FIGURE 4.12. - Steel Reinforcing Rod after corrosion test.

Length of the corroded steel rod was slightly less than 30.5 cm (1 ft).

Galvanized Steel - A 2.44 m (8 ft) galvanized steel ground rod was purchased from a local coal mine supply company. The rod was cut into 30.5 cm (1 ft) sections for testing. One section was driven 22.9 cm (9 in) into the test soil; current ranging from 0.8 to 6 amperes was passed for eight days. During current passage the presence of chlorine gas was noted by its pungent odor. A black grease-like substance appeared at the base of the exposed rod and gas bubbles were observed near the rod. Current passage was very heavy throughout the experiment and soil moisture remained high. On the eighth day current flow was stopped and the rod removed. Adhering to the outside surface was a dark brown oxide layer (ZnO, $Fe_2O_3$). The oxide layer was easily peeled from the rod, exposing a black carbonaceous liquid. After thorough scrubbing localized corrosion was noted near the soil surface and at the electrode base. Corrosion at the soil surface had worn the rod dangerously thin, suggesting a possible break with further current flow. Corroded rod length was 28.6 cm (11 1/4 in) (see figure 4.13).

Stainless Steel - Two 1.83 m long (6 ft) by 1.59 cm (5/8 in) diameter, number 304 stainless steel rods were purchased from an in-state metal distributor. Number 304 stainless steel is alloyed with 18% chromium and 8% nickel. A 30.5 cm (1 ft) electrode was cut; 23.2 cm (9 1/8 in) of the rod was placed into the soil for corrosion analysis. Current passage was heavy, ranging from 0.7 to 5 amperes and lasting for a period of eight days. During current flow a pungent chlorine gas odor was evident and a black grease-like substance appeared at the base of the exposed rod. Removal of the rod revealed a surface oxide layer ($Cr_2O_3$) which was easily peeled away. Under the oxide layer was a carbonaceous liquid. After scrubbing, the rod showed severe pitting and necking (corrosion at the soil surface) but remained bright and lustrous. The soil retained its moisture content throughout the experiment. The corroded rod length for stainless steel was 30.2 cm (11 7/8 in) (see figure 4.14).

Duriron$^R$ (SiCrFe) - Silicon, chromium, iron electrodes were donated by the Duriron Corporation of Dayton, Ohio. Although most of Duriron's commercial anodes were too large for these experiments, a few scrap pieces 45.7 cm (18 in) long by 1.27 cm (1/2 in) in diameter were located and graciously donated. SiCrFe alloy is extremely brittle and in the course of electrode preparation one was broken. Therefore the rod used in this experiment was only 21 cm (8 1/4 in) long, of which 17.1 cm (6 3/4 in) remained below the soil surface. Because of its small diameter and brittle nature the SiCrFe rod was not driven into the soil; rather it was placed in a larger diameter hole and backfilled with soil. Standard ground rod clamps could not be used; therefore a sufficiently large alligator clip provided the electrical connection. Current passage was extremely high (2 to 5.8 amperes) and lasted for four days. The shortened time period occurred for fear that the rod would overcorrode. The pungent odor of chlorine gas was very much present during the experiment and black grease-like material formed at the exposed rod's base. The plastic box cover was removed at the test conclusion, revealing an iron ring deposit a short distance from the rod. Soil adjacent to the rod appeared dry and yellowish in color. Moisture content in the rest of the box remained high,

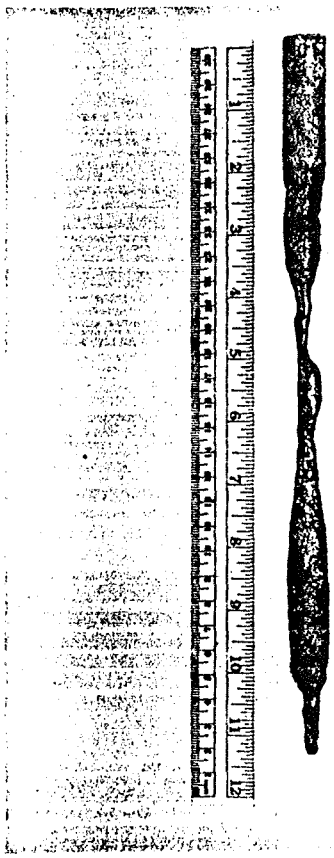

FIGURE 4.13. - Standard Galvanized Steel Rod after corrosion test.

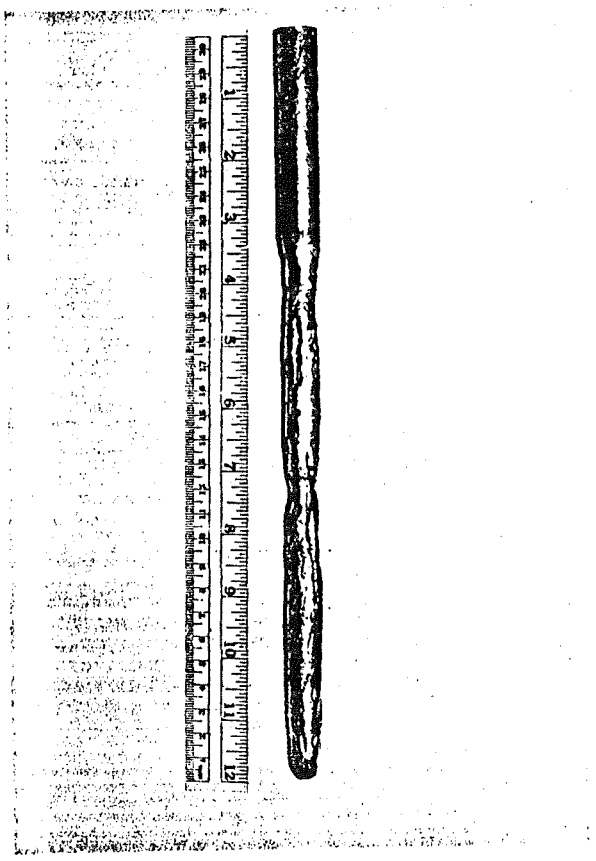

FIGURE 4.14. - Stainless Steel Rod after corrosion test.

however. Rod removal showed a large perforated surface oxide layer which was easily removed. Under the oxide layer ($SiO_2$, $Cr_2O_3$) was a black carbonaceous liquid. Thorough washing revealed uniform corrosion with no visible necking or pitting. The rod's length after corrosion was still 21 cm (8 1/4 in) (see figure 4.15).

Graphite in Soil - Four 1.27 cm by 31.1 cm (1/2 in by 12 1/4 in) graphite rods were donated by Airco Speer Corporation, Graphites Electrode Division in St. Mary's, Pennsylvania. Since graphite is easily broken, extreme care was taken in electrode preparation. An 21 cm (8 1/4 in) section of a graphite electrode was placed in a larger diameter hole and carefully backfilled with soil. The 1.27 cm (1/2 in) rod diameter was too small for conventional ground rod clamps, so a sufficiently large alligator clip was used. Current passage ranging from 4 to 5 amperes lasted for only two days due to a break in the graphite rod. A very high concentration of chlorine gas was produced during the test, causing the need for exhaust fans. Rod breakage occurred at the surface level, disconnecting the corrosion circuit. Removal of the plastic cover revealed yellowish soil adjacent to the rod and pieces of graphite in the soil. A sizable piece of graphite was removed from below the soil surface. The combined length of both pieces was 27.3 cm (10 3/4 in) (see figure 4.16). One related observation was the oxidation of metals placed in close proximity to the corroded graphite rod suggesting continued emission of $Cl_2$ gas.

Aluminum - A 54.6 cm (21 1/2 in) section of 4/0 stranded aluminum wire was used for corrosion testing. The protective insulation and oxide layer were removed before installation. The wire was buried 24.1 cm (9 1/2 in) in soil and a large alligator clip was used for electrical connection. Current levels ranged from 0.1 to 4.8 amperes for eight days. The larger current levels appeared during initial start-up; current rapidly decayed with time. A constant current of approximately 0.5 amperes continued throughout a major portion of the test period. During current passage a white salt-like substance appeared at the exposed wire base. The substance became yellowish in color with age. At the test conclusion the Al wire was removed, revealing localized corrosion near the soil surface which caused filaments of wire to separate from the main trunk. The wire surface was covered with a milkish white and red substance. After thorough cleansing the below-soil section appeared crusty and dull gray in color, suggesting the enhanced presence of aluminum oxide ($Al_2O_3$). The soil remained moist throughout the experiment. After corrosion the Al wire length was 47 cm (18 1/2 in) (see figure 4.17).

Graphite in Coke Breeze - A variation of the graphite electrode, graphite backfilled with coke breeze, was one of three special electrodes tested. Coke breeze consists of finely ground coke. The coke breeze available for testing was more granular, however. A 31.8 cm (12 1/2 in) rod, identical to the one used for graphite in soil, was placed in a 11.4 cm (4 1/2 in) diameter hole and backfilled with granular coke breeze (see figure 4.18). The graphite rod was exposed 10.8 cm (4 1/4 in) above the coke level. Current passage was light, ranging from 0.2 to 6 amperes for a period of seven days. During the test period some chlorine gas was noted, but the air concentration was low, posing no health hazard. After three days of low current flow, water was added to the soil-coke interface in an attempt to

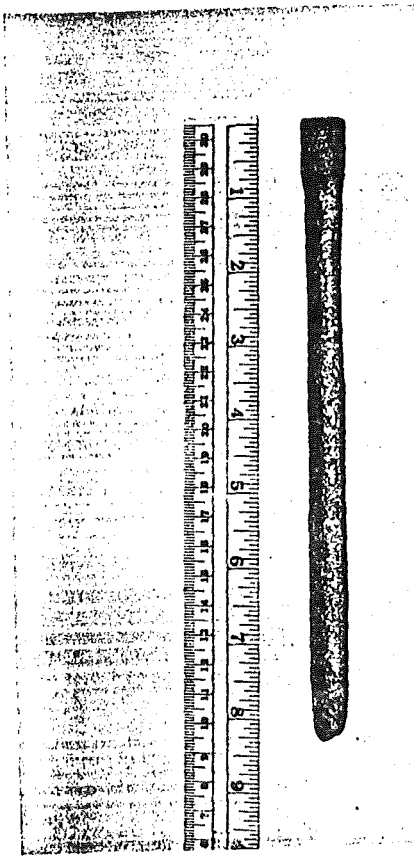

FIGURE 4.15. - Duriron$^{R}$ (SiCrFe) Rod after corrosion test.

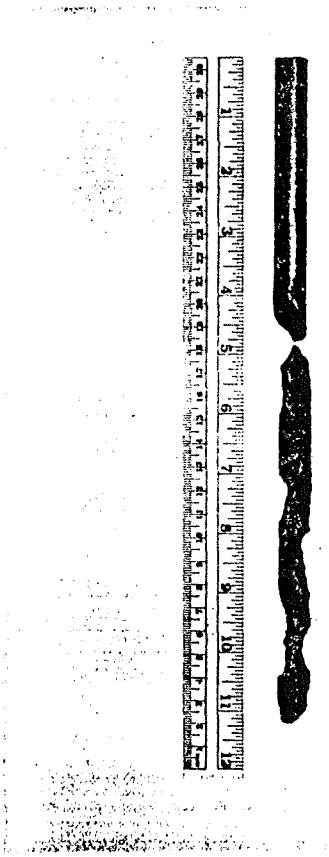

FIGURE 4.16. - Graphite Rod after corrosion test.

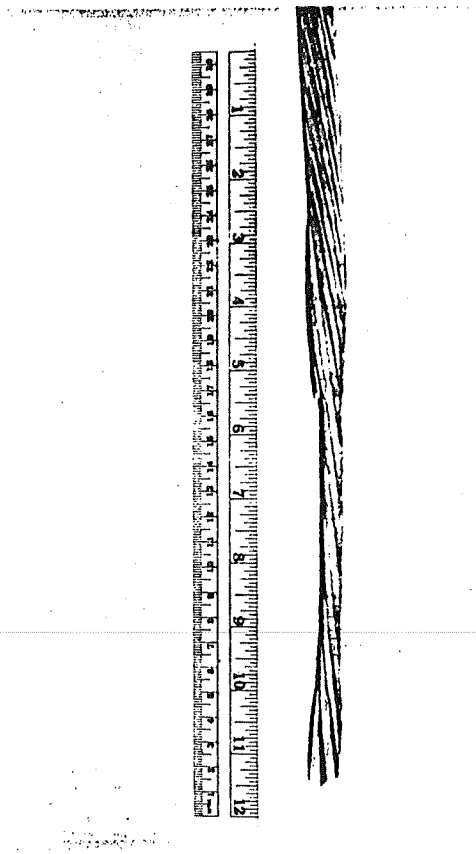

FIGURE 4.17. - Aluminum Wire (4/0) after corrosion test.

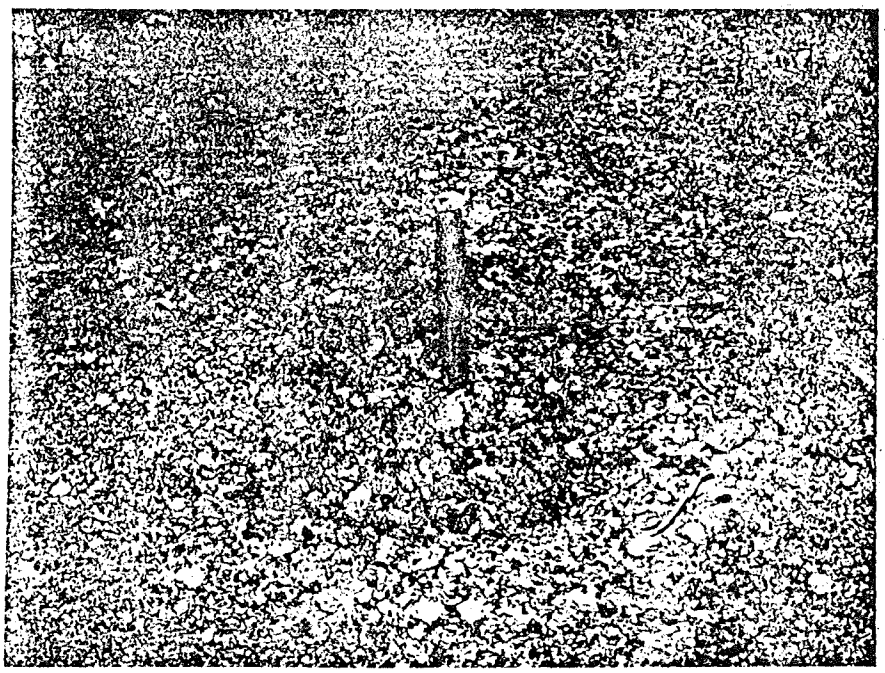

FIGURE 4.18. - Graphite Rod backfilled with granular coke breeze.

lower the circuit resistance. Following the addition of water, current flow increased and stayed high for the remainder of the test. After seven days the rod was removed. Very little corrosion or weakening was noted along the electrode body. However, 3.5 cm (1 3/8 in) of the rod's base were lost. The after-test rod length was 27.6 cm (10 7/8 in) (see figure 4.19).

Steel Rebar in Concrete - The second of three specialized electrodes consisted of a 30 cm by 1.59 cm (12 in by 5/8 in) steel reinforcing rod embedded 17.8 cm (7 in) in concrete. The concrete was 20.3 cm deep (8 in) and 15.2 cm (6 in) in diameter (see figure 4.20). The concrete-steel electrode was constructed in soil. The "concrete" used was actually a patching mix with the trade name Sakrete$^{R}$ Sand Mix. After formation the cement rod was allowed to harden for two days with the plastic box cover removed. To insure adequate concrete moisture during experimentation the hardened electrode was watered and allowed to sit covered for seven days. Due to soil erosion during watering, a layer of mud formed on top of the concrete electrode. In order to avoid error the mud was removed. Current passage was very mild, ranging from 0.2 to 0.6 amperes, and was continued for fourteen days. At the experiment's conclusion the plastic cover was lifted, revealing a symmetrical split in the cement base. The concrete electrode was extracted in two pieces, one half adhering to the steel rod. Iron deposits were visible throughout the concrete and a black carbonaceous grease-like substance coated the steel rod. By washing the intact concrete-rod section it was noted that localized corrosion occurred at the concrete surface and rod base (see figure 4.20). Moderate pitting was noted along the encased section; after corrosion length was 30 cm (11 13/16 in).

X-it$^{R}$ Rod - A sample X-it rod, 45.7 cm (18 in) by 5.4 cm (2 1/8 in), was custom-made for these experiments by C. J. Reinmuller, X-it Rod Corporation president. The rod arrived filled with salt and exit holes taped. During electrode preparation a sample of the contained salts was removed. Two substances were observed; one being a salt, the other a hydrophilic agent drawing water from the surrounding atmosphere. The electrode was placed 22.9 cm (9 in) into the box and backfilled with soil. The rod was left dormant for 18 days to allow the patented salting action time to start. To observe the self-salting action, rod-soil resistance was monitored using the Bison meter and three-electrode method (see Table 4.5). When the rod-soil resistance stabilized, current injection was started. Current flow was high, 0.6 to 4 amperes, lasting for sixteen days. Green copper oxide appeared at the exposed rod's base, thickening with time. Soil near the rod became dry and hard, making rod removal difficult. Corrosion left the rod walls very thin and breakage occurred while attempting removal. In all, three sections of rod were recovered (see figure 4.21). The rod's internal salt appeared dry and was easily lost during removal. A closer examination of the rod revealed fiberglass in the proximity of both exit holes with loosely packed salts in between. Copper oxide clung to the outer skin of the buried rod. After scrubbing, the rod walls were found to be paper thin. Localized corrosion was greatest near the surface and bottom. One additional observation: the corroded X-it rod pieces, still retaining salt, continued to draw moisture from the air even after corrosion.

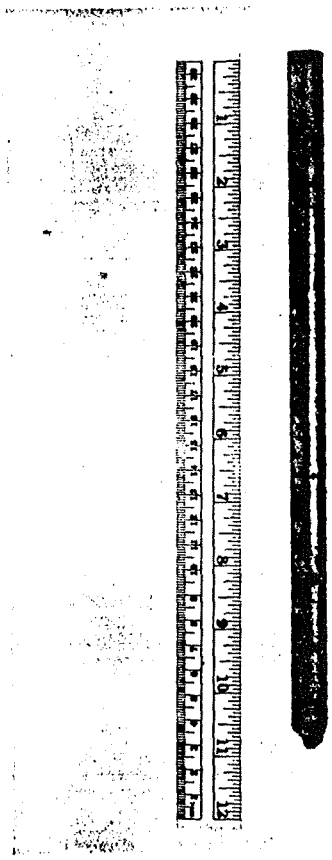

FIGURE 4.19. - Graphite Rod in coke breeze after corrosion test.

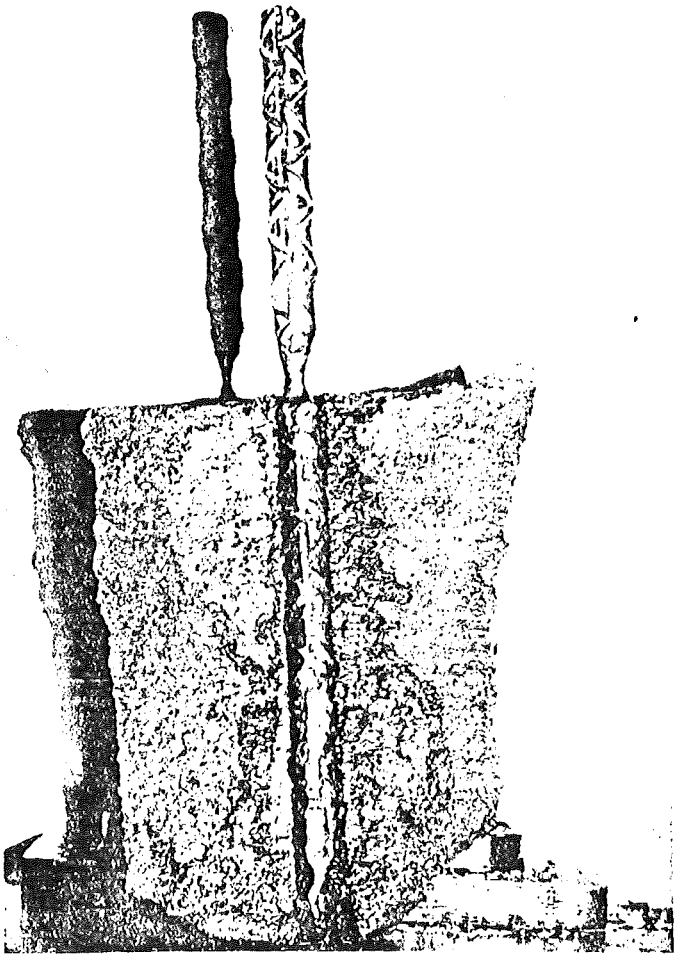

FIGURE 4.20. - Concrete-encased Rebar after corrosion test.

FIGURE 4.21. - X-it$^{R}$ Rod after corrosion test.

TABLE 4.5. - Rod-to-soil resistance of X-it Rod prior to corrosion

| Day | Rod-Soil Resistance, Ohms |
|---|---|
| Installation | 4.05 |
| 2 | 3.80 |
| 3 | 3.75 |
| 10 | 3.58 |
| 12 | 3.64 |
| 18 | 3.71 |
| After Corrosion | 6.87 |

4.5.5 Results and Discussion of Corrosion Resistance

The anode of an electrolytic corrosion cell is capable of a variety of reactions with its environment. If the cell potential is relatively low, the major reaction will be the dissolution of metallic ions into solution, for example:

$$Cu + H_2O + 1/2\ O_2 \rightarrow Cu(OH)_2.$$

For a higher cell potential the anodic reactions turn to the formation of oxygen and halogen gases,

$$2\ Cl^- \rightarrow Cl_2,$$

$$2OH^- \rightarrow 1/2\ O_2 + H_2O + 2e^-.$$

The determination of cell voltage lies in the relative nobility of the anode's oxide layer. All metallic anodes react with oxygen in the atmosphere to form skin oxides, for example:

$$2Cu + 1/2\ O_2 \rightarrow Cu_2O.$$

If the metallic oxide restricts the dissolution of metal ions (becomes noble) the cell voltage will increase. An anode which is relatively insoluable in its environment causes the cell voltage to increase until a second reaction begins. In order to have a noble anode two things must occur; the cell voltage must somehow be raised to promote secondary reactions other than anode dissolution, and the anode must not be affected by products of these secondary reactions.

Production of halogens, such as $Cl_2$ and $Br_2$, with increased cell potential causes breakdown of metallic oxide layers, thus lowering cell potential and increasing anode dissolution. In the case of insoluable anodes, such as graphite, halogen production weakens the tensile strength, causing erosion.

Each metallic anode tested produced a metallic oxide skin. Some oxides caused their anodes to become noble, raising cellular potentials and producing

gaseous oxygen and chlorine. The soil concentration of chlorine ions was very high due to external salting, thus increasing the production of $Cl_2$ and its attack on metallic oxides. A carbonaceous substance, very black in color, appears repeatedly around ground rods with high iron content. It is believed that this substance is iron-oxide (42). Every metal rod tested, except SiCrFe, showed localized corrosion at both the surface (necking) and the rod base (see figure 4.22). With continued current flow metal rods severed close to the soil surface, indicating extreme localized current flow. Necking or rapid localized corrosion above the surface is described by Fink; the phenomenon is caused by a constant bathing of that area by corrosion products pushed up from below (12). The area directly above the electrolyte surface does not produce thick oxide layers due to lack of current flow, therefore this area of the rod is very susceptible to attack by corrosive agents generated below. In the rod configuration the maximum current density is located at the base; this is also the area of lowest oxygen concentration, thus retarding oxide formation (18). Therefore accelerated corrosion at the rod's base is expected.

All rod currents were noticed to decrease with time due to dc polarization (see figure 4.23). One cause of polarization is the decreasing presence of ions necessary for anodic reactions. As accelerated reactions take place a build-up of products occurs, gradually restricting reactants from reaching the electrode surface. Because current in the electrolytic cell is dependent on this electronic-ionic exchange, the gradual decrease in reactants is reflected in a gradual decrease in current flow (53).

An experimental corrosion rate was calculated for each electrode from the weight loss (gm) and the charge passed (A-hr) (see Table 4.4). Because the corrosion rates are based on charge, the length of time a rod is corroded is unimportant. It can be argued that such corrosion rates are very specific for the type soil and procedure used; this statement is true. If one would test these same rods under different experimental conditions the results would not remain constant. In dealing with soil electrolytes and corrosion cells it is difficult to guarantee repetitive results. If all rods are exposed to similar conditions, however, a comparison is valid. Although corrosion rates cannot be taken as fact they provide a good indicator as to a rod's behavior in a salted, soil environment with moderate current flow. Table 4.6 provides a comparison of all rods tested according to experimentally determined corrosion rates. The table comments as to the practical use of each type rod. Some rods, such as graphite, are extremely resistant to corrosion but are very difficult to handle, thus increasing their cost-effective value. In fact, of the three rods most resistant to corrosion not a single one is without installation complications. If a severe ground bed corrosion problem exists, the added expense of installation may pay for itself in the future.

Theoretical calculation of corrosion rate, based on charge alone, uses Faraday's Law. Faraday's Law states that the weight lost, $W_L$, is equal to the total charge passed, Q, times the molecular weight of the metal, M, divided by Faraday's Constant, (F = 96,500 coulombs), and the metal's valence state, n,

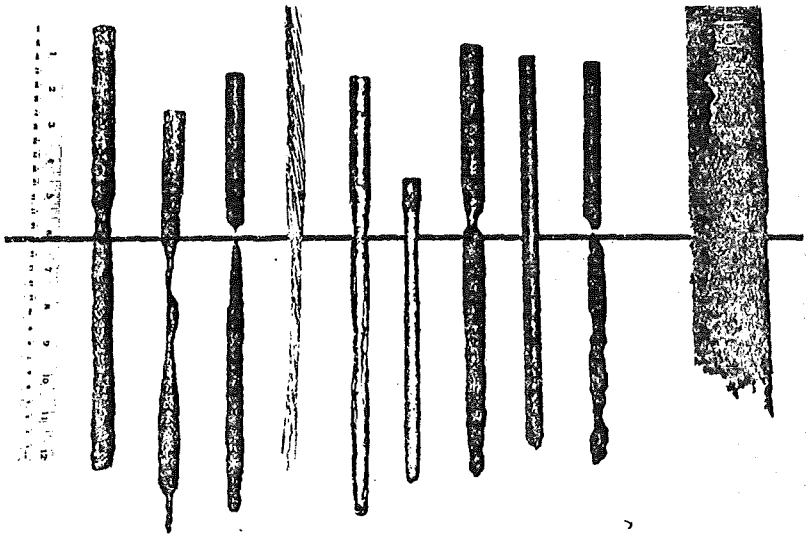

FIGURE 4.22. - Composite of all ground rods tested following corrosion. Black line indicates soil level.

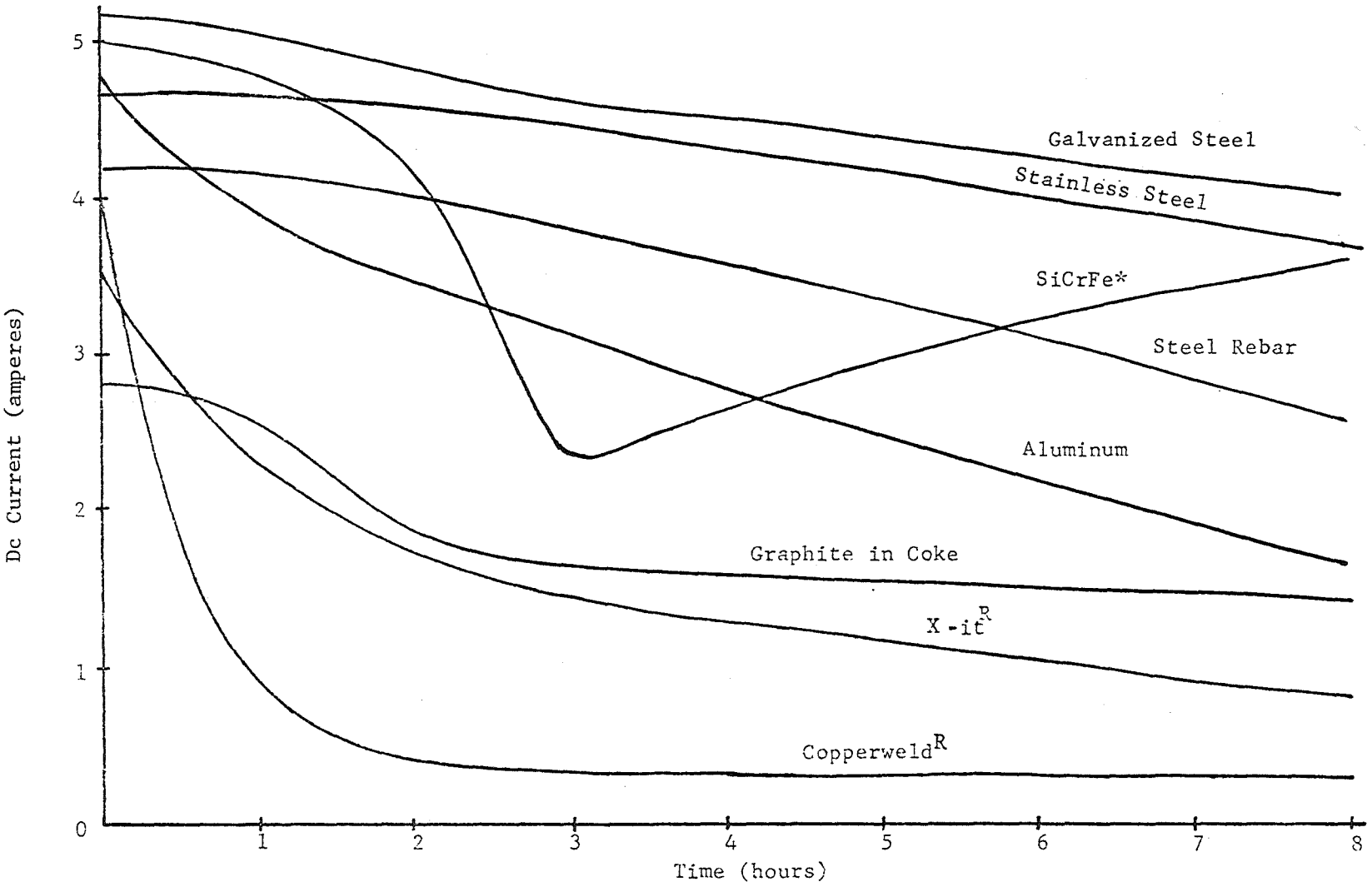


FIGURE 4.23. - Initial current passage vs time for all ground rods tested.
*oscillatory response

TABLE 4.6. - Comparison of tested ground rods

| Ground Rod | Measured Corrosion Rate, g/A-hr | Usage Comments |
|---|---|---|
| Graphite in Coke | 0.03 | Graphite is extremely brittle. Requires special installation procedure. |
| Graphite in Soil | 0.17 | Not recommended without adequate ventilation due to chlorine gas attack. |
| Duriron (SiCrFe) | 0.19 | Extremely brittle. Requires pre-drilled hole. High current density possible. Very uniform corrosion. |
| Stainless Steel | 0.31 | High current density possible. Fairly expensive. |
| Galvanized Steel | 0.44 | Currently used ground rod. Easily installed. High current density possible. |
| Aluminum | 0.58 | Low current density. Very ductile. |
| Steel Rebar | 0.63 | Used as ground rods. Very inexpensive. |
| Steel Rebar in Concrete | 0.73 | Previously used for grounding. Requires extensive installation if no reinforced concrete structure exists. Can cause weakening and even cracking of concrete structures. |
| X-it Rod | 1.21 | Requires special installation. Very expensive. |
| Copperweld | 1.33 | Most commonly used ground rod. Highly corrosive. |

$$W_L = \frac{Q\,M}{F\,n} \cdot \qquad (4.7)$$

The problem in using Faraday's Law for evaluation of corrosion is the presence of side reactions and weight loss due to erosion. Side reactions, such as the production of oxygen and halogens, cause current to flow but do not directly result in metal loss. Sometimes a section of metal will be lost due to the weakening of underlying metal, consituting erosion. Because of errors like these, rarely are accurate results obtained using Faraday's Equation for weight loss. One additional restriction in using Faraday's Equation is the assumption of metal purity. Although it is theoretically possible to predict weight loss for alloy metals, it is very difficult and requires knowledge of exact compositions (62). Alloy metal constitutents theoretically corrode according to their position on the reduction potential scale; however, the combination of some metals may accelerate or retard normal corrosion rates (43). The majority of rods tested were alloys. Frequently one metal constituted a large percentage of the total rod, however. In an attempt to predict metal loss it was assumed that the dominant metal was responsible for a majority of the weight loss. In the case of insoluable and special electrodes no prediction was attempted. Results were fairly close for alloys with one high percentage metal, such as steel; however results for plated and alloy metals with no high percentage component, such as copperweld and stainless steel, proved useless.

### 4.5.6 Ground Bed Corrosion Detection

One of the objectives of the corrosion research was to devise a way to noninvasively detect ground bed corrosion. The easiest way to detect corrosion is by examination; however, in working electrical systems the ground bed must remain intact at all times. Therefore the search began for possible alternatives to evaluate corrosion progress. After an extensive literary search, five measurable parameters existed. These five appear in Table 4.7.

TABLE 4.7. - Evaluation of ground bed monitoring techniques

| Monitoring Technique | Non-Invasive | Accuracy | Corrosion Prediction | Corrosion Monitor |
|---|---|---|---|---|
| Ground Rod - Soil Potential | 5 | 5 | 3 | 0 |
| Soil Resistivity | 5 | 5 | 3 | 1 |
| Current Integration | 5 | 5 | 4 | 3 |
| Ultrasonics* (rod length) | 5 | 4 | 0 | 3 |
| Ground Rod Resistance | 5 | 4 | 3 | 2 |

*Ultrasonics is only applicable under certain ground bed conditions.

All five methods are rated from 0 to 5 (five being the best), evaluating their ability to be used non-invasively; to give reliable results; to

predict the onset of corrosion; and to monitor corrosion progress. These ratings are derived from literary information and practical experience; their use is solely for narrowing possible alternatives.

All possible schemes adapt themselves easily to working ground beds with some reservations. Accuracy, for the most part, is good for all methods, but the last two columns narrow the field. The existance of corrosion depends on the presence of two conditions; adequate electrolytic contact and current flow. All methods, except length detection, monitor one or both conditions. If the assumption is made that corrosion exists, the problem is one of retardation and evaluation--therefore column 3 is irrelevant. Column 4 reveals four possible solutions which will be discussed in detail. Reasons for deleting the remaining solution follow:

Ground bed-to-soil potential measures the potential of ground beds with reference to a reference electrode (such as standard copper-copper sulfate, $Cu\text{-}CuSO_4$) close by. The numerical value obtained gives only an indication as to the type of corrosion present, if any (20). As long as metal is available for corrosion the potential will prevail. Therefore this method is not useful for monitoring duties. Rod-to-soil resistance, although considered possible for corrosion monitoring, will not be discussed further. Work in this area is presently being conducted for the USBM at West Virginia University. To prevent multiple investigation discussion will be limited to the soil resistivity method, a relative of rod-to-soil resistance.

Attempts to use changes in soil resistivity were reported in the previous annual report. The results were unsatisfactory for the most part, and will not be reiterated here.

Monitoring of corrosion by current integration was also covered in the previous report. A current integrator was built to make long-term data gathering easier, and several electrodes were tested. Figures 4.24 and 4.25 show the front panel and card layout of the device. Although the passage of charge could be monitored easily, it was determined that corrosion itself could not be directly assessed.

### 4.5.7 Ultrasonics

From the above results it becomes evident that other means besides current integration must be employed to monitor the onset of corrosion. If the corrosion process were uniform, current integration would be very useful. Current integration yields an average weight loss regardless of the uniformity of corrosion, however (25). If corrosion tends to be localized the threat of rod separation becomes the main concern. The problem is to find a way to detect localized corrosion non-invasively. Once again an analogous situation from industry provides a possible solution.

For a long time plant engineers had no accurate way to detect corrosive weakening in exposed pipelines. Previously, sample holes were drilled and pipe thickness recorded by use of a micrometer. This sampling technique was far from accurate and very invasive, necessitating periodic pipeline shutdowns and repairs (44). Today ultrasonics is used to measure metal thickness and thus corrosion progress.

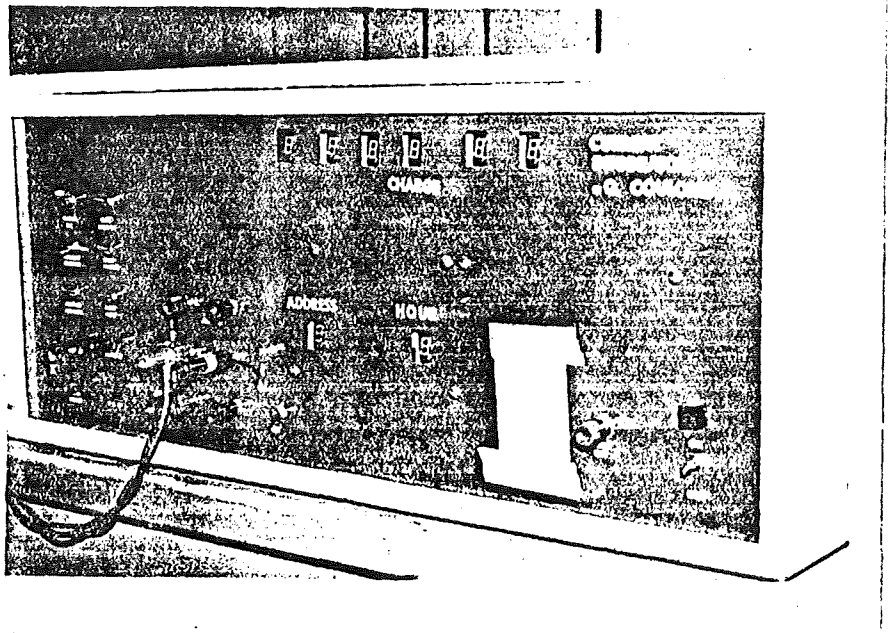


FIGURE 4.24. Long-term Electronic Integrator, front panel.

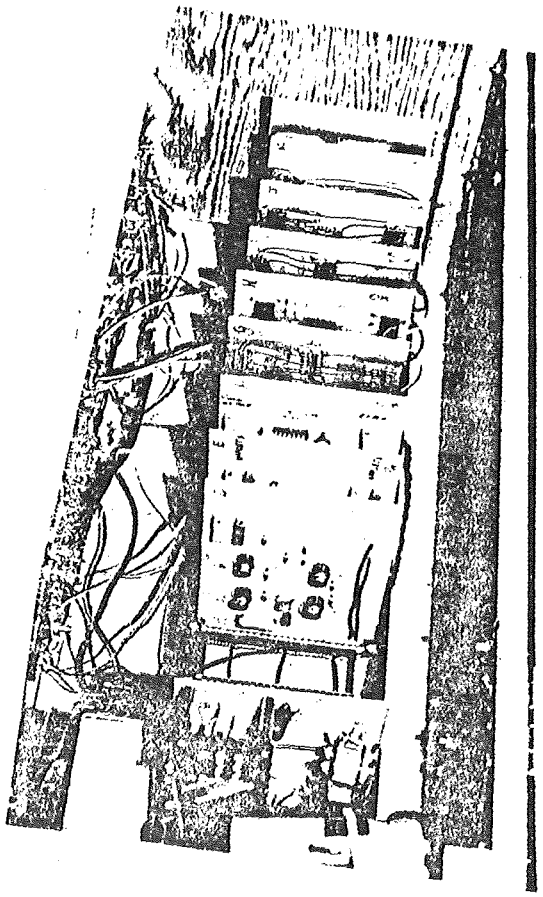

FIGURE 4.25. - Modular construction, Long-term Electronic Integrator.

Ultrasonics represents any frequency of sound higher than human hearing. High frequency vibrations are introduced to the exposed metal surface using a piezoelectric device and an appropriate sound-coupling media, such as water or grease. Depending on the properties of the material under study, the sound wave will propagate until a second interface is encountered; at this point some sound waves will be reflected back toward the transducer.

Two methods of measurement are currently used: 1) pulse echo technique is based on the time delay between an introduced burst of sound and its return echo. The pulse echo method is a function of the material used and must be calibrated prior to testing; 2) the resonance technique continuously introduces and records a sound wave which is frequency variable. Resonance occurs when the reflected wavelength, r, is equal to the test wavelength, t, which occurs when the metal thickness is n(1/2)t. Wavelength is equal to the velocity of sound divided by the sound frequency. Sound velocity is a function of the material used, so by employing a variable sound frequency and sweeping the frequency spectrum the fundamental (1/2)t frequency and subsequent harmonic frequencies n(1/2)t will show resonance. For ease of measurement calibration of the frequency scale into length units is done using a test sample of known length. The resonance method is extremely useful for very accurate thickness measurements over wide ranges.

4.5.8 Applications and Limitations

In applying ultrasonic measuring techniques to ground beds four very important requirements must be met (19):

1. the ground bed must consist entirely of ground rods, capable of propagating sound,

2. tops of ground rods must be exposed above ground, accessible for measurements,

3. tops of ground rods must be perpendicular to the rod body,

4. the ground rod must be solid and continuous (welds and threaded joints are unacceptable).

Prior to this, ultrasonics has been used extensively to measure material thickness. Non-invasive measurement of ground rod length is proposed here. If ultrasonic laws hold true, placement of the transducer on top of the rod would send a signal to the rod base which would reflect back. Using the techniques described, the length could be read directly. Corrosion or rod separation any here would alter the length reading. In the case of a severed ground rod, length readings would be less than expected. For general rod corrosion, multiple as well as base reflections would be expected (45).

Current industrial ultrasonic units are available in portable, battery operated models. These units are designed for field work, suggesting possible use for ground bed study (28). One disadvantage of the ultrasonic method is the need for a specific type of ground-bed design. Although a seemingly bothersome disadvantage, the move toward a standardized ground-bed design is inevitable.

### 4.5.9 Preliminary Tests

Following corrosion tests a preliminary feasibility study was made of ultrasonic length measurements for ground rod corrosion. Krautkramer-Branson of Stamford, Connecticut was contacted regarding the application of ultrasonic length measuring techniques to ground rods. A local distributor, R. L. Holliday Company, Pittsburgh, Pennsylvania, consented to demonstrate the use of existing equipment in ground rod measurement.

The pulse-echo method was chosen to measure various length ground rods in differing states of corrosion. Equipment employed was the Branson Model 303 Ultrasonic Flaw Detector. Initially the instrument was calibrated to a standard, out-of-soil, 2.44 m (8 ft) ground rod, showing that the instrument was capable of measuring a rod of such length. Next, a 30.5 cm (1 ft) section of rod, out-of-soil, was measured without recalibration. As expected, the instrument recorded a 30.5 cm length. In order to determine the effect of corrosion on ultrasonic readings the instrument was calibrated to an uncorroded, out-of-soil, 30.5 cm rod. Subsequent testing of out-of-soil, corroded rods revealed multiple reflections, the first being located at the point of corrosion. The effect of soil on ultrasonic length measurement was observed using the simulated ground beds previously described. No difference was noted between observations made out-of-soil and those within the soil environment. An experimental ground bed nearby provided measurements of a driven, 2.44 m (8 ft) ground rod. The top of the ground rod was prepared using a metal file and the instrument was calibrated with a 2.44 m, out-of-soil ground rod. Measurements of the in-soil rod revealed markable signal attenuation, possibly due to an over-abundance of earth moisture. However, with an amplifier gain of 80 dB, a signal at the 2.44 m mark was clearly visible. An additional signal appeared approximately 1/3 of the way down the rod. This signal could be attributed to corrosion, rod bending, or a large water pool.

These preliminary tests show that ultrasonic length measurement provides a reliable method of detecting ground rod corrosion. Instrumentation procedures are easily learned and rugged industrial equipment is available. Problems of attenuation can easily be overcome by using more powerful transducers, signal generators, and receiving amplifiers.

### 4.5.10 Conclusions

Based on test results, commercially used ground rods are most susceptible to corrosion. If a commercial ground rod must be used, galvanized steel proves the lesser of evils, being least corrosive. Corrosion resistant electrodes do exist, but these tend to be brittle, expensive and difficult to install. The stainless steel electrode provides both durability and inexpensive corrosion resistance.

Use of reinforced concrete structures as grounding electrodes tend to cause concrete deterioration and cracking. One special electrode, the X-it rod, was designed to lower rod-soil resistance. Although rod-soil resistance may be lowered with time, use of the X-it rod in a corrosive environment is not advised. With the addition of coke breeze backfill even a standard electrode's corrosion rate is cut in half.

Non-invasive monitoring of ground rod corrosion is best accomplished with both current integration and ultrasonic length measurement. Long-term current integration is reliably done using an electronic integration system with memory. Use of soil resistivity as a corrosion monitoring method proves to be unreliable and a poor indicator of ground rod corrosion.

## 4.6 GROUND BED MONITOR EVALUATION

### 4.6.1 Introduction

The Ground Bed Monitor was conceived as a tool to study time variations in the resistance characteristics of mine safety ground beds. Conversations with several mine operations people indicated that some mines had experienced loss of the safety ground bed due to electrolytic corrosion. In at least one case this loss was essentially complete but was not discovered until the bed was dug up as part of substation renovation.

A survey of the literature pertaining to ground-bed resistance revealed that seasonal effects such as freezing of the soil or periods of drought can cause significant changes in ground-bed resistance. Since no coal mine checked its bed resistance more often than twice a year (some never did), concern arose as to the number of beds which might develop excessively high resistance without the immediate knowledge of the mine personnel. It was decided to develop a continuous monitor of ground-bed resistance in order to obtain data on day-to-day variations in ground bed resistance.

As detailed in the 1975-76 Annual Report of Grant G0144138 (56), a prototype was first installed on 22 and 23 December 1975 at the Delmont Mine, near Ruffsdale, PA. It was connected to the safety ground bed, a rather large structure incorporating 21 rods. Some difficulty was experienced during the initial installation, leading to the discovery that the bed was already in a partially failed condition, having experienced a connecting wire failure some time previously. This failure had been unknown to the mine personnel and the MSHA inspector, and suggested that a continuous ground bed monitor would be a very useful device.

It was necessary to readjust and repair the prototype several times, but it was finally capable of making a continuous recording of resistance from 12 March 1976 to 20 May 1976, a period of 69 days, at which point it failed again due to destruction of its monitoring leads by small animals (squirrels, groundhogs, or other rodents). Before it failed, however, it recorded some step changes in ground bed resistance occurring as the result of the failure of another interconnecting wire on the ground bed. The actual recording of this ground bed failure suggested even more strongly that a continuous monitor was a desirable instrument.

Scrutiny of the 69-day record of ground-bed resistance revealed several occasions where electrical noise seemed to be causing undesirable effects on monitor accuracy. It was decided to rebuild the monitor to reduce the noise component creeping into the monitor from earth currents and other environmental effects. The redesign program was active for over a year, but the device was never substantially improved. The addition of very-low pass filters reduced the effects of external noise, but it increased the

internal noise figure of the monitor and made it overly sensitive to temperature. All in all, the design "improvements" served only to degrade the monitor below its original performance level. Although several attempts were made to further test the monitor, none were as successful as the original test.

The details of the ground bed monitor circuitry are covered in detail in the 1975-76 Annual Report on G0144138 (56).

The design and evaluation procedure that was carried out provided much significant information, but not necessarily the type of information that was expected. This information can be divided into two categories, that which was learned about circuit design for such an instrument, and that which was learned about ground beds themselves.

### 4.6.2 Circuit Design

After much wasted effort, it became clear that the particular circuit design approach chosen had produced a marginal design. A circuit of this type cannot be made to work well in the monitoring situation simply by improving its components, since the technology does not currently exist to do so. A fundamental limit exists in terms of the noise immunity and stability of the analog circuitry, related to 1/f, or "flicker" noise. Empirical measurements on many semiconductor devices has shown that they are subject to random noise signals whose RMS amplitude is inversely proportional to frequency (39). Since the ground bed monitor must be designed to function at very low frequencies (cycles per year), it is particularly sensitive to noise of this type. As additional filters were placed in the circuit to reduce the effects of external noise they increased internal noise generation levels to an intolerable level. When attempts were made to remove this noise with tuned filters the monitor became too sensitive to changes in temperature, since they cause the oscillator to drift as well as effect the response of the tuned filters.

It must be concluded, then, that a very-low frequency device which must remain stable under wide ranges of temperature and humidity and which must reject large unwanted signals at its inputs cannot be effectively designed using the analog circuit techniques that were originally chosen. A drastic redesign is necessary to achieve an effective monitor. This redesign would probably require the use of digital techniques. It is recommended that no further effort be expended to improve the present circuit.

### 4.6.3 Ground Bed Resistance

The ground bed monitor was designed to continuously evaluate ground bed resistance as a way of determining the integrity of the metallic structure buried within the earth, as well as to study seasonal variations in bed resistance. Although the monitor did not work well, some other aspects of the research have contributed significantly to an understanding of the situation. Most of this information was developed as part of the study of ground-bed corrosion, which is covered in detail in section 4.5. First, the experimental evidence shows that ground-bed resistance is essentially unaffected by the electrolytic corrosion process, and in many

cases the rods tested maintained their resistance characteristics after being nearly destroyed. Resistance is definitely not a sensitive indicator of corrosion damage.

Second, it appears that monitor failures are at least as likely as failures of the bed itself. In order to make its measurement the monitor requires two widely spaced electrodes and several long interconnecting wires to the various electrodes and sensors. These wires are quite small, and therefore more likely to be damaged than the large interconnecting wires that are being monitored. With respect to physical damage to bed interconnections, then, it appears to be a simpler matter to protect the bed itself than to protect the monitor connections.

Third, the corrosion studies have suggested that bed corrosion can be predicted somewhat from the soil characteristics and knowledge of the magnitude of stray current present. This means that susceptible beds can be identified. Actual corrosion damage can be checked periodically using off-the-shelf ultrasonic devices. This approach is so sensitive that damage can be detected long before bed destruction has occurred, so that periodic inspection is sufficient. Corrosion-resistant and climatically stable electrodes have also been identified, and can be installed in those locations which are suspected of developing unacceptably high bed resistance.

It is concluded then, that identification of environmental hazards, careful bed construction, physical protection of the bed, and periodic inspection using ultrasonics and visual means will provide as much assurance of bed reliability as will the use of a ground bed monitor, and at a lower total cost.

## 4.7 DEVICE TO MEASURE RESISTANCE OF CONNECTED BED

One of the most serious difficulties encountered in making field measurements of mine ground-bed resistance is the requirement that the bed be disconnected from the ground system in order to measure its resistance. Since disconnecting the bed affects the integrity of the safety ground system, mining operations should cease during the time of the measurement, and no equipment should be touched by mine personnel. In addition, having the bed disconnected can cause a possible shock hazard to the crew measuring its resistance unless power is actually shut off to the mine. Mine operators are understandably reluctant to measure the resistance of their ground beds.

It is for this reason that WVU began work on the design of an instrument to measure the resistance of a ground bed without disconnecting it. This was to be a further refinement of the ground bed monitor, described in detail in a previous annual report (56). While the monitor is able to measure the resistance of a connected bed, the bed still must be disconnected for a short time to slip a current transformer over its connecting wire to the grounding resistor. Additionally, it was found that the signal used to measure resistance was too small, and was easily swamped by stray and induced currents flowing in the ground bed.

Based on the experiences mentioned, criteria for the design of the device included:

1) compatibility with currently existing 4-terminal resistance and resistivity measuring devices, since the techniques used in these work better than any concerned alternative;

2) increased signal strength compared to instruments previously tested, hopefully up to several amperes or more; and

3) capability of measuring the resistance of a connected bed without any disruption of its connections or danger to the measuring crew or equipment.

Other criteria which were desirable included a modular construction which would couple easily to existing devices without duplicating any of their functions, field portability (lightweight, rugged, and weather resistant) and a relatively high voltage and high power capability for resistance and resistivity measurements in areas of high resistivity.

It was conceived that the instrument should be capable of several different modes of operation. It should be capable of functioning as a constant-current source for some types of measurement. This constant current mode could be used in two ways--a fixed current controlled by a front-panel adjustment or a feedback system in which the source supplies current in a way which causes the current flowing through some remote sensor to be held constant, such as the current through the ground bed itself. The device should also be capable of functioning as a constant-voltage source. This mode may be necessary in some situations, since Federal regulations require that no more than 40 volts be applied to the safety ground system.

As mentioned above, the most desirable module would be extremely flexible and capable of making various types of field measurements. Figure 4.26 shows several of the applications and connections which should be included in any further development of a ground-bed resistance measurement device.

### 4.7.1 Description of the Prototype

An elementary prototype was fabricated to evaluate the feasibility of using some of the measurement modes which had been conceived. The schematic diagram of this device is shown in figure 4.27. It is simply a current-booster amplifier which amplifies a signal received from a Bison Model 2350 Earth Resistivity Tester.* The Bison is a constant-current device which supplies approximately 25 mA to a wide range of loads. The prototype circuit is able to increase the current drive by a factor of approximately 10, but it cannot be used for a wide range of loads. It can supply only 6 volts RMS, so it will not work where the circuit impedance is greater than about 20 ohms. The meter and variable resistor are used to adjust the output current to some simple multiple of the input current (as read by the current meter on the Bison). Once this has been done, the resistance reading

---

* Reference to specific brands, equipment, or trade names in this report is made to facilitate understanding and does not imply endorsement by the Bureau of Mines.

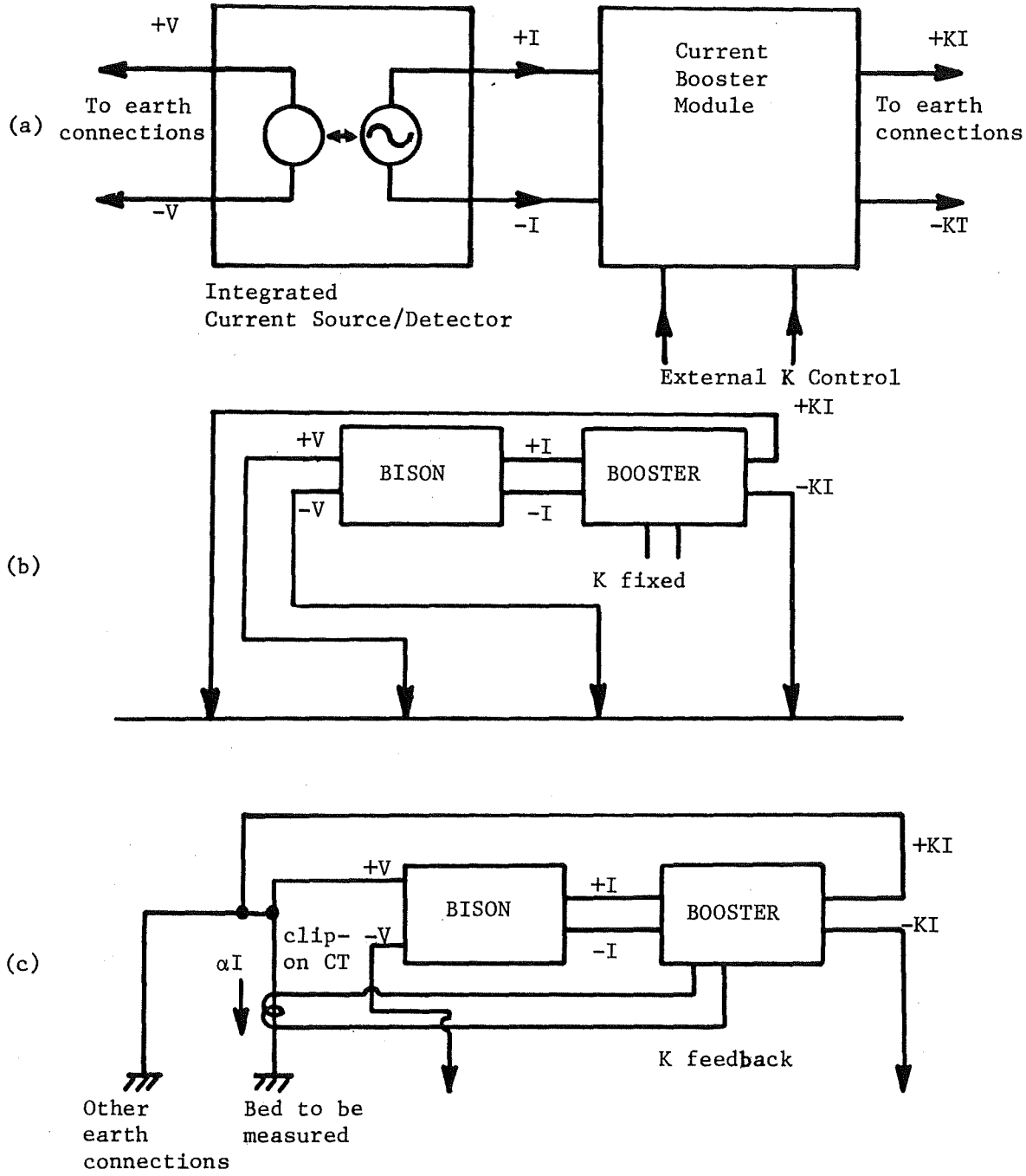


FIGURE 4.26. - Use of Booster System to make resistivity and resistance measurements. (a) Diagram of Booster System; (b) Boosted-power resistivity measurement ($\rho = \rho_{indicated}/K$); (c) Feedback control to measure resistance of connected bed. Here feedback alters K to maintain $\alpha$ constant.

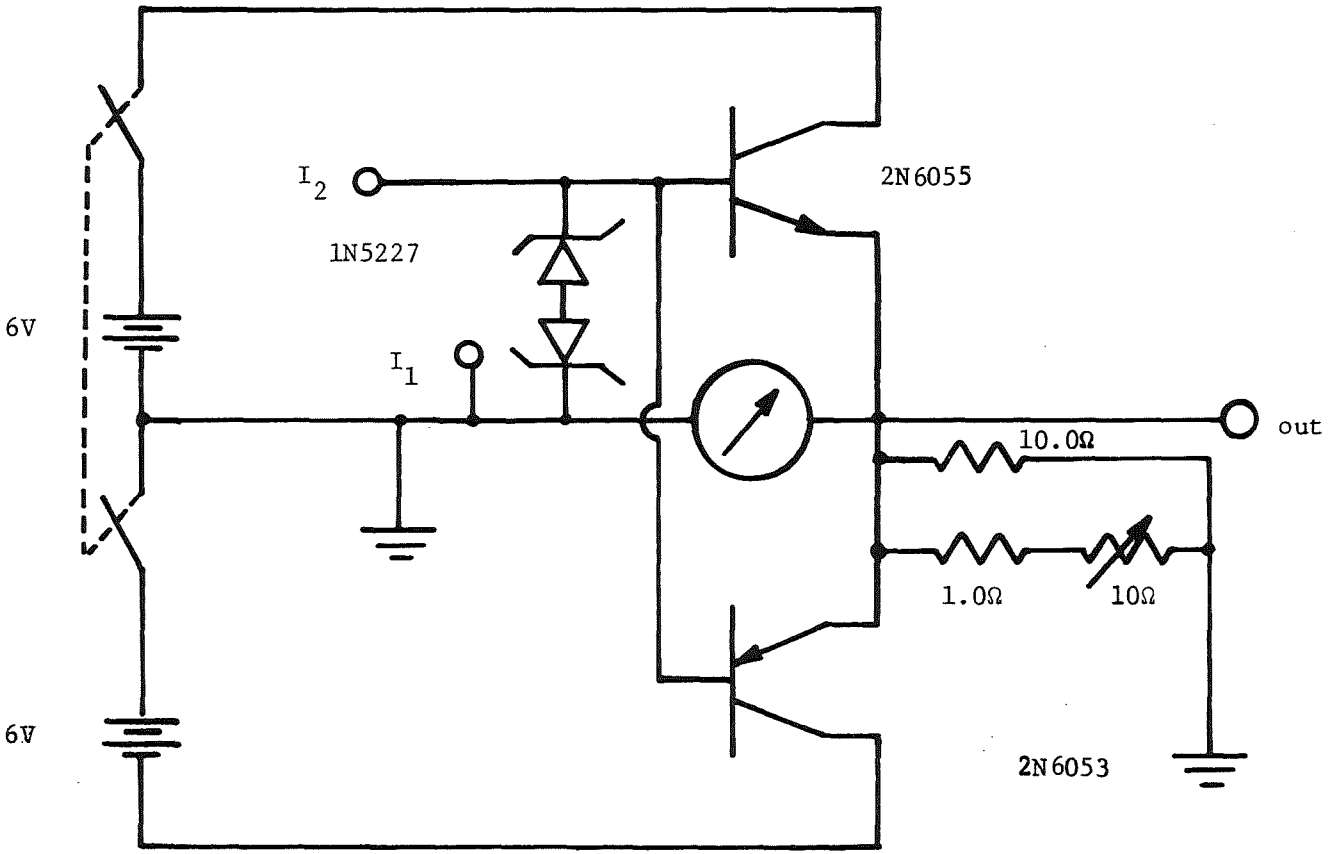


FIGURE 4.27. - Schematic of prototype booster amplifier.

obtained by the Bison is corrected by dividing it by the current multiplication factor.

The prototype has worked reliably and well for the limited range of conditions within its capabilities. It does not meet the original criteria well enough to be generally useful, however. The biggest problem is its lack of power capability.

# CHAPTER 5

# STRAY AND INDUCED CURRENTS

## 5.1 SOURCES OF STRAY DC CURRENTS

### 5.1.1 Introduction

A major source of machine-earth and inter-machine voltage is due to stray dc currents within the earth. Most of these currents are attributed to the rail haulage system which is in good contact with the mine floor. Equipment frames which rest on the mine floor are placed at the potential of earth they rest on, making a path for the dc currents via the trailing cable ground wire. Figure 5.1 shows how potentials from the haulage system cause dc to flow in the ground system. This current can damage ground-check monitors and cause extensive corrosion to the ground bed electrodes (57):

### 5.1.2 Rail Haulage

A portion of the rail leakage current enters the grounding system through the contact between mine equipment and the mine floor, thereby setting up a field. The track can be simulated by an infinite number of current generators connected between the earth (same reference point) and various points along the haulage system. Each generator develops a potential depending on its location and the earth resistance. By summing the current from the generators, the equation for rail current as a function of distance (u) is (57):

$$I_R(u) = \frac{I_m}{e^{\alpha \ell} + 1} \left(e^{\alpha \ell} + e^{\alpha(\ell - u)}\right) \tag{5.1}$$

where $\ell$ = length of track
$I_m$ = motor current
and $\alpha$ = leakage factor, given by:

$$\alpha = \sqrt{\frac{\delta}{r}} \tag{5.2}$$

where $\delta$ = longitudinal resistance of track
and $r$ = earth track contact resistance.

The total current flowing into the earth is

$$I_R \text{ max} - I_R \text{ min} = I_{TL} . \tag{5.3}$$

For the case of $I_R$ min which occurs at $u = \ell/2$, the total current is (57):

$$I_{TL} = \frac{I_m (e^{\alpha \ell/2} - 1)^2}{e^{\alpha \ell} + 1} . \tag{5.4}$$

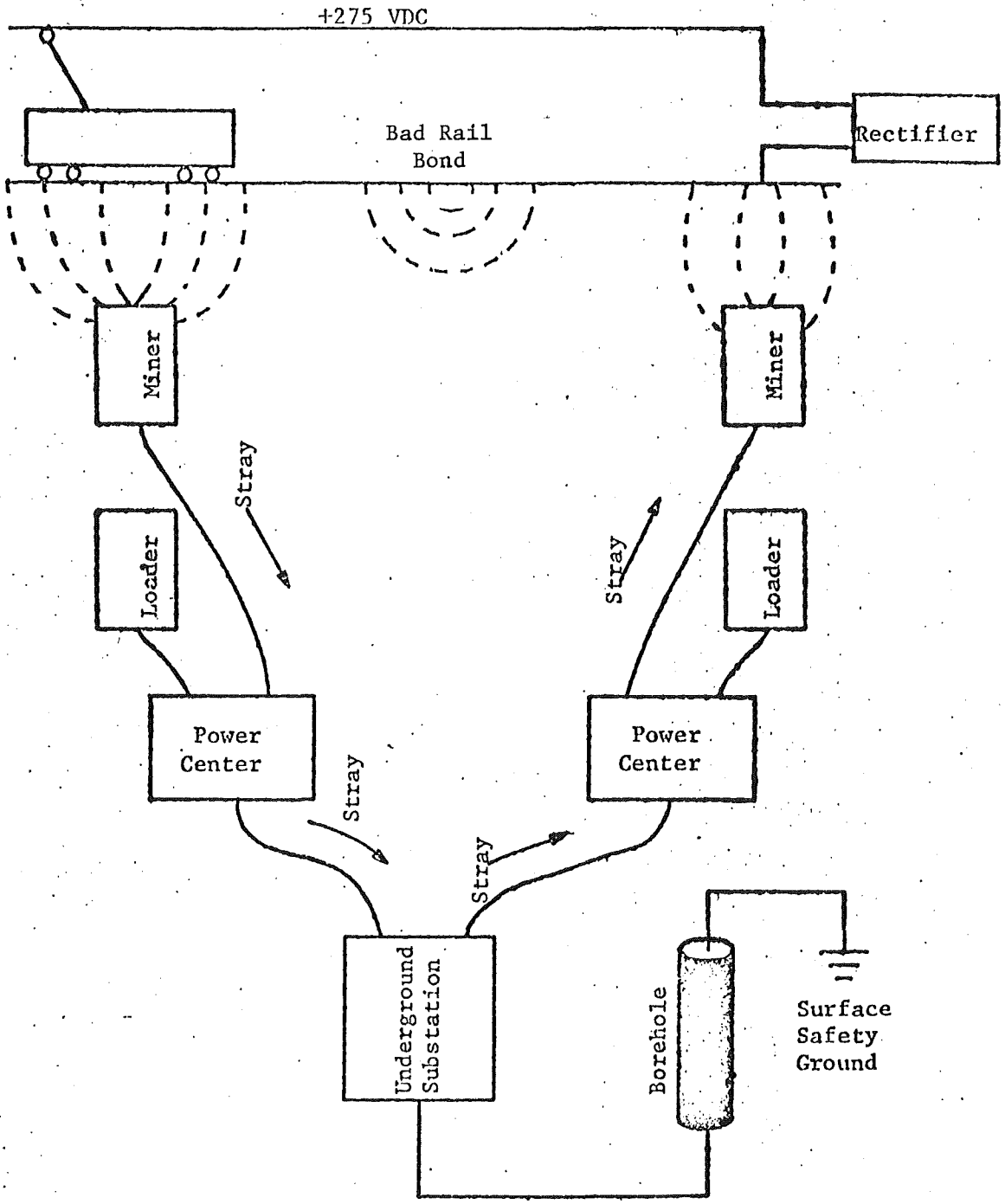


FIGURE 5.1. - Stray dc flow in safety ground system caused by potentials from rail haulage.

Figure 5.2 shows the results of these formulas. For easy field analysis, a computer program for the HP 65 programmable calculator was written (57). Once the equation for track leakage has been found, the field equation for the surrounding earth can be expressed in integral form (57):

$$V = k \int_0^{\ell} \frac{e^{\alpha u}}{\sqrt{u^2 - bu + c}} du \qquad (5.5)$$

The final expression of this equation will vary with the geometry. Figure 5.3 shows a plot of a field where there is a single rectifier at one end of the haulage system and a motor located 304.8 m (1000 ft) from the other end (63).

Several attempts were made to obtain field data for evaluating the track leakage coefficient, $\alpha$. Figure 5.4 shows the cumulative voltage drop versus distance for a section of newly laid track. The uniform voltage is indicative of good rail bonding. It was not possible to evaluate the leakage resistance since an isolated section of track is needed (56) Figure 5.5 shows the voltage drop versus distance foa another section of haulage track. Notice the discontinuity resulting in a nearly vertical line. This was the result of a broken rail bond which, since it provided isolation in the track, enabled the coefficient to be found ($\alpha$=.27). The leakage effect can be accentuated by temporarily opening a pair of opposite bonds on a track segment. This is explained in detail in a previous annual report (3, p. 36).

The following are various methods which may be employed to reduce the leakage factor.

1. Use high quality welded rail bonds.
2. Use heavy-weight rail.
3. Maintain a dry road-bed.
4. Use wooden track ties.
5. Install a track feeder wire.

The stray dc current may also be reduced by moving the safety ground equipment farther from the haulage track or insulating it from the earth (3).

### 5.1.3 Shuttle Car Grounding

The operation of dc shuttle cars and/or dc equipment can also cause significant dc current to flow in the safety ground system. Stray current flow in the ground depends on the method of grounding the dc equipment. There are several methods available for grounding dc shuttle cars which will limit the ground fault current and the machine frame potentials in case of a fault. A two-conductor shuttle car system using a diode connected from one of the conductors to the machine frame is one such method. This method is

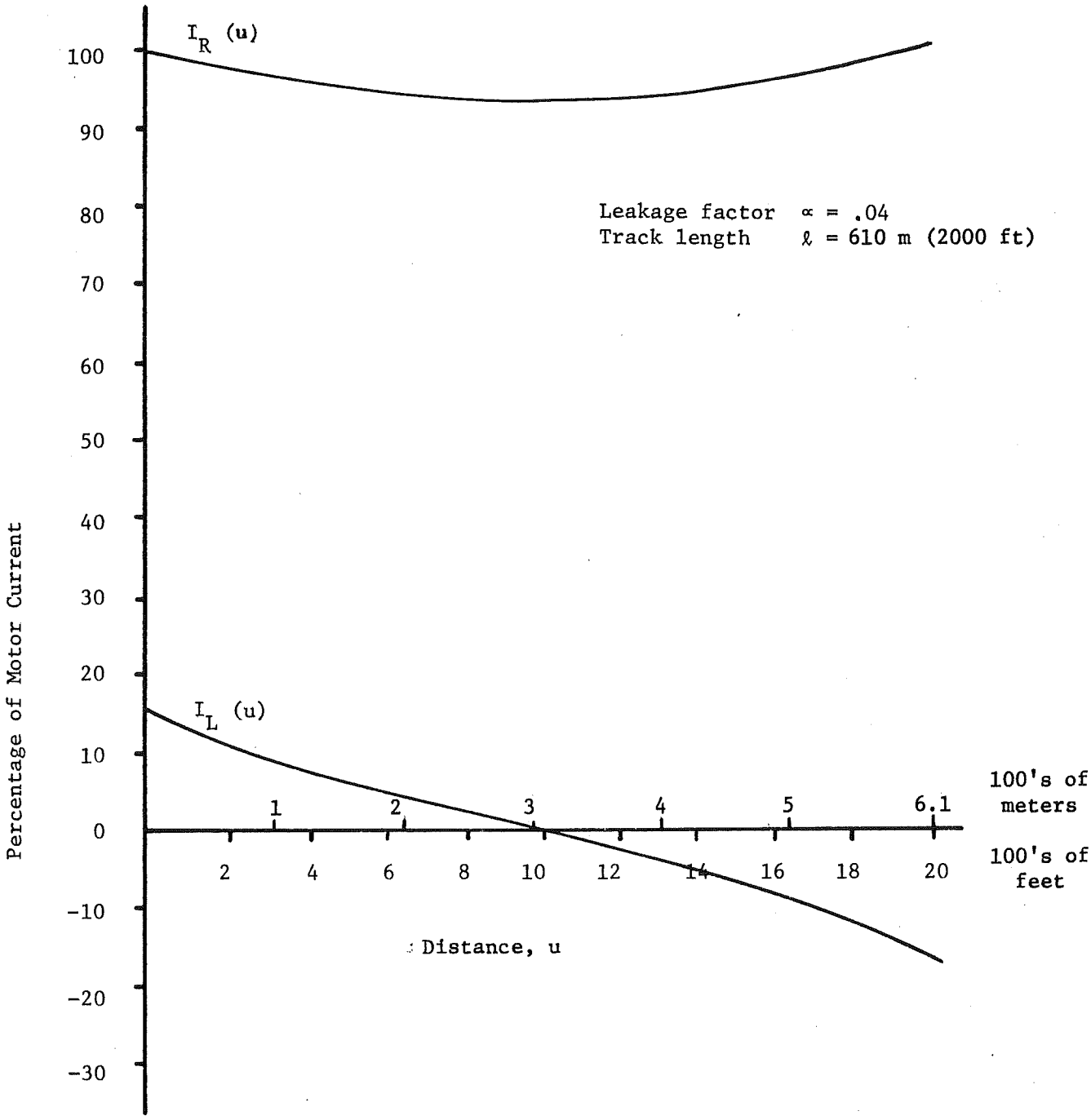


FIGURE 5.2. - Plot of theoretical rail current and leakage current density.

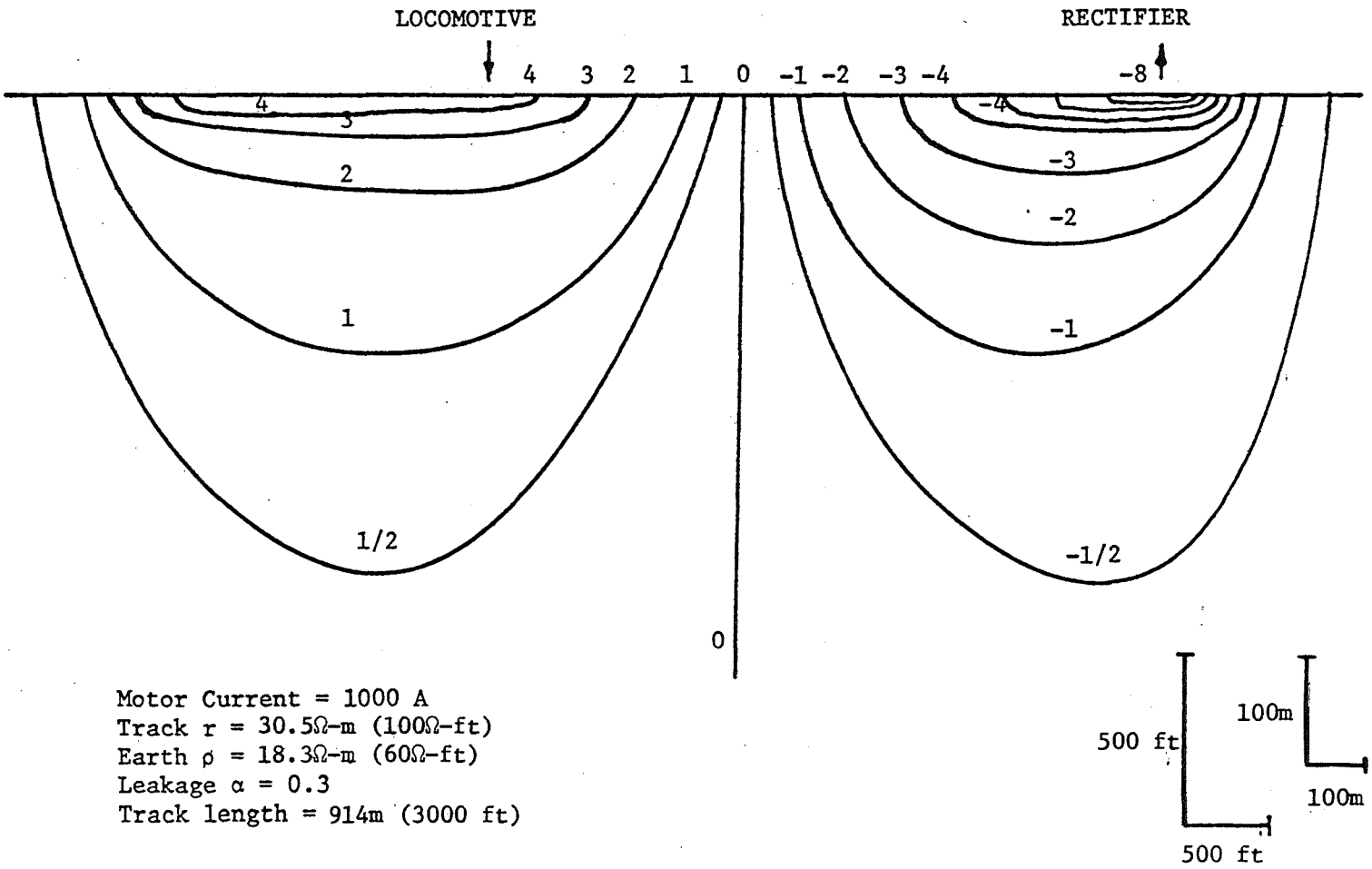


FIGURE 5.3. - Plot of calculated earth voltages.

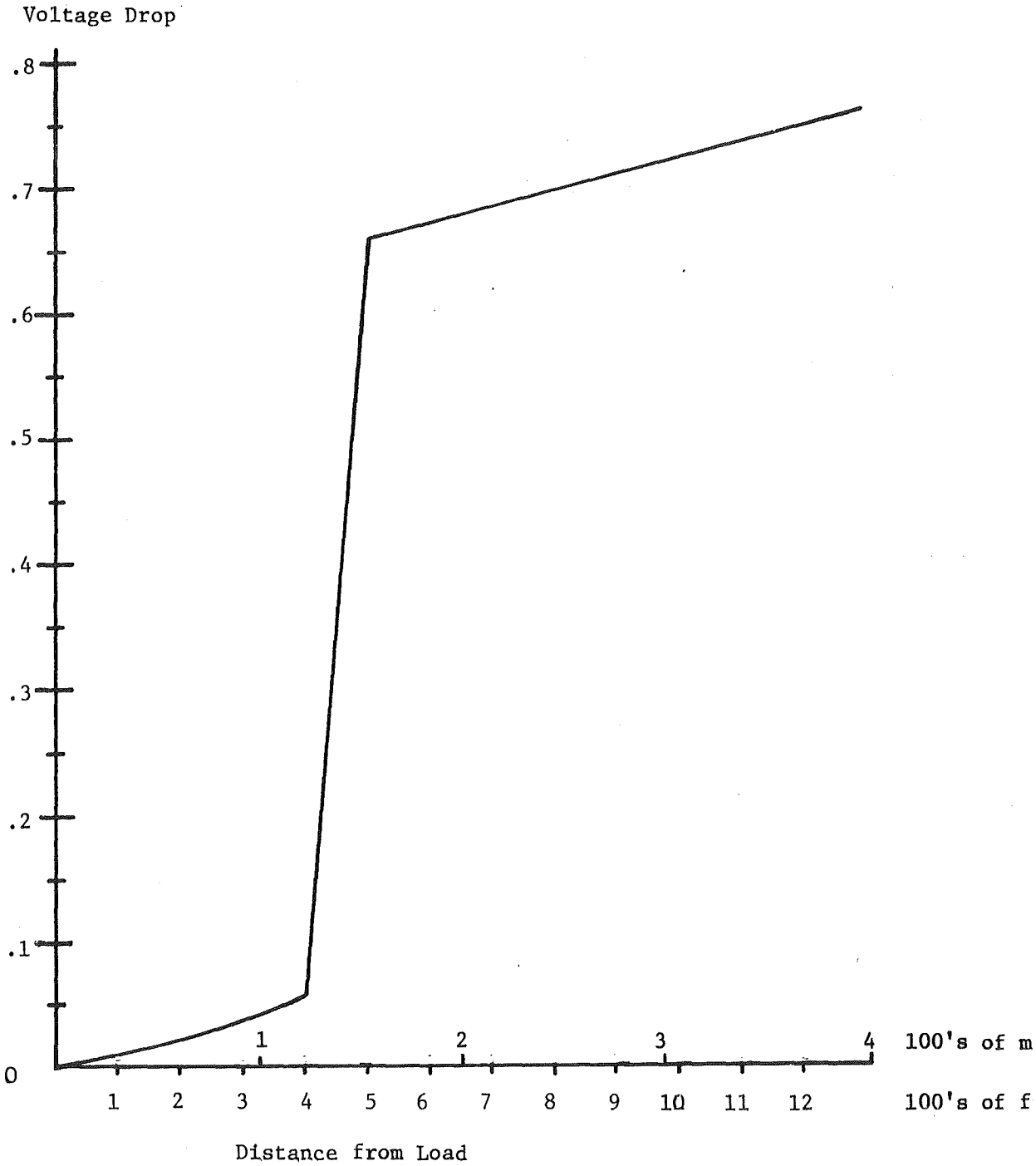


FIGURE 5.4. - Data taken at Shade Gap to determine track leakage coefficient $\alpha$.

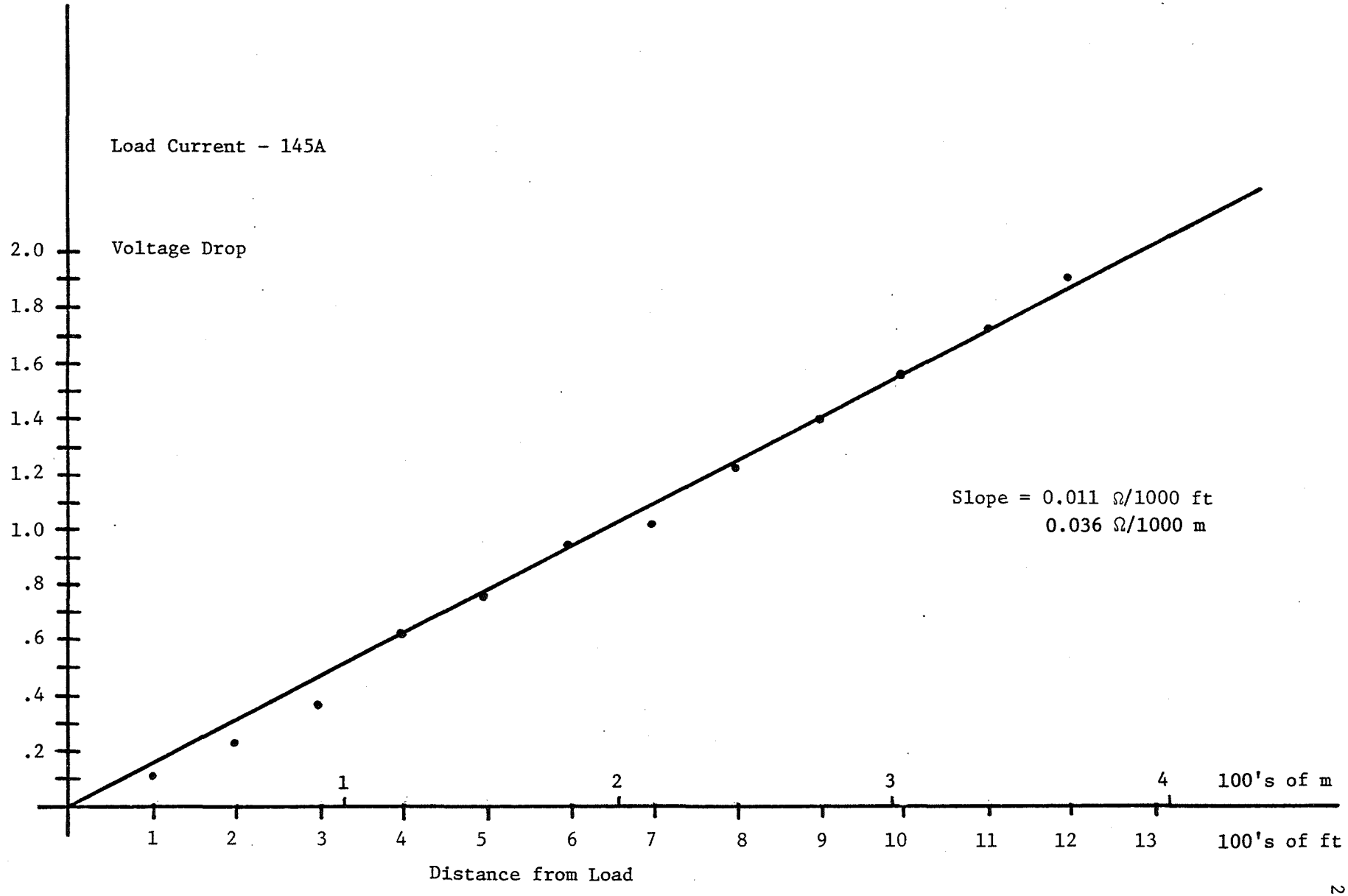


FIGURE 5.5. - Data taken to determine leakage from underground haulage track.

shown in Figure 5.6. This approach has decreased the cost of cabling to the shuttle cars, but has also caused other problems. As the car operates, heavy currents are drawn which cause significant voltage drops in the cable. This drop can amount to several tens of volts during normal operation. Since these cars are often in contact with other equipment, significant ground wire currents can be produced in the cables to the load center or rectifier. Problems also arise if there is an insulation failure on the positive conductors. If there is a short on the shuttle car, heavy current will be drawn and much sparking and burning can occur. The solution to these problems must prevent or detect immediately all short circuits between either of the dc conductors and the machine frame(63).

### 5.1.4 Cables

Another cause of stray currents within the mine grounding system is the power cable through splices, insulation breakdown, or the leakage of insulators for the trolley wires. The magnitude of leakage in a trailing cable with splices has been measured to be as high as 0.528 amperes.

In type G-GC cable, an ac current of 7% of the phase current can be induced into the ground wires in a length of 4/0 cable.

Solutions to these problems can be as easy as changing the type of cable being used, but this trial and error method can prove to be expensive to the mine operator. Another solution can be the use of monitors to check the amount of current which is added to the ground system. Another approach to the problem is to insert a non-linear impedance into the safety ground wire. This will prevent small induced ground currents but allows the heavy current to flow easily(63).

### 5.1.5 Conclusions

Most mines are presently experiencing problems which can be traced to the flow of stray currents within the safety ground system. This report has listed some of the major problem areas and possible solutions.

## 5.2 RAIL BOND RESISTANCE MEASUREMENT

### 5.2.1 Introduction

Previous reports have analyzed the leakage currents from haulage track in great detail(57). This study has shown that leakage currents from the rail can be rather large. These currents have proven to be a big problem for the mine operator, in that they render ground-check monitors inoperative and can possibly cause difficulties with protective relay coordination. The currents may also cause extensive corrosion in the mine's ground bed.

Figure 4.3 shows a possible path for the leakage currents in an underground power system. As can be seen from the figure, one of the possible causes for the leakage currents is a broken or high-resistance rail bond. Many of these defective bonds can be detected with a visual inspection, but this may not indicate if an intact bond has an unacceptably high resistance. Also, many of the bonds may be covered with several inches of coal dust, rock dust, or mud, making a visual inspection very tedious and expensive to the mine operator.

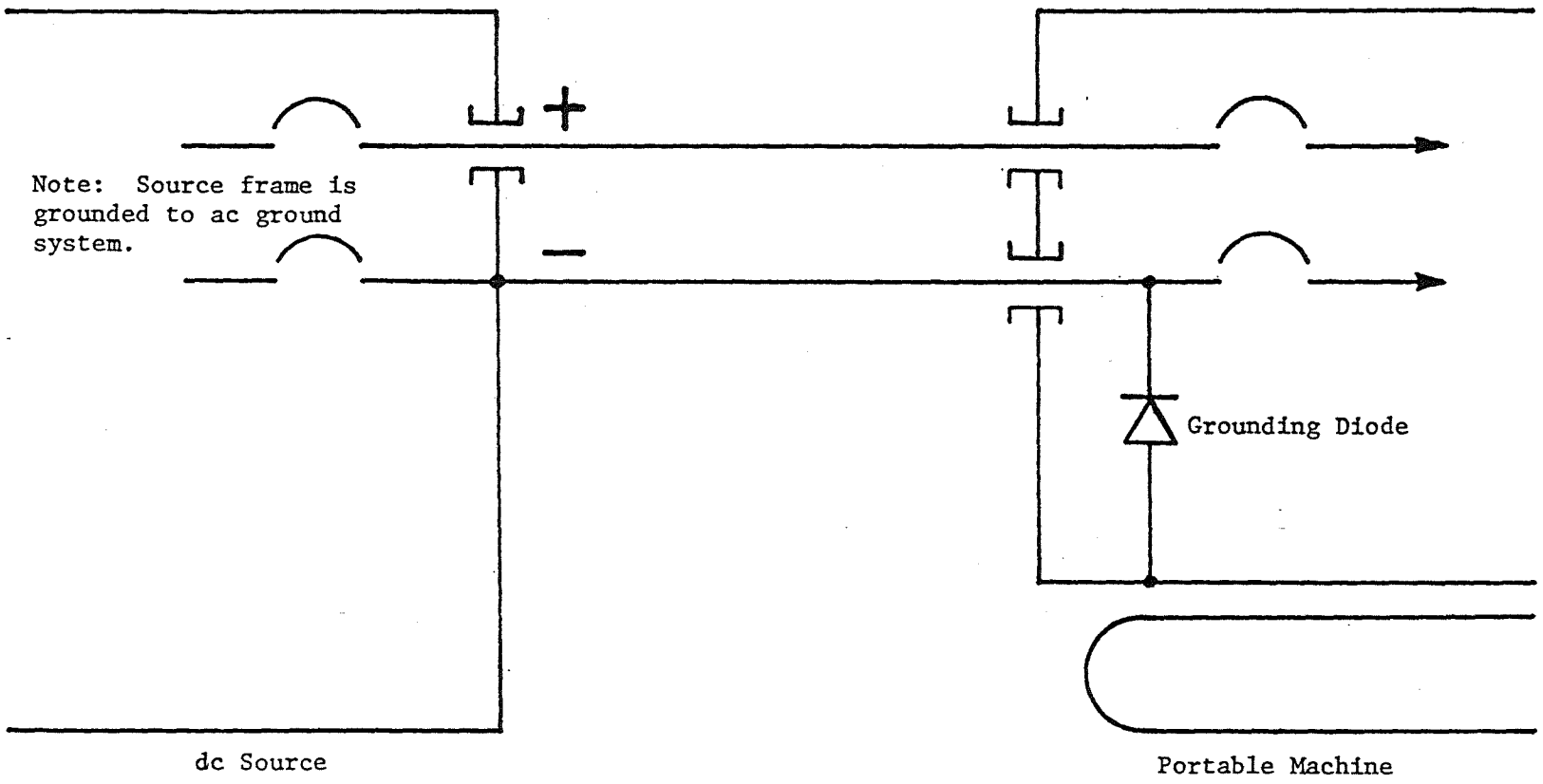


FIGURE 5.6. - Diode grounding for dc systems.

### 5.2.2 Types of Bonds

The purpose of a bond is to maintain a low-resistance contact between adjacent rail ends that will withstand the constant pressure of cars passing over the rail joints and permit expansion and contraction of the rail due to temperature changes. Presently there are three ways of bonding the track:

1. Direct weld - Whether an arc or thermit weld, this method provides a permanent connection between the two sections of rail. The direct weld provides a good physical contact, yielding a low-resistance path for the current to flow through.

2. Adhesive chemical bond - Consisting of an epoxy resin paste, the chemical bond immobilizes the rail ends at the joint. To be effective, the rails must be cleaned and sanded so that when the epoxy sets, the mechanical connection between rails will provide a low-resistance path. The epoxy also fills the voids and aids in making the joint moisture-proof. Chemical bonds are used most often where conditions prohibit a direct weld.

3. Wire rail-bond - This type consists of a 2/0 or 4/0 wire cable, usually 76 cm (30 in) in length, which is welded to each rail across the connection of the rail joint. When the bond is in place its length is shortened to 61-66 cm (24 to 26 in).

The wire bond is the most common method used today. The direct weld and chemical adhesive bonds tend to be used on sections of track which are considered as a permanent installation or in a section of the mine where a retreat is not being planned. The direct weld and chemical adhesive bonds, however, are most affected by expansion and contraction due to temperature changes and the pressure and vibration of cars passing over the rail joints.

Cross bonds, which are wire bonds interconnecting the two parallel track sections, are placed at approximately every 60m (200 ft). These bonds aid in keeping both sides of the haulage track at the same potential. Cross bonds also insure that the return conductor or section of track will not be separated from the rectifier, which would occur if a bond were to break between a section and the rectifier.

Table 5.1 gives the electrical characteristics of the rail and the rail joint.

TABLE 5.1. Electrical Characteristics of Haulage Rail

| Weight of Rail | | Resistance | | Resistance of Unbonded Joints |
|---|---|---|---|---|
| lbs/yd | lb/m | Ω/1000 ft | Ω/1000 m | Ω |
| 30 | 32.8 | 0.018 | 0.059 | 0.072 |
| 40 | 43.7 | 0.0135 | 0.0443 | 0.054 |
| 50 | 54.7 | 0.0108 | 0.0354 | 0.0432 |
| 60 | 65.6 | 0.009 | 0.0295 | 0.036 |
| 70 | 76.6 | 0.0077 | 0.0253 | 0.0308 |
| 80 | 87.5 | 0.0067 | 0.022 | 0.0268 |
| 90 | 98.4 | 0.006 | 0.0197 | 0.024 |
| 100 | 109.4 | 0.0054 | 0.0177 | 0.0216 |

A copper bond of 4/0 wire has a resistance of 0.171Ω/1000m (0.052Ω/1000 ft) (1). From this the resistance of a 76.2 cm (30 in) rail bond can be determined:

$$\frac{0.171\ \Omega}{1000\ \text{m}} \times 0.762\ \text{m} = 0.13\ \text{m}\Omega$$

By placing the rail bond across a rail joint for a 30 lb rail, the total resistance of that joint is calculated to be:

$$\frac{0.13\ \text{m}\Omega \times 0.072\ \Omega}{0.13\ \text{m}\Omega + 0.072\ \Omega} = 0.129\ \text{m}\Omega.$$

The resistance of a cross bond of 1.219m (48 in) of 4/0 wire is:

$$\frac{0.171\Omega}{1000\ \text{m}} \times 1.219\ \text{m} = 0.208\ \text{m}\Omega$$

and a 3.66m (12 ft) section of 30 lb track has a resistance of:

$$\frac{0.059\Omega}{1000\ \text{m}} \times 3.66\ \text{m} = 0.216\ \text{m}\Omega.$$

The track haulage can be modeled as shown in figure 5.7, where the admittance, Y, is equivalent to a cross bond with a resistance of 0.208 mΩ. The track resistance, along with the joints and bonds every 3.44 m (12 ft), is indicated by the impedance $Z_A$, and $Z_A'$ corresponds to the parallel section of track. With 3.66 m sections, approximately 16 sections of track are used to derive each 61 m (200 ft) run where cross bonding occurs. The impedance $Z_A$ and $Z_A'$ can thus be calculated as:

$$16(0.216 + 0.129)\ \text{m}\Omega = 5.68\ \text{m}\Omega.$$

The equivalent resistance, $Z_T$, is found by the following equation (equate $Z_A = Z_A'$):

$$Z_T = 2Z_A + \cfrac{1}{Y_A + \cfrac{1}{2Z_B + \cfrac{1}{Y_B + \cfrac{1}{2Z_C + \cfrac{1}{Y_C}}}}} \qquad (5.6)$$

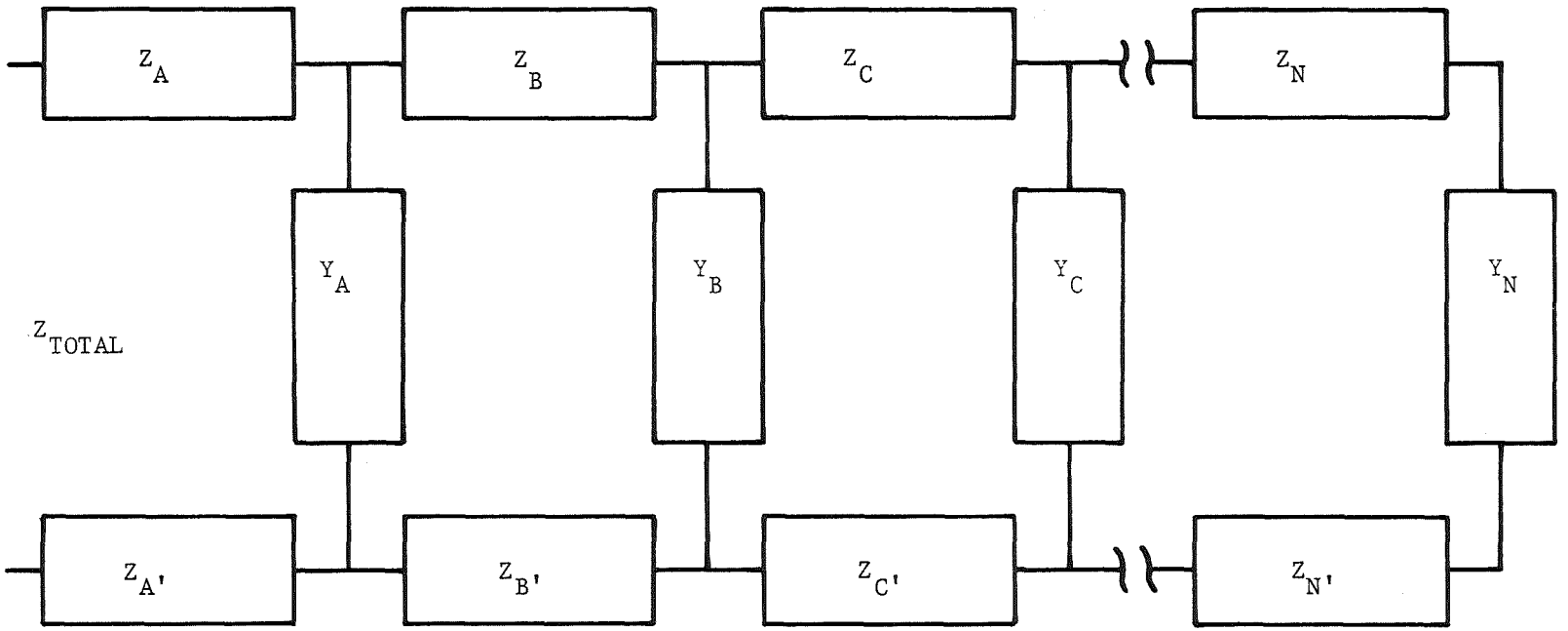


FIGURE 5.7. - Model of track haulage system.

By substituting in the values for the resistance of the track section and cross bonds which were calculated above, the total impedance for the 183 m (600 ft) section of track is 11.564 mΩ.

Figure 5.7 also shows how cross-bonding helps in maintaining a low-resistance path for the return current. Assume that a bond in the section, represented by $Z_B$, is broken. The arrows indicate that the flow of current does not pass through $Z_B$ yet but does pass through $Z_A$ and $Z_C$. The current passes from $Z_C$ through $Y_B$, $Z_B'$, and $Y_A$ to reach $Z_A$. This situation will never exist on actual haulage back, since an open bond in section $Z_B$ will not completely open the circuit at that point, but will only increase the resistance by 72 mΩ (to that of an unbonded joint).

Though figure 5.7 allows examination of track, joint, and cross bond impedances, it does not take into account the parallel path. Since the rails of the track are not electrically insulated from the mine floor, the earth on which the track is laid acts as an electrical shunt to the rails. Since the electrical conductivity of the earth is greatly increased by moisture which is found in the mines, some of the current flowing in the rails may at various points be diverted from the rails to the mine floor. The probability of diverting these currents into the ground will be greatly increased where the resistance of the track is high, that is, at points where a good low-resistance path between rails is not maintained.

### 5.2.3 Circuitry

From the calculations above, it can be seen that the resistance to be detected is very small (0.129 mΩ), but that there is a relatively large difference between a bonded and unbonded joint. With this large difference in mind, an attempt was made to develop electronic circuitry which, when transported down the track, would measure the resistance of each joint. The output of this circuitry will drive a display unit which will show the bonded joint resistance, and an alarm which will sound when the joints' resistance is above a predetermined limit.

Since the haulage rail is used as the return conductor to ground, it will contain alternating as well as direct currents. A major design requirement was that the haulage system should not have to be disconnected in order to allow measurement of the track's rail bonds. This requires that the measurement circuitry be immune to any current which might be present within the rails. This current will constantly be changing in magnitude and direction depending upon the equipment being operated at that time. For this reason a constant current source which uses a prime frequency to reduce interference from harmonics and sub-harmonics of 60 Hz is used. A 41 Hz sine wave signal is developed from an 8038 function-generator integrated circuit and passed through a buffer to prevent loading of the oscillator circuit. This signal is then placed into a constant current source, utilizing class B amplification. The output of the amplifier, which is capable of driving approximately one ampere, is passed through a transformer to two current electrodes which are in contact with the rail. The transformer is used to boost the current applied to the rails.

The voltage which is picked off the rail via the two voltage electrodes is passed through a low-pass filter with a corner frequency of 52 Hz. This is done to reduce the 60 Hz signals which will be present on the track and allow passage of the 41 Hz signal generated by the system. This input filter also contains some transient suppression to protect the sensitive electronic circuitry against power surges present on the track. The filtered voltage is then amplified and passed into the synchronous detector.

The detector operates by synchronous rectification of the signal to be detected. This is accomplished by effectively multiplying the input signal, along with its noise and interference, by a pure signal of the same phase as the operating frequency. This pure signal is derived from the circuit's oscillator and is passed through a phase shifter which will allow for any change in phase which may occur in the signal being passed to the rail. The multiplication of signals causes full wave rectification of the signal which is desired and cancels the low frequency interference (the high frequencies are attenuated by the input filter). This cancellation of low frequency occurs because the change in amplitude of a low frequency signal during a half cycle of the higher frequency signal (41 Hz) is so slight, that multiplication by the higher frequency signal produces zero output for a low frequency input. If the injected signal frequency (41 Hz) is present along with the low frequency interference, the synchronous rectifier will still produce a full wave rectified output of the injected signal.

The rectification is achieved by inputting the filtered voltage to a pair of analog switches. The pure signal (after phase shifting) is fed into two zero-crossing detectors. The control signals from these detectors operate the analog switching array synchronously with the incoming signal. The output of one switch is passed to an inverting amplifier while the other output is fed to a non-inverting amplifier. The invert/non-invert characteristic thus generates the synchronous rectification. These amplifiers are then summed and fed into a low-pass filter with a corner at 0.8 Hz to yield only a dc output which corresponds to the incoming signal from the rail which was detected.

The dc output is then passed to a comparator which allows the operator to set a range point at which an alarm or indicator can show when the output voltage is above this preset level. The output of the filter is also scaled and is input to a 3-1/2 digit voltmeter. The voltage is used to indicate the resistance of the bond being measured. Figure 5.8 is a block diagram of the bond detection circuitry.

A four-probe method is used to inject the current and measure the voltage from the rail. The four electrodes, or in this case wheels, are set up on a cart which is shown in figure 5.9. The inner two wheels are to measure the voltage across the bond, and are spaced far enough apart to allow the entire bond to be between them. The outer two electrodes are used to inject the current into the rail. A piece of V-shaped stainless steel is used to make contact between the wheels and the electronic circuitry. A spring pivot joint is placed at each end of the cart to allow for changes in the track heights at the rail joint, while keeping all four electrodes in contact with the rail.

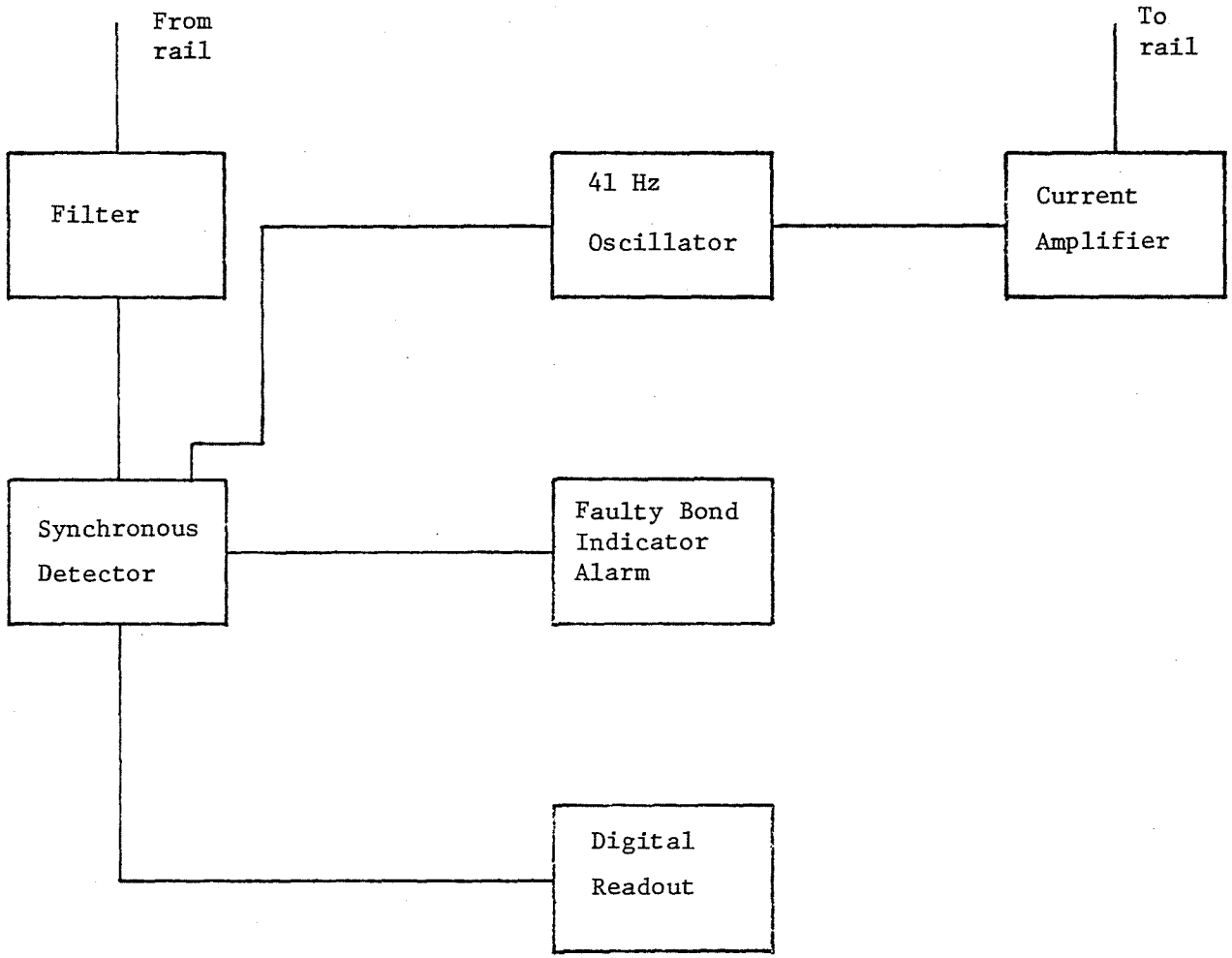


FIGURE 5.8. - Block diagram of the bond detection circuitry.

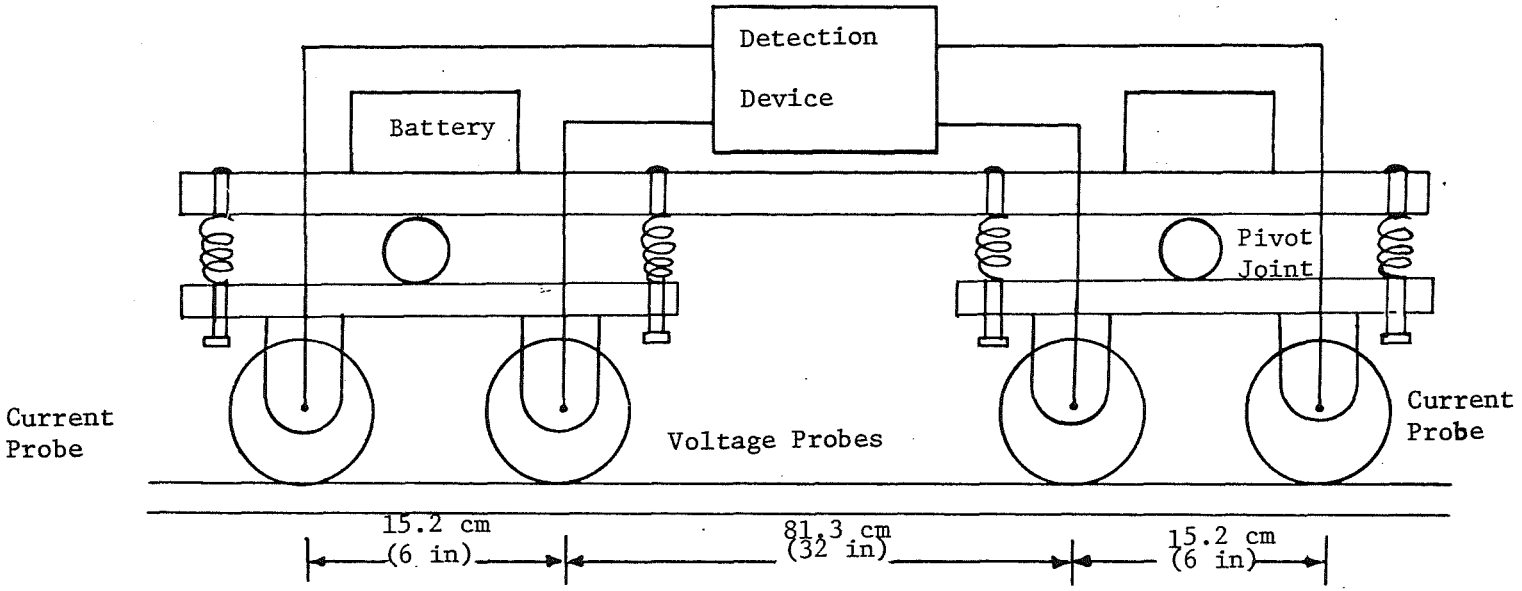


FIGURE 5.9. - Cart carrying the Broken Bond Detector.

All electronic circuitry is mounted on printed circuit cards and is housed in a NEMA standard enclosure along with the current transformer and alarm circuits. Since the amplifiers within the circuitry require both positive and negative supplies, two 12 volt automotive batteries are mounted on the cart for the power supply and weight (4).

## 5.3 SOURCES OF STRAY AC CURRENTS

As discussed in a previous annual report, "Mine Grounding Systems: Evaluation of In-Mine Grounding System and Codification of Ground Bed Construction and Measurement Techniques", dated November 16, 1977 (58), one source of stray alternating currents in mine power systems is the leakage of phase current into the mine floor and hence the safety ground system via splices in trailing cables. Figure 5.10 illustrates this situation diagramatically. The research showed that, for a wide variety of cables which were tested under simulated mine conditions, the magnitude of the leakage current is proportional to the relative humidity. In addition, current leakage increased with the number of splices in the trailing cable. Figure 5.11 depicts both of these conditions. In-mine monitoring showed that the magnitude of the leakage current varied directly in step with the level of phase current, which supports the premise that the leakage actually does occur through the trailing cable splices.

## 5.4 CABLE SPLICE RESISTANCE

Since this work was covered in an earlier report (58), it will be summarized here. The resistance of a trailing cable splice was found to vary between 4 and 21 milliohms, depending mainly on the quality of the components in the splice kit and the care with which the splice was made. Temperature measurements were made on cable splices while under full-load conditions, and the cable temperature was found to vary directly as a function of the splice resistance. Figure 5.12 shows the temperature profile for a high-quality, low-resistance splice, while figure 5.13 displays the marked increase in temperature which can be found at a badly-made cable splice. The high-resistance connections which characterize poor splices can be quickly detected by temperature measurements as shown in these figures. If not a premature cable failure or possibly a fire, with its concomitant hazard of explosion.

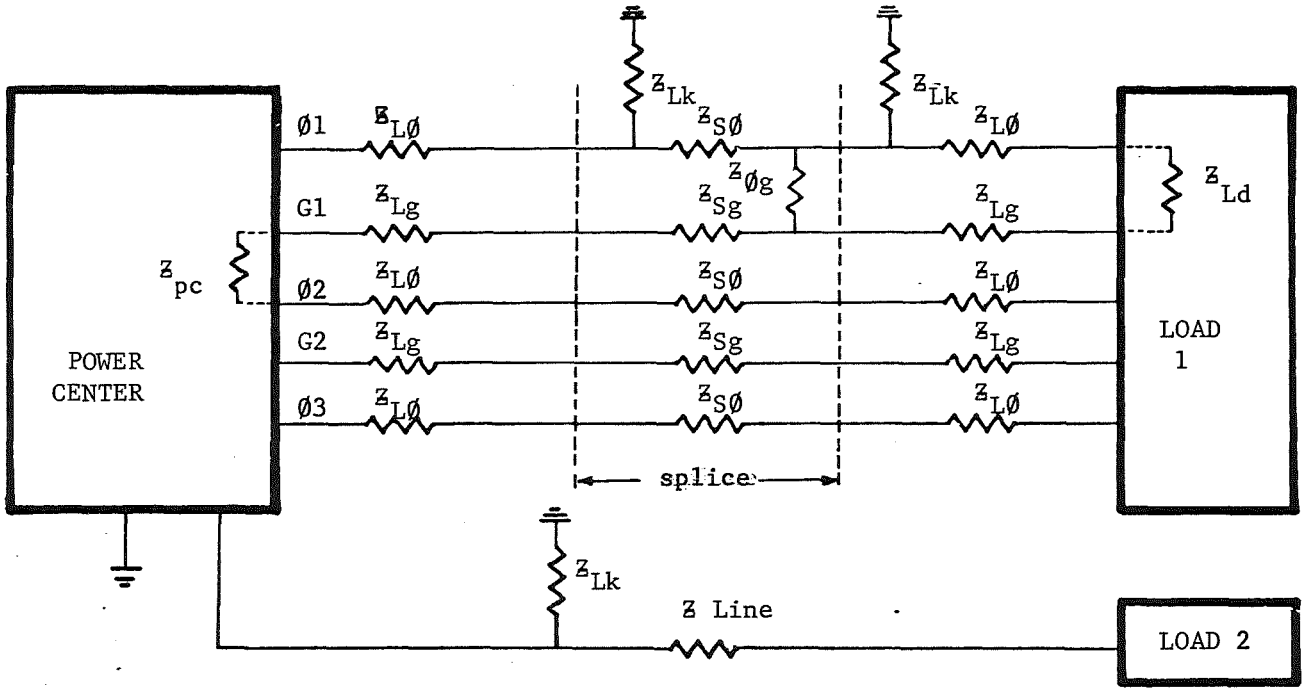


FIGURE 5.10. - Diagram of power distribution system on a mine section showing current leakage paths through a trailing cable splice.

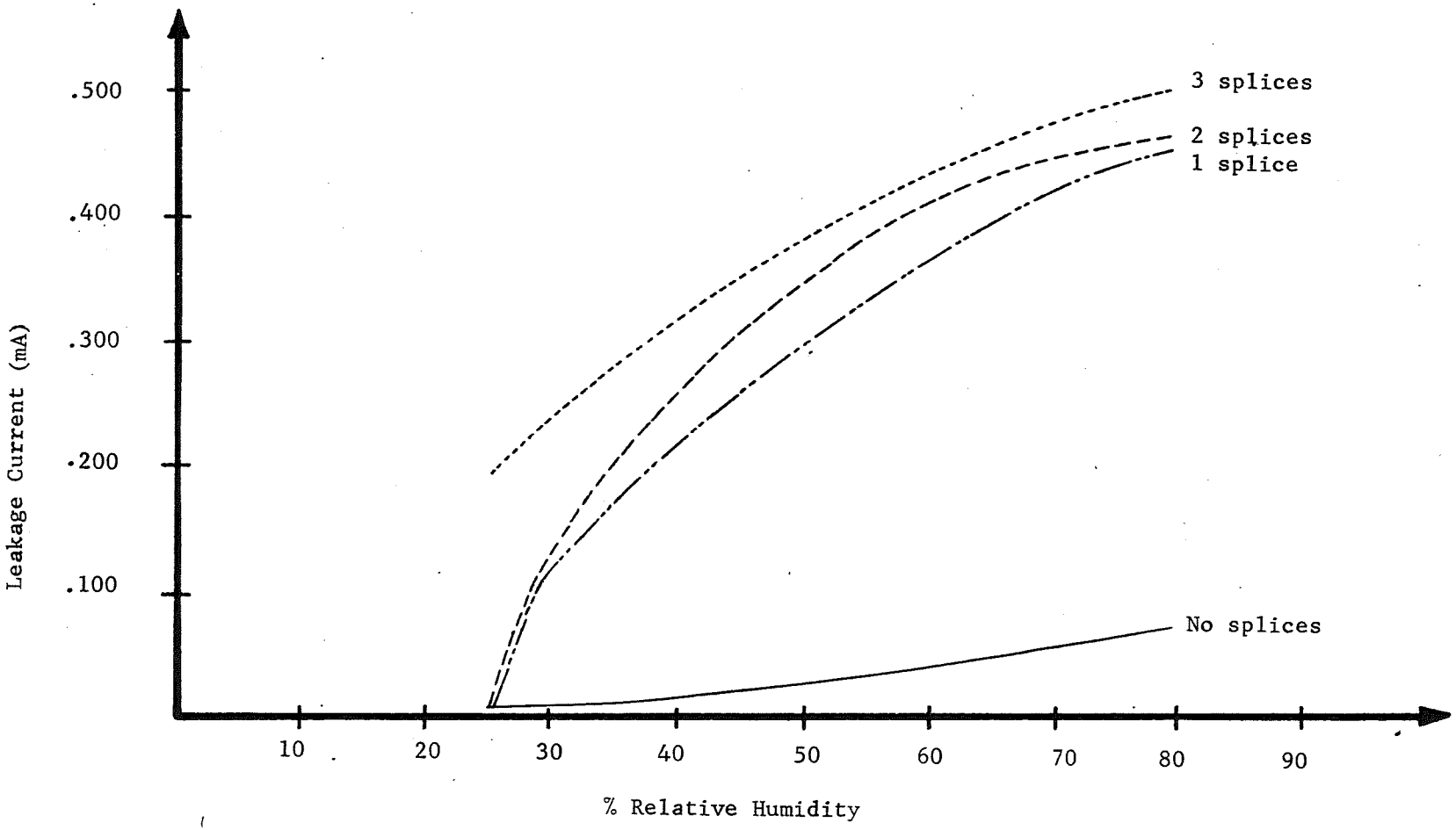


FIGURE 5.11. - Graph showing leakage current in a trailing cable as a function of the relative humidity and the number of splices in the cable.

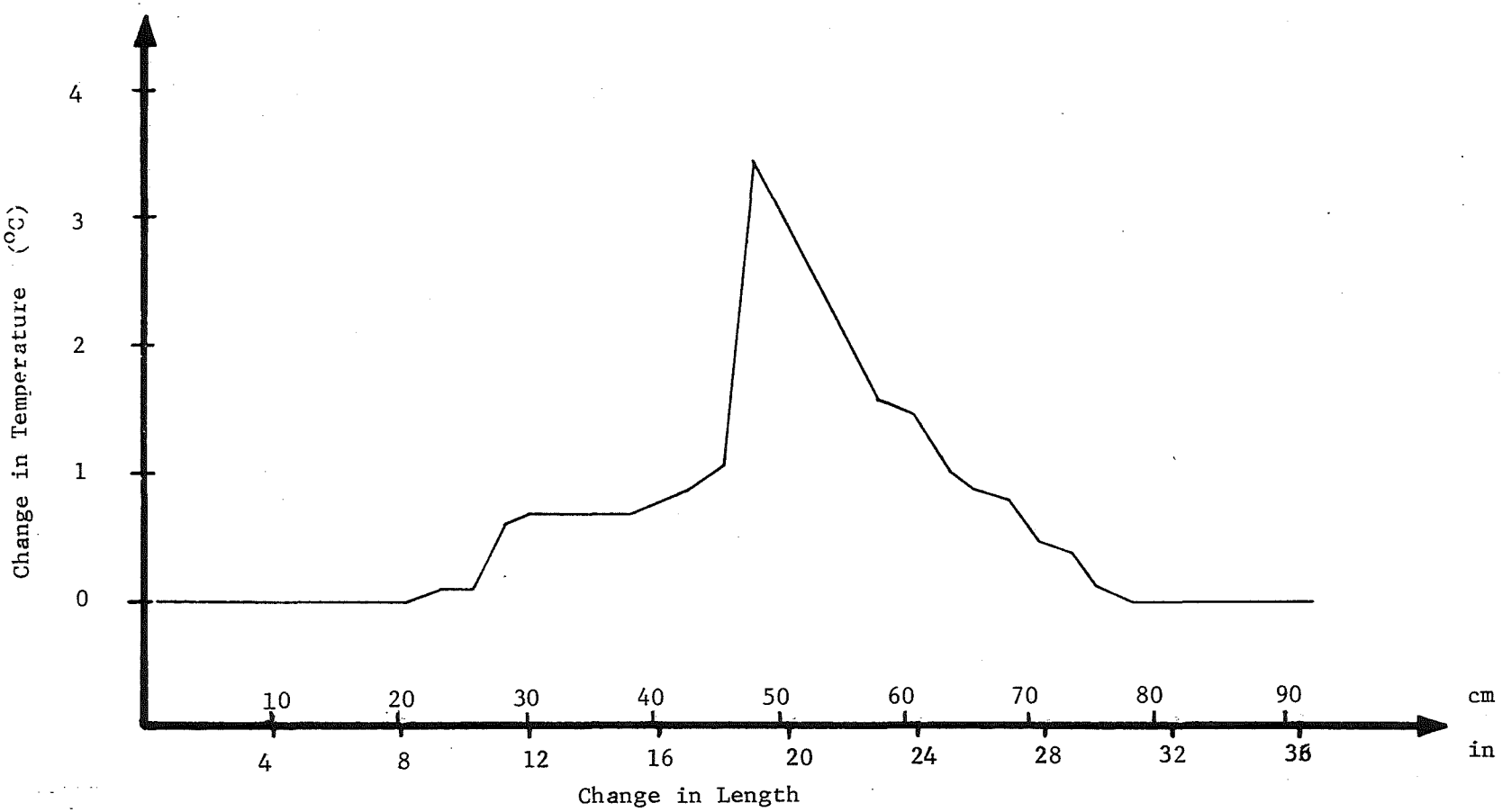


FIGURE 5.12. - Temperature profile along a good trailing cable splice.

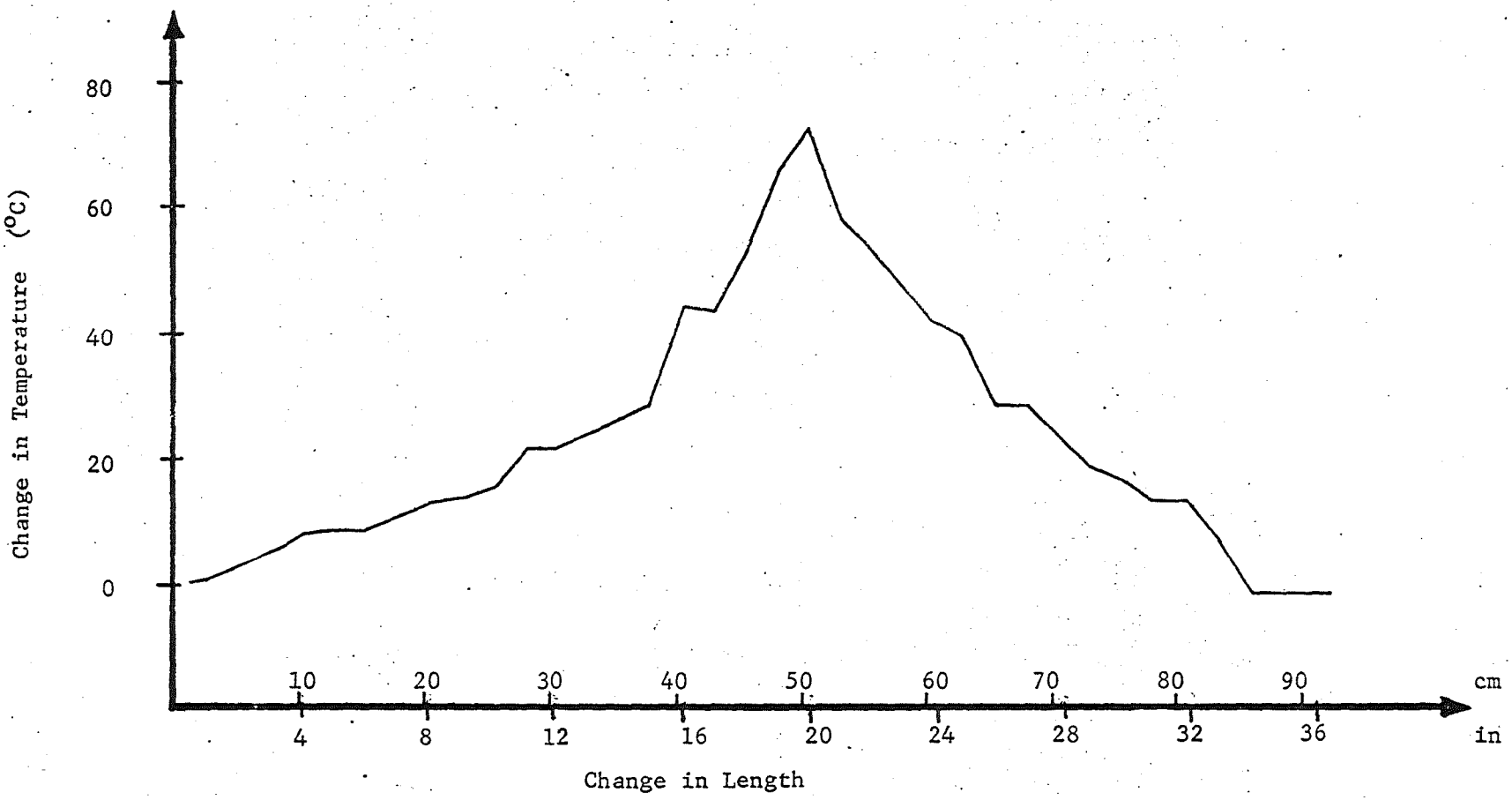


FIGURE 5.13. – Temperature profile along a bad trailing cable splice.

REFERENCES

1. Anaconda Mining Cable Data Book. August 1977, Section 1.

2. Bellashi, P. L. Impulse and 60-Cycle Characteristics of Driven Grounds. AIEE Transactions, March, 1941, pp. 123-128.

3. Bellashi, P. L., R. E. Armington, and A. E. Snowden. Impulse and 60-Cycle Characteristics of Driven Grounds - II. AIEE Transactions, 1942, pp. 349-363.

4. Brereton, D. S., and H. N. Hickok. System Neutral Grounding for Chemical Plant Power Systems. AIEE Transactions on Applications and Industry, November, 1955, p. 315.

5. Christman, A. M., W. L. Cooley, and H. W. Hill. Remote Grounding of Large Surface Electrical Equipment. Proceedings of Fourth WVU Conference on Coal-Mine Electrotechnology, August, 1978, pp. 11-1 to 11-10.

6. Cooley, W. L. Design Considerations Regarding Separation of Mine Safety Ground and Substation Ground Systems. Conference Record of IEEE Industry Applications Society Annual Meeting, 1977, pp. 976-981.

7. Costanzo, F. E. Using Graphite as Impressed Current Anode for Deep Groundbeds. Material Protection, v. 9, No. 4, April, 1970, pp. 26-32.

8. Davis, R., and J. E. M. Johnston. The Surge Characteristics of Tower and Tower-Footing Impedances. IEEE Journal, London, v. 88, 1948, pp. 453-465.

9. Dunki-Jacobs, J. R. The Effects of Arcing Ground Faults on Low-Voltage System Design. IEEE Transactions on Industry Applications, May-June, 1972, pp. 223-230.

10. Eaton, J. R. Impulse Characteristics of Electrical Connections to the Earth. General Electric Review, v. 47, October, 1944, pp. 41-50.

11. Fagan, E. J., and R. H. Lee. Use of Concrete-Encased Reinforcing Rods as Ground Electrodes. IEEE Transactions on Industrial and General Applications, v. IGA-6, No. 4.

12. Fink, C. G. Catalytic Electrolytic Generation of Oxygen. Industrial and Engineering Chemistry, v. 6, No. 6, June, 1924, pp. 566-567.

13. Fox, F. K., H. J. Grotls, and C. H. Tipton. High Resistance Grounding of 2400 Volt Delta Systems with Ground Fault Alarm and Traceable Signal to Fault. IEEE Transactions on Industry and General Applications, September-October, 1965, pp. 366-372.

14. General Electric Company. Evaluation and Feasibility Study of Isolated Electrical Distribution Systems in Underground Coal Mines. National Technical Information Service, Springfield, VA, April, 1972, pp. 1-127.

15. Gienger, J. A. Fourteen Years of Data on the Operation of One Hundred Ungrounded 240 and 480 Volt Industrial Distribution Systems. IEEE Transactions on Industry and General Applications, March-April, 1966, pp. 147-150.

16. Graeme, J. D., G. E. Tobey, and L. P. Huelsman. Operational Amplifiers, Design and Applications. McGraw-Hill, New York, 1971.

17. Greenspan, D. Discrete Numerical Methods in Physics and Engineering. Academic Press, Inc.

18. Hill, H. W. Design and Measurement of Driven-Rod Ground Beds. Unpublished M.S. Thesis, West Virginia University, 1977, p. 49.

19. Holliday, R. L. Private Interview, Morgantown, WV, February, 1976.

20. Husuck, B. Use of Pipe to Soil Potential in Analyzing Underground Corrosion Problems. Corrosion, v. 17, No. 8, August, 1961, pp. 97-101.

21. Industrial and Commerical Power Systems Committee. IEEE Recommended Practice for Grounding of Industrial and Commerical Power Systems. IEEE, New York, 1972, pp. 1-95.

22. Jung, W. C. IC Op-Amp Cookbook, Howard W. Sams and Co., Indianapolis, Indiana, 1974.

23. Kaufmann, R. H. Important Functions Performed by an Effective Equipment Grounding System. IEEE Transactions on Industry and General Transactions, November-December, 1970, pp. 545-552.

24. Keller, G. V. and F. C. Frischknecht. Electrical Methods in Geophysical Prospecting. Pergamon Press, NY, 1966.

25. Kimbark, E. W. DC Transmissions. John Wiley and Sons, Inc., NY, v. 1, 1971, p. 426.

26. King, R. L., H. W. Hill, Jr., R. R. Bafana, and W. L. Cooley. Guide for the Construction of Driven-Rod Ground Beds. U.S. Bureau of Mines, IC 8767, 1978.

27. Krauss, J. D., and K. R. Carver. Electromagnetics. McGraw-Hill, New York, 1973.

28. Krautkramer-Branson, Inc. Ultrasonic Flaw Detector USM-2. Technical Pamphlet, Krautkramer-Branson, Inc., Stamford, CT.

29. Library Programme: Laplace's Equation - LPLACE, LPLACD. University of Waterloo Computing Center.

30. Lordi, A. C. How to Safety Ground Mine Power Systems. Coal Age, v. 68, September, 1963, pp. 110-117.

31. McCoy, W. J. Cable and Some of Their Effects on the Safety Ground System. Unpublished M.S. Thesis, West Virginia University, 1977, pp. 65-95.

32. Merritt, R. P. Measurement of the Auroral Induced Current in the Trans-Alaska Pipe Line. Paper presented at the 1977 Energy Technology Conference and Exhibition, Houston, TX, September 18-23, 1977, pp. 1-3.

33. Millman, J., and C. Halkias. Integrated Electronics. McGraw-Hill, New York, 1972.

34. Monfore, G. W. Electrical Resistivity of Concrete. Journal of P.C.A. Research and Development Laboratory, v. 10, No. 2, 1968, pp. 35-48.

35. Motorola Semiconductor Data Library. Linear Integrated Circuits. v.6, Series A.

36. N.A.C.E. Laboratory Corrosion Testing of Metals for the Process Industries. N.A.C.E. Standard TM-01-69, N.A.C.E., Houston, TX, August, 1972.

37. National Semiconductor. Linear Integrated Circuits Data Book. February, 1975.

38. Orellana, E., and H. M. Mooney. Master Tables and Curves for Vertical Electrical Sounding Over Layered Structures. Interciencia, Madrid, 1966.

39. Ott, H. W. Noise Reduction Techniques in Electronic Systems. John Wiley and Sons, NY, 1976, p. 209.

40. Petropoulos, G. M. The High Voltage Characteristics of Earth Resistances, IEEE Journal, London, v. 95, 1948, pp. 59-70.

41. Regotti, A. A., and H. S. Robinson. Charging Concepts and Equipment Applied on Grounded Low-Voltage Systems. IEEE Transactions on Industry Applications, May-June, 1972, pp. 231-236.

42. Samsonov, G. V. The Oxide Handbook. IFI/Plenum, NY, 1973, pp. 320-329.

43. Shreir, L. L. Metal/Environment Reactions. Corrosion, v. 1, Newness-Butterworth, London, 1977, pp. 1-4.

44. Sidwell, R. J. Ultrasonic Gauges in Corrosion Control. Anti-Corrosion Methods and Materials, v. 19, No. 6, June, 1972, pp. 4-9.

45. Silva, J. L. Letter, Krautkramer-Branson, Inc., Stamford, CT, November 20, 1975.

46. Smith-Rose, R. L. Electrical Measurements on Soil with Alternating Currents. IEEE Journal, London, v. 75, 1934, pp. 221-237.

47. Sunde, E. D. Earth Conduction Effects in Transmission Systems. Van Nostrand, New York, 1949, pp. 67-97.

48. Tagg, G. F. Earth Resistances. Pittman Publishing Corporation, London, 1964, pp. 1-258.

49. Tagg, G. F. Resistance of Large Earth-Electrode Systems. Proceedings IEE, v. 119, No. 2, February, 1972, pp. 269-272.

50. Texas Instruments. Power Data Book. First Edition, 1977.

51. Texas Instruments. Transistor and Diode Data Book, 1973.

52. Towne, H. M. Impulse Characteristics of Driven Grounds. General Electric Review, v. 31, November, 1928, pp. 605-609.

53. Uhlig, H. H. Corrosion and Corrosion Control. John Wiley and Sons, Inc., NY, 1971, 2nd Edition, pp. 42-46.

54. Uman, M. A. Lightning. McGraw-Hill, New York, 1960, pp. 1-17.

55. U.S. Bureau of Mines. Code of Federal Regulations, Title 30. 1974, p. 387.

56. U.S. Bureau of Mines. Evaluation of Ground Beds and Ground Bed Monitors and Evaluation of Modular Ground Wire Monitor. Annual Report, USBM Grant No. GO144138, West Virginia University, May 6, 1977.

57. U.S. Bureau of Mines. Evaluation of In-Mine Grounding System and Codification of Ground Bed Construction and Measurement Techniques. Annual Report, USBM Grant No. GO144138, West Virginia University, August 1, 1975, 263-119/AS.

58. U.S. Bureau of Mines. Evaluation of In-Mine Grounding System and Codification of Ground Bed Construction and Measurement Techniques. Annual Report, USBM Grant No. GO144138, West Virginia University, November 16, 1977.

59. U.S. Bureau of Mines. Mandatory Safety Standards, Surface Coal Mines and Surface Work Areas of Underground Coal Mines. Federal Register, v. 36, No. 100, Part II, May 22, 1971, pp. 9364-9385.

60. U.S. Bureau of Mines. Statistical Evaluation and Mitigation of Inductive Interference Problems in Portable Power Cables. Annual Report, USBM Grant No. GO122088, West Virginia University, August, 1975, NTIS PB 246-386/45.

61. Weber, E. Electromagnetic Theory, Dover, New York, 1965, pp. 11-115.

62. West, J. M. Electrodeposition and Corrosion Processes. Van Nostrand Reinhold Co., London, 1971, pp. 53-54.

63. West Virginia University, Department of Electrical Engineering, and IEEE Industry Applications Society. Proceedings of the Third WVU Conference on Coal Mine Electrotechnology. August 4-6, 1976, Lakeview Inn, Morgantown, WV, pp. 11-4 to 11-10.

64. Whitt, R. O. D. Trends and Practices in Grounding and Ground Fault Protection Using Static Devices. IEEE Transactions on Industry Applications, March-April, 1973, pp. 149-157.

65. Wolf Contouring Package. Documentation developed by Goddard Space Flight Center.

66. X-it Rod Corporation. X-it Rod: A Hollow-Tube Chemically-Charged-Rod Electrode. Technical Pamphlet, X-it Rod Corporation, Beaumont, CA, 1974.

# APPENDIX A

## GROUND-CHECK MONITOR INSTRUCTIONS

# A1 MODULAR GROUND WIRE MONITOR

## A1.1 Power Connections

### A1.1.1 Ac Power

The modular ground wire monitor requires 120 V ac for power. The black and white wires in the power cord are to be connected to the 120 volt source. The black wire is internally fused so it must be connected to the high potential power connection.

The ac power for the modular monitor must come from a power source that will be on before the breakers can be closed to the cable that is to be monitored. The Under Voltage Relay (UVR) will not be energized until the monitor senses a satisfactory ground condition. Therefore, the power to the monitor must be on before the breaker can be closed.

### A1.1.2 Fusing

The monitor is internally fused with a 3AG-2A fuse. Therefore, external fusing is required only to protect the wiring.

### A1.1.3 Grounding

The green wire in the power cord is to be connected to the power center ground (see figure A1-1). This will connect the monitor chassis to the safety ground. A second green wire (in the monitor connection bundle) will be connected to the ground wire in the trailing cable. If an arc suppressor is used, the two green wires will be at different potentials. The monitor reference will not be the chassis or safety ground but will be the trailing cable ground wire. Any connection between the two green wires will bypass the arc suppressor and may lead to dangerous conditions.

## A1.2 Monitor Connections

There are seven wires coming from the monitor in one bundle. The connections of this group depend on the monitor configuration used. Each wire or pair of wires will be discussed separately. See figure A1-1 for all connections. Any wires not connected should be coiled and taped to prevent any electrical contact. Any voltages present are less than 40 volts, but extra connections may impair operation of the monitor.

### A1.2.1 UVR (Yellow, Two Wires)

The yellow wires are to be connected to the UVR. The 120 V ac source that supplies the monitor is also used to supply the UVR. The same 120 volt source also supplies the two counters. The trip counter is connected in parallel with the UVR. (Note: If the counters are removed, the UVR contacts on the relay may be rewired and an external UVR source used).

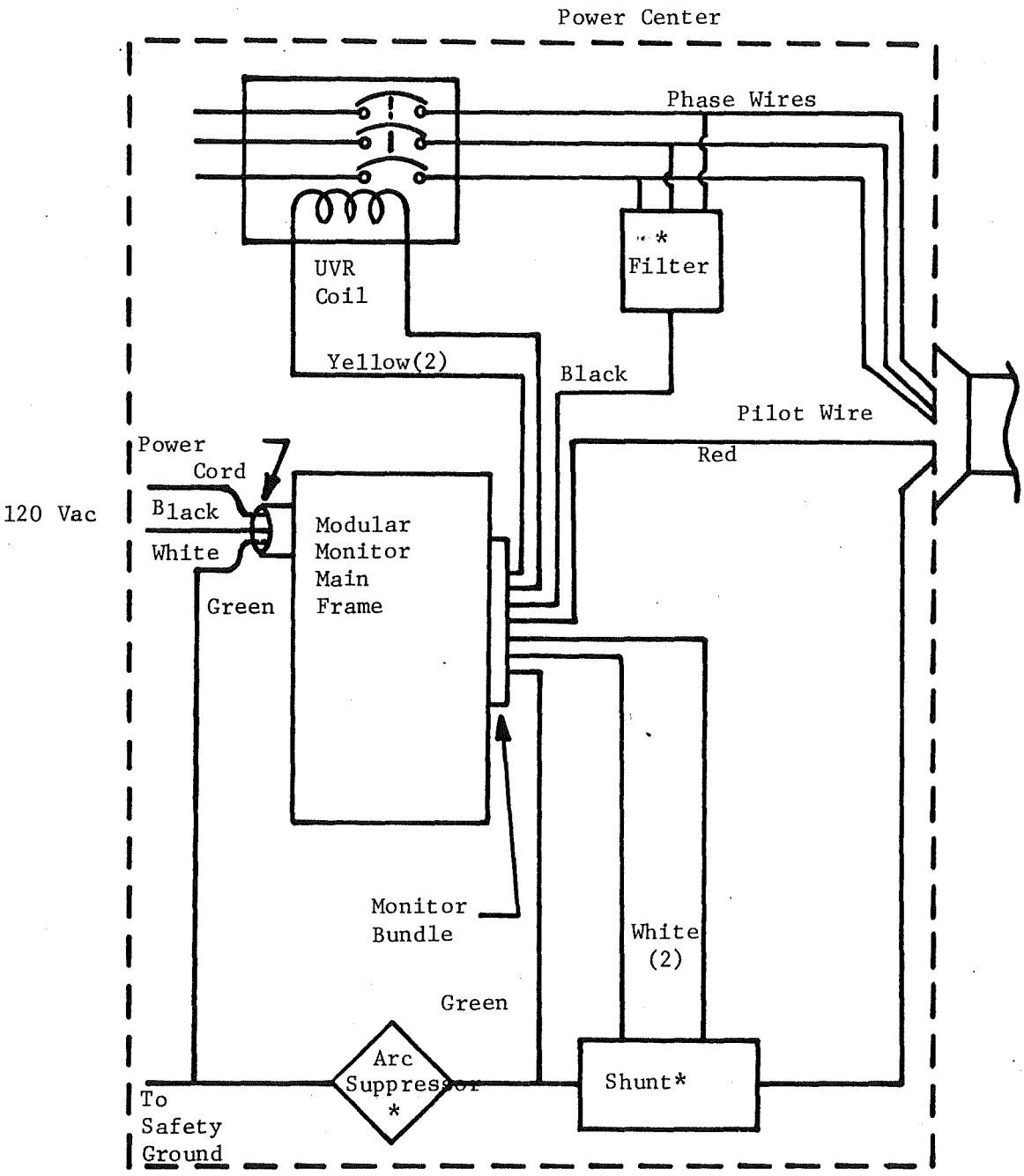


FIGURE A1-1. - Modular Monitor connection diagram.
(* external components)

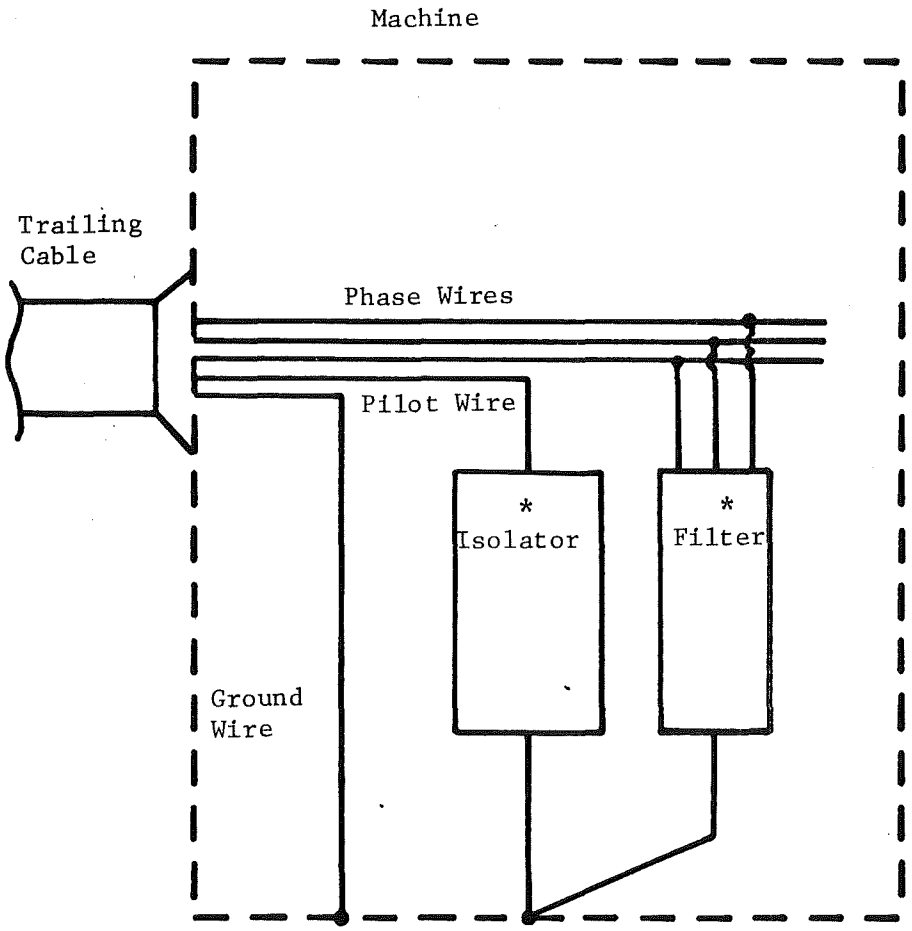


FIGURE A1-1. - (Continued).

A1.2.2 Ground Wire Connection (Green)

As discussed in the section on power connections, the green wire in the monitor bundle is to be connected to the trailing cable ground wire. If an arc suppressor and/or a shunt in the ground wire is used, the trailing cable ground wire is to be insulated from the connector or plug casing on the power center and connected to the safety ground through the arc suppressor and/or shunt. The green wire is to be connected to the inby side of the arc suppressor where the trailing cable ground wire is connected. The monitor chassis is connected directly to the safety ground and must not be connected to the trailing cable ground wire if an arc suppressor is used.

A1.2.3 Pilot Wire Connection (Red)

For cables with a pilot wire (if used), the red wire is to be connected directly to the pilot wire. See Section A1.5 on individual monitors to determine if the pilot wire is used.

A1.2.4 Audio Connection (Black)

If the monitor is to use the phase wires for the monitor signal path, the black wire is connected to the filter which in turn is connected to the three phase wires. See Section A1.5 on the use of filters and the filter connections required on the machine frame.

A1.2.5 Shunt Connections (White, Two Wires)

If a shunt detector is used in the ground wire, the two white wires are attached. These wires will be used to detect a potential caused by current in the ground wire. Both wires are to be attached, but the order is usually unimportant.

A1.3 External Components

Several external components may be used with the modular monitor. Connections to these components (marked with *) are shown in figure A1-1. The use of these components is dependent on the monitor configuration.

A1.3.1 Arc Suppressor

An arc suppressor may be required to prevent inter-machine arcing. It will not interfere with any monitor configuration. In fact the arc suppressor is required in order for the monitor to operate properly in some configurations. The discussion of the monitor modules will explain when and which type of arc suppressor is required.

A1.3.2 Filter(s)

When the pilot wire is not used or is unavailable, the monitor signal is fed to the machine end of the ground wire through the phase wires. A filter is attached to the phase wires at both ends of the cable for this purpose. Normally, the order of connection to the phase wires is unimportant. Specific installation instructions for the filters is given with the monitor configuration.

A1.3.3 Isolator

The isolation resistor is connected between the pilot wire and the ground wire connection to the machine frame. The isolation resistor (50Ω, 25 W) is used only for pilot wire installations and provides a means of detecting pilot-to-ground shorts which could mask a broken ground wire inby the short.

A1.3.4 Shunt

If a shunt is used, it is to be treated in a manner similar to the arc suppressor. The trailing cable ground wire is to be isolated from the power center frame and must pass through or connect to one end of the shunt before connection is made to the arc suppressor or frame (safety) ground. If the shunt is a current transformer, the ground wire will simply pass through the shunt on its way to the arc suppressor, or to the safety ground if no arc suppressor is used. If a diode or other type shunt is specified by the monitor module, the trailing cable ground wire is connected directly to one end of the shunt. The other end of the shunt is connected to the arc suppressor which is normally required with a diode shunt.

The monitor connections to the shunt are made as indicated. Two special terminals are provided. The order of connection is unimportant.

A1.4 Monitor Components

The modular monitor contains several components. The layout is shown in figure A1-2 and the wiring diagram of the monitor main-frame is shown in figure A1-3.

The permanent components:

1. Transformer
2. Switch
3. Fuse
4. Counters.

The replaceable components are:

1. Relay
2. Printed Circuit Boards
    a. Power-filter
    b. Power regulator
    c. Status indicator
    d. Monitor modules.

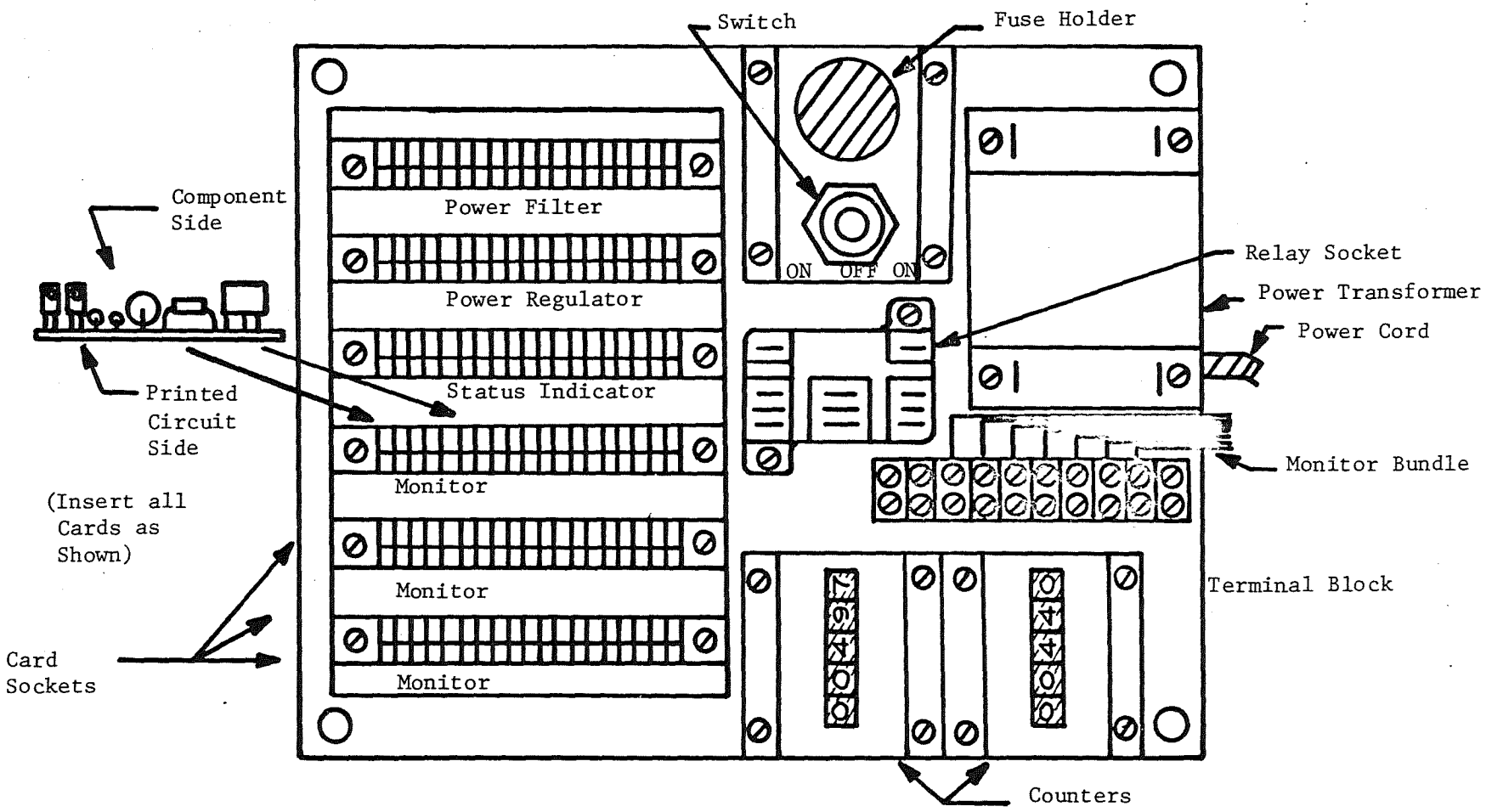


FIGURE A1-2. - Modular Monitor component layout.

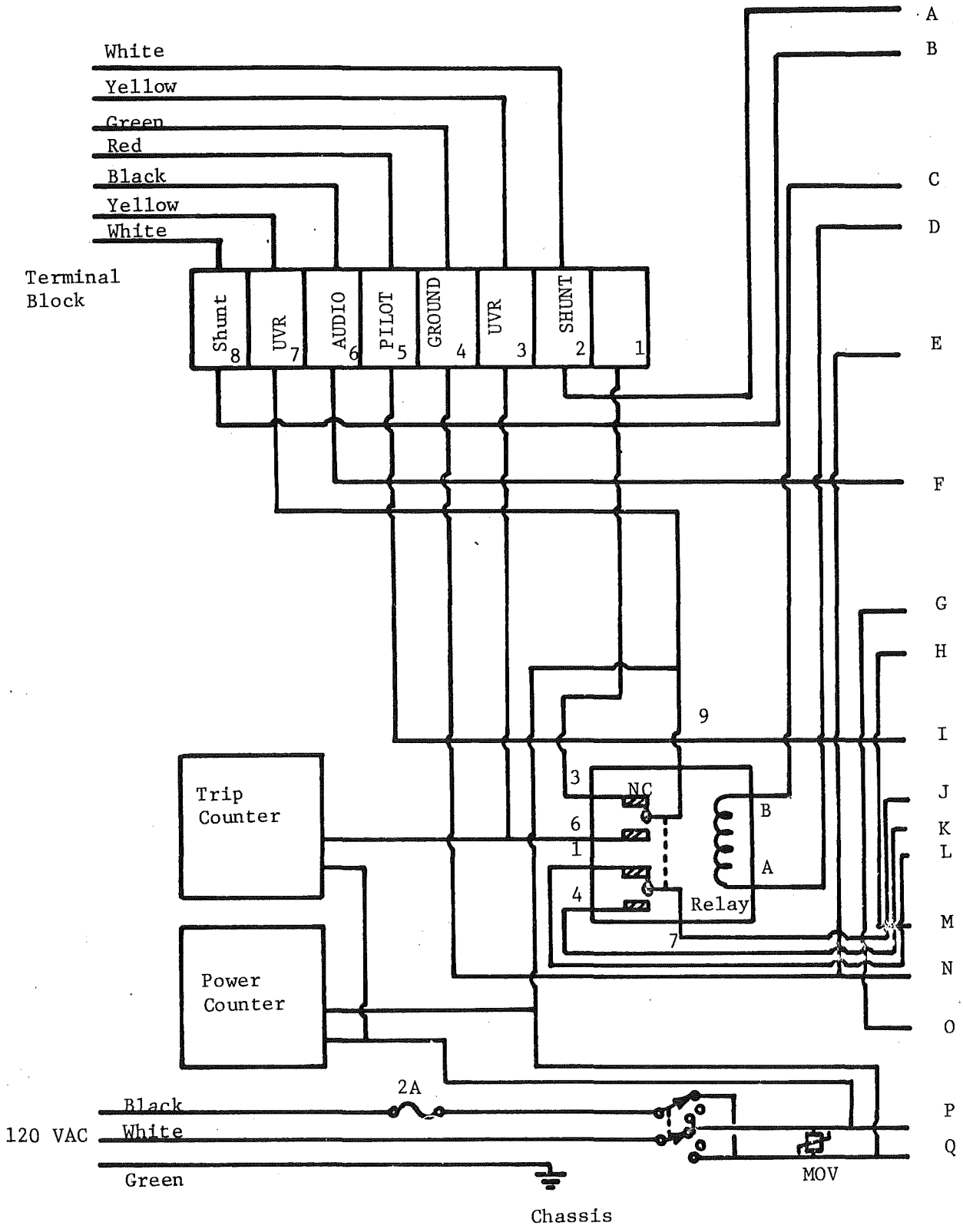


FIGURE A1-3. - Modular Monitor main frame wiring diagram.

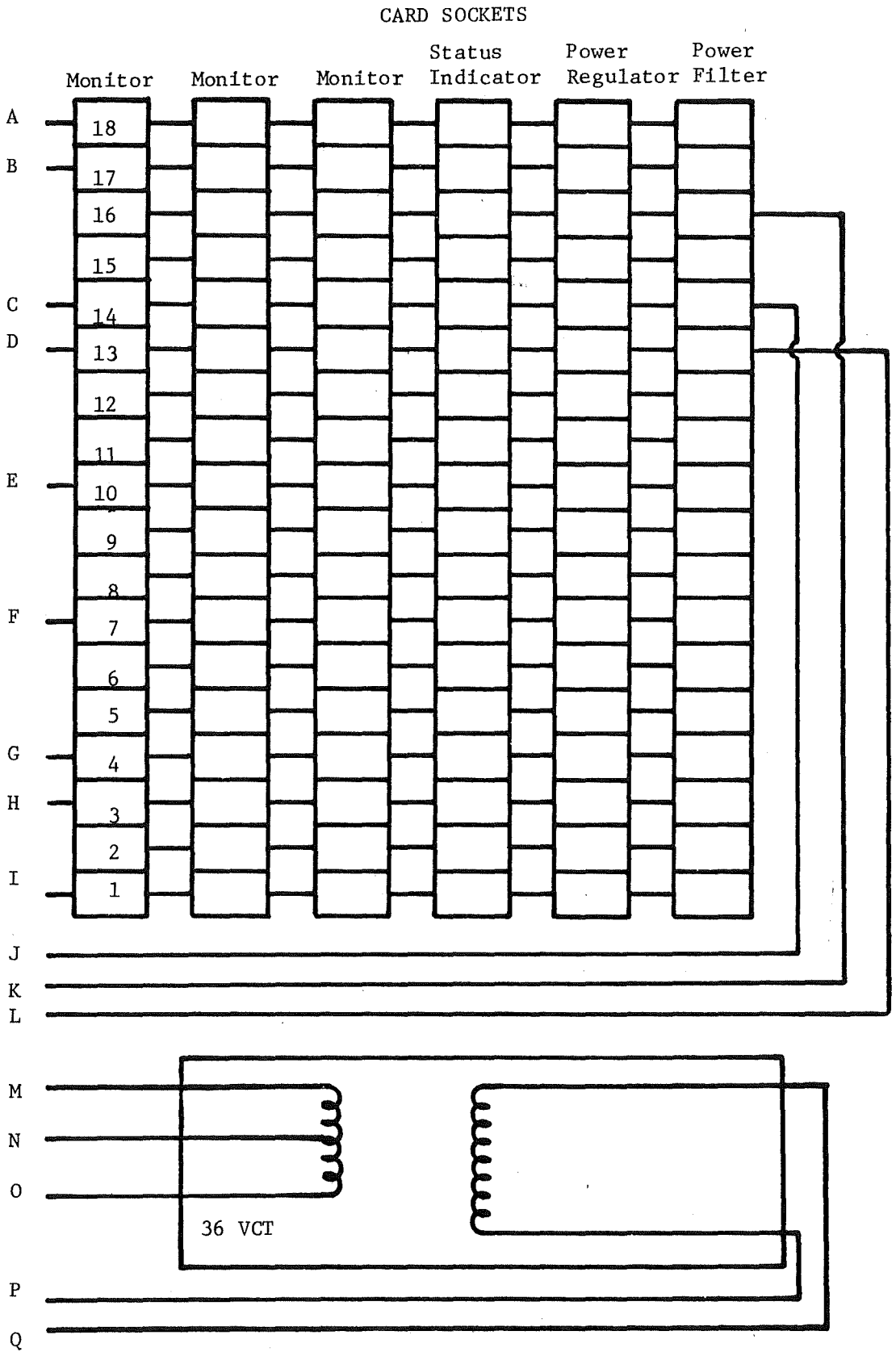


FIGURE A1-3. - (Continued).

A1.4.1 Transformer (Stancor TP-4) (120V-36 VCT)

The transformer supplies power for all functions except for the counters and the UVR. The UVR and the counters receive power from the 120 V ac input directly (power counter) or indirectly through the relay contacts (trip counter and UVR).

A1.4.2 Switch

The switch controls all power coming into the modular monitor. The switch is a three position switch with the off position in the center. The two outside positions reverse the input phase from each other. The phase reversal feature may provide better immunity to transient and stray currents for some monitor configurations.

A1.4.3 Fuse (3AG-2A)

All components in the modular monitor are protected by the fuse.

A1.4.4 Counters

The two counters are provided for field test purposes. They are powered from the 120 V ac line. The power counter counts loss of power to the monitor and counts when the monitor is turned off. The trip counter is tied through the UVR contacts on the relay and will count when power is removed from the UVR. The number of monitor trips can be found by taking the difference between the trip counts and the power counts.

A1.4.5 Relay (Potter-Brumfield KUP Series DPDT)

The relay coil is driven by the monitor and the relay contacts control the UVR. In addition, the relay contacts control the trip counter (when used) while the other set of contacts are used by the status indicator.

A1.4.6 Printed Circuit Cards

The particular set of printed circuit cards used will determine the monitoring configuration. See Section A1.5 on the cards necessary for each configuration. For card insertion, see the drawing of the modular monitor component layout for orientation.

The power-filter, power regulator, and status indicator cards are the same for all present monitors. The monitor cards will be discussed individually in Section A1.5.

A1.4.6.1 Power-Filter

The power-filter card is used to convert the 18 V ac signals to ±25 V dc. This card is used whenever dc power is required for the monitor. The ac is full-wave rectified and filtered on the card. The dc is unregulated and will fluctuate with the line voltage.

In addition to the dc outputs, a full-wave rectified but unfiltered signal is also available. This signal is used in some monitor configurations where it provides some immunity to both ac and dc stray currents. The circuit diagram and component layout are shown in figure A1-4.

A1.4.6.2 Power Regulator

The power regulator card is used whenever regulated dc signals or power are required. The input comes from the power-filter card. The unregulated dc is converted to ±12 V dc by three-terminal integrated circuit regulators. The output is limited to approximately 1 A. The circuit diagram and component layout are shown in figure A1-5.

A1.4.6.3 Status Indicator

The status indicator card is not necessary for monitoring. It is used solely to enable personnel to identify the cause of a circuit breaker trip. The circuit configuration of the status indicator card is given in figure A1-6. This configuration is not unique and may be changed in future models.

There are three indicating LEDs. The green indicator shows the position of the relay which drives the UVR. If the green light is "ON", the relay is on and the UVR is energized. If the green light is "OFF", the relay is off and the UVR is not energized.

The red indicator light shows if the monitor has tripped out the UVR. This indicator is latched on if the monitor trips out. It will remain on until reset by the pushbutton switch on the card, even though the monitor relay may again be pulled in.

The yellow indicator will show the status of the input power. If the input voltage drops below an adjustable level, the yellow light will turn on. If the monitor drops out with a low input voltage, the yellow light will be latched on. Thus, if the yellow and red lights are on, it indicates that the monitor dropped out due to low input voltage. The voltage indicator level detector may be adjusted for the monitor used. Normally, this requires laboratory facilities using a variable auto-transformer.

## A1.5 Monitor Configurations

Several monitor configurations are expected to be available. In this section, installation instructions and circuit descriptions will be given. This section will be expanded as further modules become available.

### A1.5.1 Dc Comparator (Pilot Wire Monitor)

This monitor uses a dc signal and a Wheatstone bridge arrangement to measure resistance. A comparison to a resistance level is made with a voltage comparator integrated circuit. The reference adjustment level can be varied with a multi-turn potentiometer on the monitor card. The circuit diagram and component layout for the dc comparator card are shown in figures A1-7 and A1-8.

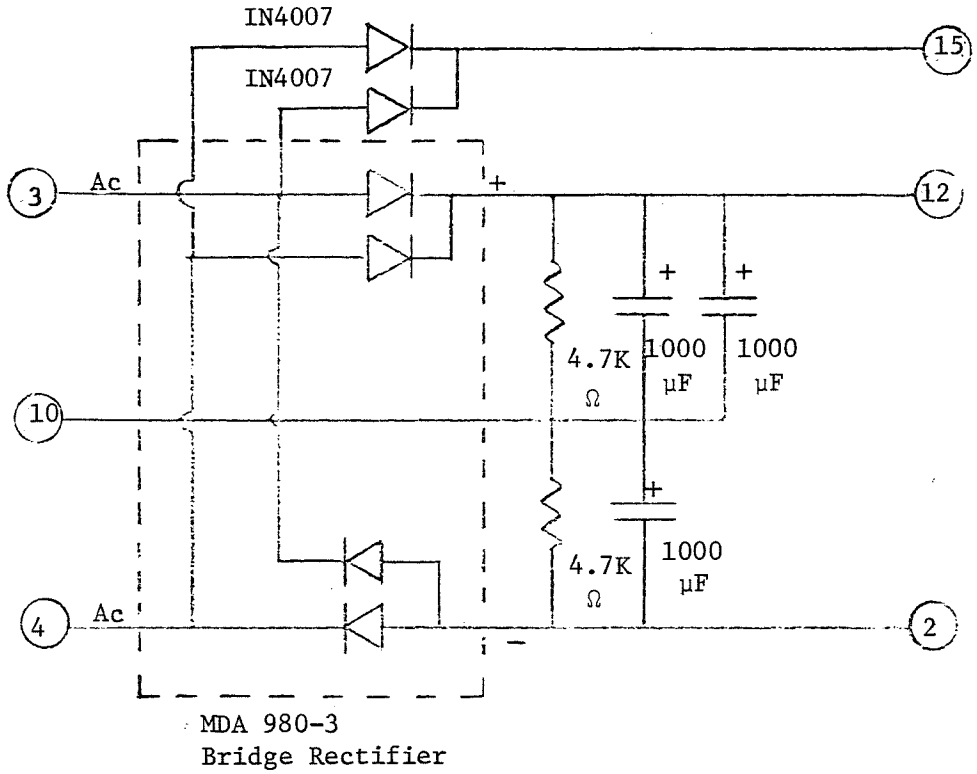


FIGURE A1-4. - Power-Filter card.

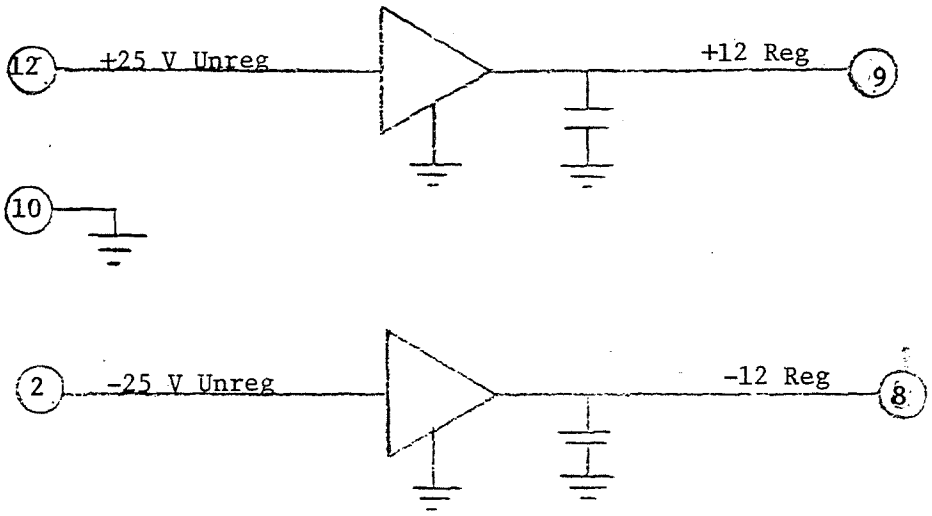


FIGURE A1-5. - Power Regulator card.

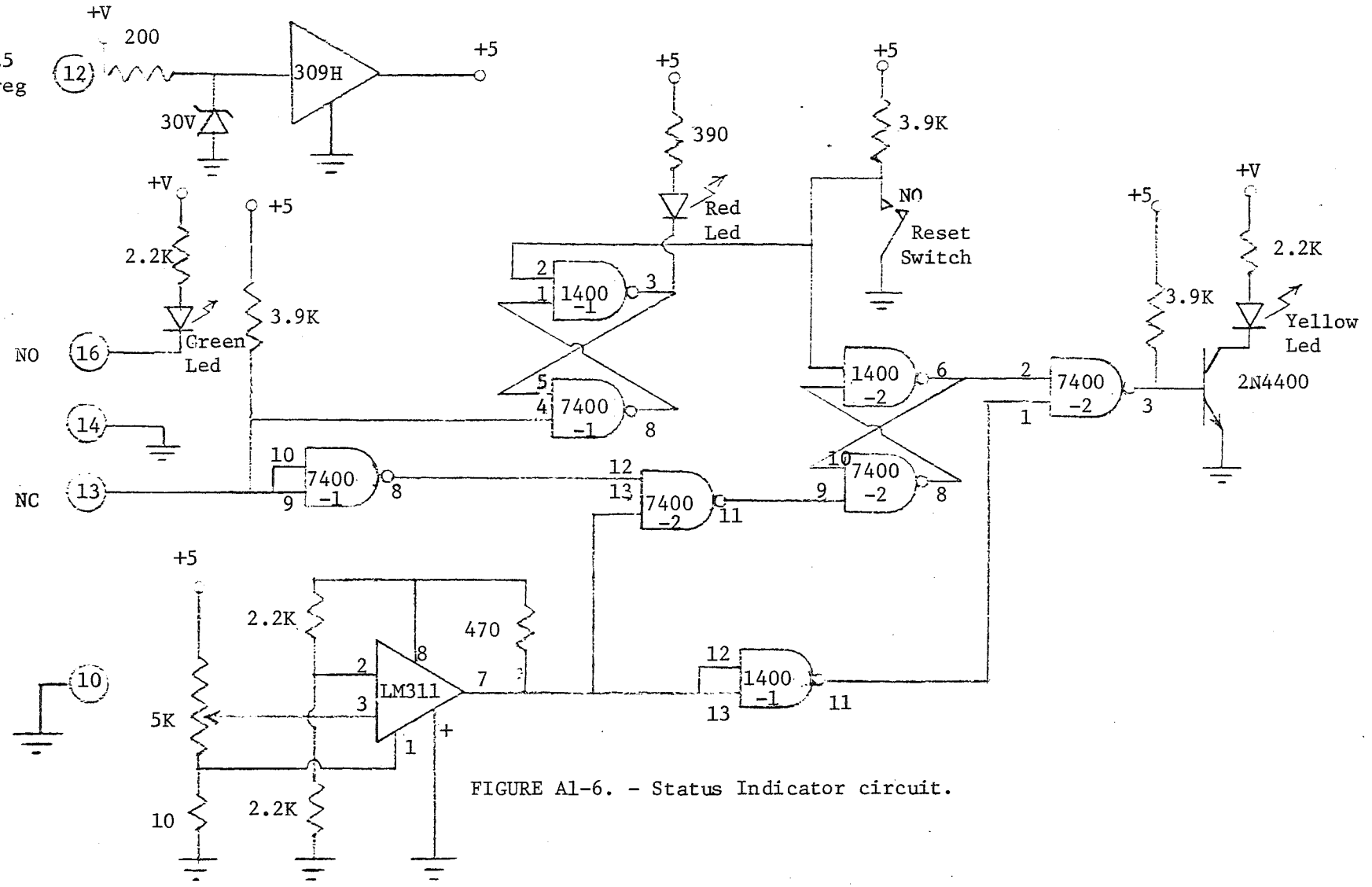


FIGURE A1-6. - Status Indicator circuit.

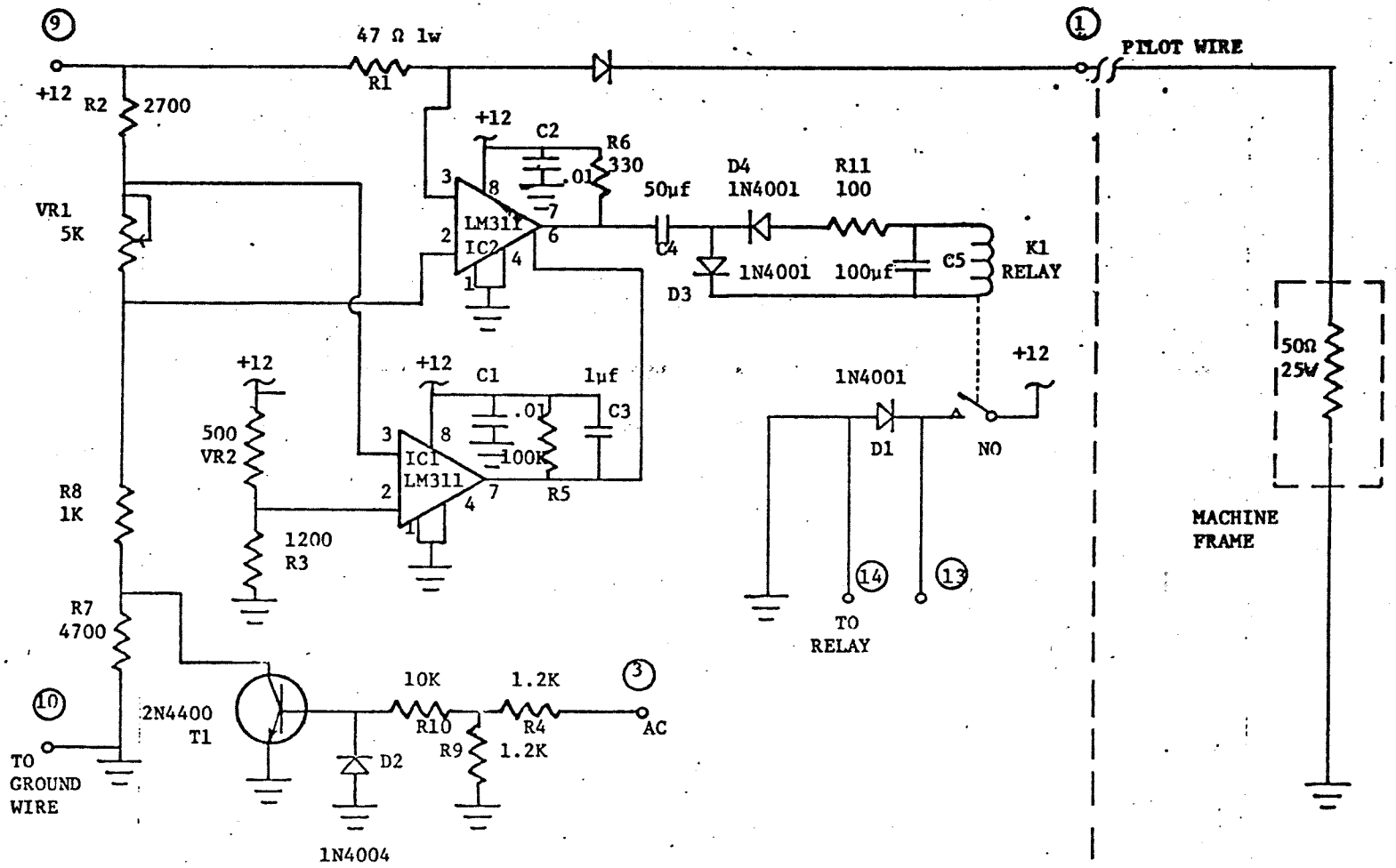


FIGURE A1-7. - Circuit diagram - Dc Comparator.

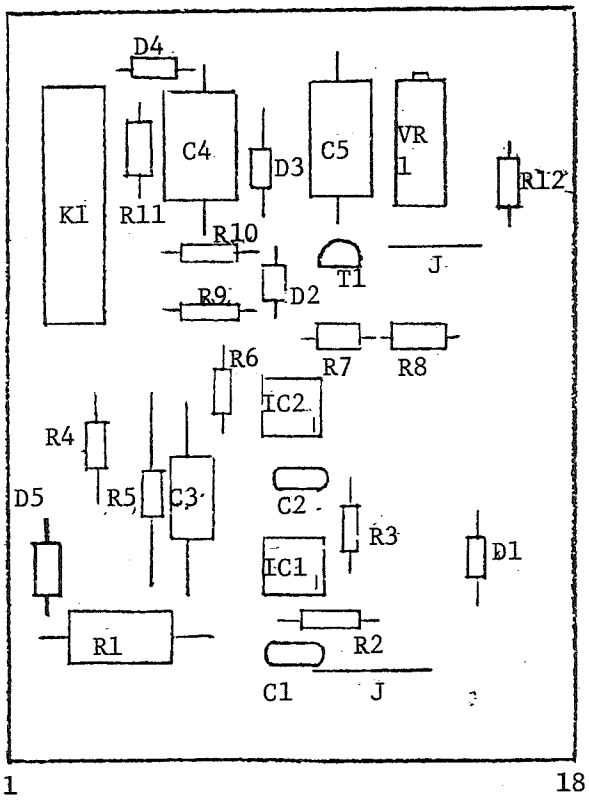


PARTS LIST

| | | | | |
|---|---|---|---|---|
| R1 | 47, 1w | C1 | .01µfd | |
| R2 | 2700, 1/4w | C2 | .01 | |
| R3 | 10K , 1/4 | C3 | 1 | 25wv |
| R4 | 1200, 1/4 | C4 | 50 | 15wv |
| R5 | 100k. 1/4 | C5 | 100 | 10wv |
| R6 | 330, 1/4 | | | |
| R7 | 4700, 1/4 | | | |
| R8 | 1k, 1/4 | IC1 | | |
| R9 | 1200, 1/4 | | LM 311 | |
| R10 | 10k, 1/4 | IC2 | | |
| R11 | 100, 1/4 | | | |
| R12 | 1800, 1/4 | | | |

| | | | |
|---|---|---|---|
| J | JUMPER | VR1 | 500 20 TURN POTENTIOMETER |
| D1,D2,D3,D4 | 1N4004 | | |
| D5 | 1m4007 | T1 | 2N4400 |

K1 Relay RR505-C INTERNATIONAL RECTIFIER

FIGURE A1-8. - Dc Comparator card-component side.

A1.5.1.1 Installation Instructions

The following modules are required:

1. Power-filter
2. Power regulator
3. Relay - 12 V dc
4. Dc comparator monitor card.

These modules should be placed in their respective sockets with the power switch turned off.

The following external components are required:

1. Arc suppressor - diode type
2. Isolator - 50 Ω, 25 W resistor on machine frame.

Connections to these components should be made as described in Section A1.3. In addition, the pilot wire must be connected to the monitor.

A1.5.1.2 Calibration

Calibration should be carried out with the monitor installed and all connections made as described above. A diode arc suppressor must be used if the monitor is to be calibrated as a continuity monitor. In this case, the monitor is simply adjusted to drop out with the ground wire open and a parallel path provided from the machine to the power center frame.

Use of this monitor as an impedance monitor is not recommended because of the likelihood of false tripping. If used as an impedance monitor, the arc suppressor is not required. Calibration is carried out with a resistor in series with the pilot wire. The resistance value used will be the desired drop-out value. The potentiometer on the monitor card is adjusted to just drop out with the resistor in place. The resistor is then removed.

A1.5.1.3 Circuit Operation

This monitor uses a Wheatstone bridge measurement. This measurement is against the calibration setting on the variable resistor VR1. The comparison is made with the voltage comparator IC2. In addition this same circuit tests for a pilot-to-ground short. The short-circuit test is made during the self-checking cycle.

Self-checking is accomplished using the transistor T1 to momentarily lower the comparison voltage on the resistor string that makes up one-half of the bridge. The test signal is driven by 60 Hz ac. The test sequence moves the comparison voltage down by approximately four volts for every one-half cycle. The upper level is the high impedance test under normal conditions. The lower level is the short circuit or minimum resistance test.

If the measured potential is outside this range, the comparator will not switch. The comparator must be continually switched in order to drive the charge pump which drives a reed relay K1. If the comparator stops switching, C5 will lose its charge and the relay will open.

The comparator IC1 is used to check the bridge resistor string. A high voltage caused by an open resistor in the string will be detected by IC1. The output of IC1 will in turn disable IC2.

A1.5.2 Ac Comparator (Pilot Wire Monitor)

The ac comparator monitor is similar to the dc comparator monitor. It is a pilot wire type and requires an arc suppressor if used as a continuity monitor. Either a diode or saturable reactor arc suppressor may be used. Figures A1-9 and A1-10 show the circuit diagram and component layout.

A1.5.2.1 Installation Instructions

The following modules are required:

1. Power-filter
2. Power regulator
3. Relay - 12 V dc
4. Ac comparator monitor card.

These modules should be placed in their respective sockets with the power switch turned off.

The following external components are required:

1. Arc suppressor - diode or saturable reactor
2. Isolator - 50 Ω, 25 W resistor on machine frame.

These components are to be connected as described in Section A1.3 In addition, the pilot wire must be connected to the monitor.

A1.5.2.2 Calibration

Calibration should be carried out with the monitor installed and all connections made as described above. If the monitor is to be used as a continuity monitor an arc suppressor must be used. In this case, the monitor is simply adjusted to drop out with the ground wire open and a parallel path (low resistance) provided from the machine frame to the power center frame.

This monitor may be used as an impedance monitor, but this is not recommended because of the likelihood of false tripping. If used as an impedance monitor, the arc suppressor is not required. Calibration is carried out with a resistor in series with the pilot wire. The resistance

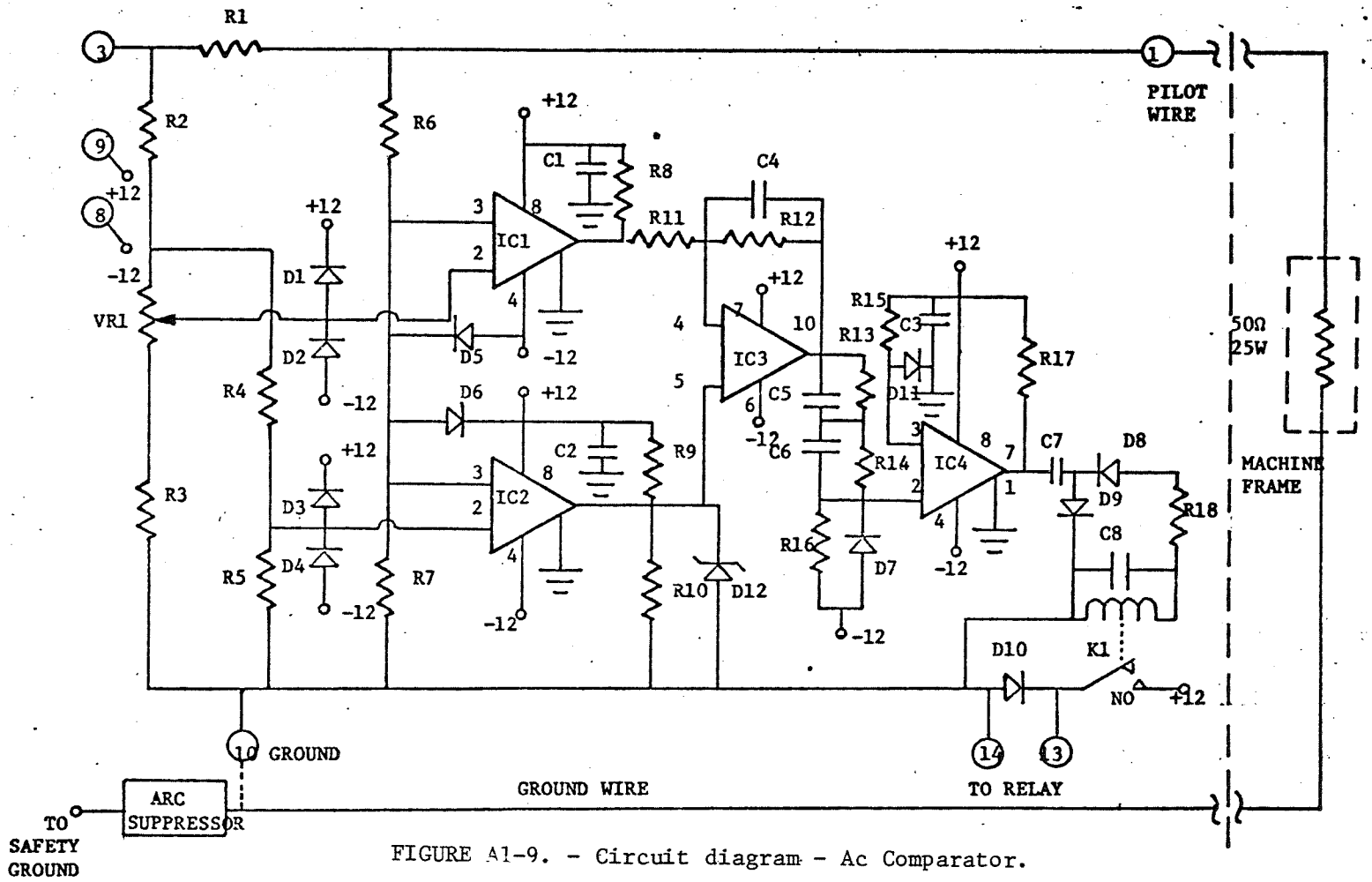


FIGURE A1-9. - Circuit diagram - Ac Comparator.

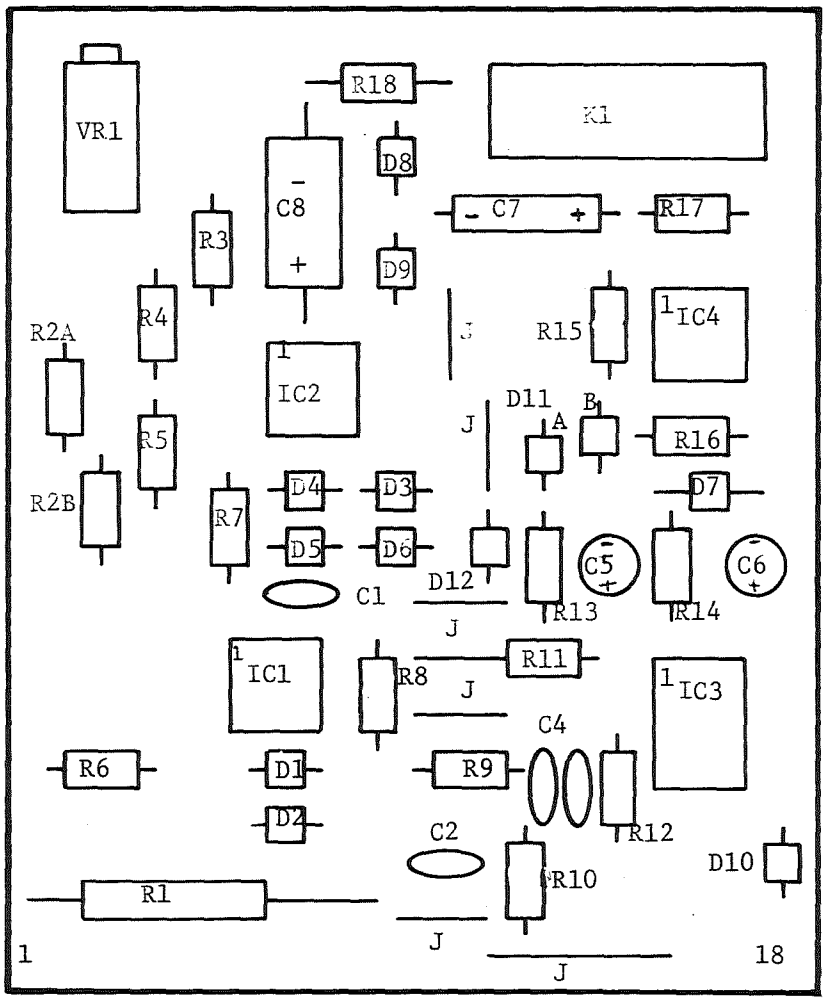


PARTS LIST

| | | | |
|---|---|---|---|
| R1 | 33Ω 2w | IC1,2,4 | LM311 |
| R2A | 15K | IC3 | LM741 |
| R2B | 1.5K | | |
| R3 | 8.2K | VR1 | 500Ω |
| R4 | 56K | K1 | Relay |
| R5 | 100K | | RR505-C |
| R6,R7 | 1K | | International |
| R8,R9 | 2.2K | | Rectifier |
| R10 | 1.2K | J - Jumper | |
| R11 | 2.2K | | |
| R12 | 2.7K | | |
| R13,R14 | 10M | | |
| R15 | 1K | | |
| R16 | 39K | | |
| R17 | 220 | | |
| R18 | 10 | | |
| | | | |
| D1-D6 | 1N4148 | | |
| D7-D10 | 1N4001 | | |
| D11A,B | 1N4148 | | |
| D12 | 5.1V Zener | | |
| | | | |
| C1-C3 | 0.1 µf | | |
| C4A,B | 0.1 µf | | |
| C5,C6 | 5.6 µf | | |
| C7,C8 | 100 µf | | |

FIGURE A1-10. - Ac Comparator card-component side.

used is the desired drop-out value. The potentiometer on the monitor card is adjusted to just drop out with the resistor in place. The resistor is then removed and the pilot wire is connected to the monitor.

A1.5.2.3 Circuit Operation

This monitor uses a Wheatstone bridge measurement. Two voltage comparator integrated circuits are used to detect a high and a low impedance value. Thus it measures both a high impedance ground and a short between the pilot and ground wires.

The input signal to the bridge is 60 Hz ac. Thus the comparators switch on and off every one-half cycle. As long as the impedance measurement voltage lies between the two reference voltages, the outputs of the two comparators are "out of phase" with each other. These two signals are subtracted with the operational amplifier circuit. The output of the operational amplifier is clamped to -12 volts and the peak voltage is compared to a fixed level with a third comparator.

As long as the outputs of the two comparators are out of phase, the output of the clamp circuit will go above the comparator threshold. The comparator output will be switched at a 60 Hz rate. The switching output drives a charge pump to hold in relay K1.

If the impedance measurement potential goes outside the comparator window, the output of the two comparators IC1 and IC2 will be in phase and the output of the operational amplifier will be very small. The clamp prevents the peak threshold from being reached. If either comparator IC1 or IC2 fails in any mode, its output will remain in a steady-state. The other comparator will continue to switch. But when the two signals are subtracted, the output of the operational amplifier will not reach the threshold of the comparator IC4.

## A2 MULTIPATH MONITOR

### A2.1 Introduction

The multipath monitor is designed to monitor up to five parallel connections of machine frames to the ground wire as discussed in Section 2.4 of this final report. This is accomplished by placing a series tuned filter between the pilot and machine frames where the ground connections are to be monitored. Each filter is tuned to a different frequency. The monitor changes its output frequency to the resonance frequency of each filter in sequence so that each ground connection can be checked independently.

This monitor is intended to be used where more than one machine frame connection is to be monitored by a single ground check monitor. Typical applications would be where a motor and starter box are some distance apart and separately connected to a common ground wire, or where several independent pieces of portable equipment are run in parallel from a common power bus.

A filter is to be connected between the pilot wire and each machine frame. Each filter must be tuned to a different frequency from the others. Five different filters are available marked A, B, C, D, or E. The corresponding switch on the chassis is to be "ON" if the filter is used and "OFF" if the filter is not used. For calibration purposes, a RUN/STOP switch is provided, and a single step switch can be used to cause the oscillator to move to the next frequency in sequence. An indicator light will show which frequency step is presently active. The frequency of each step must be tuned with the complete monitoring system in operation. An additional step "0" is added as an internal check for the monitor logic and to test for a pilot-to-ground wire short.

Another pair of indicator lights will show the impedance level presently detected. The level will be either high or low. The impedance tripping level can be adjusted. A low level should be measured for each step that has its corresponding filter. A high level should be measured for each step with a missing filter and for the check step "0".

### A2.2 Installation

The installation of the multipath monitor is similar to most other ground check monitors. Some differences will occur, however, because of the unique properties of this monitor.

#### A2.2.1 Filters

The filters are to be mounted in the machine frames to be monitored. Each frame must have a different filter; that is, each filter must be tuned to a different resonant frequency. The filter is to be connected between the pilot wire and the chassis of the machine. This will place the filter in series with the machine frame ground connection.

#### A2.2.2 Frequency Calibration

Frequency calibration is to be carried out with all filters connected.

Because some interaction occurs between filters, any change in the number of filters used will require that the system be recalibrated.

Frequency calibration is a fairly simple procedure. A voltmeter is provided for this purpose.

The calibration procedure is as follows:

1. Set RUN/STOP switch to STOP.

2. Advance step indicator to desired step by depressing the single step switch.

3. Adjust the corresponding frequency adjustment potentiometer for a minimum reading on the voltmeter if the filter for this step is connected. If the filter for this step is omitted, tune for a maximum reading. Step "0" is a special case, and need only be tuned for a high impedance reading. The maximum voltage expected is approximately 10 volts.

In order to insure that a particular step frequency is not tuned to an incorrect filter, stop on the desired step and momentarily disconnect the filter. The voltmeter should read high and the high impedance light should come on if the impedance level detector has been properly calibrated. The approximate frequencies of each step are given in Table A2.1.

TABLE A2.1. - The approximate frequencies of each step of the Multipath Monitor

$f_o$ = 5000 Hz
$f_A$ = 2952 Hz
$f_B$ = 3280 Hz
$f_C$ = 3645 Hz
$f_D$ = 4050 Hz
$f_E$ = 4500 Hz

A2.2.3 Impedance Calibration

The multipath monitor is intended to be used as a continuity monitor. Minor frequency drift in the oscillator and filter resonance preclude its use as an impedance monitor. For calibration purposes, a resistor is placed in series with the pilot wire which is normally bypassed with a momentary open, normally closed switch.

Proper adjustment of impedance will be attained when the low impedance indicator is on for all steps with filters and the high impedance indicator is on for all steps without filters. In addition, the high impedance indicator should go high in any state where it is normally low if the filter is disconnected.

## A2.3 Principles of Operation

Describing the circuitry of the multipath monitor can best be accomplished by describing the signal processing functions. The details of the circuit can then be easily understood by anyone familiar with electronic circuitry. A block diagram of the circuit is shown in figure A2-1 and the detailed circuit diagram is shown in figure A2-2.

### A2.3.1 Impedance Measuring Circuit

The discussion will start with the voltage controlled oscillator (VCO) and continue in the direction of signal flow. The VCO has its frequency controlled by the D/A converter. There are 6 frequency outputs from the VCO; one at each filter resonance, and one ($f_o$) which is not at the resonance of any filter. The output of the VCO goes to a power amplifier and from there to the pilot wire. Inasmuch as the output of the power amplifier has a constant amplitude, the resistor R and the branch filter network act as a voltage divider. The voltage which goes to the filter circuit is a measure of the impedance seen looking toward the filters. At a filter resonance, this voltage will be low if the ground connection impedance is low.

A bandpass filter (270-48,000 Hz) is used to reduce the stray signals, particularly 60 Hz signals, into the synchronous rectifier. A square wave signal from the VCO is brought into the synchronizing control. This control circuit is used to control the switching of the synchronous rectifier and is adjusted to compensate for the phase delay through the power amplifier.

The synchronous rectifier is switched in synchronism with the audio frequency signal. The phase of every other half cycle is reversed. The result is full wave rectification. Signals not synchronized with the audio frequency will be rejected, with their output averaging zero. The output of the synchronous rectifier goes through a low-pass filter to eliminate the ripple before going to the magnitude comparator.

The magnitude comparator compares the output of the synchronous rectifier with an adjustable reference voltage to determine if the impedance is above or below the set value. Red and green indicators are used to indicate the status of the comparator output.

### A2.3.2 Frequency Control Circuits

The VCO frequency is changed in steps from one frequency to another in sequence. This is controlled by a ring counter. The ring counter has eight positions but only five are required by the branch filters. Thus, the three remaining are used for the reference state "0". The frequency, $f_o$, will be on for approximately three times as long as the other frequencies. The step signal is produced by the output of a divide-by-64 counter which in turn is driven by the output of the VCO. Thus, the VCO will remain at one frequency for 64 cycles during normal operation.

The output of the ring counter goes through a buffer/driver circuit which drives a voltage level control to change the frequency of the VCO. The

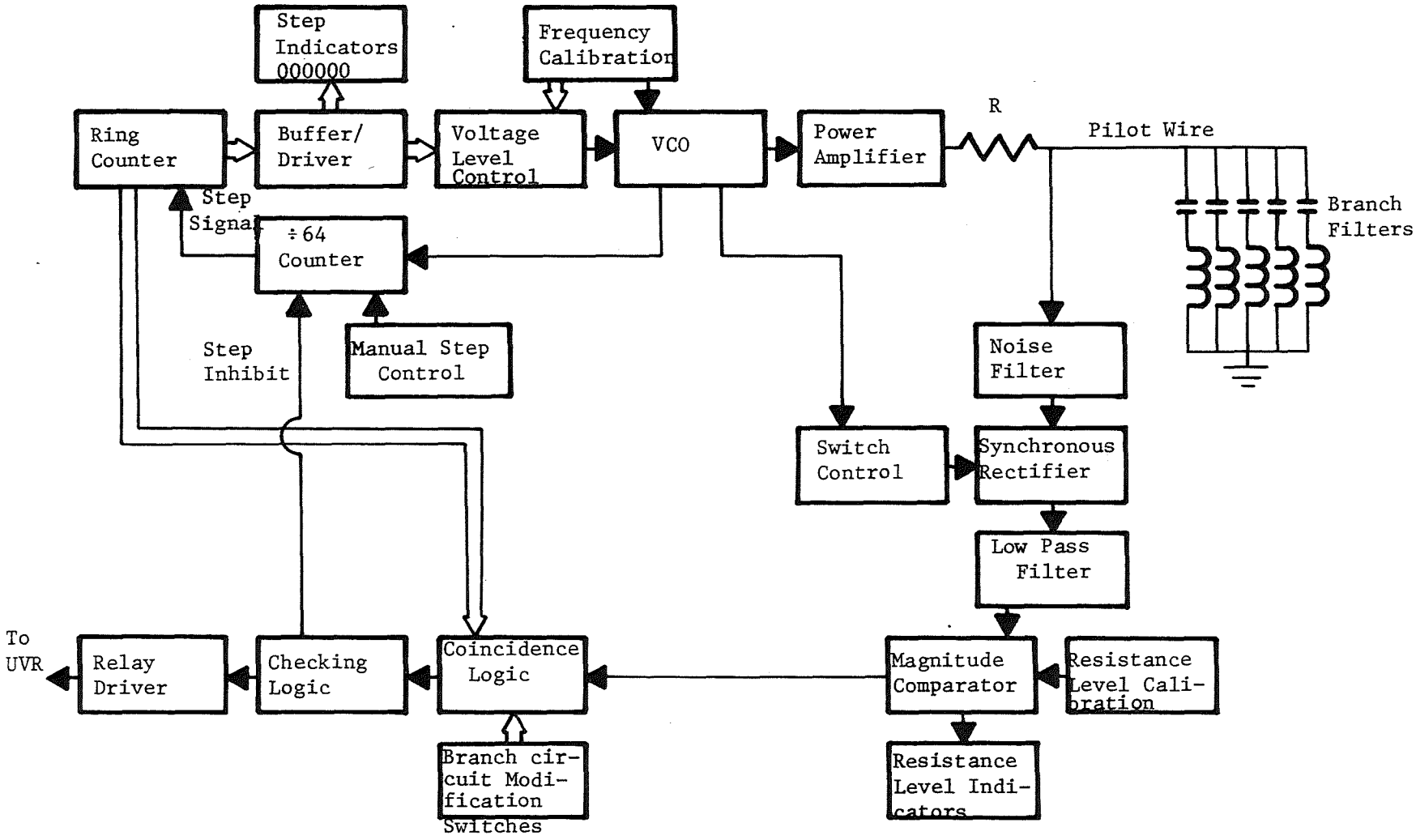


FIGURE A2-1. - Block diagram of Multipath Monitor.

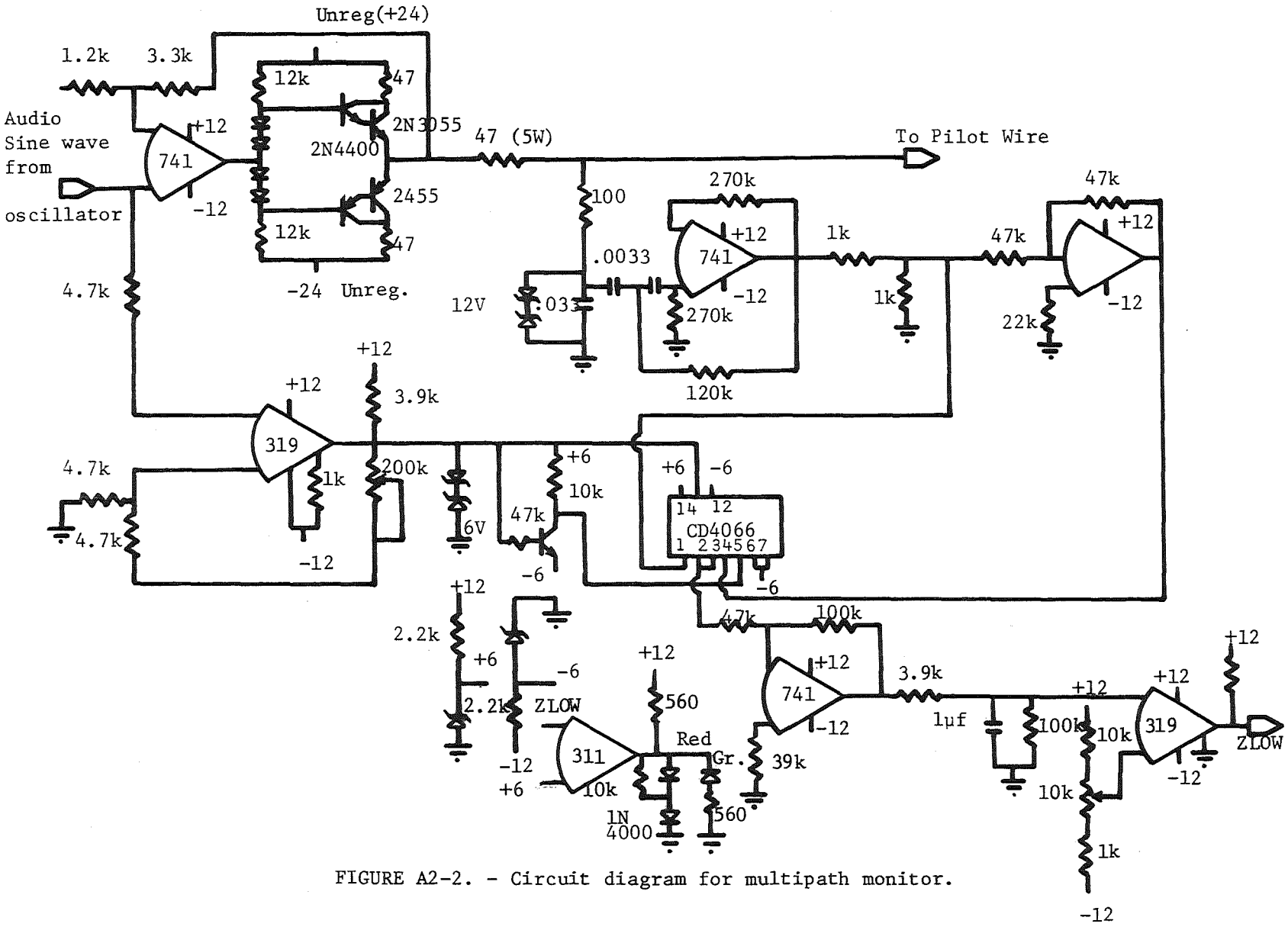


FIGURE A2-2. - Circuit diagram for multipath monitor.

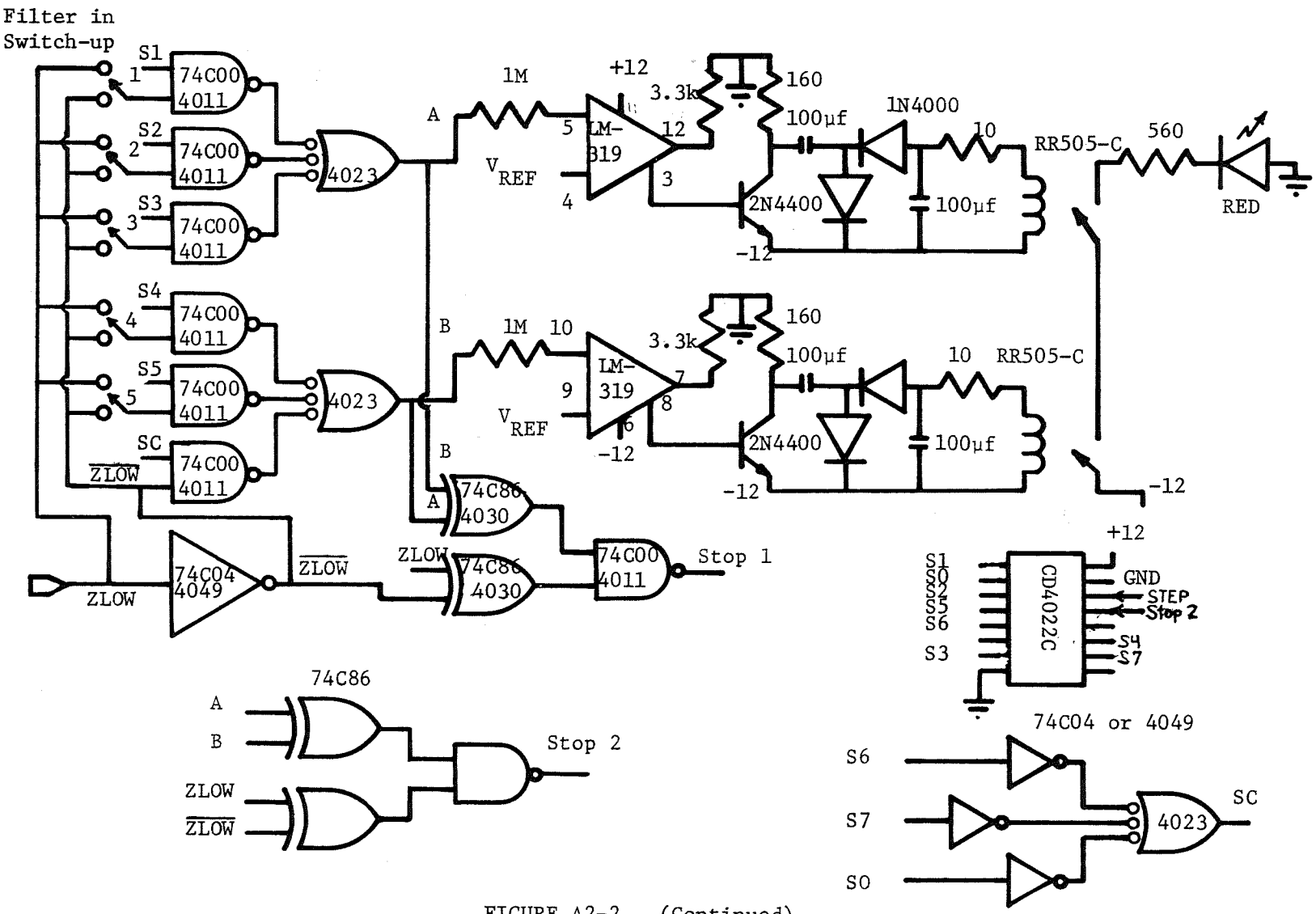


FIGURE A2-2. (Continued).

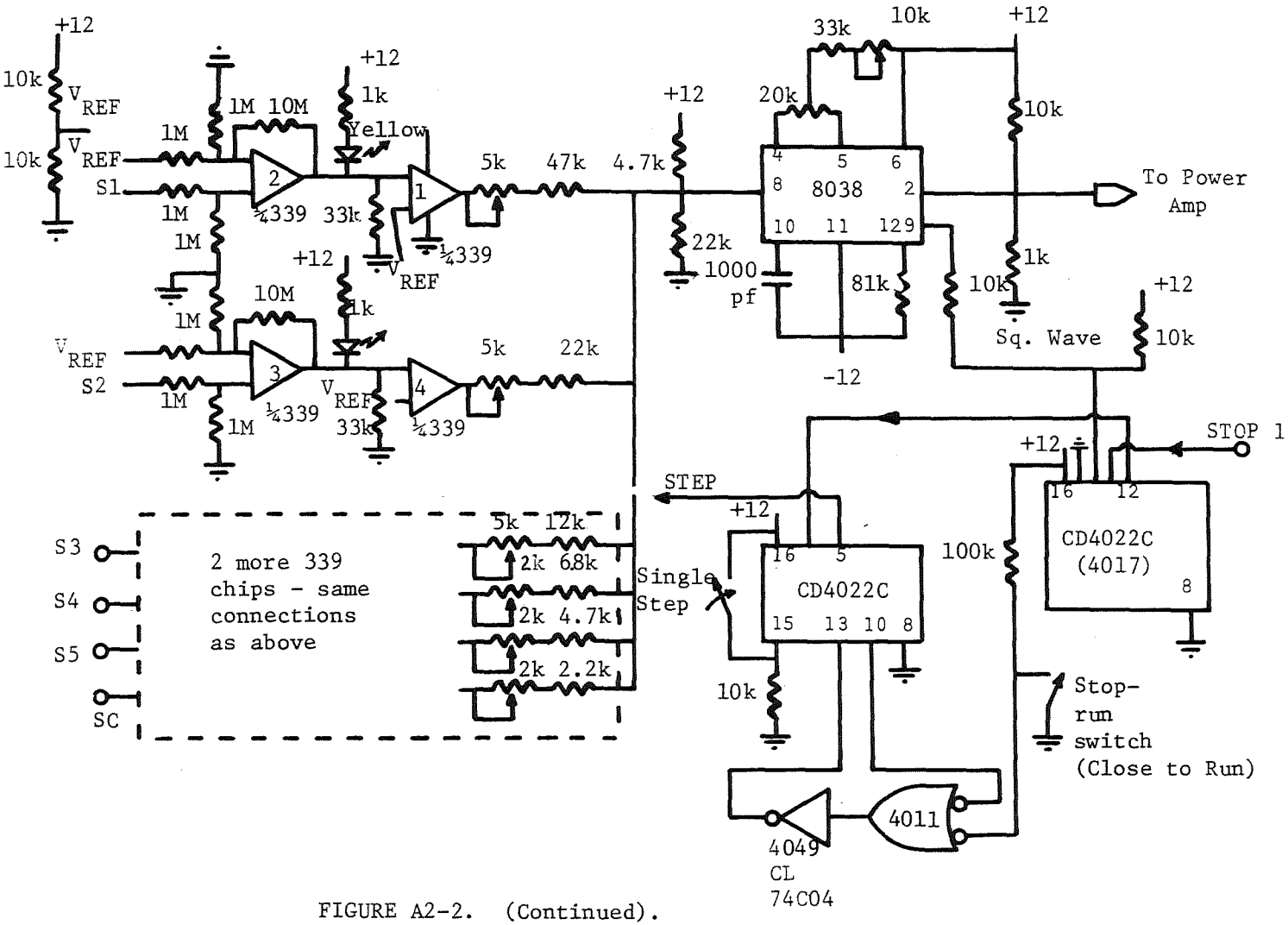


FIGURE A2-2. (Continued).

buffer/driver also drives a set of LED's to indicate the present state of the ring counter.

The step signal may also be controlled manually with a RUN/STOP switch and a single step switch. This feature is required for calibration and servicing purposes.

A2.3.3 Control Logic

A comparison of the state of the ring counter and the output of the impedance level comparator is accomplished in the coincidence logic circuit. It should be noted that the desired impedance level is a function of the filters inserted in the circuit. The output of the coincidence logic circuit goes two places: the failsafe relay driver, and the step inhibit of the divide-by-64 counter.

The step inhibit control stops the divide-by-64 counter from counting if the coincidence logic detects an incorrect impedance level in the present state. Thus, the ring counter will not be advanced if an error is detected in the monitoring circuit. Several other logic circuits will also inhibit the counter if circuit failures occur in several parts of the system. Servicing personnel may readily determine which grounding branch the problem is in by observing the step indicators and the resistance level indicator.

The UVR relay driver is made up of two low-power relay contacts in series. Each of the low power relays is driven by a charge pumping circuit which will stop if the input signal fails to cycle. Thus, if the stepping circuitry is inhibited by some failure either in the logic circuits or in the grounding circuit, the low-power relays will open, causing the UVR to drop out.

# APPENDIX B

## OPERATIONS MANUAL FOR THE POTENTIAL GRADIENT PLOTTER

## B.1 INTRODUCTION

The potential gradient plotter is used for making field measurements to obtain a continuous fall-of-potential profile near ground beds and electrical machinery used commonly in mines. It is self-contained and has built-in circuitry that accomplishes three things at once.

1. Generation of a current signal ranging from 0 to 100 mA.
2. Voltage measurement.
3. Distance measurement.

The voltage and distance signals are transmitted to the Y and X inputs of an X-Y recorder to obtain a continuous profile of voltage versus distance.

## B.2 OPERATING PRINCIPLE

Consider figure B-1 where E is the reference electrode near which a fall-of-potential profile is desired. An alternating current is injected between electrode E and a remote auxiliary electrode B. A wheeled electrode A travels between E and B. A plot of the potential difference between A and E as a function of distance from E would appear as in figure B-2. Curve #1 is obtained for a small spacing between B and E while curve #2 has a flat mid-portion and results from large electrode spacings. The presence or absence of a near flat mid-portion in the fall-of-potential is a test of whether or not the auxiliary electrode is far enough from the reference electrode.

## B.3 CONSTRUCTION AND GENERAL APPEARANCE

Figure B-3 is an isometric sketch of the wheel assembly with the main parts appropriately labeled.

The aluminum wheel which makes contact with the ground is 0.91 m (3 ft) in circumference and is 1.27 cm (1/2 in) thick. It has 30 equally spaced holes drilled circumferentially at a distance of 10.2 cm (4 in) from the center. The circular arc obtained by the radial projections through adjacent holes is 3.05 cm (0.1 ft). This is illustrated in figure B-4.

An infrared emitter and infrared detector are mounted on either side of the wheel in teflon pieces. One end of each teflon piece is hollowed out a little into a concave surface, and on each surface the emitter and detector are fixed by means of an adhesive. Electrical leads are taken out of the other end. The teflon pieces are mounted inside spring loaded sockets so that the concave surfaces are flush with the wheel surface. This does not hamper the wheel movement since teflon is self-lubricating. All extraneous infrared light is thus cut off and the infrared device is made very sensitive. The infrared emitter and infrared detector are mounted at the same radial distance of 10.2 cm (4 in) from the wheel center as the 30 holes, so that when each hole comes in line with the emitter and detector, an infrared signal is transmitted from emitter to detector and an impulse is generated which corresponds to 3.05 cm (0.1 ft). A series of impulses is generated as the wheel rolls along. These are fed into a counter circuit for display as

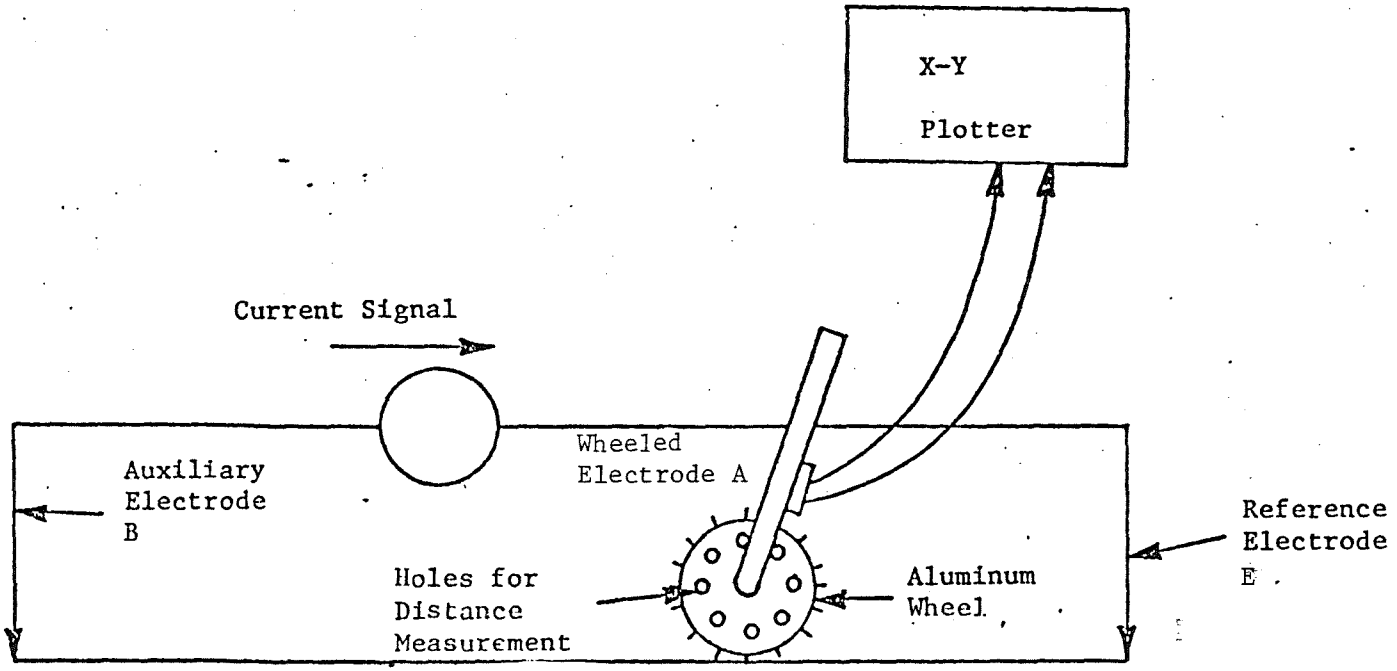


FIGURE B-1. - Illustration of the operating principle of the plotter.

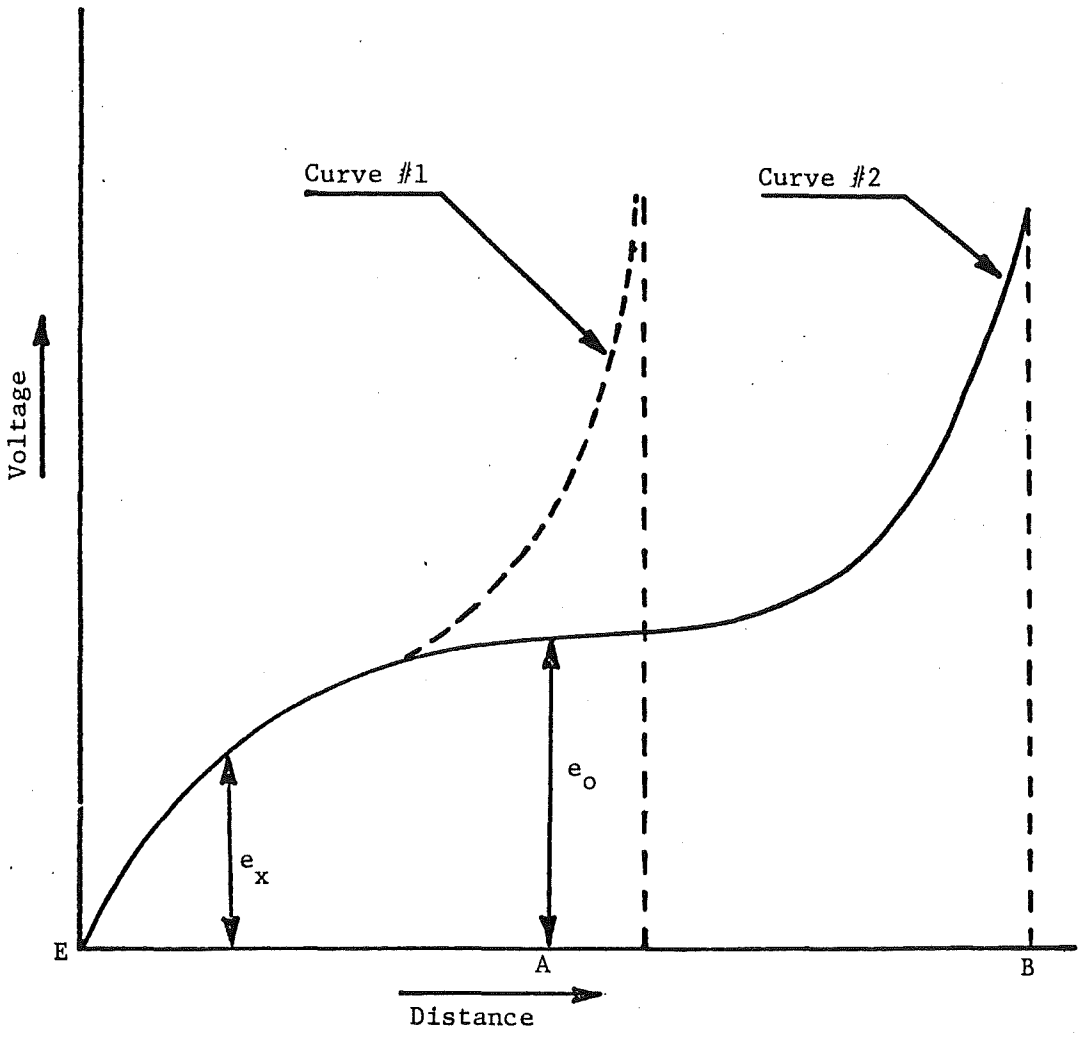


FIGURE B-2. - Fall-of-potential curve.

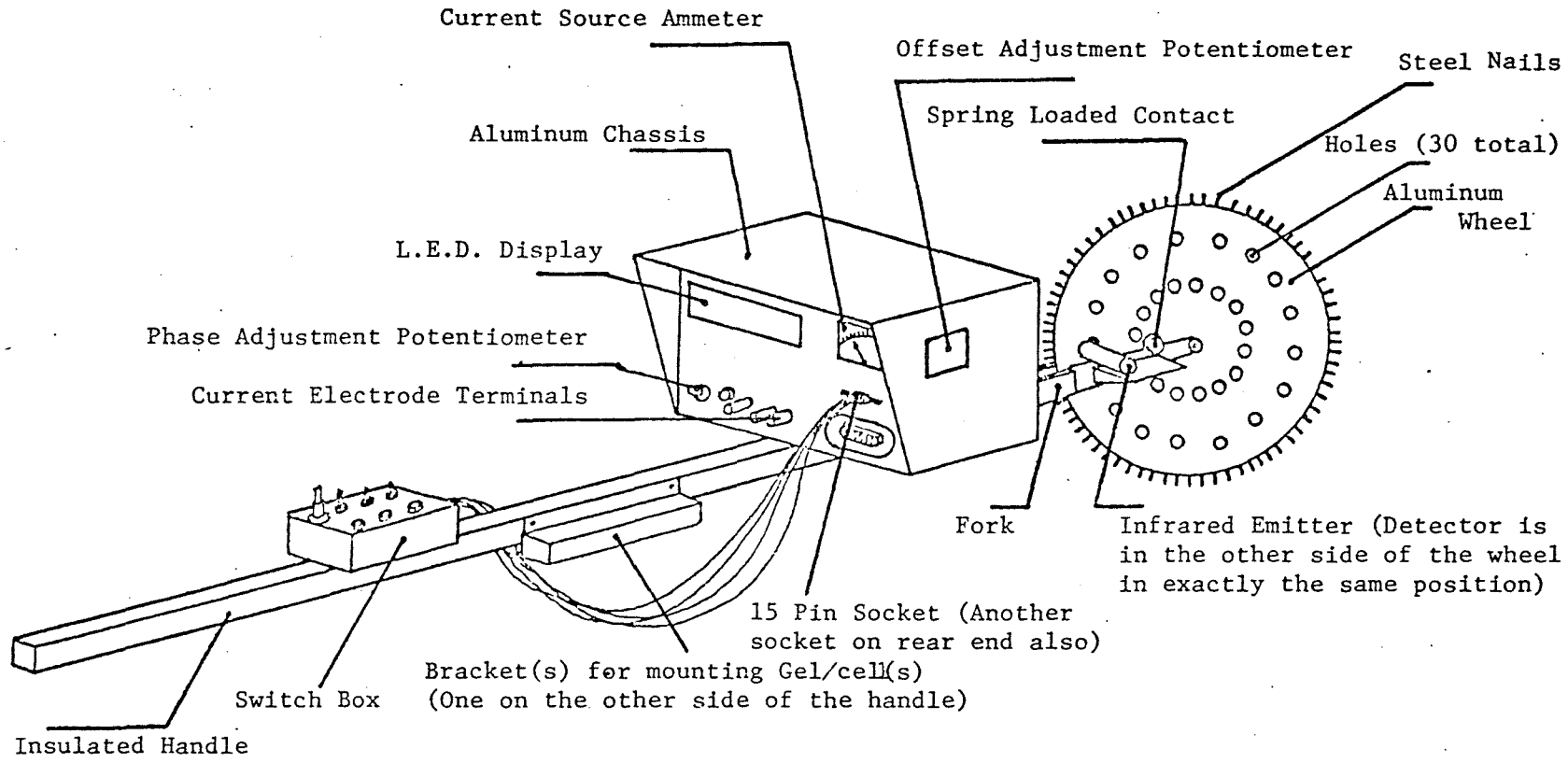


FIGURE B-3. - Isometric sketch of the wheel assembly.

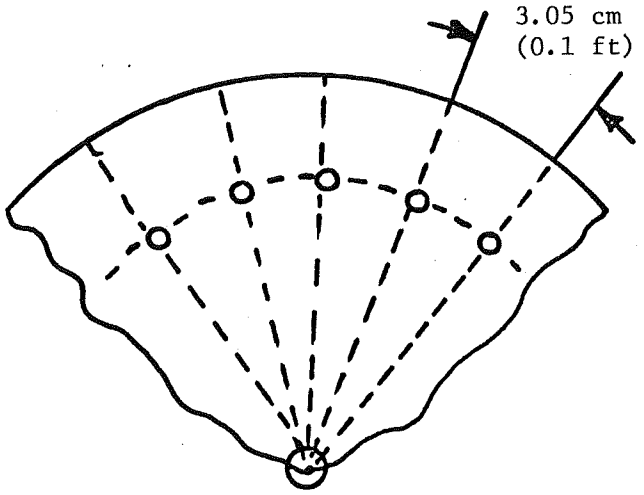


FIGURE B-4. - Magnified view of a radial arc between holes.

well as for conversion into an analog signal for feeding to the x input of an X-Y recorder.

Steel nails are driven along the wheel rim projecting 0.32 cm (1/8 in) from the rim. This insures better contact between the wheel and earth, especially when the surface is grassy.

The voltage signal is actually transmitted to the detecting circuit through the aluminum wheel which acts as the conducting medium.

The wheel is linked to a well-insulated handle through a fork and provides for smooth motion as it is pushed along. The handle is well-insulated to avoid any possibility of a parallel current path through the operator's body. A spring loaded electrical contact grazes the surface of a circular copper strip which is screwed onto the wheel to insure better contact.

The electronic circuitry is housed in a lightweight aluminum chassis with an overall dimension of 25.4 cm x 15.2 cm x 17.8 cm (10 in x 6 in x 7 in) and is mounted on the lower end of the wheel handle. Incoming and outgoing terminations, L.E.D. distance display unit, test points, phase adjustment potentiometers, and the current source ammeter are mounted on the chassis at convenient locations.

The circuit control buttons, switches, and current magnitude potentiometer are mounted on a smaller box at the upper end of the handle within easy reach of the operator. The connections between the box and the main chassis are done with single core multi-stranded wires. Wires of different colors are selected for different terminations so they can be easily identified at the chassis, and the wires are terminated in a 15 pin plug-in type socket which can be easily pulled out of or inserted into a 15 pin plug where all wiring from the printed circuits terminate. The circuitry inside the chassis can therefore be easily isolated when required in order to carry out laboratory tests or repairs.

Two 12 volt Gel/cells mounted adjacent to the chassis supply power to the complete circuit. Each Gel/cell has a continuous capacity of 1.5 ampere hours and with the total current consumption of the circuit being 250 mA, the batteries will have a 6-hour cycle when fully charged. This is more than sufficient for one experimental run.

The complete wheel unit weighs 23 pounds.

## B.4 BLOCK SCHEMATICS

### B.4.1 Constant Current Source

Figure B-5 is the block schematic of the constant current source. An 11 Hz square wave voltage signal is generated and fed through a potentiometer into a voltage-controlled current source circuit. The output is a constant current signal whose magnitude is adjusted by varying the input potentiometer. This output is fed to the ground resistance. A metering circuit monitors the output current and generates a proportional signal for feeding into a microammeter calibrated to a full scale reading of 100 milliamperes.

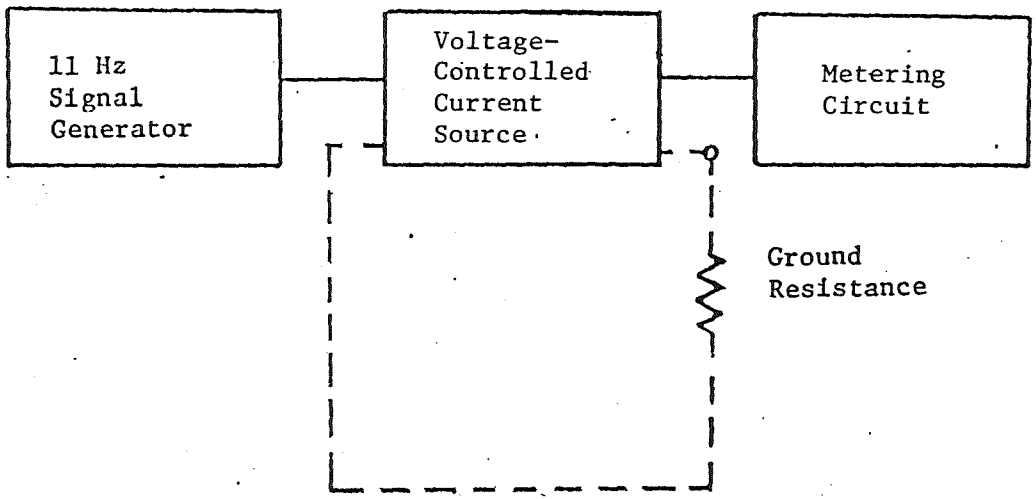


FIGURE B-5. - Block schematic of constant current source.

### B.4.2 Distance Measurement Unit

Figure B-6 is the block schematic of the distance measuring unit. An infrared emitter generates a signal which is picked up by an infrared detector when one of the 30 wheel holes is in line with the emitter/detector. The 2-volt impulses are fed to a Schmitt Trigger circuit which generates 5-volt pulses. This is fed to an UP-DOWN switching circuit whose outputs are fed to the input stage of an UP-DOWN binary counting chain as well as to the input stage of an UP-DOWN B.C.D. counting chain. The 10 most significant bits of the binary counting chain output are fed to a digital-to-analog converter for generating the X input signal to the X-Y plotter. The 16-bit output of the B.C.D. counting chain is fed into a set of four 7 segment drivers whose outputs are connected to four L.E.D. displays. The display is normally off and can be turned on by depressing a push button connected to appropriate points in the circuit. A one decimal display accuracy is obtained.

### B.4.3 Voltage Detecting Unit

Figure B-7 is the block schematic of the voltage detecting unit. Synchronous detection is used to detect and filter only the voltages corresponding to the injected current signal. The injected current signal is also fed simultaneously to the input of a buffer as well as to the input of a difference amplifier. The buffer output goes through a phase-shifting circuit to the input of a zero-crossing detector. The phase-shifter brings the reference signal and the detected signal in phase, while the zero crossing detector generates two square wave signals that are 180° out-of-phase with each other. The signals are fed into an analog switching device.

The detected signal from the wheeled probe is fed to the inverting input of the difference amplifier. The current reference signal is fed to the non-inverting input. The difference amplifier output is proportional to the difference of the two input signals and is therefore proportional to the difference of potential between the reference electrode and the wheel. This signal is also fed to the analog switching device. The detected signal is chopped at a rate determined by the frequency of the two signals from the zero crossing detector. The analog switch output consists of two halves of the input signal, the positive half and the negative half. The negative half is inverted and the two signals are summed and fed to a low pass filter whose output is a dc signal corresponding to the 11 Hz signal. This is fed to the Y input of the X-Y recorder.

## B.5 CIRCUIT DIAGRAMS

### B.5.1 Power Supply

Figure B-8 is the power supply circuit diagram. Figure B-9 is the component layout on the printed circuit board. The ±12 volt supply from the Gel/cells is fed through 5 volt regulators to get a regulated ±5 volt supply. The ±12 volt and ±5 volt supplies are used for the complete circuitry.

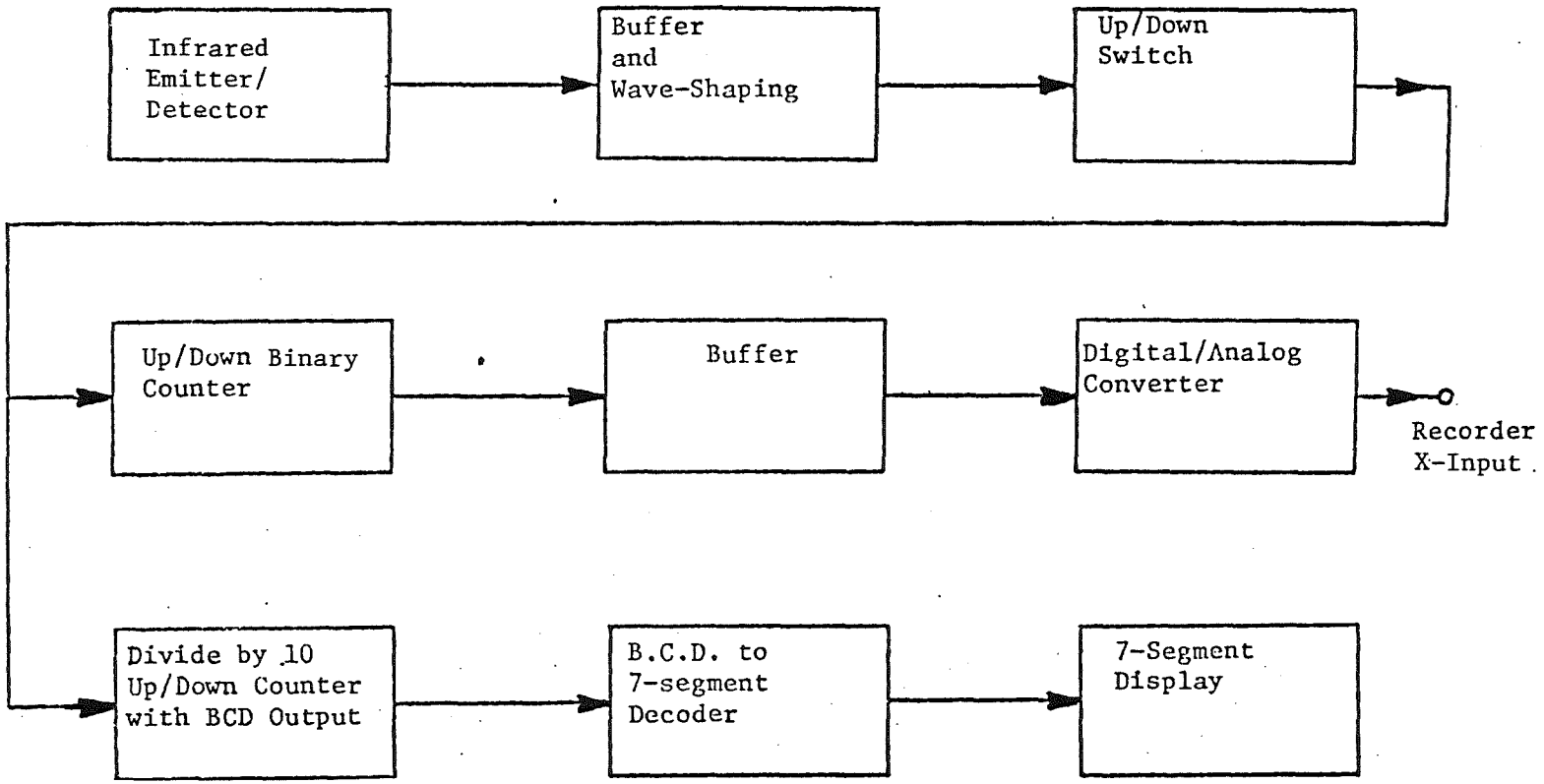


FIGURE B-6.- Block schematic of distance measuring unit.

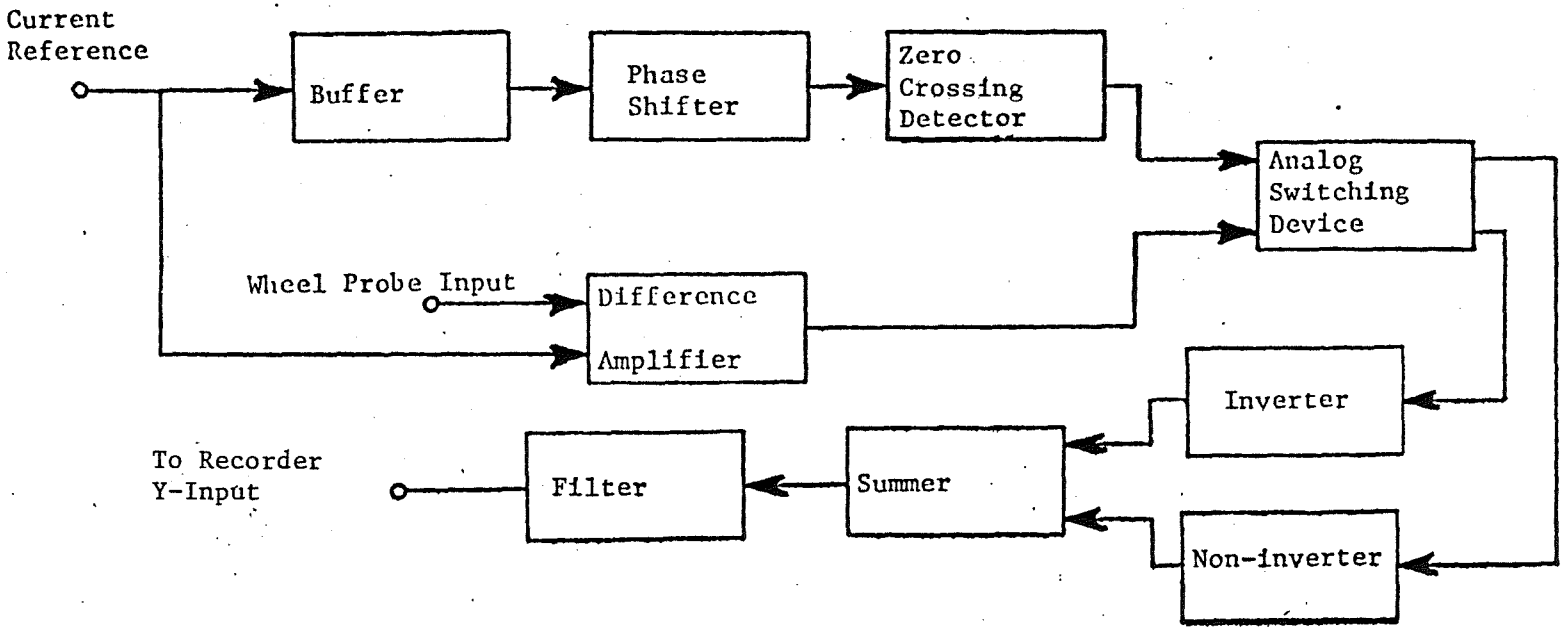


FIGURE B-7. - Block schematic of the voltage detecting unit.

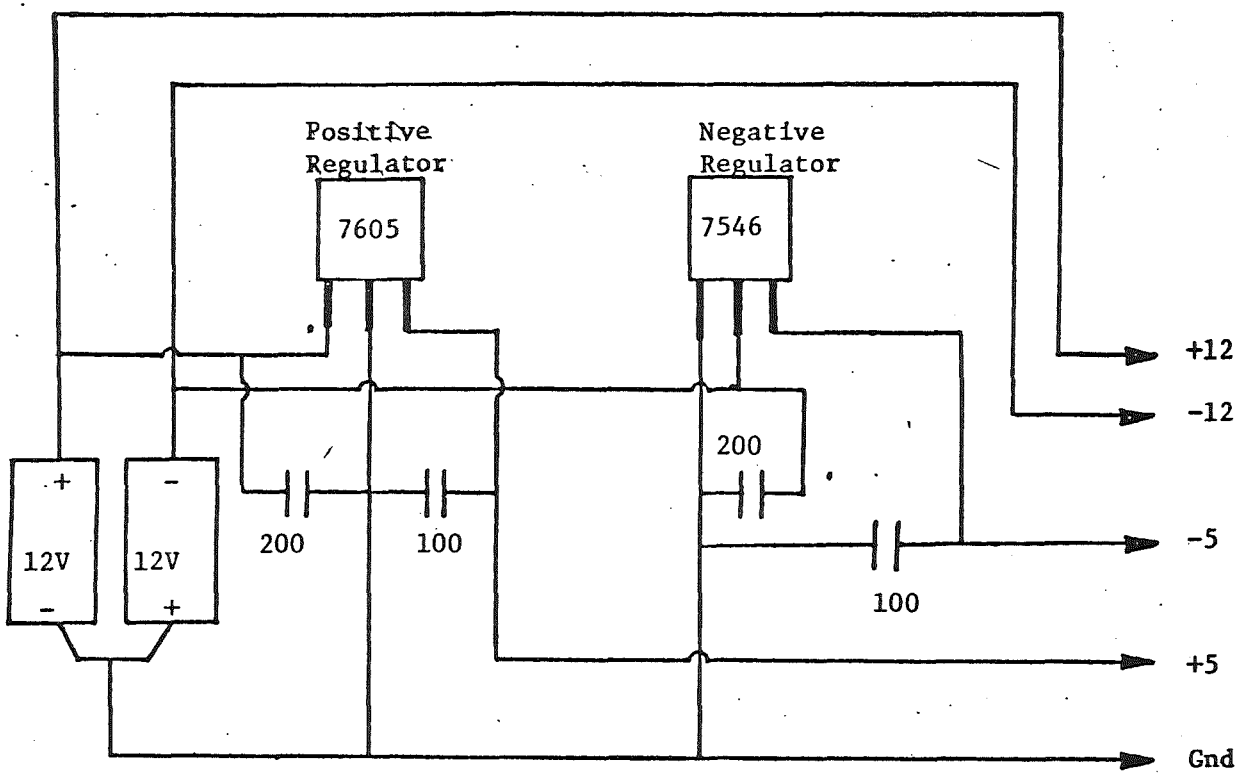


FIGURE B-8. - Power supply circuit diagram.

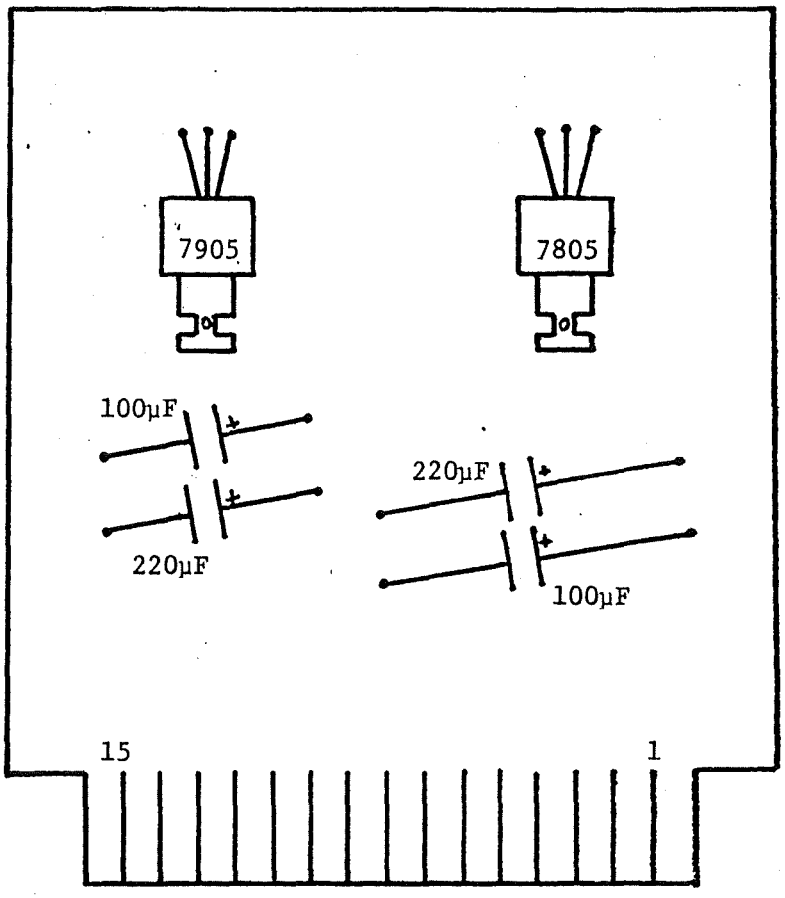


7805 - Positive voltage regulator
7905 - Negative voltage regulator

FIGURE B-9. - Power supply printed circuit board--component layout.

### B.5.2 Current Source

Figure B-10 is the circuit diagram of the current source and figure B-11 is the component layout on the printed circuit board. The 555 integrated circuit timer chip generates a 11 Hz square wave signal by a proper selection of resistors and capacitors for a 50% duty cycle.

A 741 operational amplifier chip in conjunction with a 4400 and 4402 complementary transistor pair is used in the push-pull mode to deliver a current of up to 100 mA. An adjustable potentiometer at the output of the 555 chip adjusts the current magnitude to the desired level.

A 1458 (dual 741) operational amplifier chip is used to rectify a small fraction of the output current from the current source, in conjunction with two 1N914 diodes and by a proper selection of resistor and capacitor values. The output is connected in series with a microammeter (range 0 to 100 μA) calibrated to read 0 to 100 mA full scale.

### B.5.3 Voltage Detector Circuit

Figure B-12 is the circuit diagram of the synchronous detector. The component layout on the printed circuit board is shown in figure B-13. The chip functions are below:

Chip A - For input buffer and phase shifting.
Chip B - Differential amplifier for voltage pick-up and current reference input.
Chip C - Zero crossing detector.
Chip D - Analog switching device.
Chip E - Summing and filtering.

### B.5.4 Distance Circuit

Figures B-14 and B-15 are drawings of the distance measuring circuits for analog output and display, respectively. Figures B-16 and B-17 show the component layout on the printed circuit boards. The functions of the various chips are below:

74C14 - Schmitt trigger for shaping the input pulses and generating output 5-volt square pulses.

74C00 - Logic switch whose two outputs are connected to the count-up and count-down inputs of a counting chain. While counting up, the count-down input is high, and vice-versa while counting down.

74C193 - Synchronous UP-DOWN counter with a 4-bit binary output. Three such chips are cascaded by connecting the "carry" and "borrow" outputs of each stage to the count-up and count-down inputs of the next stage to generate a 12-bit binary output.

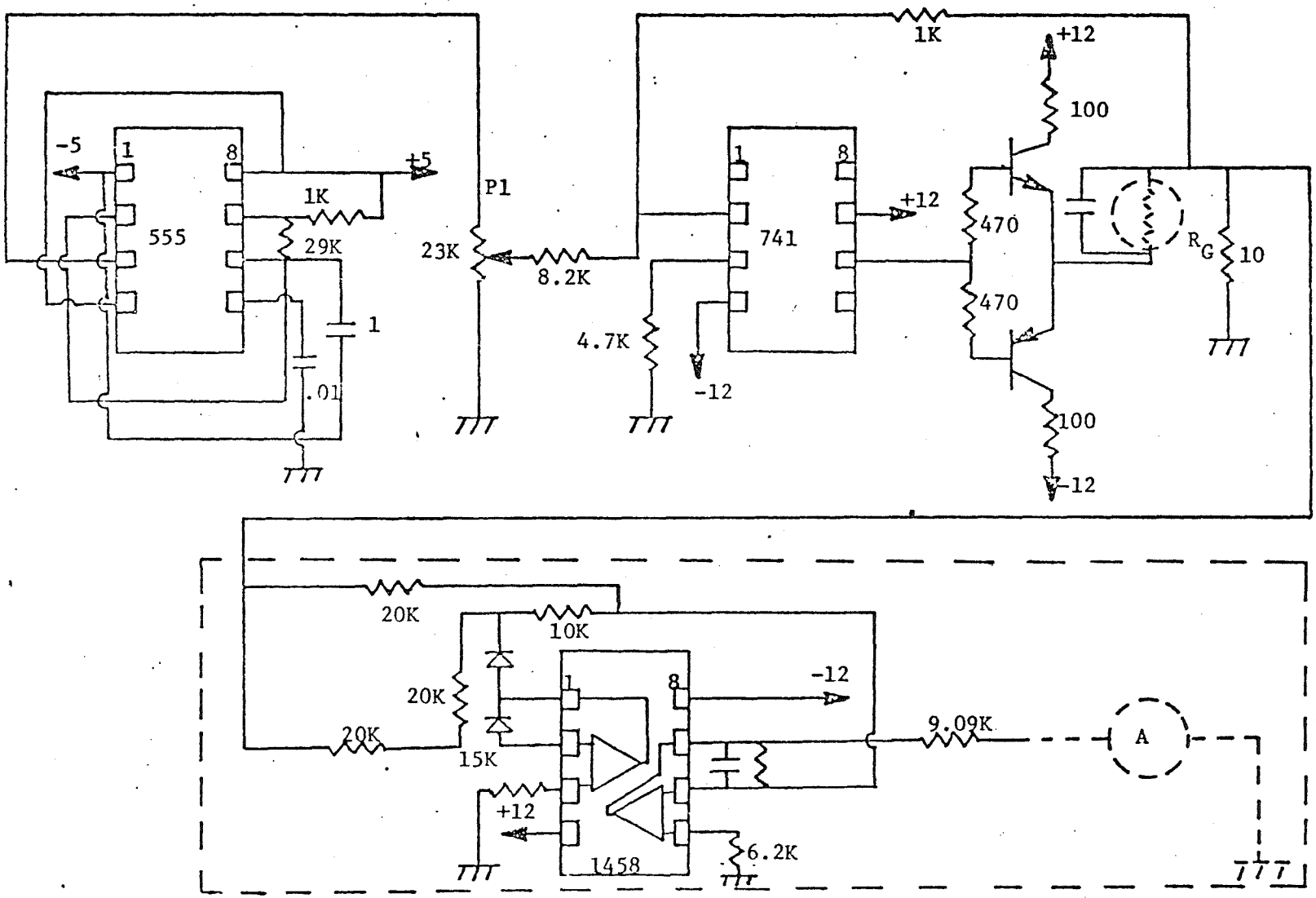


FIGURE B-10. - Constant current source and metering circuit - IC interconnections.

Note: Invert all IC chips before inserting (note how pins are numbered)

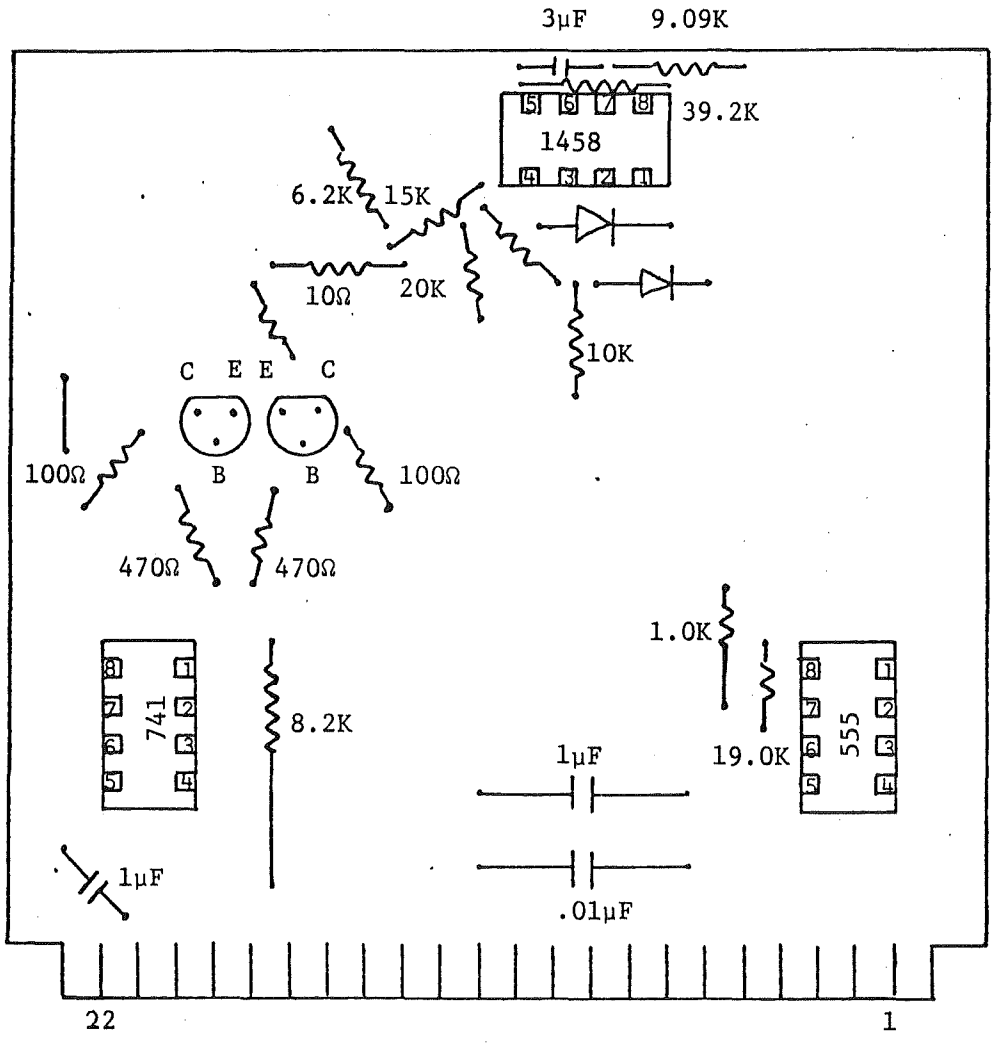


FIGURE B-11.- Current source printed circuit board--component layout.

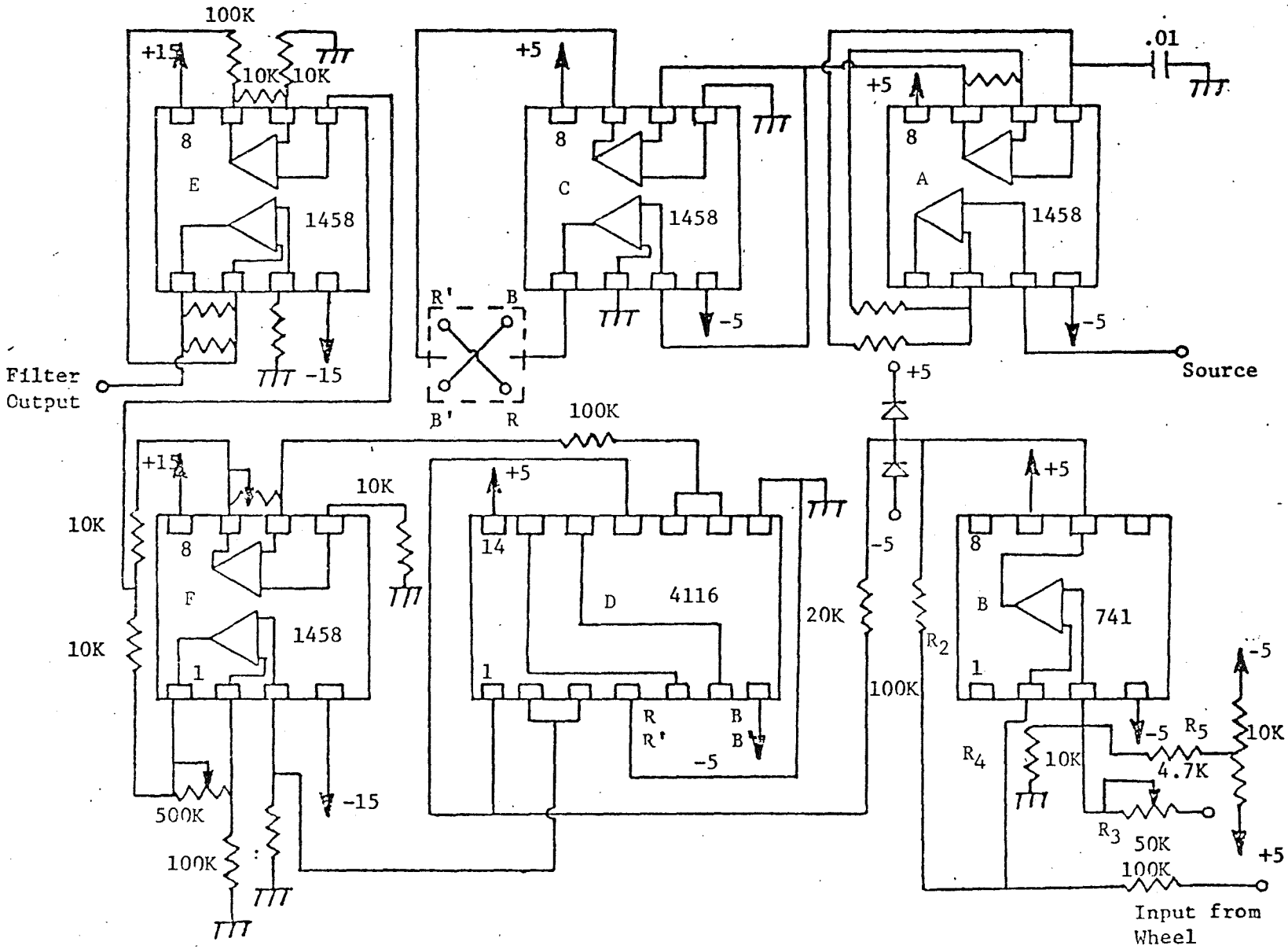


FIGURE B-12.- Synchronous detector-IC connections.

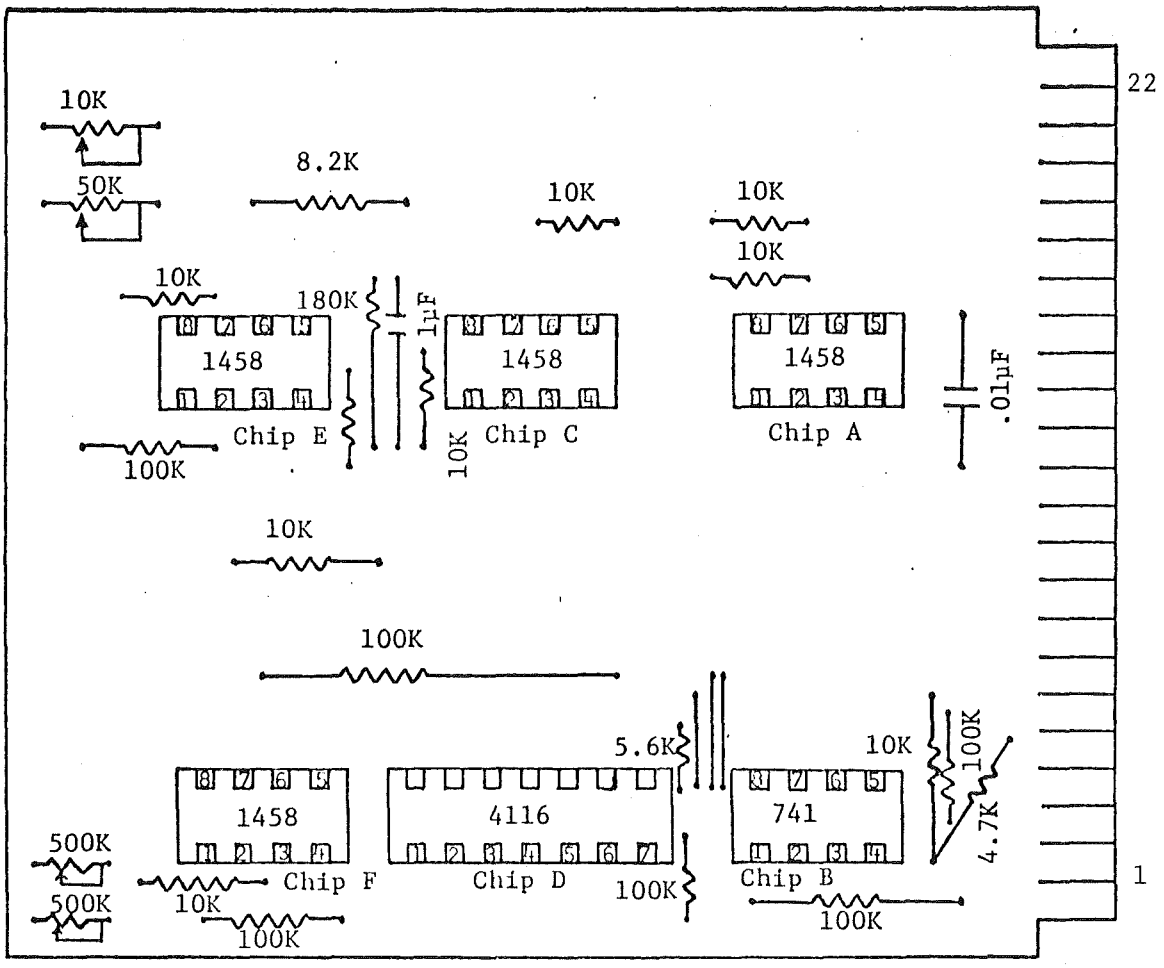


FIGURE B-13. - Synchronous detector printed circuit board--component layout.

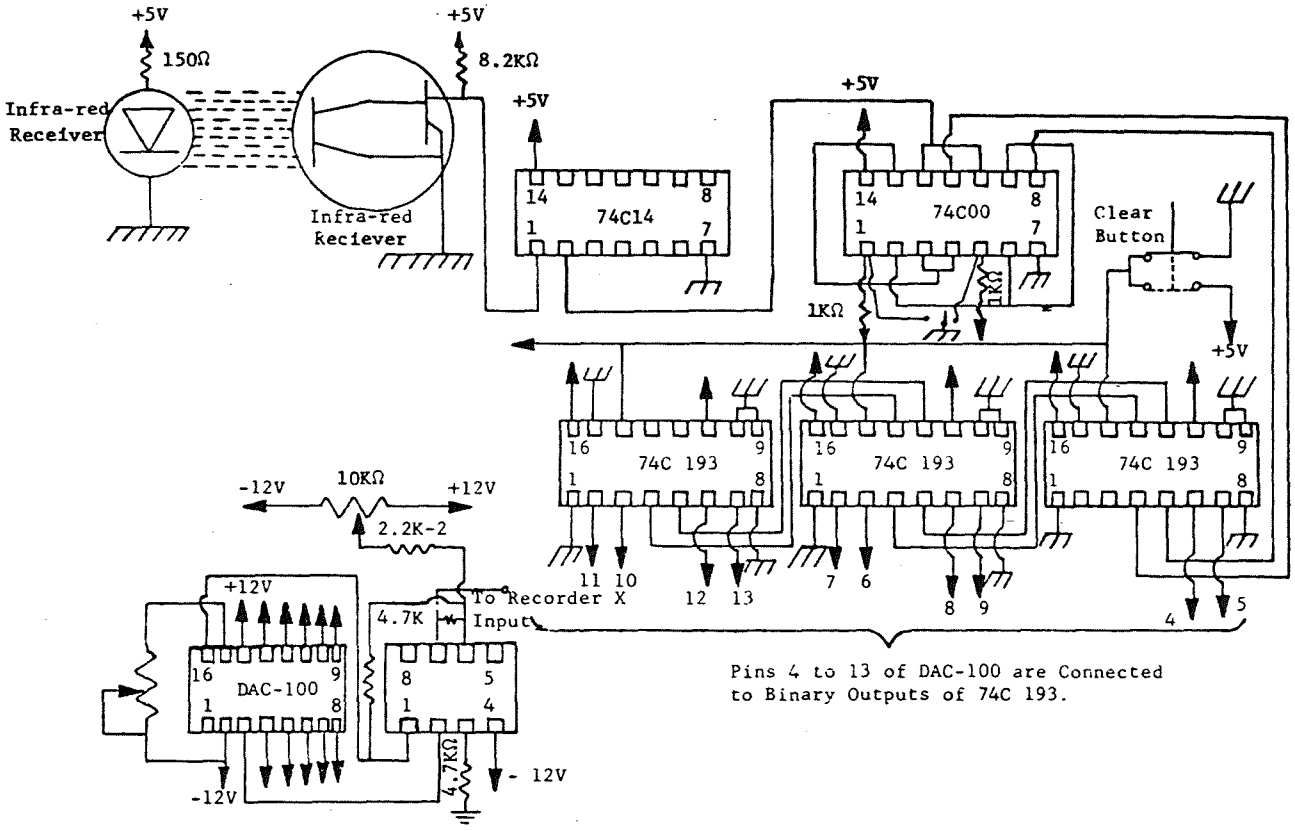


FIGURE B-14. - Distance measuring circuit using infrared emitter/receiver.

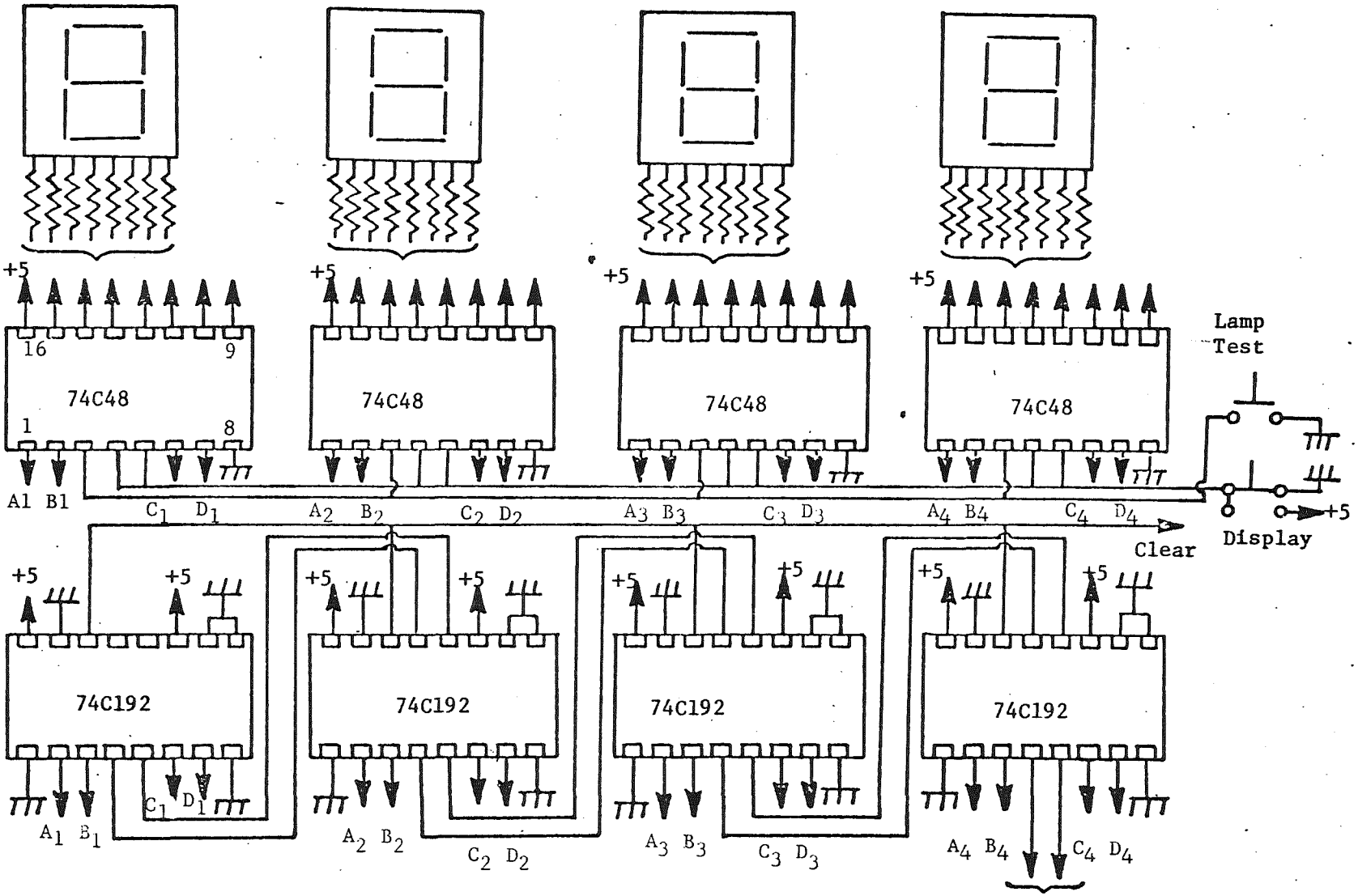


FIGURE B-15. - Display unit-IC connections.

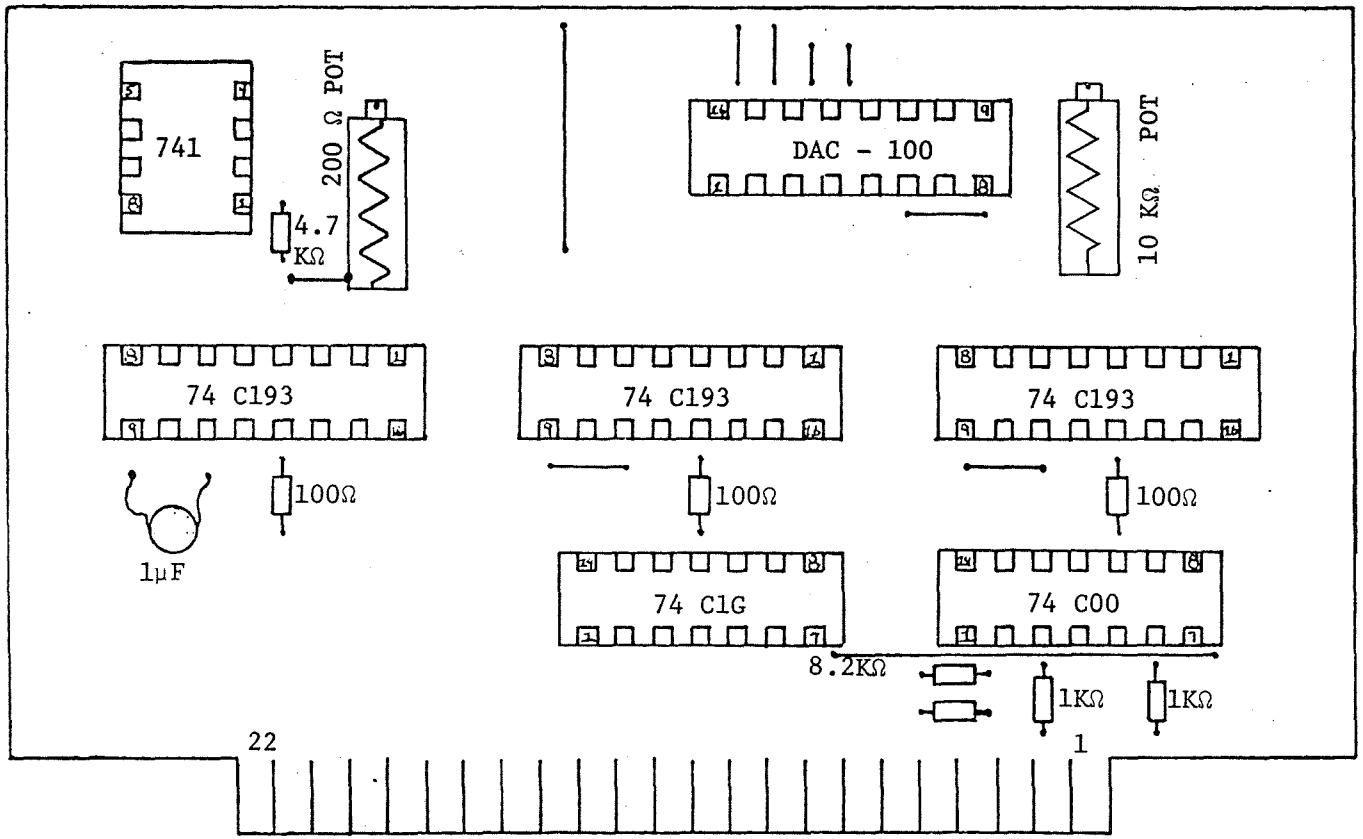


FIGURE B-16. - Distance circuit (analog output) printed circuit board -- component layout.

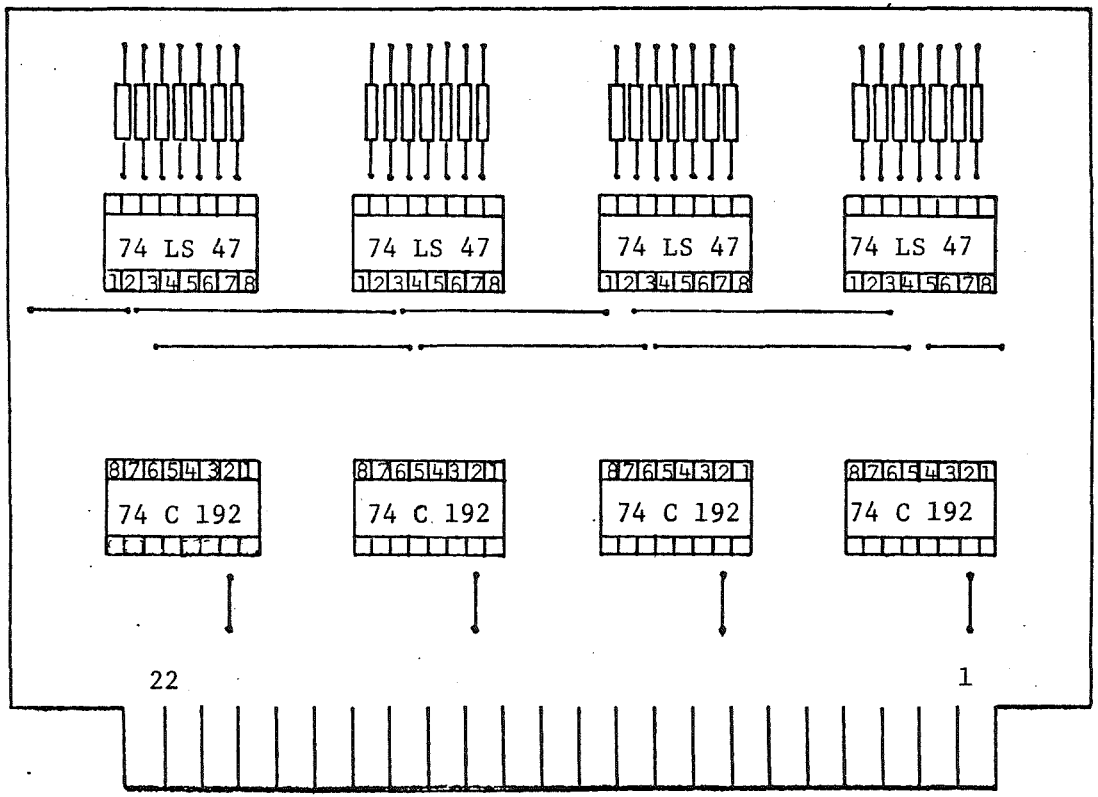


FIGURE B-17. - Distance display printed circuit board--component layout.

DAC-100CC - Ten bit digital-to-analog converter. This generates an analog output for a 10 bit binary input. The ten most significant bits of the 74C193 counting chain are connected to the inputs of the D/A converter.

1458 (Dual 741) - One of the 741 amplifier inputs is connected to the D/A converter output. The output of this 741 is connected to the input of a second 741 amplifier, which serves to offset the output voltage. The D/A converter gives a complementary 1's output, and so an offset voltage is necesary to get an output of 0 to 10 volts.

74C192 - UP-DOWN synchronous counter with a B.C.D. output. Input signal comes from the 74C00. Four counting chips are cascaded by connecting the "carry" and "borrow" outputs of each stage to the count-up and count-down inputs of the next stage.

74LS47 - B.C.D.-to-7 segment converter. Output signals from this chip are connected to the 7-segment inputs of an L.E.D. display. Input signals come from 74C192. Four such converters are used, one corresponding to each converter.

## B.6 WIRING DIAGRAMS

The following wiring diagrams contain detailed information on terminal interconnections and other external connections that can enable the user to easily trace the wiring for repairs.

B-18 Wiring diagram of the main chassis.
B-19 Wiring connections of the Gel/cell.
B-20 Wiring connections of the infrared emitter/detector.
B-21 Wiring connections of the switch box.
B-22 Pin connections for infrared device and voltage pick-up.
B-23 Pin connections between main box and switch box.

Wires are cross referenced on the drawing so that they can be easily traced.

## B.7 OTHER ACCESSORIES FOR MEASUREMENT

1. Two reels of special non-kinking cable with high resistance insulation are required for injecting a current between the reference and auxiliary electrode.

2. Two alloy steel rods, 1.27 cm (1/2 in) in diameter and 0.61 m (2 ft) long, are used as the reference and auxiliary electrodes. They have cross-bars on which the reels can rest. One of the rods is tied to the machine (around which the field distribution is desired) and is the reference electrode. The other rod is the auxiliary electrode.

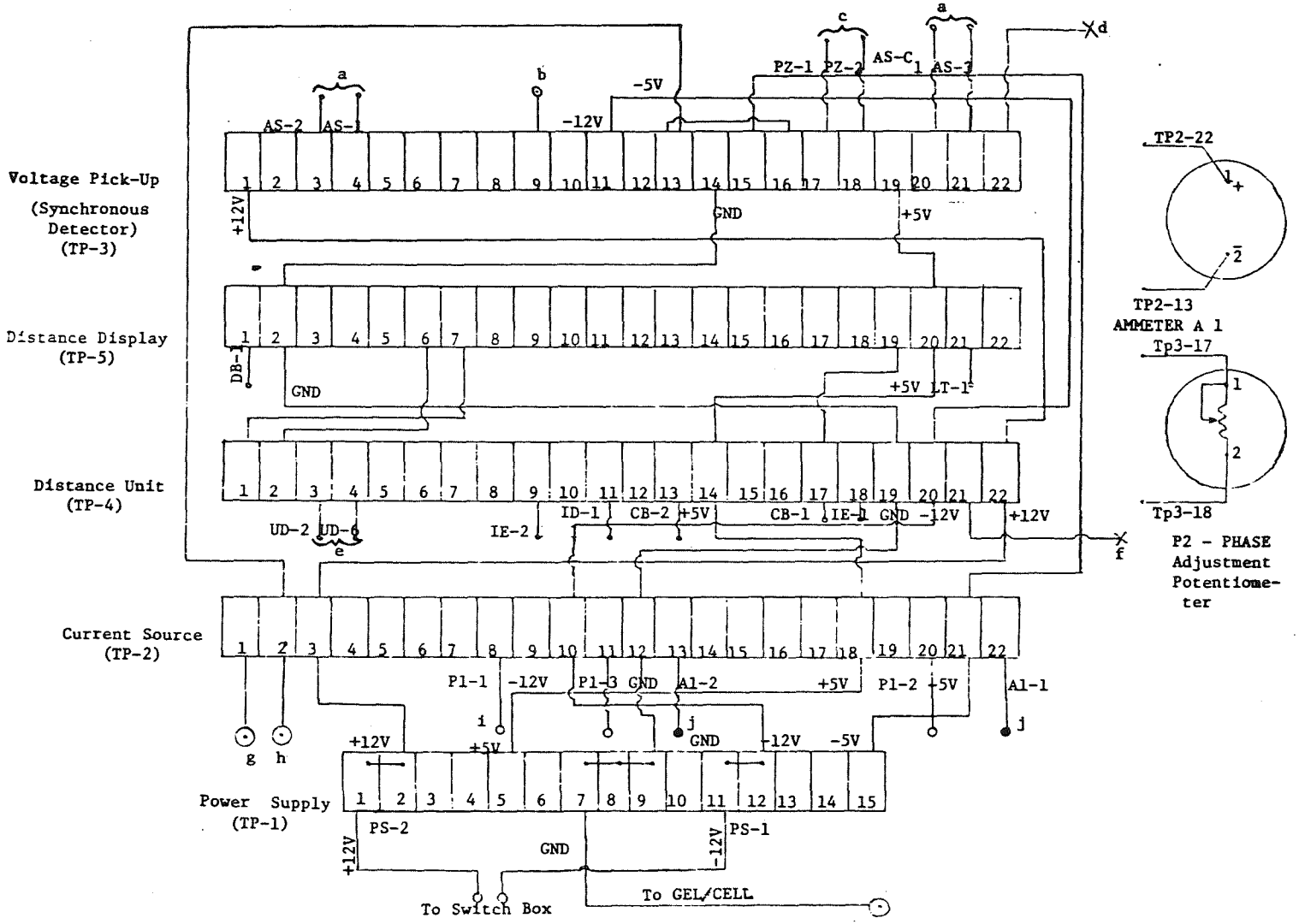


FIGURE B-18. - Wiring diagram of the main chassis (Legend on following page).

Legend for Figure B-18

⊙ Termination on chassis suitable for banana jacks
∘ Connection to multipin plug
• Connections within chassis
× Connections to 4 wire cable terminals

a To analog switch
b Test point
c Phase potentiometer
d Recorder Y-input
e To UP-DOWN switch
f Recorder X-input
g Auxiliary electrode
h Reference electrode
i To current potentiometer
j To ammeter

This drawing must be read in conjunction with drawings figure B-19 through figure B-23.

All wirings are cross referenced so they can be easily traced. Some examples are given below:

Pin 3 of terminal strip TP-3 has a wire labeled AS-2 and ending in a —o. This wire is connected to a 15 pin socket and figures B-22 and B-23 should be checked. In figure B-22, pin 10 of the 15 pin socket is labeled TP3-3 and this is pin 3 of terminal TP-3.

Pin 1 of TP-2 has a wire ending in ⊙ and reads auxiliary electrode. The wire has a banana jack terminal. The chassis terminals should be checked to see the label that corresponds to the above. Figure B-3 shows where the terminal is located.

Pin 22 of TP-2 has a wire labeled A1-1 and ends in a —●. This is an interconnection within the chassis and should be found in this drawing. Ammeter A1 labeled TP2-2 is obviously the wire.

Strips TP-2 to TP-5 are mounted one above the other in exactly the same order as shown in figure B-18. TP-1 is mounted horizontally adjacent to the above four.

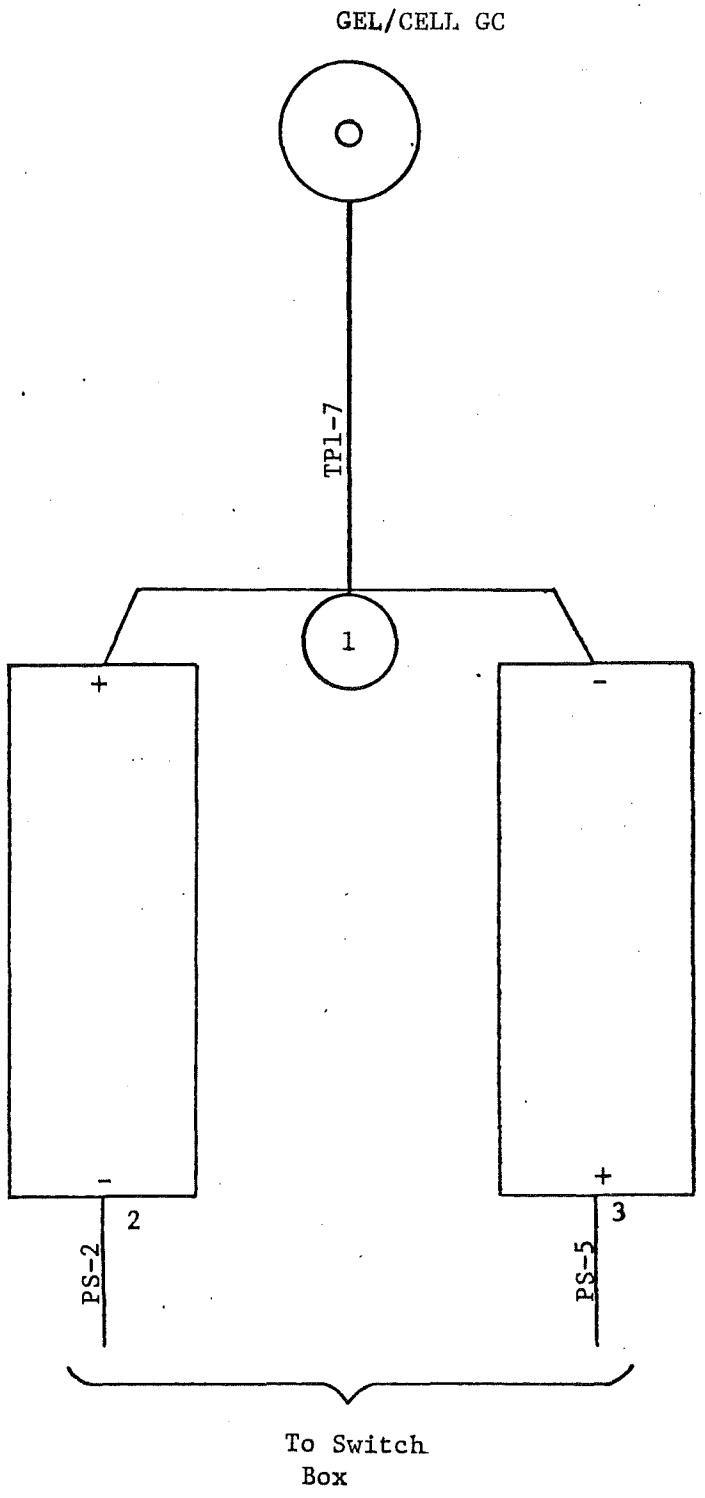


FIGURE B-19. - Wiring connections of the Gel/cells

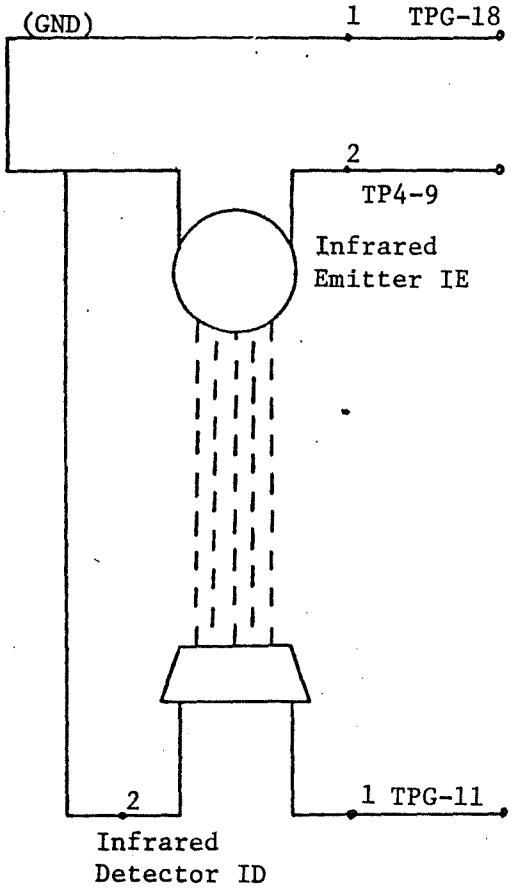


FIGURE B-20. - Wiring connection of the infrared emitter/detector.

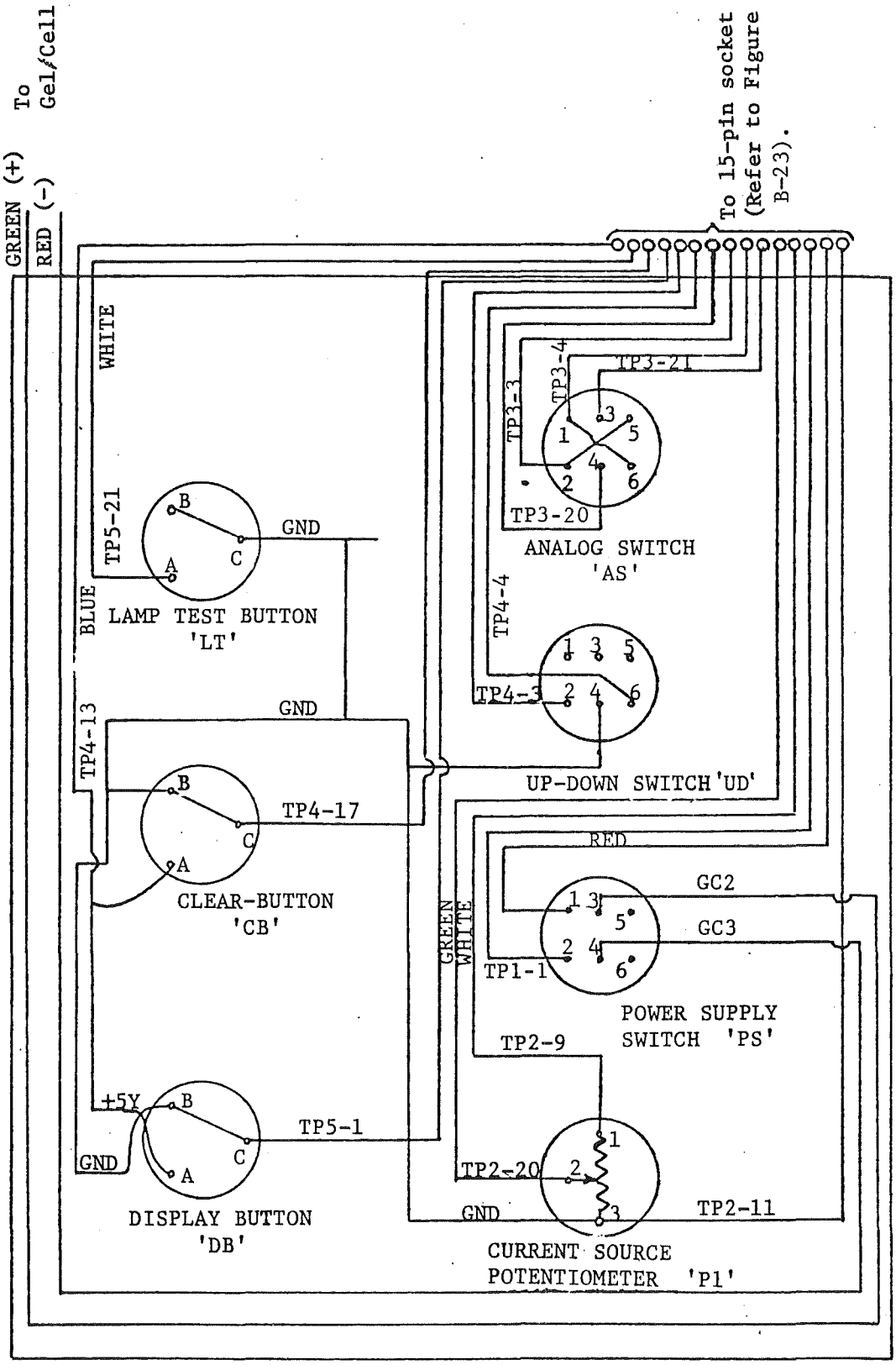


FIGURE B-21. - Wiring connections of switch box (as seen from inside the switch box).

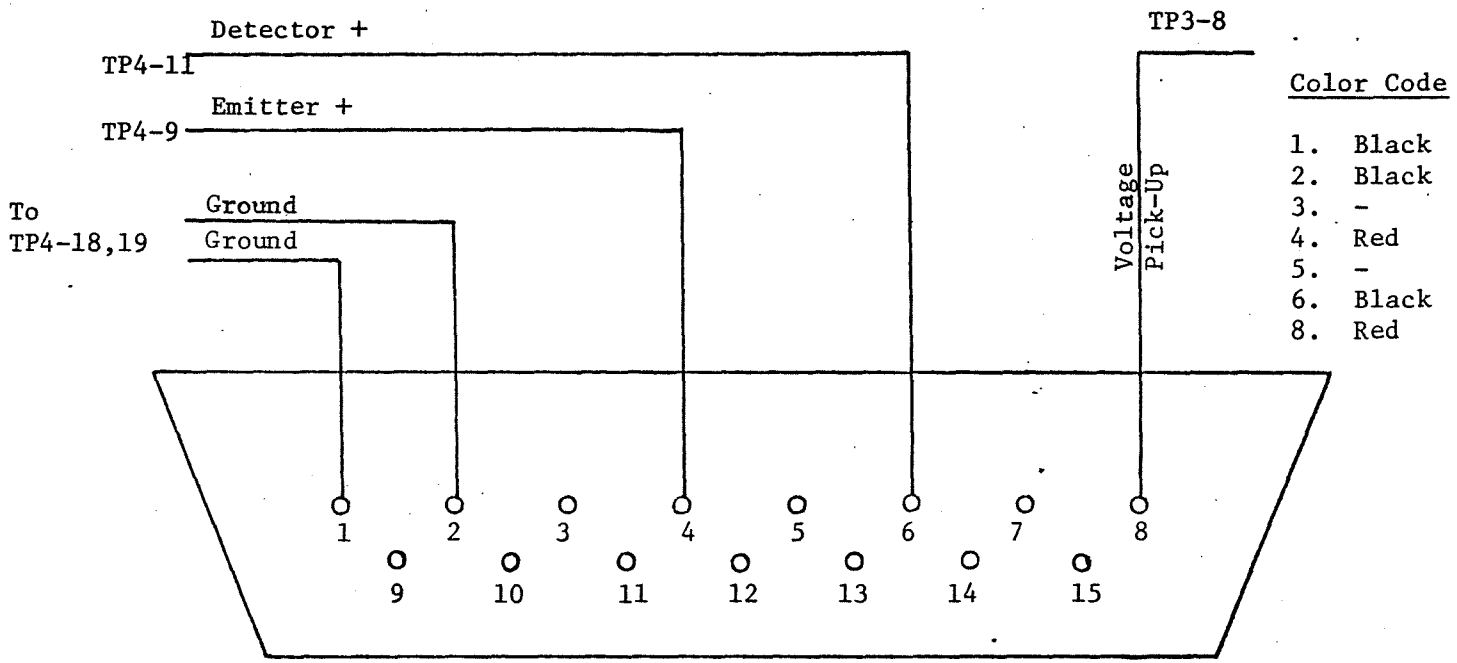


FIGURE B-22. - Multipin connections for infrared device and voltage pick-up (from socket into chassis).

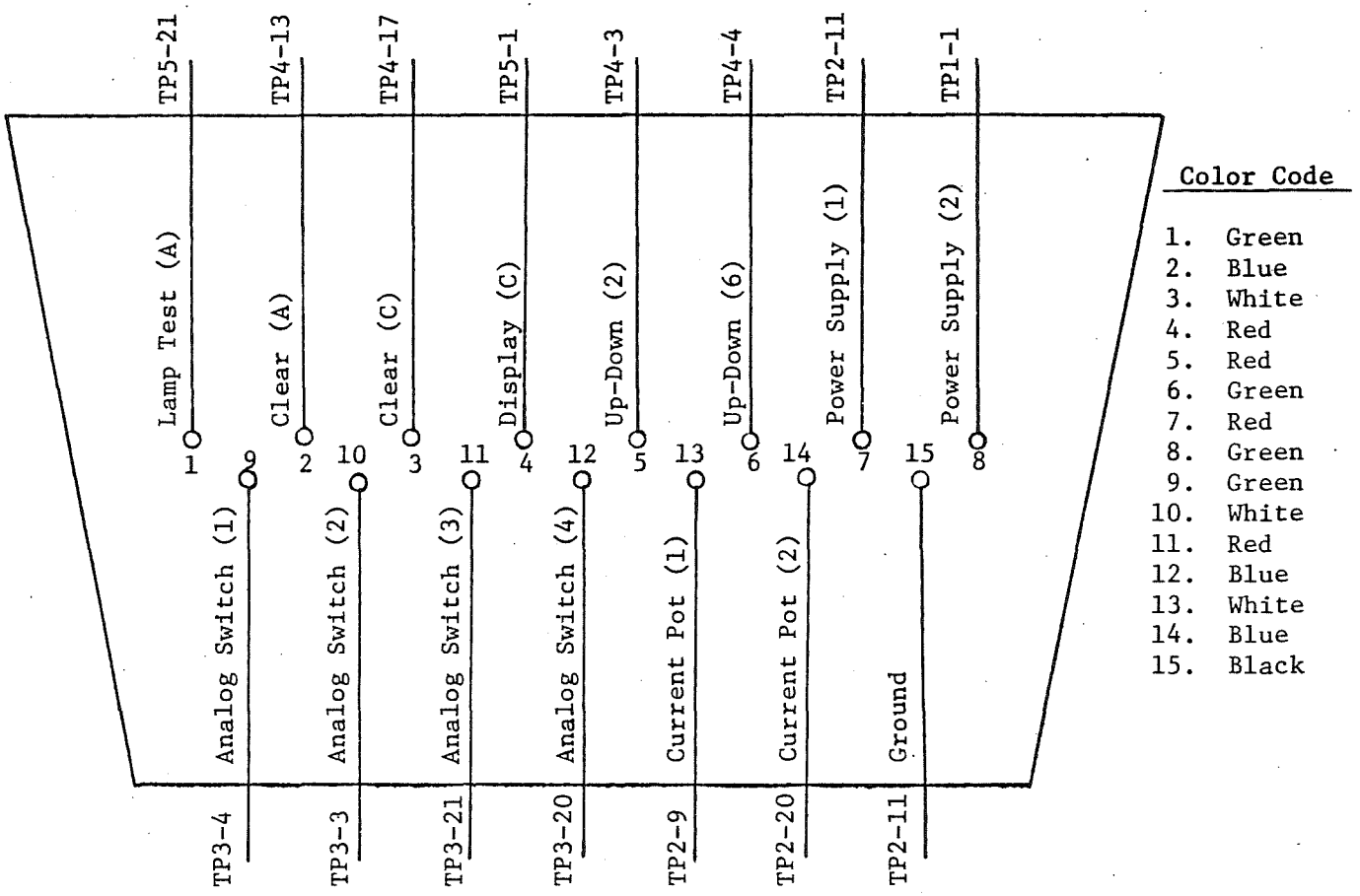


FIGURE B-23. - Multipin connections between main box and switch box.

3. A 76.2 m (250 ft) long, 4 conductor shielded cable transmits the voltage and distance signals from the wheeled electrode to the X-Y recorder.

4. An X-Y recorder with an adjustable scale range 50 mV to 1 V per inch and which can record on 8" x 11" paper.

5. A thyristor inverter operating with input supply from a car battery generates 120 V, 60 Hz supply for the X-Y plotter.

6. A hammer, screwdriver set, and 3 or 4 short wire lengths with grippers will be needed.

## B.8 CALIBRATION

There are very few calibration adjustments and these are listed below.

1. Distance unit adjustment

Referring to figure B-16, the 10 kilohm potentiometer is adjusted to get a zero output signal by observing the output voltage between pins 19 and 21 on a digital voltmeter. Next with the UP-DOWN switch in the DOWN position, the wheel is rotated through a distance between two holes. The voltage reading should be about 10 volts. The 200 ohm potentiometer $P_2$ is adjusted to get a full scale of 10 volts (or whatever voltage is desired). This corresponds to a distance of 124.8 (409.5 ft).

2. Voltage detector offset adjustment

This is a field adjustment. After the electrodes are installed and supply switched on, the wheel is physically shorted to the reference electrode and the Y output of the unit is observed on a voltmeter. The 50 kilohm potentiometer (shown in figure B-13) is adjusted to get zero volts.

## B.9 INSTALLATION AND MEASUREMENT PROCEDURE

This will proceed according to the following steps.

1. Make a small sketch showing the reference object and traverses proposed to be made with the gradient plotter. Decide on a tentative location for the auxiliary electrode at a distance 10 to 12 times the largest dimension of the reference object.

2. Hammer the reference and auxiliary rods in the selected positions, about one foot into the ground. The reference rod is clamped to the reference object.

3. The two reels are slid through the cross-bars of the rods (one reel for each rod). The wires are then unrolled and plugged into the reference and auxiliary current terminals of the plotter.

4. The 4-conductor cable is unrolled to a sufficient length (depending upon the largest traverse). One end of the cable terminates in a 4-pin socket and is insetted and screwed onto the corresponding plug on the main chassis of the plotter. The other end terminates in 2 plugs. The black plug is inserted into the recorder X terminals. The red plug goes into the recorder Y terminals.

5. A battery (car battery type) is connected to the battery terminals of the inverter. The supply cord of the X-Y recorder is plugged into the inverter output terminals.

6. The plotter supply is switched on. The current magnitude potentiometer is rotated to get an indication of 100 mA on the ammeter. If not, drive the auxiliary electrode deeper in the ground. If still not successful, try locating the auxiliary electrode in a low resistance area, until full deflection is obtained. Next, the offset adjustment for the voltage detector (described in section B.8) is done.

7. The X-Y recorder supply is switched on. A plot is obtained by making a trial directly to the auxiliary electrode. A profile similar to curve #1 in figure B-2 indicates that the auxiliary electrode spacing should be increased, after which another trial run should be conducted until a near-flat mid-portion is obtained.

8. A series of traverses are now made in the desired areas. A set of measurements is thus obtained. A typical setup for obtaining field measurements with the plotter is shown in figures B-24 and B-25.

## B.10 TROUBLESHOOTING AND MAINTENANCE

| Problem | Cause/Solution |
|---|---|
| 1. Complete rotation of current potentiometer does not result in full scale deflection of current ammeter. | Auxiliary electrode may not be driven deep enough or may be in high resistance soil. Drive electrode deeper and check. Or try another location for the auxiliary electrode. Also make sure cable reels have good contact with the rods. |
| 2. Recorder goes negative in the X direction. | Reverse the X input terminals |
| 3. Recorder goes negative in Y direction. | Reverse the Y input terminals. |
| 4. Recorder readings are very highly noisy | Check if negative terminals of X and Y inputs are shorted to recorder shield ground. If not, short them. |
| 5. No current being injected at all into the ground Ammeter shows zero. | Reels might have fallen off from cross bars. Put them back on the cross bars. Reel terminals might have gotten disconnected from the plotter current input terminals. Reconnect. |

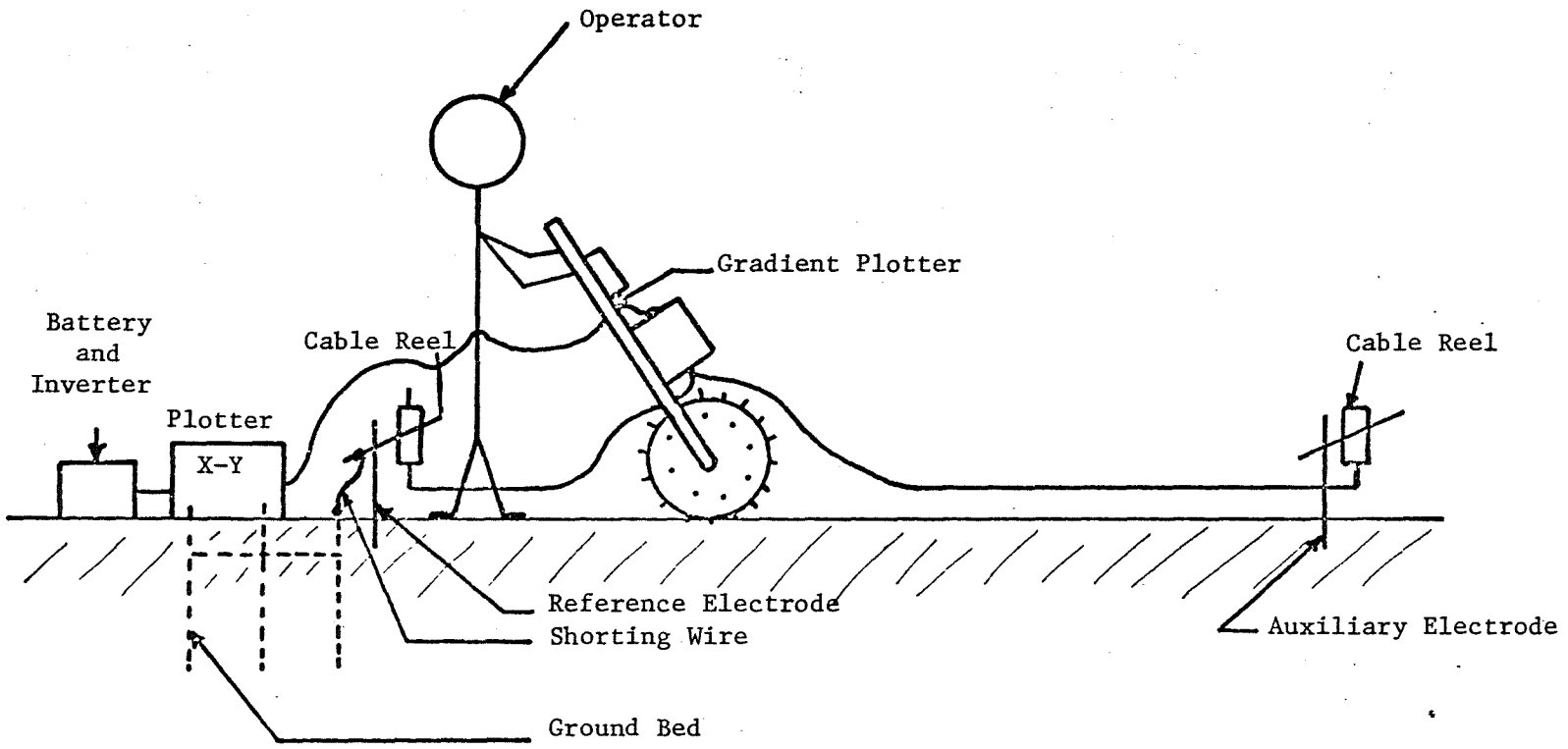


FIGURE B-24. - Typical set-up for obtaining field measurements with the plotter.

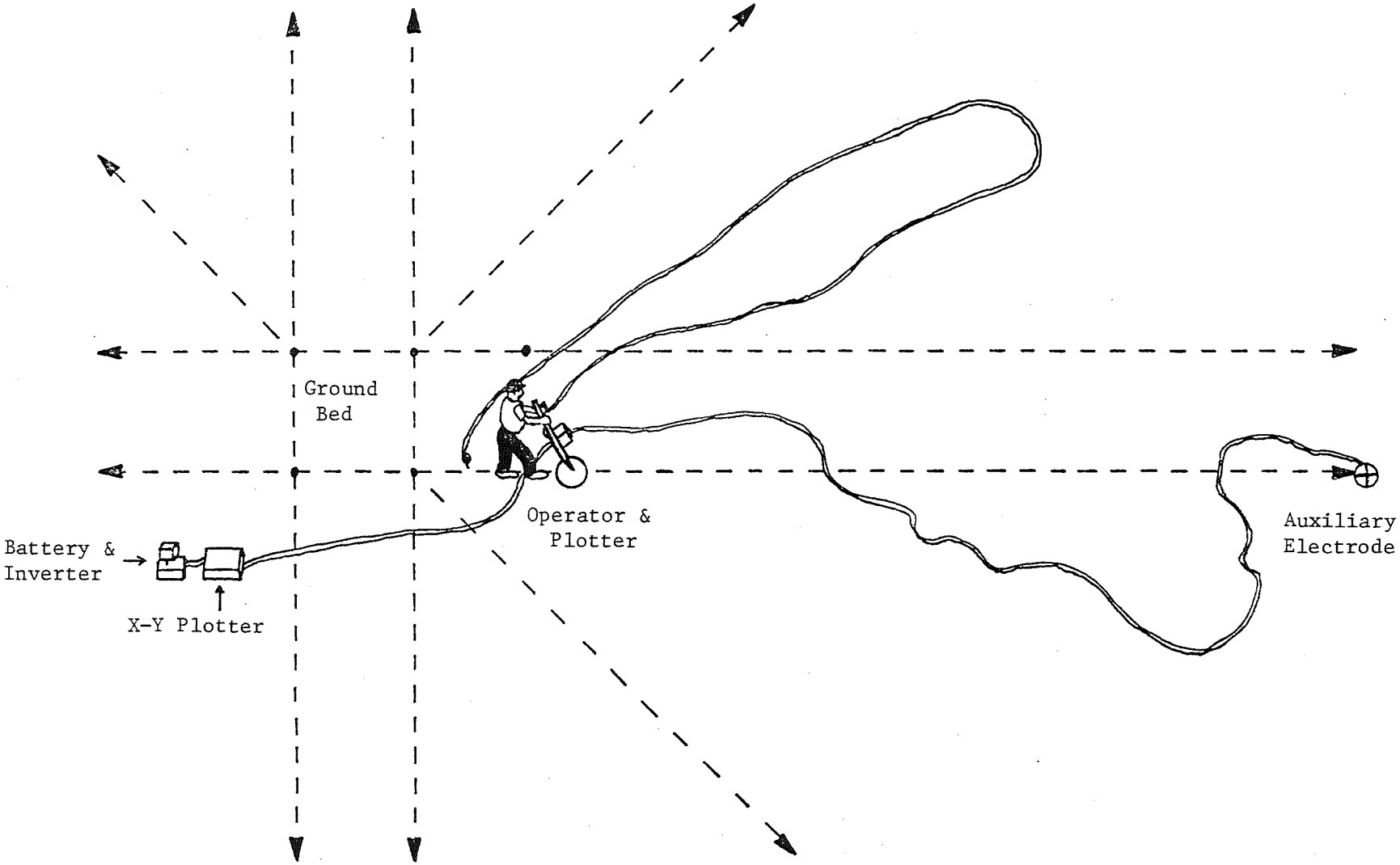


FIGURE B-25. - Perspective view of operation of gradient plotter.

| Problem | Cause/Solution |
|---|---|
| 6. No readings at all on the X and Y inputs | Probably a conductor cable is not well connected. Check and reconnect. If this does not work, check for broken leads, and reconnect. |

Maintenance: Gel/cells need to be charged after every field trip.

## B.11 LIST OF SPARE PARTS

| | | |
|---|---|---|
| 1. | 555 IC Chip | 2 pieces |
| 2. | 4400 Transistor | 2 pieces |
| 3. | 4402 Transistor | 2 pieces |
| 4. | 1458 IC Chip | 12 pieces |
| 5. | 741 IC Chip | 6 pieces |
| 6. | 4116 CMOS Chip | 2 pieces |
| 7. | H13B1 Photo Coupled Interrupter Module (GE Make) | 1 set |
| 8. | 74C14 CMOS Chip | 2 pieces |
| 9. | 74C00 CMOS Chip | 2 pieces |
| 10. | 74C193 CMOS Chip | 6 pieces |
| 11. | DAC-100-CC D/A Converter (PMI Make) | 1 piece |
| 12. | 74C192 CMOS Chip | 6 pieces |
| 13. | 74LS47 CMOS Chip | 6 pieces |